University of Alberta

The Use of Multi-Axis Force Transducers for Orthodontic Forces and Moments Identification

---

By

Hisham Badawi

A thesis submitted to the Faculty of Graduate Studies and Research
in partial fulfillment of the requirements for the degree of

Doctor of Philosophy
in
Orthodontics and Medical Sciences

Department of Dentistry

©Hisham Badawi
Fall 2009
Edmonton, Alberta

Permission is hereby granted to the University of Alberta Libraries to reproduce single copies of this thesis and to lend or sell such copies for private, scholarly or scientific research purposes only. Where the thesis is converted to, or otherwise made available in digital form, the University of Alberta will advise potential users of the thesis of these terms.

The author reserves all other publication and other rights in association with the copyright in the thesis and, except as herein before provided, neither the thesis nor any substantial portion thereof may be printed or otherwise reproduced in any material form whatsoever without the author's prior written permission.

Library and
Archives Canada

Published Heritage
Branch

395 Wellington Street
Ottawa ON K1A 0N4
Canada

Bibliothèque et
Archives Canada

Direction du
Patrimoine de l'édition

395, rue Wellington
Ottawa ON K1A 0N4
Canada

Your file Votre référence
ISBN: 978-0-494-51221-0
Our file Notre référence

NOTICE:
The author has granted a non-exclusive license allowing Library and Archives Canada to reproduce, publish, archive, preserve, conserve, communicate to the public by telecommunication or on the Internet, loan, distribute and sell theses worldwide, for commercial or non-commercial purposes, in microform, paper, electronic and/or any other formats.

The author retains copyright ownership and moral rights in this thesis. Neither the thesis nor substantial extracts from it may be printed or otherwise reproduced without the author's permission.

AVIS:
L'auteur a accordé une licence non exclusive permettant à la Bibliothèque et Archives Canada de reproduire, publier, archiver, sauvegarder, conserver, transmettre au public par télécommunication ou par l'Internet, prêter, distribuer et vendre des thèses partout dans le monde, à des fins commerciales ou autres, sur support microforme, papier, électronique et/ou autres formats.

L'auteur conserve la propriété du droit d'auteur et des droits moraux qui protège cette thèse. Ni la thèse ni des extraits substantiels de celle-ci ne doivent être imprimés ou autrement reproduits sans son autorisation.

In compliance with the Canadian Privacy Act some supporting forms may have been removed from this thesis.

While these forms may be included in the document page count, their removal does not represent any loss of content from the thesis.

Conformément à la loi canadienne sur la protection de la vie privée, quelques formulaires secondaires ont été enlevés de cette thèse.

Bien que ces formulaires aient inclus dans la pagination, il n'y aura aucun contenu manquant.

Canada

Examining Committee

Roger Toogood, Mechanical Engineering

Paul Major, Dentistry

Jason Carey, Mechanical Engineering

Giseon Hoe, Dentistry

Christoph Bourauel, External Examiner

Gary Faulkner, External Examiner

Abstract

Many of the undesirable side effects that occur during orthodontic treatment can be attributed directly to a lack of understanding of the physics involved in a given adjustment of an orthodontic appliance. A large number of variables in orthodontic treatment are not within our control, such as growth and tissue response to appliances. However, the force placed on the tooth should be a controllable variable ([1]), and careful study of the physics underlying our clinical application, can help in reducing those undesirable side effects. If researchers and clinicians can quantify the force systems applied to the teeth, they can better understand clinical and histologic responses.

Orthodontic force systems used in everyday orthodontic mechanics are considered indeterminate force systems, in other words, there are too many unknowns to determine the different components of these force systems. Until recently, much of the literature was restricted to experimental two-dimensional analyses of the biomechanical aspects of orthodontic force systems, and computer modeling of three-dimensional analyses. Very little evidence exists in the literature regarding three dimensional experimental measurement and analysis of orthodontic force systems ([2]). Force system measurements were made on one or two tooth models, however in order for us to understand the orthodontic force systems we need to simultaneously, measure in 3D, the forces being applied on every tooth in the dental arch.

With the very recent technological advances in force/torque sensors technology, data acquisition and data representation, it became possible to measure those forces and reveal the force systems we are applying to the

dentition. The purpose of this PhD research study is the design and construction of an experimental device that is capable of revealing the details of the force systems used in modern day orthodontic mechano-therapy of continuous arch technique.

Preface

My research interests started soon after joining the MSc in Orthodontics specialty training program at the Eastman Dental Institute in London, England. I kept asking myself a number of "what if" questions, "*What if we were able to measure the forces we apply on our patients' dentition during orthodontic treatment*", "*what if we were able to identify the most clinically efficient orthodontic force system*". Those questions were troubling, they were thought to be impossible to resolve, considering the technical challenges that face the orthodontic research community.

Soon after graduating from my specialty-training program, I joined the Orthodontic department at the University of Alberta, determined to devise a method that can be used to answer those questions. I embarked on this seemingly impossible task with the help of a group of individuals (Orthodontists and Engineers) as driven as I was to prove that it is possible to answer those questions. Six years passed, through which we put numerous hours of work, and encountered many formidable obstacles, and finally, we are here to declare "mission accomplished". We are now able to answer many of those daunting questions, only to find that my journey in the field of orthodontic research has just begun.

This research journey was only possible with the help of many individuals. My wife, without whom this would never have been possible, stood by me, endured and sacrificed to allow me to fulfill my dream. My research supervisors believed in me and were willing to walk this uncertain road with me.

Acknowledgement

I would like to acknowledge those who helped me throughout my journey:

My wife Asma, she was a source of enlightenment and a passionate supporter. Her sacrifice and her hard work were admirable.

My parents for helping me all along, words cannot do them justice. Without their support this would not have been possible.

My supervisory committee who taught me, so I will never forget.

Paul Major, who believed in me and supported me.

Roger Toogood, the most intelligent person I have ever met.

Steve Ward, who was instrumental with his help and encouragement throughout the last five years.

All my Family, friends and colleagues who directly or indirectly made a difference.

Table of Contents

1 CHAPTER ONE: INTRODUCTION 1

2 CHAPTER TWO: LITERATURE REVIEW 4

2.1 Principles of Biomechanics.. 5

2.1.1 Force.. 5

2.1.2 Moment 6

2.1.3 Couples.. 7

2.2 Orthodontic mechanical concepts 9

2.2.1 Centre of resistance 9

2.2.2 Centre of rotation 10

2.2.3 Moment of couple to moment of force ratio (Mc/Mf).. 11

2.3 Biological Response to Forces 15

2.3.1 Physiological Stress of the Periodontium.. 16

2.3.2 Optimum Orthodontic forces.. 17

2.4 Orthodontic Force systems.. 19

2.4.1 Force system from an ideal arch.. 19

2.4.2 V-Bends.. 21

2.5 The Edgewise Appliance 26

2.5.1 Development of the Edgewise Appliance 26

2.5.2 Modifications of Edgewise Appliances.. 27

2.5.3 Materials of Modern Edgewise Appliances 28

2.6 Torque.. 32

2.6.1 Third order moments.. 33

2.6.2 Factors Contributing to Losses in Third Order Movements.. 34

2.7 Self-ligating brackets 43

2.7.1 Low friction produced by self-ligation 44

2.7.2 Reduction in treatment time and chair-side time with self-ligation 49

2.7.3 More accurate archwire engagement with self-ligation 50

2.7.4 Active Vs Passive Self-ligation 52

2.8 Force system determination 56

2.8.1 Force system analysis (Force Resolution) 56

2.8.2 Finite Element Analysis 58

2.8.3 Force Measurements 58

2.9 Purpose of the study 59

3 CHAPTER THREE: DEVELOPMENT AND EVALUATION OF MEASUREMENT REPEATABILITY OF AN ORTHODONTIC TORQUE MEASURING APPARATUS 60

3.1 Introduction 61

3.2 Apparatus 63

3.2.1 Hardware: 63

3.2.2 Software 70

3.2.3 Error analysis 70

3.3 Materials 74

3.4 Results 75

3.5 Discussion 82

3.6 Conclusions 86

3.7 Future research 88

4 CHAPTER FOUR: DESIGN, CONSTRUCTION AND OPERATION OF THE ORTHODONTIC SIMULATOR 89

4.1 Introduction **90**

4.2 Hardware: **92**

4.2.1 Force/torque transducers 92

4.2.2 Temperature chamber 96

4.2.3 OSIM Device 96

4.2.4 Data acquisition Hardware 107

4.2.5 Coordinate measurement 110

4.2.6 Transformations 116

4.3 Software **121**

4.3.1 Sign convention 137

4.4 Error analysis **138**

4.5 Simulating a high upper cuspid **144**

5 CHAPTER FIVE: RESULTS 146

5.1 Overview **147**

5.2 0.014" NiTi wire results **153**

5.2.1 Mesio-distal forces (F_x) 153

5.2.2 Fy Bucco-lingual forces 160

5.2.3 Fz Occluso-gingival forces 166

5.2.4 Mx Moments (Bucco-Lingual Moments) 173

5.2.5 My Moments (Mesio-Distal Moments) 179

5.2.6 Mz Moments (Disto-Buccal/Mesio-Buccal Moments) 185

5.3 0.018" NiTi wire **191**

5.3.1 Mesio-distal forces (Fx) 191

5.3.2 Fy Bucco-lingual forces 199

5.3.3 Fz Occluso-gingival forces 205

5.3.4 Mx Moments (Bucco-Lingual Moments) 212

5.3.5 My Moments (Mesio-Distal Moments) 218

5.3.6 Mz Moments (Disto-Buccal/Mesio-Buccal Moments) 224

5.4 0.014" x 0.025" NiTi wire 230

5.4.1 Mesio-distal forces (Fx) 230

5.4.2 Fy Bucco-lingual forces 237

5.4.3 Fz Occluso-gingival forces 243

5.4.4 Mx Moments (Bucco-Lingual Moments) 250

5.4.5 My Moments (Mesio-Distal Moments) 256

5.4.6 Mz Moments (Disto-Buccal/Mesio-Buccal Moments) 262

5.5 Summary of Results 268

5.6 Forces produced by 0.014" wire 270

5.7 Forces produced by 0.018" wire 277

5.8 Forces produced by 0.014"× 0.025" wire 284

5.9 The effect of archwire size and dimension on the force system 291

5.9.1 The effect of the wire size and dimension on Fx 291

5.9.2 The effect of the wire size and dimension on Fy 294

5.9.3 The effect of the wire size and dimension on Fz 296

5.9.4 The effect of the wire size and dimension on Mx 298

5.9.5 The effect of the wire size and dimension on My 300

5.9.6 The effect of the wire size and dimension on Mz: 302

5.10 Conclusion 304

6 CHAPTER SIX: DISCUSSION 306

6.1 The challenges faced during the development the Orthodontic Simulator (OSIM) 310

6.2 High upper cuspid simulation 314

6.3 Future research 324

6.3.1 PDL compliance simulation: 324

6.3.2 Horizontal connector modification: 325

6.3.3 Motorizing the micrometers: 325

6.3.4 Future experiments: 326

7 REFERENCE LIST 328

8 APPENDIX 341

8.1 OSIM 0.014" Display 342

8.2 OSIM 0.018" Display 349

8.3 OSIM 14x25 Display 356

List of Figures

Figure 2-1: Rotation about the center of rotation caused by the application of a pure force in the absence of a moment; where the Mc/Mf ratio is zero (uncontrolled tipping)........12

Figure 2-2: Translation tooth movement, through the simultaneous application of a force and a moment of a couple at the bracket; where the Mc/Mf ratio equals 1 13

Figure 2-3: wire attachment geometry defined by the inter bracket distance (L) and the angles of the brackets at position A and B (θ_A and θ_B) ([3])........20

Figure 2-4: Six basic geometries based on the ratio θ_A / θ_B. Classes are independent of interbracket distance ([3])........20

Figure 2-5: forces and moments produced by a step bend in a wire ([38])........22

Figure 2-6: geometry of a V bend ([38])........23

Figure 2-7: Mesiodistal placement of the apex of the V bend in two planes of space ([38]).23

Figure 2-8: force systems produced by anterior Vbends. A, V bend between central incisors gives equal and opposite couples. B, step bends between central and lateral incisors give vertical forces and unidirectional couples. C, Summation of A and B. ([38])........24

Figure 2-9: Typical load-deflection curve of superelastic NiTi........31

Figure 2-10: Third order couple is added at the bracket to produce a counter acting moment that is equal in magnitude but opposite in direction to the force induced moment. 33

Figure 2-11: Deviation angle: Measurement of the amount of axial rotation that the archwire must rotate within the bracket slot until contact is made between the edges of the archwire and the walls of the bracket slot. 35

Figure 2-12: Friction........45

Figure 2-13: force resolution........57

Figure 3-1: Deviation angle........61

Figure 3-2: bracket/wire assembly torsion testing apparatus........64

Figure 3-3: (a) Conical wire support dies; (b) Schematic of the torsion application system and wire support dies 67
Figure 3-4: Schematic of the alignment system. (a) Unaligned wire and bracket. Possible motion of both turntables is shown. (b) Aligned bracket and wire and rotation motion required by both turntables. 68
Figure 3-5: Bracket mounting and alignment assembly 69
Figure 3-6: Moments measured for error analysis showing no plastic deformation of wire or bracket 72
Figure 3-7: torque expression of one bracket wire combination repeated 10 times 73
Figure 3-8: Variation in the torque measurement increases as angle of torsion increases 80
Figure 3-9: Torque expression of the four brackets 80
Figure 4-1: Orthodontic Simulator (OSIM) in a temperature chamber 91
Figure 4-2: Nano 17 force sensors 92
Figure 4-3: Compound Loading Range of Nano17 transducer 95
Figure 4-4: temperature chamber and temperature controller 96
Figure 4-5: OSIM major components 98
Figure 4-6: OSIM tooth connector 99
Figure 4-7: load-cell to tooth connector, (a) Vertical micrometer (b) Horizontal micrometer (c) Tooth adapter 100
Figure 4-8: bracket-mounting jig 103
Figure 4-9: tooth-mounting guide 104
Figure 4-10: transfer template 105
Figure 4-11: data acquisition hardware 109
Figure 4-12: Global point of origin determination 111
Figure 4-13: Transducer point of origin determination 113
Figure 4-14: the tooth point of origin determination 114
Figure 4-15: the bracket point of origin determination 115

Figure 4-16: Positional transformations T1, T2 and T3 are required to calculate T4 required for the force system transformation from the load-cell coordinate system to the tooth coordinate system. 117

Figure 4-17: Typical positional transformation matrix 118

Figure 4-18: force system transformation 119

Figure 4-19: LabView control panel 122

Figure 4-20: OSIM dataflow 123

Figure 4-21: OSIM display 124

Figure 4-22: OSIM software user interface 125

Figure 4-23: World to load-cell transformation matrices 125

Figure 4-24: World to tooth transformation matrices 126

Figure 4-25: tooth to bracket transformation matrices 127

Figure 4-26: X Y and Z component display of force components 128

Figure 4-27: Force vector display 128

Figure 4-28: color gradient display of force magnitude 129

Figure 4-29: sampling window 130

Figure 4-30: samples view 131

Figure 4-31: Error analysis window 132

Figure 4-32: Force and moment error analysis 133

Figure 4-33: Overload protection window, force or moment overload threshold input window 134

Figure 4-34: Overload alert 134

Figure 4-35: Multi-sample Display 135

Figure 4-36: tooth alerts of teeth experiencing F_x higher than 0.4N 135

Figure 4-37: OSIM sample playing options 136

Figure 4-38: (a) Calibration arm (b) Testing weight applied in F_y (c) Testing weight applied in F_x (d) Testing weight applied in F_z 139

Figure 4-39: Simulated high upper right cuspid 145

Figure 5-2: Sample 2D graph showing the different graph components 151

Figure 5-3: Sample 3D graph showing the different graph components 152

Figure 5-4: 0.014” NiTi, Fx Mesio-distal forces 95% confidence intervals 154

Figure 5-5: 0.014” Fx force on tooth #13 156

Figure 5-6: 3D 0.014” Fx graphs means EL, ASL and PSL brackets 159

Figure 5-7: 0.014” Fy Bucco-lingual forces 95% confidence intervals 161

Figure 5-8: 3D 0.014” Fy graphs means EL, ASL and PSL brackets 165

Figure 5-9: 0.014”Fz Occluso-gingival 95% confidence intervals.....................167

Figure 5-10: 0.014” Fz load deflection of tooth #15 and #11 showing the “W” pattern.168

Figure 5-11: 0.014” Fz force on tooth #13 170

Figure 5-12: 3D 0.014” Fz graphs, means EL, ASL and PSL brackets 172

Figure 5-13: 0.014” Mx Bucco-lingual crown torque, 95% confidence intervals 174

Figure 5-14: 3D 0.014” Mx Bucco-lingual crown torque graphs, means EL, ASL and PSL brackets 178

Figure 5-15: 0.014” My mesio-distal crown tip, 95% confidence intervals.....................180

Figure 5-16: 3D 0.014” My mesio-distal crown tip, graphs, means EL, ASL and PSL brackets.....................184

Figure 5-17: 0.014” Mz rotation around the long axis, 95% confidence intervals 186

Figure 5-18: 3D 0.014” Mz rotation around the long axis graphs, means EL, ASL and PSL brackets 190

Figure 5-19: 0.018” NiTi, Fx Mesio-distal forces 95% confidence intervals 192

Figure 5-20: 0.018” Fx force on tooth #13.....................195

Figure 5-21: 3D 0.018” Fx graphs means EL, ASL and PSL brackets.....................198

Figure 5-22: 0.018” Fy Bucco-lingual forces 95% confidence intervals 200

Figure 5-23: 3D 0.018” Fy graphs. Means EL, ASL and PSL brackets.....................204

Figure 5-24: 0.018” Fz Occluso-gingival 95% confidence intervals.....................206

Figure 5-25: 0.018” Fz load deflection of tooth #15 and #11showing the “W” pattern..207

Figure 5-26: 0.018” Fz force on tooth #13 209

Figure 5-27: 3D 0.018” Fz graphs. Means EL, ASL and PSL brackets.....................211

Figure 5-28: 0.018” Mx Bucco-lingual crown torque, 95% confidence intervals 213

Figure 5-29: 3D 0.018” Mx Bucco-lingual crown torque graphs, means EL, ASL and PSL brackets 217

Figure 5-30: 0.018" My mesio-distal crown tip, 95% confidence intervals 219

Figure 5-31: 3D 0.018" My mesio-distal crown tip, graphs, means EL, ASL and PSL brackets 223

Figure 5-32: 0.018" Mz rotation around the long axis, 95% confidence intervals 225

Figure 5-33: 3D 0.018" Mz rotation around the long axis graphs, means EL, ASL and PSL brackets 229

Figure 5-34: 0.014"x 0.025" NiTi, Fx Mesio-distal forces 95% confidence intervals 231

Figure 5-35: 0.014" x 0.025" Fx force on tooth #13 234

Figure 5-36: 3D 0.014" x 0.025" Fx graphs means EL, ASL and PSL brackets 236

Figure 5-37: 0.014"x 0.025" Fy Bucco-lingual forces 95% confidence intervals 238

Figure 5-38: 3D 0.014" x 0.025" Fy graphs means EL, ASL and PSL brackets 242

Figure 5-39: 0.014" x 0.025" Fz Occluso-gingival 95% confidence intervals 244

Figure 5-40: 0.014"x 0.025" Fz load deflection of tooth #15 and #11showing the "W" pattern 245

Figure 5-41: 14"x25" Fz force on tooth #13 247

Figure 5-42: 3D 0.014"x 0.025" Fz graphs, means EL, ASL and PSL brackets 249

Figure 5-43: 0.014"x 0.025" Mx Bucco-lingual crown torque, 95% confidence intervals 251

Figure 5-44: 3D 0.014"x 0.025" Mx Bucco-lingual crown torque graphs, means EL, ASL and PSL brackets 255

Figure 5-45: 0.014"x 0.025" My mesio-distal crown tip, 95% confidence intervals 257

Figure 5-46: 3D 0.014"x 0.025" My mesio-distal crown tip, graphs, means EL, ASL and PSL brackets 261

Figure 5-47: 0.014"x 0.025" Mz rotation around the long axis, 95% confidence intervals 263

Figure 5-48: 3D 0.014"x 0.025" Mz rotation around the long axis graphs, means EL, ASL and PSL brackets 267

Figure 5-49: 0.014" wire, Fx, Fy, Fz, Mx, My and Mz graphs 271

Figure 5-50: 0.018"wire, Fx, Fy, Fz, Mx, My and Mz graphs 278

Figure 5-51: 0.014"x 0.025" wire, Fx, Fy, Fz, Mx, My and Mz graphs 285

Figure 5-52: Standardized Fx graphs of 0.014", 0.018"and 0.014"x 0.025" NiTi wires.293

Figure 5-53: Standardized Fy graphs of 0.014", 0.018"and 0.014"x 0.025" NiTi wires.295

Figure 5-54: Standardized Fz graphs of 0.014", 0.018"and 0.014"x 0.025" NiTi wires.297

Figure 5-55: Standardized Mx graphs of 0.014, 0.018"and 0.014"x 0.025" NiTi wires..299

Figure 5-56: Standardized My graphs of 0.014", 018" and 0.014"x 0.025" NiTi wires..301

Figure 5-57: Standardized Mz graphs of 0.014", 0.018"and 0.014"x 0.025" NiTi wires 303

Figure 6-1: Example of five brackets, the middle bracket is out of alignment, aligning force F 320

Figure 6-3: two types of sliding in orthodontics..........322

Figure 8-1: 0.014" 1mm loading OSIM display..........342

Figure 8-2: 0.014" 2mm loading OSIM display..........343

Figure 8-3: 0.014" 3mm loading OSIM display..........344

Figure 8-4: 0.014" 4mm OSIM display..........345

Figure 8-5: 0.014" 3mm unloading OSIM display..........346

Figure 8-6: 0.014" 2mm unloading OSIM display..........347

Figure 8-7: 0.014" 1mm unloading OSIM display..........348

Figure 8-8: 0.018" 1mm loading OSIM display..........349

Figure 8-9: 0.018" 2mm loading OSIM display..........350

Figure 8-10: 0.018" 3mm loading OSIM display..........351

Figure 8-11: 0.018" 4mm OSIM display..........352

Figure 8-12: 0.018" 3mm unloading OSIM display..........353

Figure 8-13: 0.018" 2mm unloading OSIM display..........354

Figure 8-14: 0.018" 1mm unloading OSIM display..........355

Figure 8-15: 14x25 1mm loading OSIM display..........356

Figure 8-16: 14x25 2mm loading OSIM display..........357

Figure 8-17: 14x25 3mm OSIM display..........358

Figure 8-18: 14x25 2mm unloading OSIM display..........359

Figure 8-19: 14x25 1mm unloading OSIM display..........360

List of Tables

Table 2-1: Force system by class (^{3}) 21

Table 3-1: Maximum full-scale measurement uncertainties for Nano 17 transducer (error), (ATI Automation, NC)..64

Table 3-2: Sensing ranges and resolution of the sensor using a Data Acquisition Card (ATI automation, NC) 65

Table 3-3: Coefficient of variation, error analysis..73

Table 3-4: Repeated measures analysis of variance (pair-wise comparison) 78

Table 3-5: Descriptive statistics..79

Table 4-1: Maximum full-scale measurement uncertainties for Nano 17 transducer (error) (provided by the manufacturer, ATI automation, NC) 93

Table 4-2: sensitivity change sure to temperature change for the Nano17 (ATI Automation, NC)..96

Table 4-3: Tooth sizes (Burlington growth study) used for locating the application points in the OSIM device 105

Table 4-4: X, Y and Z coordinates of the points of application for maxillary arch relative to the OSIM global point of origin 107

Table 4-5: Sign convention 137

Table 4-6: Load cell force errors..142

Table 4-7: Load cell moment error..143

Table 5-1: Sign convention 150

Table 5-2: 0.014" wire Fx Force data at 1mm increments..155

Table 5-3: 0.014" wire Fy force data at 1mm increments..162

Table 5-4: 0.014" wire Fz force data at 1mm increments 169

Table 5-5: 0.014" wire Mx moment data at 1mm increments 175

Table 5-6: 0.014" wire My data at 1mm increments 181

Table 5-7: 0.014" wire Mz data at 1mm increments 187

Table 5-8: 0.018" wire Fx force data at 1mm increments..193

Table 5-9: 0.018" wire Fy force data at 1mm increments 201

Table 5-10: 0.018" wire Fz force data at 1mm increments 208

Table 5-11: 0.018" wire Mx moment data at 1mm increments 214

Table 5-12: 0.018" wire My moment data at 1mm increments 220

Table 5-13: 0.018" wire Mz moment data at 1mm increments 226

Table 5-14: 0.014" x 0.025" wire Fx force data at 1mm increments 232

Table 5-15: 0.014" x 0.025" wire Fy force data at 1mm increments 239

Table 5-16: 0.014" x 0.025" wire Fz force data at 1mm increments 246

Table 5-17: 0.014" x 0.025" wire Mx Moment data at 1mm increments 252

Table 5-18: 0.014" x 0.025" wire My moment data at 1mm increments 258

Table 5-19: 0.014"x 0.025" wire Mz moment data at 1mm increments 264

List of Equations

Equation 2-1: Calculation of the moment of a force 6

Equation 2-2: Friction 46

Equation 4-1: Error in the loaded axis 140

Equation 4-2 140

1 Chapter One: Introduction

Study of the biophysics of tooth movement can yield important information. If researchers and clinicians can quantify the force systems applied to the teeth, they can better understand clinical and histologic tooth responses. Therefore, in order to make valid judgments about the response of teeth to orthodontic forces, clinicians first must fully define the force systems acting on those teeth.

Many of the undesirable side effects that occur during orthodontic treatment can be attributed directly to a lack of understanding of the physics involved in a given adjustment of an orthodontic appliance. A large number of variables in orthodontic treatment are not within our control, such as growth and tissue response to appliances. However, the force placed on the tooth should be a controllable variable ([1]), and careful study of the physics underlying our clinical application, can help in reducing those undesirable side effects.

Orthodontic force systems that result from the continuous arch technique used in everyday orthodontic mechanics are considered indeterminate force systems, in other words, there are too many unknowns to determine the different components of these force systems. Force system measurements have been made on one or two tooth models, however in order for us to understand the orthodontic force systems we need to simultaneously, measure in 3D, the forces being applied on every tooth in the dental arch. Until recently, much of the literature was restricted to experimental two-dimensional analyses of the biomechanical aspects of orthodontic force systems, and computer modeling of three-dimensional analyses. Very little evidence exists in the literature regarding three dimensional experimental measurement and analysis of orthodontic force systems ([2]). This is partly due to the problem inherent in studying the response of a tooth subjected to a force system, which is much more complex and difficult to solve than those of simple measurements of forces. A tooth's response to a force can be studied at three levels: the clinical level, the cellular and biochemical level, and the stress-strain level. The clinical level allows the study of phenomena such as the rate of tooth movement, pain response, and tooth mobility. The cellular level gives insight into the dynamics of the biology of tooth movement and the dynamics of bone and connective tissue. The ability to determine the level of stress in different areas of the PDL, which is the most important and least understood stress strain level, may well offer the best means of correlating the application of force on a tooth with the tooth's response ([3]).

With the very recent technological advances in force/torque sensors technology, data acquisition and data representation, it became possible to measure those forces and reveal the force systems we are applying to the dentition. The purpose of this PhD research study is the design and construction of an experimental device that is capable of revealing the details of the force systems used in modern day orthodontic mechano-therapy of continuous arch technique.

2 Chapter two: Literature review

2.1 Principles of Biomechanics

2.1.1 Force

A "force" is an action that changes, or tends to change the state of motion or the internal state of stress of the body upon which it acts. It is a vector quantity that can be represented either mathematically or graphically. A complete description of a force must include its magnitude, direction and point of application. The magnitude in orthodontics is traditionally expressed in the units of grams (gm), however the correct unit to be used is Newtons (N), the conversion factor from grams to Newtons is 1 gm = 0.00981 N or 1 N = 101.9716 gm. The direction of a force is discerned by observing the line of action of the vector of the force. The point of application is the exact location of the application of a force on a body.

Teeth are often acted upon by more than one force. Since the movement of a tooth is determined by the net effect of all forces on it, it is necessary to combine applied forces to determine a single net force. Alternatively, there may be a force on a tooth that we wish to break up into components, that are parallel and perpendicular to one plane of reference, in order to determine the magnitude of force in each of these directions ([2]).

2.1.2 Moment

The Moment of a force is a measure of its tendency to cause a body to rotate about a specific point or axis. This is different from the tendency for a body to move, or translate, in the direction of the force. In order for a body to rotate, the force must act upon the body so that it does not pass through the center of mass of the body. The moment of any force can be calculated at any point within the body. The body will not rotate if the sum of moments on the center of mass is zero.

The moment arm or lever arm is the perpendicular distance between the line of action of the force and the point about which the moment is determined. Therefore, the magnitude of the moment of force acting about a point or an axis, is directly proportional to the distance of the force's line of action from the point or axis. It is defined as the product of the force (F) and the moment arm (d). A moment is expressed in units of Newton-millimetres. A moment also has a sense; it is either clockwise or counter-clockwise, which applies only in two dimensions, in 3D the moment is presented as a vector. The most common way to express a moment is

$$\boldsymbol{Moment} = \boldsymbol{Force} \times \boldsymbol{Distance}$$

Equation 2-1: Calculation of the moment of a force

The moment of a force taken about any point that lies on its own line of action is zero. The moment of several forces about a point is simply the algebraic sum of their component moments about the same point.

It is clear that a moment at the center of mass of a free body depends upon the relationship of the line of action of the force to the center of mass. However teeth present an additional complication, they are not free to move in response to a force, they are restrained by the periodontal structures which are not uniform around the tooth ([2]). In a restrained body such as a tooth, a point analogous to the center of mass is used, this is called the center of resistance ([4,5,6]). In orthodontics, a moment is a measure of the tendency of the tooth to rotate, this tendency is produced by two ways. First, if a single force is applied and does not act through the center of resistance of the tooth, this moment, the moment of force, is quantitatively equal to the magnitude of the applied force multiplied by the perpendicular distance between the line of the applied force and center of resistance (Equation 2-1). Second, a moment can also be applied through a couple,

2.1.3 Couples

A special case of moments is a couple. A couple consists of two parallel forces that are equal in magnitude, opposite in sense and do not share a line of action. It does not produce any translation, only rotation ([2]). The resultant force of a couple is zero. But, the resultant of a couple is not zero; it is a pure moment. The moment of a couple is the product of the magnitude of one of the forces and the perpendicular distance between their lines of action.

The magnitude of the couple is independent of the reference point and its tendency to create a rotation will remain constant. The resultant of a number of couples sharing the same axis direction is their algebraic sum. A couple cannot be put in equilibrium by a single force. A couple can only be put in equilibrium, by a moment or another couple of equal magnitude and opposite direction anywhere in the same plane or in a parallel plane. It does not matter where a couple is applied to an object, the net effect is a moment equal to the magnitude of one of the forces multiplied by the distance between them (^{2}). The couple is a free vector, in the sense that the couple's tendency to cause rotation is independent of the point of application of the couple.

2.2 Orthodontic mechanical concepts

2.2.1 Centre of resistance

In orthodontics, the center of resistance is conceptually similar to the center of mass. It is the point on the tooth where a single applied external force would produce translation, i.e. all points within that tooth moving in parallel, straight lines, parallel to the line of action of the force. This type of movement is referred to in orthodontics as bodily movement ([6,7]). The location of the center of resistance is dependent on the root length, number, attachment, morphology, level of alveolar bone height and crown size ([8,9,10]).

When a force does not act through the center of resistance, it causes the tooth to simultaneously translate and rotate. Rotation is movement of a body whereby no two points on the body move in the same direction. When a moment results from a force that does not pass through the center of resistance, it is called "Moment of Force". When the moment is the result of a couple, it is called "Moment of Couple". Since brackets attach to the crowns not the roots, limited opportunities exist in orthodontics where it is possible to apply a force at a bracket that also acts through the tooth's center of resistance. Burstone and coworkers ([7]) studied the location of center of resistance. First in 1969, they reported that the center of resistance of a central incisor is at a point apical of the alveolar crest by 40% of the distance measured between the alveolar crest and the apex of the root. This conclusion was based on the assumption that the shape of a single rooted tooth approaches that of a parabola. The center of resistance of anterior teeth was reported at one third to one-half the root length as measured apically from the alveolar crest, whereas for posterior teeth it is located 0.3 to 0.4 the distance from the alveolar crest to the apex of the root (5,6,11). Nagerl, using an experimental model reported that the centers of resistance varied according to the transverse direction of the loading (12). Yoshida found that the location of the center of resistance depended more on the palatal bone height and very little on the labial bone height (13). In addition, he confirmed the earlier finding that the center of resistance is located 1/3 the alveolar bone height measured from the alveolar crest. Tanne *et. al.* (4,5) used laser holography and found the center of resistance to be 9.9 mm apical to the bracket of a central incisor and 1/3 of the root length measured apically from the alveolar crest.

2.2.2 Centre of rotation

Orthodontic tooth movement is generally described as tipping, bodily movement and root movement. The point of application of the force is an important determinant of the center of rotation; by varying the location of the point of application occluso-apically, we can alter the position of the center of rotation. Another way to alter the position of the center of rotation is what most multibanded appliance techniques employ, which is the application of a force and a moment (couple) at the bracket counteracting the moment of the force (Figure 2-2) (5).

A single force acting through the center of resistance of the tooth can produce translation or bodily tooth movement where the center of rotation is at infinity. If a couple is placed anywhere on a tooth the center of rotation is created near the tooth's center of resistance only if the tooth is considered as a free body, in fixed orthodontic appliances the center of rotation resulting from the couple is more likely to be the midpoint of the bracket. Unlike pure translation, pure rotation does not produce a uniform stress distribution in the PDL, but rather a uniformly varying distribution, with the highest stress at the root apex and the next highest at the alveolar crest ([2]). No stress can be found on the center of rotation, which is located at the level of the root where the stress is zero. Pure translation (center of rotation at infinity) and pure rotation (center of rotation near the center of resistance) can be considered the two basic types of tooth movement.

Other locations of the center of rotation can be created by combining pure rotation and pure translation, in other words, any center of rotation can be produced by combining a single force through the center of resistance of the tooth, and a couple if a proper force/couple ratio is used ([14]). Hence, control of the center of rotation during tooth movement is based on two components. First, placement of a single force through the tooth's center of resistance and second, use of a couple of proper direction and magnitude that counteracts the moment of the force ([14,15]). The location of the center of rotation is a function of the distance between the point of application and the center of resistance, which is equivalent to the Moment to Force ratio. The center of rotation can be very close but it can never reach the center of resistance, except when only a couple is applied on a single unrestrained tooth.

2.2.3 Moment of couple to moment of force ratio (Mc/Mf)

When a force and a couple are being applied, the type of tooth movement is determined by the ratio (Mc/Mf) between the applied moment (Mc) of a couple and the applied moment (Mf) of the force ([4,11,13,16]). If orthodontic brackets are subjected to pure forces in the absence of moments the result will be uncontrolled tipping of the teeth, since the moment of couple/moment of force ratios (Mc/Mf) equals zero (Figure 2-1). The centers of rotation are presumed to be just apical to the centers of resistance for teeth with Mc/Mf ratios equivalent to zero (Mc = 0) ([15]). However, if the Mc/Mf ratio is increased through the application of (couples) moments, the centers of rotation may move apically, increasing the potential for translatory tooth movements.

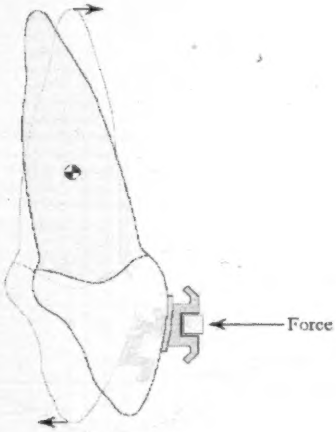

Figure 2-1: Rotation about the center of rotation caused by the application of a pure force in the absence of a moment; where the Mc/Mf ratio is zero (uncontrolled tipping)

Pure bodily tooth movements occur if the Mc/Mf ratio equals one, in other words the moment of the couple is equal in magnitude and opposite in direction to the moment of force, yielding a net moment of zero at the center of resistance of the tooth ([2]) (Figure 2-2). Bodily movement implies that the center of rotation is located at infinity from the centers of resistance. If the applied moment of a couple exceeds the moment of the force, the M/F ratios will surpass the proportional (finite) values. In these instances, the centers of rotation are located occlusal to the centers of resistance, allowing root movements to exceed those of the crowns ([2,11,16]).

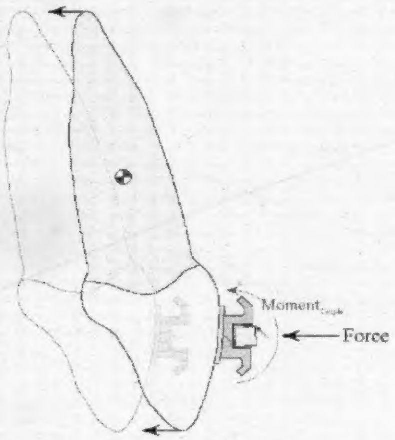

Figure 2-2: Translation tooth movement, through the simultaneous application of a force and a moment of a couple at the bracket; where the Mc/Mf ratio equals 1

Despite the fact that the concept of moment to force ratio and its effect on the center of rotation has been extensively studied in orthodontic literature, it is limited in its applicability in orthodontic everyday practice. The concept of moment to force ratio is only applicable when considering a single tooth in two dimensions. In other words this concept is no longer useful when we consider two or more teeth attached to a wire, therefore in multibanded orthodontic appliances using the continuous arch technique the concept of moment to force ratio is of no value.

2.3 Biological Response to Forces

When forces are applied to the teeth, the crowns are instantaneously (elastically) displaced 60-80 micrometers in the direction of the forces ([17,18]). Movements arise primarily from compression of the periodontal ligaments and secondarily from deformation of the alveolar bone ([19]). If forces are sustained in sufficient intensity and duration, a delayed metabolic response will induce remodeling of the surrounding bone ([14]). It has been suggested that initiation of bone remodeling was related to force magnitude, peaking at optimal ranges while displaying lower responses at excessive or inadequate levels. Recently, investigators have determined that the rates of tooth movement are dependent on force magnitudes, where heightened rates of movement are proportional to the applied forces, up to a point after which an increase in stress causes no increase in the rate of tooth movement ([20,21,22]). Forces applied to the teeth may be classified as continuous or intermittent. Investigators have demonstrated that sustained "continuous" light forces are those that produce tooth movements most efficiently ([18,23]). By using orthodontic appliances, clinicians can manipulate forces and moments imposed upon the teeth, thus controlling the rate, pattern and direction of tooth movement.

2.3.1 Physiological Stress of the Periodontium

In contemporary orthodontics, physiological tooth movement may be explained by many theories, one of which is the pressure-tension hypothesis. This theory stipulates that in response to forces, areas of the periodontal ligament encountering pressure will experience bone resorption, whereas areas sustaining tension will undergo deposition ([24,25]). Large variations in root morphologies may elicit different biological responses to forces of similar magnitudes, thus the concept of periodontal ligament stress has emerged as part of the understanding of orthodontic tooth movement ([26]). Schwarz (1932) first determined that stress levels of 20-26 g/cm^2 were sufficient to produce movement of the teeth. Since that time, no consensus has been reached with respect to the optimum stresses required for tooth movement ([20,27,28,29,30]). Recently, using a canine model, Pilon *et al* ([22]) demonstrated that rates of tooth movement were not significantly different for applied stress levels that ranged from 100 g/cm^2 to 400 g/cm^2.

2.3.2 Optimum Orthodontic forces

There is conflicting evidence in the literature concerning the force level that results in optimal tooth movement. The optimal orthodontic force is related to the root surface area, and mechanical and biological properties of the periodontal ligament ([17,31]). The current concept of optimal force is based on the hypothesis that a force of a certain magnitude and temporal characteristics (continuous Vs intermittent, constant Vs declining) would be capable of producing a maximum rate of tooth movement, without tissue damage and with maximum patient comfort. Optimum force may differ for each individual and for different teeth within the same individual, which makes the objective of identifying the optimum orthodontic force very complicated ([15]). The forces applied to the crowns of the teeth, are distributed over the entire supporting structure and so are the stresses and strains. From a cellular point of view the distribution of stress (force per unit area), distortion of the periodontal ligament (strain), and bone deformation (strain) are critical factors ([32]). The Orthodontic force as an extrinsic mechanical stimulus starts a biological cellular response that aims to restore equilibrium by remodeling of the periodontal supporting tissues ([33]).

A recent study by Ren *et al.* showed that there are large variations in current literature; they were unable to find definitive evidence regarding the optimal force level for orthodontic tooth movement ([34]).

From a clinical viewpoint, two major problems related to tooth movement can be considered. The first is the problem of identifying the optimal force magnitudes for tooth movement, it is not possible at the time due to the lack of evidence to determine the optimum force magnitude. The second problem is identifying the type of force system required to produce a desired movement. The force systems resulting from the continuous arch technique are unknown to us, again due to the lack of evidence. This PhD research project is aimed at understanding the nature of these complicated force systems.

2.4 Orthodontic Force systems

2.4.1 Force system from an ideal arch

When an archwire is placed in the mouth a complicated set of forces is produced at each tooth. These force systems are very complicated to describe, since the situation is statically indeterminate, in other words, there are too many unknowns to calculate the forces using the laws of statics ([3,35]). In order to have a better understanding of the force systems that are generated on each tooth in an ideal arch, Burstone and Koenig studied the force systems in one plane of space (sagittal only) of two tooth segments by summing series of two tooth force systems. In a situation of two tooth segment the wire will apply a force and a moment at each bracket. They concluded that only if the geometry of the attachments on the teeth is accurately described (Figure 2-3), can we determine the force system acting on those attachments ([3,35]). And they identified six different arrangements that produce distinctly different force systems (Figure 2-4), and described the force systems of each resulting tooth configuration very broad terms (Table 2-1). The arrangements differed in the angulations of the two teeth as well as the directions of those angulations. One of the main conclusions of Burstone and Koeing was that the relative magnitude of the moments depends exclusively on the ratio of angulation of each bracket to the interbracket axis (θ_A/θ_B). They reported a predictable ratio of the moments produced between two adjacent brackets which remained constant regardless of the interbracket distance or the cross section of the wire used. They concluded that very small changes in the ratio between θ_A/θ_B can readily alter the force system. (3,35,36).

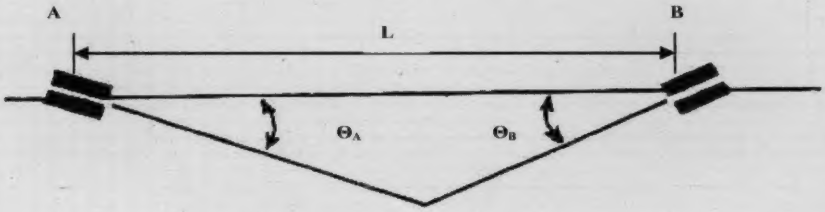

Figure 2-3: wire attachment geometry defined by the inter bracket distance (L) and the angles of the brackets at position A and B (θ_A and θ_B) (3)

CLASS:	I	II	III	IV	V	VI
$\frac{\theta_A}{\theta_B}$	1.0	0.5	0	-0.5	-0.75	-1.0
LOWER LEFT QUADRANT	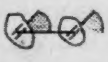	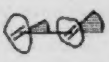	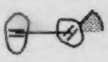	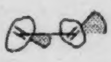	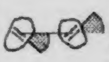	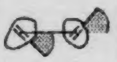

Figure 2-4: Six basic geometries based on the ratio θ_A / θ_B. Classes are independent of interbracket distance (3)

Class	I	II	III	IV	V	VI
θ_A / θ_B	1.0	0.5	0	-0.5	-0.75	-1.0
M_A / M_B	1.0	0.8	0.5	0	-0.4	-1.0
Force system at wire	↑ ↓ ↺ ↺	↑ ↓ ↺ ↺	↑ ↓ ↺ ↺	↑ ↓ ↺	↑ ↓ ↻ ↺	↻ ↺
Force system on tooth	↓ ↑ ↻ ↻	↓ ↑ ↻ ↻	↓ ↑ ↻ ↻	↓ ↑ ↻	↓ ↑ ↺ ↻	↺ ↻

Table 2-1: Force system by class (3)

However in the previous study the authors analyzed the force system on the two tooth segment in one plane only. Adding more teeth to those segments will undoubtedly alter the force systems, and the position of the teeth within the curvature of the dental archform is bound to have an effect on the force system. Therefore, three dimensional measurements of the force system on all teeth in the dental arch is the only way to understand these complex force systems.

2.4.2 V-Bends

The forces developed when a straight wire is engaged are determined by the relationship between the bracket of the individual tooth and the wire (37). The V bend has many names, depending on its purpose and its position. Between the incisors it is called an "Artistic Bend", in the canine region it is called a "gable bend", and anterior to molars depending on the orientation, a "tip back bend" or a "toe in bend" (37). Burstone and Koeing in another classic paper about the proper wire bending in clinical applications studied the force systems produced by step bends and V- bends acting on two tooth segments, using an analytic technique. They found that a step bend between two brackets would produce unidirectional couples of equal magnitude and horizontal or vertical forces, depending upon the plane of activation (Figure 2-5). In addition, they found that the mesiodistal position of the step bend does not alter the force system appreciably.(38)

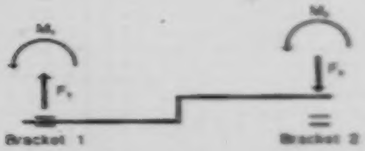

Figure 2-5: forces and moments produced by a step bend in a wire (38)

On the other hand they reported that the force system produced by a V bend depended on the mesiodistal position of the apex of the bend (Figure 2-6). When the apex of the V-bend is centered between the two brackets (a/L = 0.5, Figure 2-6) the moments at each bracket are equal and opposite in direction. As the bend is moved to the left towards bracket 1 the ratio will change (a/L is 0.4, M_2/M_1 becomes 0.3). The moments at the brackets are unequal, with the moment furthest away from the V bend being one-third the magnitude of the other moment. As the V-bend is moved further towards bracket 1 and a/L becomes 0.33, then no moment whatsoever is found at bracket 2. Finally if the bend is moved farther towards bracket 1 and a/L becomes 0.2, the moment at bracket 1 becomes one third of bracket 2 and both moments are in the same direction. Figure 2-7 demonstrates the application of V bend variations and resultant force system. These fundamental relationships according to Burstone hold true regardless of the interbracket distance. As the a/L ratio changes, so does the magnitude of the force. When the V bend is centered, equal and opposite couples are produced and hence there is no vertical force. As the V bend is moved towards bracket 1, the force increases in a Non-linear manner (37,38).

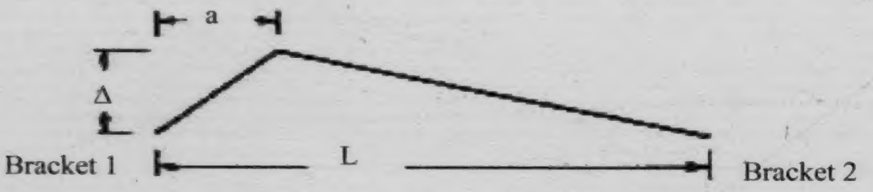

Figure 2-6: geometry of a V bend (38)

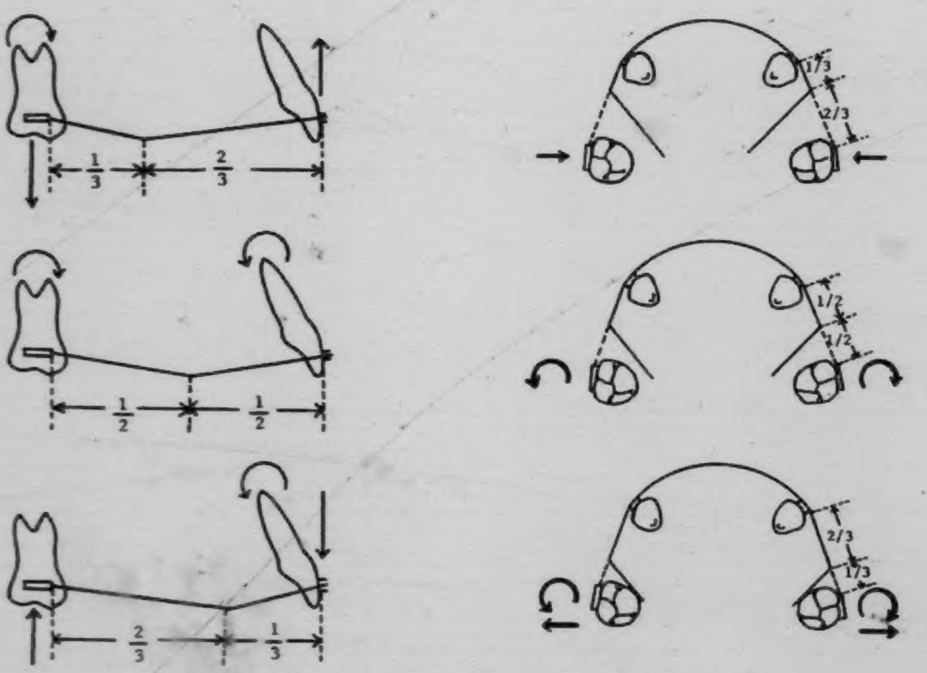

Figure 2-7: Mesiodistal placement of the apex of the V bend in two planes of space (38)

When a V bend is placed between the two centrals the result is equal and opposite moments. This is shown as the block A of the diagram (Figure 2-8). A step bend (second order bend) between the central and the lateral incisor will result in unidirectional moments and vertical forces shown in block B of the diagram (Figure 2-8). The total force system is quite complex, with moments on all the incisors tending to move the roots distally more on the centrals than on the laterals. There are intrusive forces on the lateral incisors and extrusive forces on the centrals (37,38).

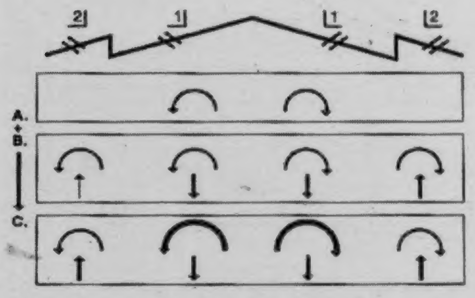

Figure 2-8: force systems produced by anterior Vbends. A, V bend between central incisors gives equal and opposite couples. B, step bends between central and lateral incisors give vertical forces and unidirectional couples. C, Summation of A and B. (38)

Burstone, coworkers, and many others, studied those bends ignoring the play present within the brackets, the bracket wire interface plays a significant role in determining the eventual force system acting on the teeth. Moreover, all the previous studies lack the potential for clinical applicability because these studies are focused on two dimensional force systems of two tooth segments, rendering the application of their findings to three dimensional force systems of three or more teeth severely limited. There need to be experimental validations and further investigations of the nature of the resulting force systems in three dimensions when all teeth in the dental arch are included in those applications mentioned above.

2.5 The Edgewise Appliance

2.5.1 Development of the Edgewise Appliance

Edward H. Angle introduced the edgewise orthodontic appliance in 1928. Unlike previous removable appliances that could only produce simple tipping movements, the edgewise design permitted control over tooth position in three dimensions ([15]). The edgewise system used attachments with rectangular slots that were fastened to the teeth with formable metal bands. The attachments were machine milled to internal dimensions of 0.022 inches in height and 0.028 inches in depth. These components were soldered onto the bands, then shaped and cemented to teeth. Archwires were fabricated by drawing bar stock though mandrels of various shapes and sizes. The largest dimension archwire produced was 0.022 inches by 0.028 inches, to engage the walls of the bracket slot. Activation of the appliance was accomplished by contouring wires to the dental arches and then engaging them into each attachment with stainless steel ligation wires. In this configuration, the clinician could precisely control crown and root position. Although considered as the mainstay of multi-banded fixed appliance therapy, the edgewise design had many disadvantages. Band fitting was often time consuming and caused discomfort to the patient during placement. Final occlusion could only be achieved by placing compensatory bends in the archwire due to the orthogonal orientation of the attachment slots. Interproximal space closure caused from the interposed band material was often necessary after appliance removal.

2.5.2 Modifications of Edgewise Appliances

Cecil C. Steiner in 1953 revised Angle's design by reintroducing an attachment with a slot dimension of 0.018"inches by 0.028 inches. Steiner demonstrated that smaller dimension archwires could elicit similar tooth movement without the discomfort experienced by patients upon whom Angle's full dimension edgewise appliances were used. Thereafter, development of epoxy adhesives in the 1960s permitted orthodontic bands to be replaced by bondable attachments. Initially limited by bond failures, bonded brackets eliminated many shortcomings of banded appliances. It enhanced esthetics, improved oral hygiene, caused less gingival irritation and eliminated the need to close interproximal spaces. Improving upon the edgewise appliance further, Lawrence F. Andrews introduced the straight wire appliance in 1974 ([39]). This system minimized the need for wire bending by incorporating specific angulations directly into the bracket bases. Values for first, second and third order dimensions were derived from the study casts of 120 untreated patients whom were deemed to have ideal occlusions. These specific dimensions are referred to as the Andrew's prescription, and are still a popular part of clinical orthodontics. The use of the straight wire system reduced treatment time and obtained more idealized tooth positions. Shortly after the introduction of the straight wire appliance, investigators began modifying Andrew's prescription in order to improve root parallelism, crown angulations and occlusal contact patterns. Many of these prescriptions have remained in orthodontics, and are named after their developers ([39,40,41,42,43,44,45]).

2.5.3 Materials of Modern Edgewise Appliances

Most metallic attachments are made from AISI 300 series stainless steels (303, 304, 304L, 316, 316L, 317) and AISI 600 (17-4 PH, 17-7 PH), others are made from titanium alloys. Stainless steel contain approximately 16-18% chromium and 8-10% nickel. Chromium furnishes the steel with its resistance to corrosion, whereas nickel acts as a stabilizing element that maintains the austenite phase at room temperature. Other alloying elements are added to the base composition to provide the steels with different material properties. Some of the alloying elements include manganese, silicon, phosphorus, sulfur, and molybdenum. The characteristics that are provided by these elements, and the biocompatibility of this series of stainless steels, make them very suitable for the fabrication of orthodontic appliances. Orthodontic brackets are fabricated by sintering, casting or metal injection molding.

The engineering of nickel-titanium (NiTi) alloys has made remarkable progress since the original work at the Naval Ordinance Laboratory in the early 1960s. An ideal NiTi wire should retain a stable predesigned archform at mouth temperature and yet be formable at lower room temperatures. In other words, it should be possible to engage the wire into the brackets during a reasonable time interval, and only later should the wire recover its ideal arch form and apply light, predictable, constant, and continuous force to the dentoalveolar structures ([46]). Superelasticity is determined by the typical crystallographic characteristics of NiTi; the lattice of the alloy can be present in 2 phases: martensite and austenite. In the martensitic phase, the lattice is body-centered (cubic or tetragonal); in the austenitic phase, it is face-centered (hexagonal close packed). In response to temperature or stress variations, the crystal structure undergoes deformations in which the molecular arrangement is modified without a change of the atomic composition. The alloys essentially undergo a reorganization to meet the new environmental conditions ([47,48]). The transformation from the austenitic to the martensitic phase (thermoelastic martensitic transformation) is reversible. At lower temperatures, the alloy is completely present in the martensitic phase until the increase in temperature causes the progressive transformation into austenite. An interesting feature of these thermoelastic alloys, is the so-called shape memory effect, which has remarkable clinical applications, the wire in the austenitic phase is able to "memorize" a preformed shape, including specific orthodontic archforms. By lowering the temperature, the alloy is transformed into martensite and becomes pliable and easily deformed. However, every time the temperature rises, the wire will remember and recover the ideal archform. The technical name of the phenomenon is one-way shape memory effect.

The superelasticity of NiTi wires is correlated to the coexistence of the 2 phases, the austenitic phase of a superelastic wire is stiffer than the martensitic phase, but both are stiffer than a superelastic wire in phase transition, when both crystalline structures (austenitic and martensitic) exist. This happens with the application of stress on the austenitic wire which causes a deflection that generates a local martensitic transformation and produces stress-induced martensite (SIM). However, the SIM is unstable, and if the wire is maintained at oral temperature it undergoes reverse transformation to the austenitic phase as soon as the stress is removed. In orthodontic clinical applications, SIM forms where the wire is tied to brackets on misaligned teeth so that the wire becomes noticeably pliable in the deflected areas. In those areas, the wire will be superelastic and the load-deflection curve will show a superelastic plateau (Figure 2-9), where the increase in strain does not produce a proportional increase in stress.

When the alloy is completely transformed into austenite, the stress-strain curve follows the regular pattern of other alloys, such as stainless steel, with a direct proportionality between applied stress and resulting strain and basically lacking the typical superelastic plateau. For NiTi orthodontic alloys, austenite is the prevalent phase intraorally, while only a small percentage of martensite is present in the grain structure. This property, termed pseudoelasticity, can be considered a localized stress-related superelastic phenomenon. ([49,50,51]) The pseudoelastic (stress-related) and thermoelastic (temperature-related) behaviors of NiTi alloys are more complex and interdependent than expected ([52,53]).

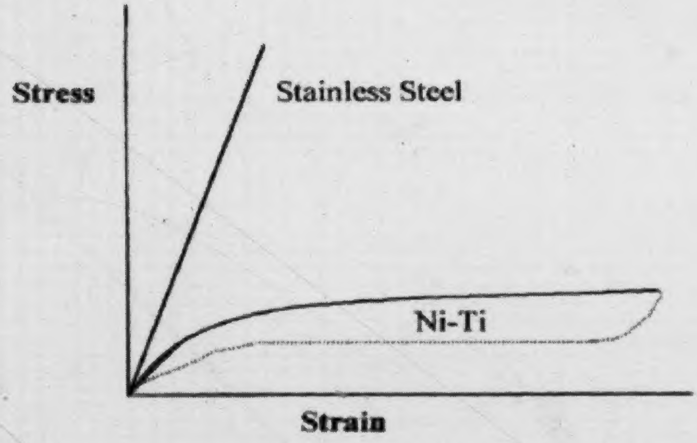

Figure 2-9: Typical load-deflection curve of superelastic NiTi

2.6 Torque

Three-dimensional control of tooth movement is generally accepted to be the strongest attribute of Angle's edgewise appliance. After being first described in 1928, orthodontists have repeatedly modified Angle's design to optimize third order tooth positions ([40,41,43,44,45,54]). Many orthodontists believed that labiolingual inclinations of maxillary and mandibular incisors are the critical determinants of pleasing dental esthetics, intra-arch occlusion and orthodontic stability ([15]).

Placing a rectangular archwire in a rectangular attachment slot makes third order control possible in contemporary fixed appliances. Brackets deliver forces and moments from the archwire to the teeth causing physiologic tooth movement. In this section, our emphasis will be on third order tooth movement, or what is clinically referred to as "torque".

Theoretical third order forces and moments can be calculated from the nominal dimensions of archwires and brackets outlined by the manufacturers, where deviations may be attributed to intrinsic variations in archwire cross-sectional diameters ([55,56,57,58]), bracket slot dimensions ([56,58,59,60]), archwire edge beveling ([60,61]), compounding second order moments ([62]) and bracket deformations ([63,64]). Extraneous factors also influence third order moments, including bracket placement errors ([65]) and irregularities in tooth morphology ([66,67]).

2.6.1 Third order moments

Third order tooth movements describe any longitudinal tooth displacements in the labiolingual direction (68). Failure to control incisor inclinations during orthodontic treatment may lead to excessive uprighting of the teeth; jeopardizing esthetics, occlusion and stability (2,69). To preserve root inclinations of the incisors during retraction, the force systems at each bracket must then be equivalent to forces with no moments at their centers of resistance (2,7,70,71). To satisfy this condition, third order couples must be added at each of the brackets to produce counter acting moments equal in magnitude but opposite in direction to the force induced moments (Figure 2-10). Such added moment of a couple is commonly termed 'labiolingual torque'. The principal advantage of edgewise appliances are that they permit clinicians to apply torques to the teeth by placing activated rectangular archwires into rectangular bracket slots (72,73,74).

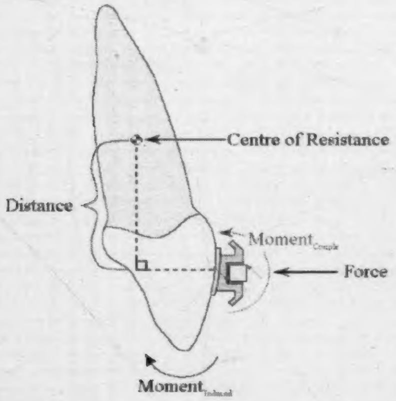
Centre of Resistance
Distance
$\text{Moment}_{\text{Couple}}$
Force
$\text{Moment}_{\text{Induced}}$

Figure 2-10: Third order couple is added at the bracket to produce a counter acting moment that is equal in magnitude but opposite in direction to the force induced moment.

2.6.2 Factors Contributing to Losses in Third Order Movements

2.6.2.1 Third Order Deviation Angles

Most orthodontic treatments are undertaken with archwires that are slightly smaller than the bracket slots. Tolerances for appliances are normally manifested as reduced archwire dimensions and increased slot dimensions ([75]). Failure of the archwires to fully occupy the bracket slots, may compromise the control offered between the archwire and bracket slot ([60,76]). When rectangular archwires are axially rotated within the bracket slots, the wires will rotate freely until their corners engage the walls of the slots. The amount of angular rotations that wires must acquire until contact is made, are entitled "deviation angles" or "torsional play" (Figure 2-11).

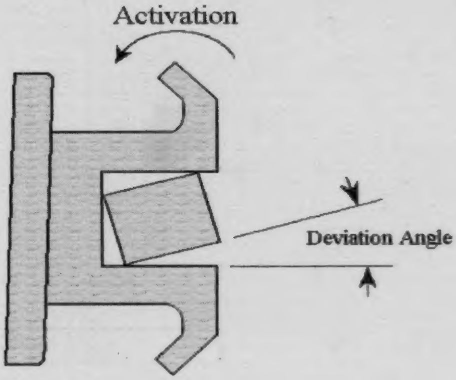

Figure 2-11: Deviation angle: Measurement of the amount of axial rotation that the archwire must rotate within the bracket slot until contact is made between the edges of the archwire and the walls of the bracket slot.

When archwires rotate past such threshold deviation angles, the applied stress will be transmitted through the attachments to the periodontal ligaments of the teeth thereby inducing third order movements. Activations of wires below these angles result in the absence of tooth movement. Although orthodontists generally acknowledge the presence of torsional play, many are unaware of their absolute magnitudes and their variability ([55,56,57,61]). Understanding these values is therefore critical, to evaluate the detriments imposed upon accurate tooth placements encountered during orthodontic treatment.

Based on a theoretical model, Dellinger ([77]) in 1978 calculated deviation angles of 1.5° to 9.6° and 0.66° to 18.9°, for 0.018"and 0.022 inch edgewise brackets, engaged by archwires of nominal dimensions. Schwaniger described a range of 0° to 15° for deviations of 0.019x0.025" inch wires in standard

0.022 inch slots (78), whereas Creekmore (79) in 1979 demonstrated angular deviations of 2.0° to 16.7° and 1.0° to 27.4°, for appliances of comparable specifications. These findings were in close agreement with those from Hocevar (80,81) in 1981, who later found deviations of 15°, 17.5°, 20° and 25° for 0.019x0.025, 0.020x0.016, 0.019x0.026 and 0.017x0.025" stainless steel wires in 0.022x0.028 inch standard edgewise brackets. Assessing rotational magnitudes of rectangular wires in vitro, Raphael *et al.*, (82) and Lang *et al.*, (69) demonstrated similar trends with the twisting of archwires in molar buccal tubes. However, it has since been shown that deviation angles are affected not only by variations in the dimensions of archwires and bracket slots, but also by archwire edge beveling (55,57). As a result, deviation angles encountered in laboratory and clinical settings are always much larger than those calculated from theoretical models.

2.6.2.2 Dimensional Variations of Orthodontic Archwires

Clinicians often assume that wire and bracket slot tolerances are those stated by manufacturers (72). As variations in nominal dimensions are encountered amongst all orthodontic appliances, orthodontists should have a working knowledge about the accuracy of appliance dimensions prescribed for a particular malocclusion, so that optimal moments of torque can be delivered to induce the required tooth movements. Variance in archwire dimensions may be multi-factorial in origin, arising from inconsistencies during appliance fabrication or from defects within the constituent metals. Although manufacturers generally fail to state the tolerances for archwires in product brochures, their dimensions are within 0.00025-0.0005 inches of the stated values ([57,77]). If archwires of reduced nominal dimensions are engaged into attachment slots, the resulting deviation angles may be greater than those of idealized bracket/wire combinations. As these effects are generally attributed to less wire material filling the slot space, more rotation by the archwire may be necessary to facilitate slot engagement. The magnitudes of these deviation angles may vary with the tolerances of the wires, but they generally follow the trend of inverse proportionality where, wires with smaller nominal dimensions will elicit larger increments of angular deviation. Therefore, in order to sustain particular moments of torque with nominally reduced wires, larger increments of activation may be imperative. Analyzing the effects of archwires with reduced dimensions, Dellinger ([77]) calculated theoretical deviation angles that could be attained by wires with tolerances of ±0.0005 inches. This investigation revealed increases of 26.2% to 79.4% and 1.8% to 204.5% in angular deviations, using respectively 0.018"inch and 0.022 inch edgewise brackets with common sized archwires. Other researchers have investigated the effects of reduced wire dimensions on deviation angles and third order moments ([55,56,57,61,62]). These studies each demonstrated similar findings to those of Dellinger, who found archwires of reduced dimensions, gave larger deviation angles and therefore smaller moments of torque. Thus, the actual dimensions of archwires are important, since the derived torques will be less than those derived from wires of nominal dimensions.

2.6.2.3 Dimensional Variations of Orthodontic Brackets

Analogous to dimensional variations sustained by archwires, orthodontic brackets also possess tolerances that affect their respective clinical performances. For example, bracket bodies are generally fabricated by casting, forging or metal injection molding processes ([64]). These processes create slot tolerances of ±0.0003 inches, torque angle tolerances of ±1.0° and in-out tolerances of ±0.001 inches. To enhance clinical and mechanical efficiency of their bracket systems, manufactures purposely develop slot dimensions greater than stated nominal dimensions ([14]). For example, Creekmore ([79]) first assessed the effects of bracket slots with larger tolerances on deviation angles through specific increments of activation. For ideal archwires (0.016x0.016 inches through full dimension), Creekmore revealed ranges of torsional play for 0.01845 inch and 0.02225 inch slot brackets (±0.00025) to be 2.0° to 16.7 ° and 1.0 ° to 27.4 °, respectively. Comparable investigation by Odegaard *et al* ([55]) and Meling *et al* ([56,57,61]), accounted for statistically significant variations in bracket slot dimensions relative to their torsional efficiencies. These studies were in agreement with Creekmore, verifying contributions of larger slot dimensions to heightened angular deviations, and thus diminished moments of torque.

2.6.2.4 Edge Beveling of Orthodontic Archwires

Rather than being drawn through dies, rectangular archwires are fabricated from round stock by rolling. This process creates wires with beveled (rounded) edges. Although not generally stated by manufacturers, the radii of these edges vary by $2\text{-}4\text{x}10^{-6}$ inches ([14]). Relative to archwires without beveling, wires with rounded corners require larger labiolingual torques to produce moments of similar magnitudes. Beveled edges therefore become critical factors during third order tooth movements, since the reduced diagonal dimensions of beveled archwires require heightened angles of engagement relative to idealized wires (55,58,60,61,82). Analyzing the variability of torque expression as a function of edge beveling on archwires, Sebanc *et al* (60) demonstrated larger measured deviation angles of actual wire specimens, when compared to values of theoretically non-beveled wires of similar dimensions. Edge beveling gave measured deviation angles that differed from theoretical values by 0.2° to 12.9°, corresponding to 3% to 63% reductions in applied torque. Interestingly, due to smaller bevel radii, Sebanc's study demonstrated that nickel-titanium archwires yielded smaller deviation angles relative to stainless steel wires of comparable nominal sizes. Further, the largest edge bevels were observed on wire specimens composed of beta-titanium. Larger radii of beta-titanium archwires compared to stainless steel arise from the inability of manufacturers to square the corners during rolling (60). Many investigators (57,61,62) have evaluated third order moments generated by specific bracket/archwire combinations. They concluded that considerable variation exists in the tolerances of orthodontic appliances, and that these variances are clinically "unacceptable", since they detrimentally reduce the magnitudes of torsional moments that should otherwise be delivered.

2.6.2.5 Deformation of Orthodontic Brackets

The integrity of slot dimensions after the application of forces and moments is one of the principal specifications for orthodontic brackets. Because of the high stresses that may be present within the slots of brackets, third order couples created by rectangular archwires may be sufficient to cause elastic, plastic or creep deformation of the brackets. The ability of orthodontic brackets to resume their shape after the cessation of stresses (archwire activation) is the result of the inherent elasticity of their constituent materials ([14]). The clinical significance of deformation of orthodontic brackets is the loss of torque that may arise from creating larger internal slot dimensions during archwire activation. Plastic deformation on the other hand is a form of permanent deformation that remains after all stresses are removed. When large third order activations are applied to metallic attachments, the tie wings will rapidly deform when the elastic limits of these components are exceeded. Plastic deformation arises from the movement (slip) of atoms or molecules past one another. Bracket slots that have been plastically deformed will permit greater amounts of torsional play thereby diminishing the magnitudes of forces transmitted in third order ([83]). Flores ([63]) determined yield stresses necessary to deform fourteen brands of commercially available 0.018"inch stainless steel brackets. They revealed that moments ranging from 3500 g-mm to 9300 g-mm were sufficient to elicit permanent deformations. These findings were confirmed by Kapur, ([64]) who later determined significant mean slot deformations of both stainless steel and titanium attachments when subjected to 45° labiolingual torque applications. Kapur's study demonstrated deformations up to 0.013 inch for 0.022 inch stainless steel brackets, and distortions to 0.001 inch for 0.018"inch titanium brackets tested in vitro. Their results illustrate that slot dimensions of metallic attachments tend to permanently, deform when subjected to sufficiently large third order moments.

Creep or time dependent strain is another mechanism of deformation to which orthodontic brackets may become susceptible during activation. Creep deformation occurs when the stress is less than the materials elastic limit, and is dependent on both the applied stress and working temperature ([14]). When either the stress or temperature is increased, the amount of permanent strain with time will likewise increase. Creep may be considered a form of viscous flow that is imparted by thermal agitations of atoms or molecules over time.

2.6.2.6 Anatomical Factors Affecting Third Order Movements

Straight wire appliances as described by Andrews are designed to control the three-dimensional position of teeth in the arch ([39,41]). The incorporation of these techniques is based on the assumption that tooth morphologies are identical for all patients. On the contrary, teeth vary considerably with respect to crown to root orientations, facial contours and incisogingival heights ([66]), which causes variances in torque delivered by pre-adjusted appliances bonded to the facial surfaces of the teeth ([67]). Taylor ([84,85]) attributed large variations in the shapes of maxillary central incisors from the apparent curvatures of their crown and root axes. Delivanis and Kuftinec ([86]) found the crowns of upper central incisors in Class II div 2 patients were angulated more lingually than those from other malocclusions. Bryant *et al* ([87]) determined maxillary central incisor collum angles (crown-root angulation) to be as high as 25.5°. Variations in the incisogingival lengths of the teeth are also prevalent within the general population ([41,87]). In an investigation to quantify anatomic differences of maxillary central incisors, Bjorndal *et al* ([88]) noted that incisogingival lengths varied up to 3.4 mm between patients. Attempts to measure facial crown morphologies of central incisors have been made using tangent lines or surface angles that approximate the mid facial points of their anatomic crowns ([77,89]). Dellinger ([77]), Carlsson and Ronnerman ([90]) found an angular deviation of 22.25° and 13°, respectively, for facial surface angles of maxillary permanent central incisors. Bryant *et al* ([87]) revealed a range of 17° for labial surface angles for upper central incisors. Since this range is similar to that of various appliance prescriptions, these facial deviations likely negate the subtle differences between prescriptions, whose third order range of activations are between 7-22°).

2.6.2.7 Effect of Bracket Placement Errors on Third Order Movements

A significant but often overlooked source of variation in the expression of buccolingual torque, are clinical bracket placement errors. According to Balut *et al* ([65]) the effects of these errors make the use of straight wire appliances "unjustifiable". Using a mathematical model Germane *et al* ([66]) demonstrated that a 1mm difference in bracket height could lead to a 10° loss of torque. Balut *et al* ([65]) determined that a 4° variance could arise from placement errors between 0.34-1.80mm. Miethke and Melsen ([67]) reported that positioning discrepancies larger than 0.4mm can influence torques by 2-10°. This then raises the question whether straight wire techniques are appropriate for contemporary orthodontics.

2.7 Self-ligating brackets

Over the past century and since the birth of the discipline of orthodontics in the early 1900s, a number fundamental changes took place that altered the manner in which orthodontics was practiced, the introduction of cephalometrics, the introduction of bonding to enamel and the introduction of bracket prescriptions, to name a few. The development and evolution of the orthodontic bracket over the last 100 years is nothing short of impressive. The most recent of those developments is the introduction and the widespread adoption of the self-ligating orthodontic bracket systems.

Conventionally ligated brackets are believed to have a number of disadvantages, high friction, force decay of the elastomeric ties which leads to less than perfect archwire engagement, time consuming ligation and oral hygiene concerns are a few of those shortcomings ([91]). These disadvantages motivated orthodontists and orthodontic suppliers to develop better brackets.

The term "self-ligating bracket" refers to a class of orthodontic brackets that include built in methods of ligation, cover or clasp which encloses or otherwise retains the arch wire within the slot of the bracket ([91]). Designs for such brackets have been around for a surprisingly long time, the earliest designs date as far back as the 1930s. Many of those designs have been patented, however, a small number became commercially available. New designs for self-ligating brackets continue to appear, and the popularity of those brackets is on the rise. The major incentive for the development of those brackets has been the faster ligation and shorter chair-side time required for archwire insertion and removal. In view of the fact that self-ligating brackets are gaining popularity, it became necessary to review the characteristics of those brackets and examine the differences between different designs. This new and different ligating mechanism requires minor, and in the view of some, major changes in the treatment mechanics.

These brackets have been around for a long time, but never gained widespread use because of many factors. Breakages were unacceptably common, breakages took place because those brackets contained a movable part, the ligating mechanism. It took orthodontic suppliers a relatively long time to produce robust self-ligating brackets. Moreover, it took even longer to convince the orthodontic community that those brackets do indeed present an advantage over conventional brackets, which is an ongoing debate within the orthodontic community. The supposed theoretical advantages of self-ligating brackets include low friction ([91,92,93]), faster archwire insertion and removal ([91,93,94]) and more accurate full archwire engagement ([91,94]). We will discuss each one of those advantages separately.

2.7.1 Low friction produced by self-ligation

Friction is the collective term used to describe resistance to orthodontic tooth movement, or the resistance to sliding of orthodontic brackets along archwires. Friction is a very complicated phenomenon, when a body slides across a surface, there is a resistance to this motion due to the interaction between the body and the surface (Figure 2-12). The causes of friction are molecular attraction or adhesion between the materials, surface roughness of the materials, and deformation resistance in the case of soft materials. Adhesion is the molecular force resulting when two materials are brought into close contact with each other. Trying to slide objects against each other requires breaking these adhesive bonds. Surface roughness is a factor when the materials are rough enough to cause abrasion, at the microscopic scale, many irregularities in each surface are apparent and it is the interlocking of these irregularities that gives rise to friction. Friction in orthodontic literature has been attributed to molecular adhesion and interlocking of surface irregulaties. When one of the materials is relatively soft, much of the resistance to movement is caused by deformations of the objects or by a plowing effect, this phenomena is referred to as "Binding" in orthodontic literature. Orthodontic litereature makes the distinction between friction (molecular adhesion and interlocking of irregularities) and Binding (deformation of the surfaces or the plowing effect) ([95]). In material sciences, friction includes those three phenomena.

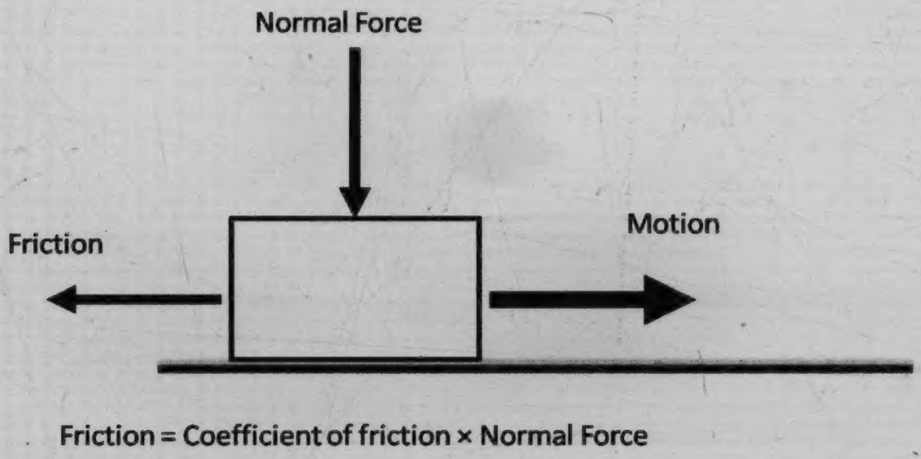

Figure 2-12: Friction

The frictional force is a product of the coefficient of friction and a force acting perpendicular to the contacting surfaces (Equation 2-2). This perpendicularly acting force is referred to as the "normal force". Frictional forces are proportional to the normal force and independent of the contact area between the two surfaces. The magnitude of the coefficient of static friction depends on the nature of the two surfaces, what material they are made of, the relative roughness, temperature and lubrication.

$$friction = coefficient\ of\ friction \times normal\ force$$

Equation 2-2: Friction

The coefficient of friction, μ is a number related to the two specific surfaces that are in contact with each other. Although there are charts listing average values of the coefficient of friction for various materials, the only true way to establish the number is by experiment and testing or empirical measurements, there are no good formulae or equations to predict μ. The coefficient of friction can range between 0 and 1. In the case where a surface is soft, the coefficient of friction is not a simple number, it may be dependent on the area of the surfaces, the amount of deformation, the amount of adhesion, the shape of the surfaces. What this means is that although the standard friction equation holds in most cases, the coefficient of friction will only hold for a specific configuration, and experimental assessment is the only way to understand this complex phenomenon.

Friction in orthodontics is due to contact between the archwire and the bracket components, the heavier the contact the higher the friction. Friction in orthodontics arises from:

- Ligation mechanism applying a force normal to the archwire surface
- The contact between the archwire and the bracket slot walls during tooth movement and bracket sliding.

Friction is influenced by bracket material, width, archwire material, diameter, cross-sectional shape, presence of active torque, Bracket/wire angulation, saliva and method of ligation ([95,96,97,98]).

Binding on the other hand is much more difficult to analyze. Binding is the term used to describe friction when a body stops sliding along the surface, the edge of the body starts plowing into the surface. In orthodontics, a bracket edge would create a notch into the archwire surface (the bracket plows into the wire). Binding has been subdivided into elastic binding and physical notching ([95]). Resistance to sliding has been presented as the combination of friction and binding (RS = Fr + Bi). Binding begins to contribute to the resistance to sliding when the bracket edges start plowing into the archwire; in order for this to happen, the archwire slot and the wire need to be at a certain angle. The angle at which the archwire first contacts the edges of the slot walls is called the critical contact angle (θ_c). At this angle the bracket edges are pushing against the wire at two opposing non-collinear points, this situation has been referred to as elastic binding ([95]), however it can be considered an extension to the definition of friction, since the bracket is now applying normal forces to the wire at two different locations. At greater θ_c the bracket may physically notch the surface of the wire thus adding more resistance to sliding, this is binding in the orthodontic traditional sense.

Elastomeric modules and stainless steel ligature ties have been shown to produce 0.4-1 N (approximately 40-100gm) of frictional forces with a wide variation in the literature from as low as 31gm to as high as 247gm per bracket ([97,98,99,100,101,102]). Self-ligating brackets on the other hand have been demonstrated to produce much lower friction than conventionally ligated brackets ([85,92,95,96,103,104,105]). However, it is difficult to ascertain how accurately any laboratory simulation of friction reproduces the true in vivo situation. Some studies reported little difference in friction between Self Ligating Brackets (SLB) and conventional brackets when the wires are active (critical contact angle exceeded ([106]). However most evidence suggests that even with active wires, the difference in the resistance to sliding remains to be significant although less dramatic ([92,95,96,102,107]). However, in a recent review publication, Ehsani et al could not find sufficient evidence to claim that with large wires in the presence of tipping and/or torque and in arches with considerable malocclusion, self-ligating brackets produce lower friction compared to conventional brackets ([108]).

Before drawing any conclusions from the evidence that SLB have less friction than conventional brackets, we need to decide if low friction should indeed be considered an advantage. Some clinicians believe that vibrations from intra-oral masticatory forces can substantially reduce friction ([109,110]), and that binding between the archwire and the bracket is the only real source of resistance to sliding. In one of those cited studies it was not clear how the vibrations were applied, instead finger perturbations were randomly applied. In the other study friction was found to be reduced by 85% and 80% for 21x25 SS and 19x25 SS respectively and by 27% and 19% for 19x25 TMA and 0.016 SS respectively. In the latter study a vibrating machine that produced 1.35 Hz or 81 cycles/min seem to be too excessive and not what would be expected from chewing forces. This study's results however suggest that oral vibrations are effective in reducing resistance to sliding for large rectangular SS archwires only. It remains unclear how significant the effect of vibration is on friction in the oral environment.

It is very difficult to design an experimental design that can answer the questions surrounding friction in orthodontics. Many factors come into play, and the true in vivo conditions are nearly impossible to completely replicate. The bulk of evidence suggests that until better scientific evidence is available, it is necessary to consider friction a key player in orthodontic mechanotherapy rather than discounting it categorically. Material science considers binding as part of friction, orthodontists however tend to differentiate between friction and binding. A good theoretical exercise is to consider a situation where two hard surfaces have no friction, it would be impossible to produce binding between those two surfaces. Friction precedes binding, and unless friction is present, binding situations would not develop. Therefore, high friction is more likely to lead to binding than low friction situations, and masticatory vibrations are a factor that influence friction but are not likely to eliminate it.

2.7.2 Reduction in treatment time and chair-side time with self-ligation

The principal objective behind the development of earlier self-ligating brackets was the faster ligation and archwire removal and insertion. With the development of elastomeric ligatures, this incentive somewhat diminished. However with the current trends towards the use of low friction mechanics, self-ligating brackets are gaining popularity, and the added advantage of quicker ligation is considered a significant advantage. Some investigators found a 7 months and 7 visits reduction in treatment time ([illegible]) while others found a 4 months and 4 visits reduction in treatment time ([illegible]). One research looked at the ligation time and found that the ligation of Damon SL brackets required 24 seconds less per arch compared to conventional ligation. A modest decrease but considering that the self-ligating brackets currently available are much easier to use and quicker to ligate than earlier designs, we expect archwire ligation timesavings to be more significant than what was shown in those studies.

In a recently published randomized clinical trial, it was found that self-ligating brackets were no more efficient than conventionally ligated brackets during tooth alignment (111).

2.7.3 More accurate archwire engagement with self-ligation

Theoretically, self-ligating brackets employ a ligation mechanism that is either open or close, partial ligation and loss of control between appointments should not be happening. That is true if the ligation mechanism was completely robust and breakages free. In reality, breakages still happen, and bracket doors disintegrate and accidentally open, which leads to loss of control. Having said that unlike an elastomeric ligature, if the ligation mechanism is the self-ligating bracket is intact the tooth will remain under control and archwire progression will proceed as planned.

2.7.4 Active Vs Passive Self-ligation

There are a number of ligation mechanisms employed in different designs of self-ligating brackets. Those can be broadly classified as passive and active. Active self-ligating brackets usually include a clip that maintains a certain amount of pressure on the wire. Passive self-ligating brackets on the other hand form a rectangular lumen with no active component within the brackets. The debate over which ligating mechanism is better within the orthodontic community has been inconclusive. In theory, the ligation mechanism is likely to have an effect on the friction, In-out alignment and torque expression. We will discuss each of those separately.

2.7.4.1 Friction

Low friction mechanics is what most self-ligating bracket (SLB) suppliers consider their most significant advantage over conventional brackets. It has been shown that all SLB have significantly less friction than conventional brackets ([92,95,97,112,113,114]). Most evidence have shown that passive brackets have less friction than active ([92,95,96,103,115,116]). Some studies concluded that some active SLB have higher friction than conventional brackets, possibly a function of the material of which the bracket clip is made ([105,115]) other studies found that active SLBs have less friction than passive SLB ([112]). The friction debate in orthodontics is a very complicated one especially when we consider friction of active and that of passive SLB and how any difference can translate into clinical difference.

2.7.4.2 In/Out alignment

Let us consider a 0.018" aligning archwire in a passive self-ligating bracket. 100% alignment will not be achieved using this type of wire, the Damon brackets for instance have a 0.027" of slot depth, and an 0.018" wire will not be able to fill the slot completely therefore full alignment is not achieved. There can be 0.009" malalignment (difference between 0.027' and 0.018") even after the wire had fully expressed itself, and became completely passive. For new users of passive self-ligation this observation is generally made during the initial alignment stage with a round wire, after noticing that the lower incisor edges are not completely aligned. The same 0.018" wire will produce full expression of the brackets in/out prescription and alignment is generally achieved using this wire when active SLB is used, such as InOvation and Speed brackets. The reason is that the slot depth in those active SLBs is 0.018", which means that a 0.018" wire would completely fill the slot and no play between the wire and the bracket would exist.

Let's now consider aligning archwires larger than 0.018" used with a passive bracket, the larger the horizontal dimension of the wire the better the in/out alignment, hence the unconventional horizontally full sized 0.014"x 0.025" and 0.016"x 0.025" aligning archwires recommended to be used with the Damon brackets. In active SLB the horizontal dimension of the wire does not matter from in/out alignment point of view as long as it is greater than the 0.018" threshold. Therefore, the use of traditional wires with a horizontal dimension of 0.025" is not entirely justifiable.

2.7.4.3 Torque

Torque in orthodontics is the term used to describe third order control. Preadjusted edgewise brackets have a rectangular slot that is oriented at a predetermined angle to the base of the bracket; this angle is the torque prescription. Torque expression of orthodontic brackets has been the subject of numerous research papers over the years ([56,83,117]). However, torque expression of self-ligating brackets has been studied in one study by the author, we are not aware of any similar investigations. Four self-ligating brackets were investigated, two representing active and the other two representing the passive self-ligating brackets. The experimental method eliminated the effect of the prescription and the study focused on the differences in torque expression that may arise from structural differences between the four brackets. We found that the amount of archwire bracket slop was less for active self-ligating brackets as opposed to passive self-ligating brackets, and that the active self-ligating brackets seem to have slightly better torque control, a direct result of the active clip of those brackets applying a normal force on the wire into the bracket slot. We found that clinically applicable range of torque activation was larger for the active self- ligating brackets than the passive self-ligating brackets. For the passive self-ligating brackets on average, there was about 15 degrees of play between a 19x25 SS archwire and the bracket slot. This 15 degree play is enough to negate and neutralize the majority of torque prescriptions available. For instance, +17 degrees of torque in an upper central incisor bracket is equivalent to +2 degrees. +12 degrees of torque is actually equivalent to using round wires with no toque control. A follow up study employing the same method was carried out using the more recent self-ligating design of the Damon Mx bracket. The data show that there is no significant difference in torque expression between active and passive self-ligating brackets.

2.8 Force system determination

2.8.1 Force system analysis (Force Resolution)

A concurrent coplanar force system is a system of two or more forces whose lines of action intersect at a common point. However, all of the individual vectors might not actually be in contact with the common point. These are the most simple force systems to resolve with any one of many graphical or algebraic options. A parallel coplanar force system consists of two or more forces whose lines of action are parallel, this is commonly the situation when simple beams are analyzed under gravity loads. Which can be solved graphically, but are combined most easily using algebraic methods. Non-concurrent and non-parallel system consists of a number of vectors that do not meet at a single point and none of them are parallel. These systems are essentially a jumble of forces and take considerable care to resolve, an orthodontic fixed appliance is an example.

Any system of known forces can be combined into a single force called a resultant force or simply a resultant. The resultant is a representative force, which has the same effect on the body as the group of forces it replaces. One can progressively combine pairs or small groups of forces into resultants. Then another resultant of the resultants can be found and so on, until all of the forces have been combined into one force. Resultants can be determined both graphically and algebraically. It is important to note that for any given system of forces, there is only one resultant.

It is often convenient to decompose or resolve a single force into two or three distinct forces. These component forces, when acting together, have the same external effect on a body as the original force. Finding the components of a force can be viewed as the converse of finding a resultant. There are an infinite number of components for any single force, the correct choice of the pair to represent a force depends upon the most convenient geometry. For simplicity, the most convenient is often the coordinate axis of a structure.

Pairs of components that correspond with the X and Y-axis are known as the rectangular cartesian components of a force. Rectangular components can be thought of as the two sides of a right angle, which are at ninety degrees to each other. The resultant of these components is the hypotenuse of the triangle. The rectangular components for any force can be found trigonometrically, $F_x = F \cos \theta$, $F_y = F \sin \theta$.

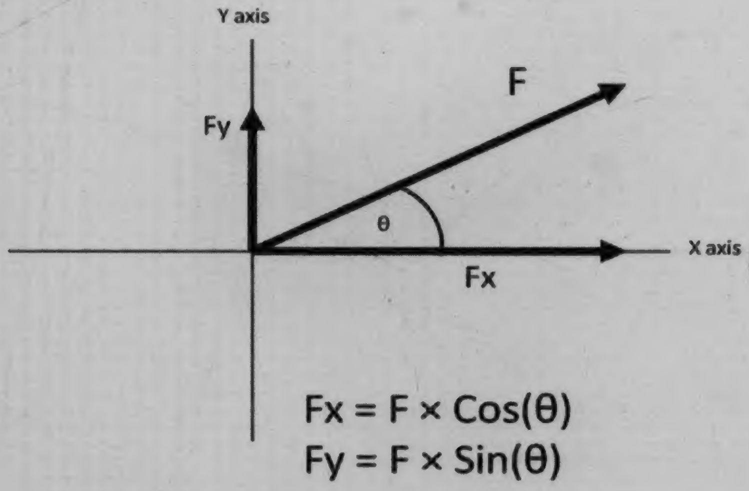

Figure 2-13: force resolution

2.8.2 Finite Element Analysis

In addition to analytic methods and laser holography, numeric techniques have been used to determine centers of rotation under different loading conditions and estimate stress in the PDL. These techniques use a three-dimensional finite element method. The tooth and the alveolar process are broken into elements, by accurately determining the shape of the elements and the constitutive mechanical behavior of each element. Centers of rotations are determined using assumed forces on the teeth ([8,31,118,119,120]).

2.8.3 Force Measurements

The forces delivered by an orthodontic appliance can be determined by direct measurement with suitable instruments or, partly, by mathematical calculation ([35,118,121]). The load deflection rates of orthodontic springs can be measured with either electronic strain gauges or mechanical gauges. Most orthodontic appliances deliver a relatively complicated set of forces and moments, which makes it impossible to analyze and very difficult to measure.

2.9 Purpose of the study

Orthodontic biomechanics is central to the development of the discipline of orthodontics, however ironically it is one of the least understood areas in orthodontics. The introduction of the continuous arch technique and the application of new superelastic alloys made the biomechanical applications in orthodontics even more complicated and difficult to study and analyze. Contemporary full arch fixed appliances create force systems that are so complex; we are still to date incapable of modeling or estimating their components, even with the support of the most powerful computer systems. There are too many unknowns, and too many assumptions are made in order to simulate those force systems in computer models. Force system measurements were made on one or two tooth models, however in order for us to understand the orthodontic force systems we need to three-dimensionally measure the forces being applied on every tooth in the dental arch simultaneously.

With the very recent technological advances in force/torque sensors technology, data acquisition and data representation, it became possible to measure those forces and reveal the force systems we are applying to the dentition. The purpose of this PhD research study is the design and construction of an experimental device that is capable of revealing the details of the force systems used in modern day orthodontic mechano-therapy of continuous arch techniques.

3 Chapter three: Development and Evaluation of Measurement Repeatability of an Orthodontic Torque Measuring Apparatus

3.1 Introduction

Correct axial inclination of anterior teeth is considered essential for providing good occlusal relationships in orthodontic treatment. This axial angulation is referred to as torque in orthodontic literature. Under-torqued upper incisors affect the arch length and the space requirements within the dental arch, and it has been shown that for every 5° of anterior inclination, about 1 mm of arch length is generated ([122]).

Orthodontic brackets bonded to teeth have a rectangular slot placed during manufacturing in a way that provides the desired torque prescription. Orthodontic torque expression can be achieved by gradually filling the bracket slot with a rectangular wire, by increasing the archwire dimensions throughout the treatment. However, dimensions of the final working archwire never reach the full dimensions of the bracket slot, therefore, a percentage of the torque that is built into the bracket is lost due to the play between the archwire and the bracket slot, this is referred to in the literature as the deviation angle (Figure 3-1)

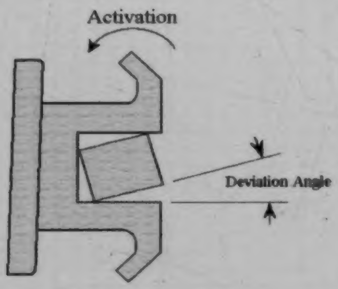

Figure 3-1: Deviation angle

This amount of play has been theoretically calculated and experimentally measured. Theoretical moments can be calculated from the nominal dimensions of archwires and brackets given by the manufacturers. However, it has been shown that there is a considerable discrepancy between the theoretical and the measured bracket archwire play ([60]). This play often extends to 100% of the prescribed torque, which is equivalent to using round wires with no torque prescription ([117]).

Deviations from those calculations can be attributed to intrinsic variations in archwire cross-sectional diameters ([55,58,62]), bracket slot dimensions ([56,58,60]), archwire edge beveling ([60,61]) and bracket deformations ([63,64]) . Other factors also have an impact on orthodontic moments (torque), including bracket placement errors ([65]) and irregularities in tooth morphology ([66,67]). Therefore, due to these variations in torque expression resulting from variations in brackets and archwires, accurate prediction of third order moments using the archwire and bracket dimensions provided by the manufacturer is impossible. An experimental approach was designed to measure torque expression of orthodontic brackets.

3.2 Apparatus

The bracket/wire assembly torsion device in Figure 3-2 was developed with the collaboration of members of the Departments of Dentistry and Mechanical Engineering. The novel apparatus has the capability of applying pure torsion to the wire using a force zeroing technique by maintaining perfect vertical and horizontal alignment between the wire and the bracket slot. The apparatus also measures load and moments on the bracket as well as rotation of the archwire. The instrument is composed of the following hardware and software components:

3.2.1 Hardware:

3.2.1.1 Force/torque transducer (Figure 3-2, g)

An ATI Industrial Automation Nano17® load cell was used to measure the three force and three moment components of the applied load. The compact transducer is the smallest load cell available in the market that uses silicon strain gauges to sense forces. The transducer's silicon strain gauges provide high noise immunity and allow high overload protection. Silicon gauges provide a signal 75 times stronger than conventional foil gauges. This signal is amplified resulting in near-zero noise distortion. Table 3-1 shows the error of measurement for this force sensor. The transducer is rated for maximum loads of 25 N of transverse forces (Fx, Fy), 35 N axial force (Fz) and 250 Nmm moments in all three axes. The resolution of the load measurements are

1/1280 and 1/256 for forces and moments, respectively. Cell overload occurs at 127 times the rated loads.

	Calibration	Fx	Fy	Fz	Tx	Ty	Tz
Nano17	SI-25-0.25	1.50%	1.50%	2.00%	1.50%	1.75%	2.00%

Table 3-1: Maximum full-scale measurement uncertainties for Nano 17 transducer (error), (ATI Automation, NC)

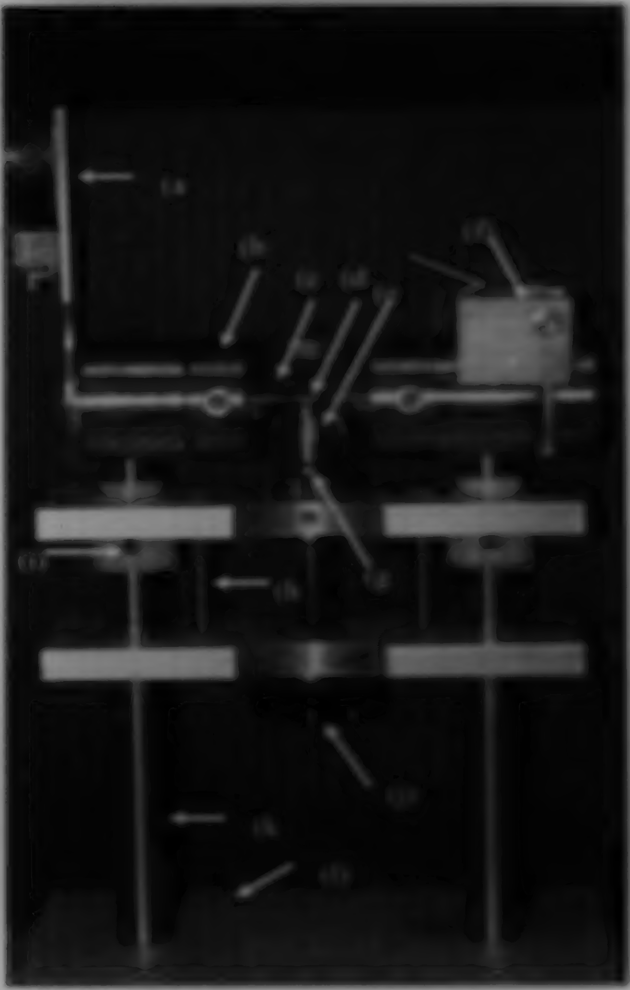

Figure 3-2: bracket/wire assembly torsion testing apparatus

3.2.1.2 Data acquisition card

The load cell was used in conjunction with a Data Acquisition Card (DAQ 16-Bit E series NI PCI-6033E, 100 kS/s, 16-Bit, 64-Analog-Input Multifunction DAQ, National Instruments, Austin, TX) recommended by the transducer manufacturer. The DAQ card recommended by the transducer's manufacturer was used in order to achieve maximum resolution. The capabilities of the DAQ system are listed in Table 3-2.

SI-25-0.25	Fx	Fy	Fz	Tx	Ty	Tz
Sensing ranges (±N)	25	25	25	250	250	250
Resolution DAQ card (N)	1/1280	1/1280	1/1280	1/256	1/256	1/256

Table 3-2: Sensing ranges and resolution of the sensor using a Data Acquisition Card (ATI automation, NC)

3.2.1.3 Inclinometer (Figure 3-2, a)

The USDigital T2-7200-1N inclinometer, (a) of Figure 3-2, was used to measure the torsional rotation of the wire. The inclinometer has a 360° rotation range with a 0.05° resolution. Since the system is under no extreme condition, no damping option was selected. The inclinometer was attached to the opposite end of the apparatus from the worm gear system.

3.2.1.4 Twist mechanism (Figure 3-2, b, c, f)

The twist mechanism was designed to apply a controlled degree of pure twist on the wire. The wire support substructure is responsible for the application of the torque and the measurement of the twist angle. The wire support substructure, a rigid assembly, is fully rotated by the worm gear, thus imposing the same rotation at both ends of the structure. Therefore, both worm gear and inclinometer undergo the same torsional rotation. This component consists of the support tube which is a rigid steel tube fixed to the base of the device. This tube received the rotating tube (Figure 3-2, b) into which the conical dies were fitted.

A rotating tube assembly was machined to receive the conical wire support dies. Setscrews on the side of the tube were placed in order to hold the conical dies in place and prevent any movement of the dies relative to the rotating tube as well as apply pressure on the dies that would friction hold the wire in the groove.

Two collinear conical steel dies (Figure 3-2, c and Figure 3-3, a & b) were mounted within the rotating tube assembly (Figure 3-2, b) to rigidly hold the wire. The mounted conical steel dies were used to secure the archwires on either side of the brackets during testing to facilitate the consistent application of torque to the brackets. Each of those dies was split in half and a groove was machined down the middle of each half so that when the two halves were joined there was a lumen that will receive the rectangular wire. Four types of dies were constructed, with lumen dimensions of 0.021"×0.025", 0.019"×0.025", 0.018"×0.025" and 0.017"×0.025".

The conical steel dies had another groove on the outer surface that received a key on the inside surface of the tube rotating assembly. This key maintains consistent and accurate positioning of the conical dies within the rotating tube.

A worm gear torsion system (Figure 3-2, f) was mounted on the support structure. This worm gear applies controlled rotation of the rotating tube.

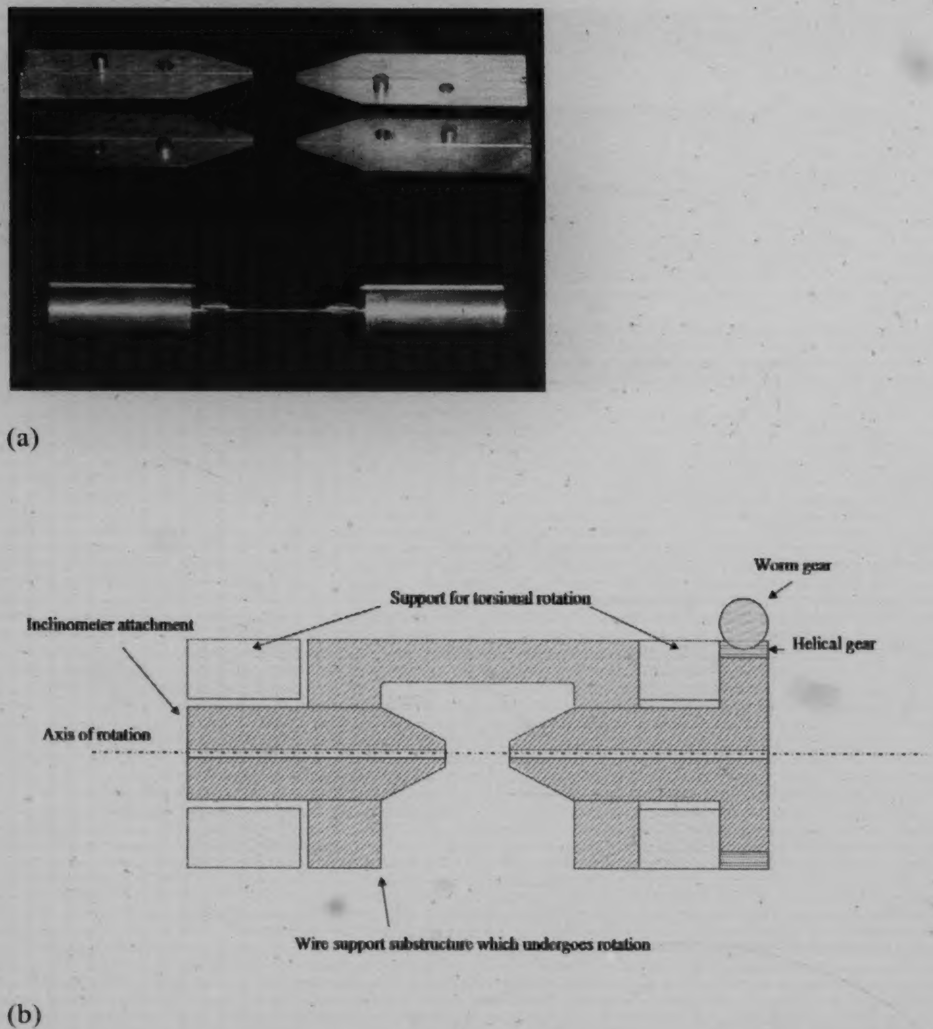
(a)
Worm gear
Support for torsional rotation
Inclinometer attachment
Helical gear
Axis of rotation
Wire support substructure which undergoes rotation
(b)

Figure 3-3: (a) Conical wire support dies; (b) Schematic of the torsion application system and wire support dies

3.2.1.5 Bracket mounting mechanism (Figure 3-4 & Figure 3-5)

The adjustability of the position of the bracket is due to a planar dual turntable alignment system which is seen schematically in Figure 3-4. The bracket mounting assembly was made of three components, the load cell adapter, Base turntable and Secondary positioning turntable. The load cell adapter was made of stainless steel and was bolted on to the load cell. It was designed to have a tight fit with the base turntable. This rigid adapter will transfer the load to the load cell. The base was designed to have a close fit with the load cell adapter with no play between those two parts. The base however was free to rotate around a vertical axis. This rotation provides the small adjustment needed in order to align the centre of the bracket with the centre of the wire.

The secondary turntable was made of steel and designed to fit into the base turntable at an offset centre of rotation of the base turntable. This geometry allows the adjustment of the bracket position so that the centre of the bracket coincides with that of the wire. This secondary turntable is free to rotate with the base in order to achieve parallelism between the bracket slot axis and the wire axis. The orthodontic brackets were mounted on the secondary turntable, and epoxy resin was used for bonding the brackets to the turntable.

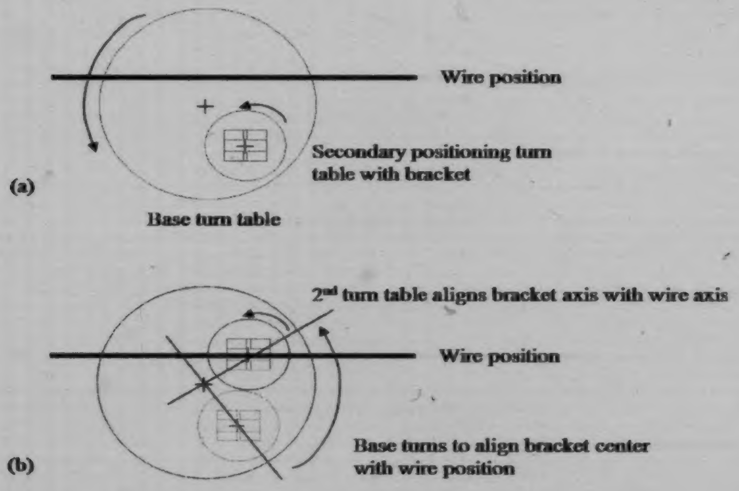
Wire position
Secondary positioning turn table with bracket
(a)
Base turn table
2nd turn table aligns bracket axis with wire axis
Wire position
Base turns to align bracket center with wire position
(b)

Figure 3-4: Schematic of the alignment system. (a) Unaligned wire and bracket. Possible motion of both turntables is shown. (b) Aligned bracket and wire and rotation motion required by both turntables.

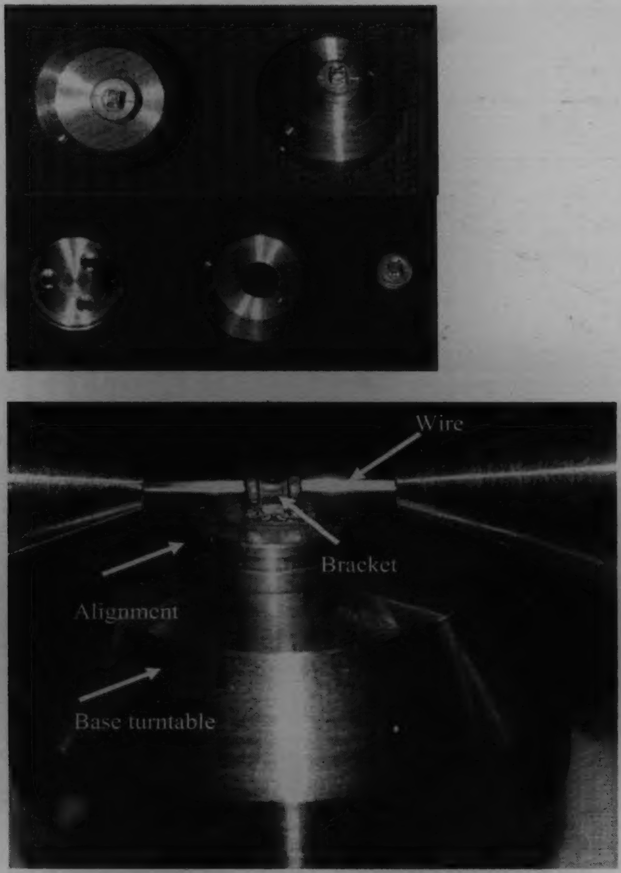

Figure 3-5: Bracket mounting and alignment assembly

3.2.1.6 Vertical adjustment mechanism (Figure 3-2)

The vertical adjustment system, which moves the load cell and the planar adjustment system vertically, is composed of two low friction guide rails, a central screw to drive the motion and a dual spring system to maintain contact between the load cell and the lower platform at all times. The vertical adjustment assembly was designed in order to facilitate mounting the brackets within the bracket mounting assembly then raising the brackets in order to engage the archwire. Different brackets that will be tested will have different vertical profiles, therefore vertical adjustability was required in order to make sure no vertical load was applied on the bracket.

3.2.1.7 Base support

A steel base was used to provide stability for the system during testing. The base was lined with soft rubber lining to help reduce vibrations that would affect the load cell and the inclinometer readings.

3.2.2 Software

LabView Data Acquisition Software (National Instruments, Austin, TX) was used to acquire the signal from the transducer and log it to file. The same software was used to acquire the signal from the inclinometer. The output was presented as a LabView front panel interface which showed the readings for the three force and the three moments in the X, Y and Z axes. The moment Tx is the one of interest for the purpose of torque measurement. Fx, Fy, Fz, Ty and Tz were monitored during data gathering in order to confirm that a pure couple was being applied. As the wire assembly is twisted to apply the desired moment, the moment value as well as the angle of twist was logged to file.

3.2.3 Error analysis

We expect to find considerable variations in the torque expression of different brackets, however any variation in our measurements can result from variations from the measurement device. In order to quantify the variation of the measurement device error analysis was conducted while controlling for the variation resulting from the brackets and the wires. Five tests were carried out, a new wire and a new bracket were used for each test (0.019" X 0.025" SS with Damon2 brackets). For each bracket/wire combination, the test was repeated 10 times recording torque measurements for 19 angles starting at zero and ending at 57, this range was chosen to avoid permanently deforming the stainless steel wire (Figure 3-6). Figure 3-7 shows 10 load deflection curves of one bracket wire combination. A higher variability in data is usually expected when the mean increases, therefore the coefficient of variation was used to evaluate the standard deviation of the data as a percentage of the mean for two angles (Table 3-3). The average coefficient of variation was 35%. Repeated measurements of the same bracket and wire showed very small amounts of variation (0.1 to 1.2 Nmm), the variations were higher at large angles. The measurement error of the Force/Torque transducer was 1.5 % (Manufacturer's specification, Table 3-1). The error analysis showed that this experimental technique was reliable and consistent.

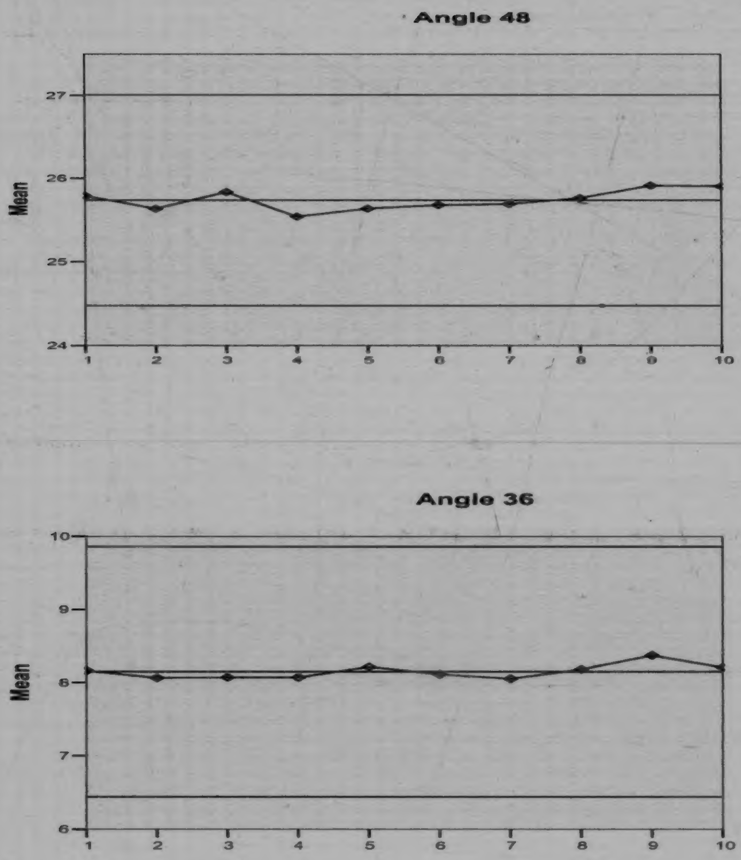

Figure 3-6: Moments measured for error analysis showing no plastic deformation of wire or bracket

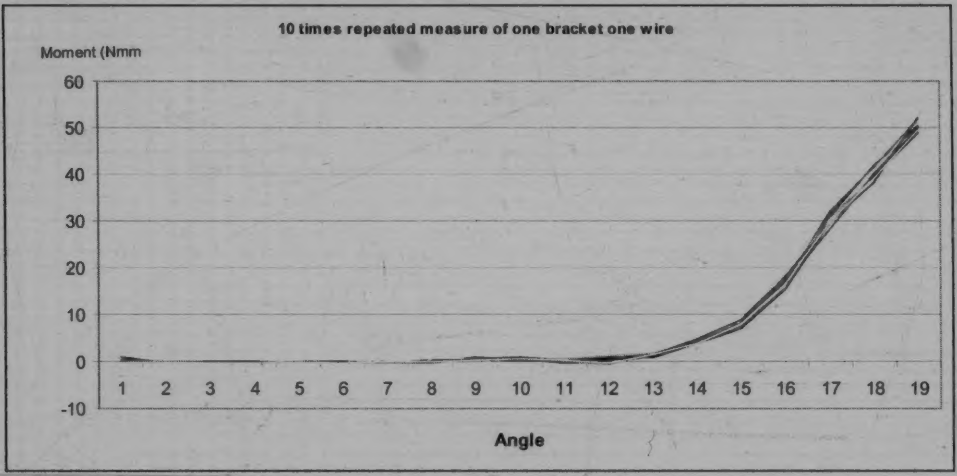

Figure 3-7: torque expression of one bracket wire combination repeated 10 times

	Angle	Mean	SD	CV
Bracket 1	36	12.703	0.207	1.63
	48	28.809	0.162	0.56
Bracket 2	36	8.703	0.317	3.64
	48	23.863	0.107	0.45
Bracket 3	36	3.0745	0.2417	7.86
	48	23.184	0.239	1.03
Bracket 4	36	9.644	0.438	4.54
	48	24.443	0.311	1.27
Bra[illegible] 5	36	6.638	0.347	5.23
	48	28.398	0.203	0.72

Table 3-3: Coefficient of variation, error analysis

3.3 Materials

A pilot study was conducted using 7 Speed brackets and 10 Damon2 brackets. For detecting a difference between the brackets 5 Nmm with $\alpha = 0.05$, $\beta = 0.1$ sample size was calculated to be 81, 40, 19, 54 for angles 12°, 24°, 36°, 48° respectively. Those calculations were averaged and a sample size of 50 was determined to be adequate in order to conduct this study.

Fifty upper right central incisor brackets of each of the four types of brackets (200 brackets in total) included in the study (In-Ovation/GAC, Bohemia, NY; Speed/Strite industrial, Cambridge, ON, Canada; Damon2/ORMCO, Orange, CA; Smart Clip/3M Unitek, Monrovia, CA) were mounted on stainless steel cylinders (secondary turn table, Figure 3-5). Epoxy adhesive (Loctite, E-20HP, Hysol, Henkel Corporation, Rocky Hill, CT) was used to bond the brackets to the cylinders after treating the surfaces with Methyl Ethyl Ketone. A bracket mounting jig was used for bonding all brackets. The epoxy was allowed to fully cure before testing the brackets. The brackets' torque prescription did not affect our method since the true zero torque position was used as a base line reference for all brackets.

3.4 Results

Kolmogrov-smirnov test was used to evaluate the data statistically to confirm normal distribution. The data was distributed normally among all the groups except for the Speed bracket at angle 12°. The mean moment of couple (torque) for the four self-ligating brackets was compared at four angles (12°, 24°, 36° and 48°). Repeated measures analysis of variance and multivariate analysis of variance was conducted (SPSS 13 statistical package, Chicago, IL) to identify any significant differences between brackets (Table 3-4).

Descriptive statistics for the four bracket types is provided in Table 3-5. There was considerable variation among the torque measurements within each type of bracket. For the Speed brackets this variation was between 1.97 to 11 Nmm, for the In-Ovation brackets it was 3.7 to 16.7 Nmm, for the Damon2 brackets it was 1.4 to 11.2 Nmm, and for the Smart Clip brackets it was 2.8 to 14.2 Nmm. This variation was small for small torsion angles and increased as the torsion angle increased (Figure 3-8).

On average, the angle of engagement (the angle at which torque was first expressed) for both Speed and In-Ovation brackets was found to be at 7.5° of torsion. The same angle of engagement for Damon2 and Smart Clip brackets was found to be 15° of torsion (Figure 3-9).

Clinically effective torque has been suggested to be between 5-20 Nmm (123,124, 25). The angle of torsion at which the lower limit of the above range (5 Nmm) is achieved was 15° for the active self-ligating brackets and 22.5° for the passive self-ligating brackets. For the active self-ligating brackets the angle of torsion at which the upper limit of the above range (20 Nmm) is achieved was 31°, however, it was 34.5° for the passive self-ligating brackets (Figure 3-9).

The active self-ligating brackets produced higher levels of torque (moment) up to 35° of torsion. Any torsion beyond this point resulted in linear increase in the moments generated by the Damon2, Smart Clip and the In-Ovation brackets. As for the Speed bracket, further increase in torsion beyond this point did not result in increases in the moments generated at the same rate as the previous three brackets. The moment generated by the Speed bracket reached a plateau where the increase in torsion did not result in increase in moments generated (Figure 3-9).

At 12 degrees of torque there was no significant difference between Damon2 and Smart Clip brackets as well as between the Speed and In-Ovation brackets. There was however a statistically significant difference between Damon2 and both Speed and In-Ovation, and Smart Clip and both Speed and In-Ovation (Table 3-4).

At 24 degrees of torque, again there was no significant difference between Damon2 and Smart Clip brackets as well as between the Speed and In-Ovation brackets. However there was a statistically significant difference between Damon2 and both Speed and In-Ovation, as well as between Smart Clip and both Speed and In-Ovation. Speed and In-Ovation brackets delivered statistically significant higher torque than did Damon2 and Smart Clip brackets at angles 12° and 24° (Table 3-4).

At 36 degrees of torque the only statistically significant difference was between In-InOvation and both Speed and Smart Clip brackets. At 48 degrees of torque the most significant difference was between Speed and the other brackets. Speed delivered significantly less torque than the other brackets. There was also a significant difference between Damon2 and Smart Clip brackets (Table 3-4).

Angle	Bracket comparisons		Mean difference	Significance	95% confidence interval for	
					Lower bound	Upper
12°	Damon2	In-	-2.360856	.001	-3.895220	-.825660
		Smart	.079858	1.000	-1.123982	1.283698
		Speed	-1.547906	.000	-2.489863	-.606027
	In-Ovation	Smart	2.438904	.002	.679556	4.198254
		Speed	.812240	.685	-.792006	2.416486
	Smart	Speed	-1.626654	.007	-2.922644	-.330664
24°	Damon2	In-	-6.408882	.000	-8.942213	-3.875551
		Smart	-.999664	.876	-3.532266	1.532938
		Speed	-6.348830	.000	-8.841366	-3.856294
	In-Ovation	Smart	5.910358	.000	2.571693	9.249023
		Speed	.568872	.998	-2.751660	3.889404
	Smart	Speed	-5.341386	.000	-8.198997	-2.483775
36°	Damon2	In-	-4.553988	.248	-10.538813	1.430837
		Smart	2.231154	.816	-2.904407	7.366715
		Speed	.892980	.996	-3.781141	5.567101
	In-Ovation	Smart	6.767642	.018	.806477	12.728807
		Speed	5.411864	.049	.000815	10.822913
	Smart	Speed	-1.348874	.959	-3.768654	1.070906
48°	Damon2	In-	1.088862	.999	-6.553111	8.730835
		Smart	8.092258	.012	1.227513	14.957003
		Speed	27.475906	.000	21.516432	33.435380
	In-Ovation	Smart	6.993596	.167	-1.327848	15.315040
		Speed	26.376644	.000	18.759847	33.993441
	Smart	Speed	19.382348	.000	12.378642	26.386054

Table 3-4: Repeated measures analysis of variance (pair-wise comparison)

Angle	Bracket	Mean	Std.	N
12º	Damon2	.45336	1.488591	50
	In-Ovation	2.81372	3.702820	50
	Smart	.37478	2.772042	50
	Speed	2.00132	1.978374	50
24º	Damon2	5.52642	3.894859	50
	In-Ovation	12.43524	6.922984	50
	Smart	6.52486	5.402589	50
	Speed	11.86672	5.239754	50
36º	Damon2	23.23314	9.632597	50
	In-Ovation	27.76902	12.478563	50
	Smart	21.00160	9.492177	50
	Speed	22.35034	6.686943	50
48º	Damon2	55.83124	11.181229	50
	In-Ovation	54.73262	16.690271	50
	Smart	47.73866	14.180880	50
	Speed	28.35618	11.008746	50

Table 3-5: Descriptive statistics

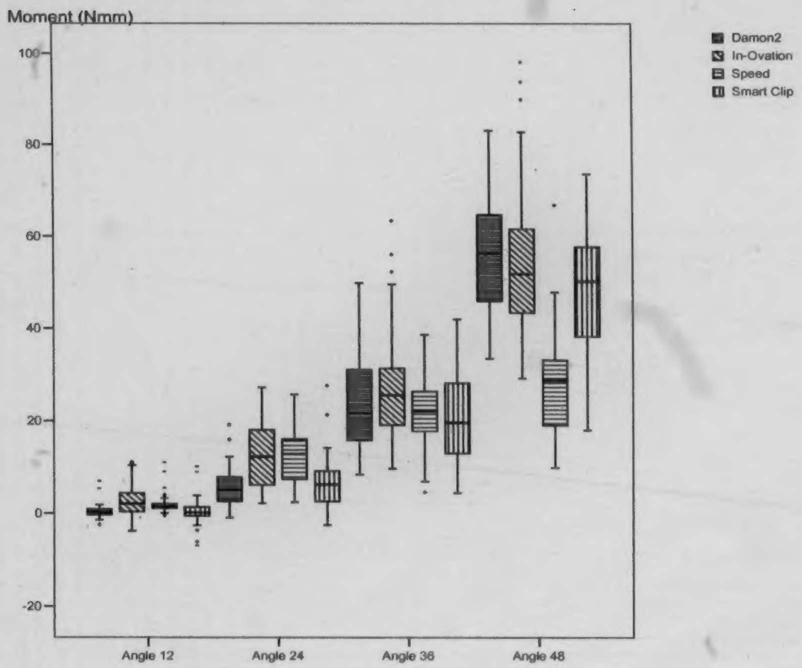

Figure 3-8: Variation in the torque measurement increases as angle of torsion increases

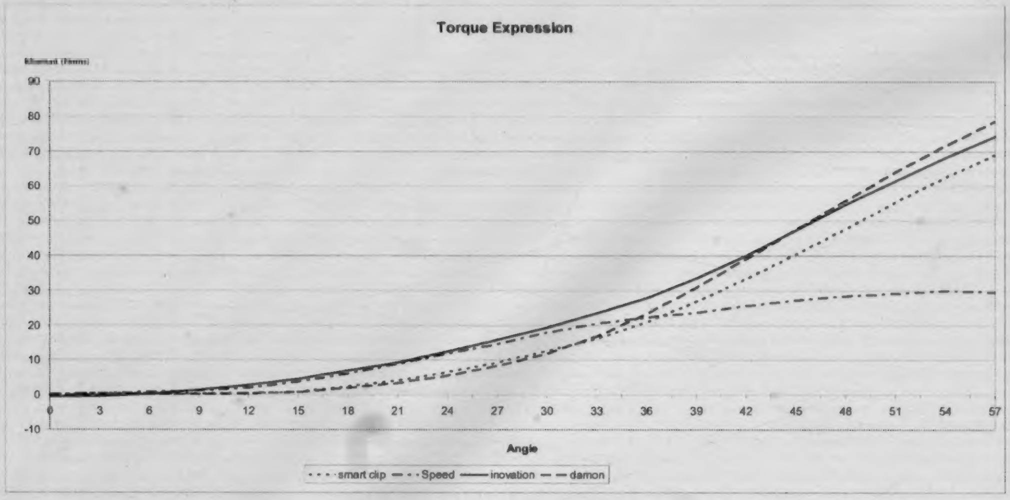

Figure 3-9: Torque expression of the four brackets

3.5 Discussion

The applied load in this study delivered a torsional moment of a couple directly to the bracket to simulate orthodontic torque application. This load was measured for four commercially available self-ligating bracket systems. We found no statistically significant difference in torque expression between the Damon2 and the Smart Clip brackets at angles 12°, 24° and 36°. There was however a statistically significant difference between the two brackets at angle 48°. There was no statistically significant difference between the In-Ovation and the Speed brackets at angles 12° and 24°. There was however, a statistically significant difference between the two brackets at angles 36° and 48° (Table 3-4).

The torque expression of Damon2 and Smart Clip brackets followed a similar pattern, characteristic of passive self-ligating brackets. Torque started to be expressed at angle 15° of torsion compared to an angle of 7.5° for the Speed and In-Ovation brackets, characteristic of active self-ligating brackets. For the Damon2 and Smart Clip brackets the value of the deviation angle (the amount of this axial rotation that the wire is permitted to undergo before contact with the slot walls is made) was found to be greater than that of the theoretically calculated one based on the nominal archwire and bracket slot sizes. This is consistent with previous research on torque expression of conventional brackets ([117,126]). For the Speed and the In-Ovation brackets the actual deviation angle was less than the theoretically calculated one. This can only be explained by the active ligating mechanism that seems to reduce the amount of archwire play in the bracket slot.

Clinically effective torque has been suggested to be between 5-20 Nmm ([123,124,125]). This range of torque was expressed at 15° - 31° of torsion for the active self-ligating brackets, and at 22.5° – 34.5° of torsion for the passive self-ligating brackets. In this study, in order to standardize the experiment, rigid clamps were used to hold the wire on either side of the tested brackets. In a clinical situation, the wire is held by brackets on either side, where there would be a certain degree of play. Therefore, two clinically useful conclusions can be drawn based on the above finding. First, the range of clinically useful torsion using active self-ligating brackets is likely to be larger than that for the passive self-ligating brackets (16 degrees for the active self-ligating brackets and 12 degrees for the passive self-ligating brackets). Second, *In Vivo,* meaningful torque control can only be achieved if torsion in the wire is higher than 15° and 22.5° for active self-ligating brackets and passive self-ligating brackets respectively. This amount of torque is much higher than most torque prescriptions available commercially. Future research might need to investigate ways to use brackets instead of rigid claps on either side of the tested brackets, without compromising the experimental technique.

The difference between the load deflection curves of the Speed and In-Ovation brackets seems to be due to the material from which the clip mechanism is made. The Speed clip is made of Nickel Titanium, and the load deflection curve of the Speed bracket was consistent with what would be expected of a Nickel Titanium alloy (Figure 3-9). The In-Ovation bracket clip is made of Stainless Steel and the load deflection curve of the In-Ovation bracket was consistent with what would be expected of a Stainless Steel alloy. The In-Ovation bracket followed a similar load deflection curve as the Damon2 and the Smart Clip brackets; however, the torque expression for the In-Ovation bracket started much earlier than the other two.

Within the data for each of the four brackets the amount of variation was considerable. For the Speed brackets this variation was between 1.97 to 11 Nmm, for the In-Ovation brackets it was 3.7 to 16.7 Nmm, for the Damon2 brackets it was 1.4 to 11.2 Nmm, For the Smart Clip brackets it was 2.8 to 14.2 Nmm (Table 3-5). This variation was small for small torsion angles and increased as the torsion angle increased.

This variation can be attributed to the bracket, wire or the experimental technique. Testing of the wires is underway as a part of another study focusing on orthodontic wire characteristics. The preliminary results show that the 0.019" X 0.025" Stainless Steel wires are very consistent. The error analysis showed that this experimental technique was quite reliable and consistent, the measurement error of the transducer was 1.5% and the average coefficient of variation (standard deviation as a percentage of the mean) was 2.7% (Table 3-3). Repeated measurements of the same bracket and wire showed a very small amount of variation. Figure 3-6 confirms that during data collection for the error analysis the wires and the brackets were not permanently distorted, the graph does not show any pattern of decrease in the loads as measurements are done.

It was concluded that the significant amount of variation in measurements resulted from structural variation in the brackets, specifically the archwire slot size. As with any other product, the manufacturing of brackets results in some variation in their size and characteristics, including dimensional accuracy and torque prescription consistency ([117]). Various bracket manufacturing processes such as injection-molding, casting and milling can affect the accuracy of the prescribed torque values, and this has been reported to be in the order of 5% to 10% ([117]). A number of researchers investigated slot size of orthodontic brackets and found that all brackets tested were oversized, anywhere between 5% and 17% ([126]). Investigators ([57,61,62]) who evaluated third order moments generated by specific bracket/archwire combinations, concluded that considerable variation exists in the tolerances of orthodontic appliances, and that these variances are clinically unacceptable since they reduce the amount of third order control that otherwise should be present using those wire/bracket combinations.

3.6 Conclusions

- The active self-ligating brackets seem to have better torque control, a direct result of the active clip of those brackets forcing the wire into the bracket slot.
- The amount of archwire bracket slop was considerably less for active self-ligating brackets as opposed to passive self-ligating brackets.
- The active self-ligating brackets were expressing higher torque values than the passive self-ligating brackets at clinically usable torsion angles (0°-35°).
- The passive self-ligating brackets produced lower moments at low torsion angles and started producing higher moments at high torsion that cannot be used clinically.
- Clinically applicable range of torque activation was larger for the active self- ligating brackets than the passive self-ligating brackets.
- All the brackets showed significant variation in the torque expressed which seems to be attributed to the variation in the bracket slot dimensions. Damon2 and Speed brackets were relatively more consistent than Smart Clip and In-Ovation brackets.
- Based on our findings, there is a need for future research to investigate torque expression on all maxillary anterior teeth simultaneously.
- This research warrants a closer look at the usefulness of multiple bracket prescriptions in the light of the very wide variation in torque

expression and the high degree of bracket archwire slop in passive self-ligating bracket systems.

3.7 Future research

This novel experimental technique will facilitate the testing of torque expression of orthodontic brackets. Advantages of such a technique is that it allows the researcher to apply, and record pure moment to the orthodontic brackets around one axis, without applying any other moment or force which might confound the results.

Different commercially available orthodontic brackets can be tested and compared with regards to torque expression. Different bracket/wire ligation mechanisms (elastics, Stainless steel wires or self ligation systems) can be tested and compared.

4 Chapter four: Design, Construction and Operation of the Orthodontic Simulator

4.1 Introduction

In order to understand orthodontic tooth movement, orthodontists need to study the mechanics of orthodontic appliances to define and quantify the force systems applied to the teeth. Many of the undesirable tooth movements that occur during orthodontic treatment can be attributed directly or indirectly to the lack of understanding of the physics of tooth movement. The large number of variables influencing orthodontic treatment, such as growth and biological tissue response to appliances, cannot be fully controlled. However, the force applied to the tooth should be a controllable variable ([1]). Careful study of the physics underlying orthodontic clinical applications can help reduce undesirable side effects, and provide the ability to accurately determine the level of stress in different areas of the periodontal ligament, this would offer the best means of correlating applied force to the tooth's response ([3,15]). Until recently, most of the orthodontic biomechanics literature was restricted to two-dimensional experimental studies, and more recently to three-dimensional computer modeling. Very little evidence exists in the literature regarding three dimensional experimental measurements and analysis of orthodontic force systems ([2,127,128,129,130,131,132,133]). Three-dimensional force and moment measurements are needed to study orthodontic force systems in three dimensions. Those measurements need to be simultaneously performed on all teeth in a dental arch. The sensors used for measurement, must therefore be small enough to be incorporated on all teeth in a simulated dental arch. Three-dimensional force and moment measurement technology (multi-axis force transducers) is commercially available but not in tooth size dimensions. Using such sensors in orthodontic research requires complicated engineering designs, micro-machining and specialized software development. The purpose of this paper is to report the design construction and measurement validation of a device capable of measuring forces and moments in three dimensions on all fourteen teeth in the dental arch simultaneously and in real-time, when fixed orthodontic appliances are used.

The orthodontic simulator (OSIM, Figure 4-1) was built and tested through collaborative work between the Departments of Orthodontics and Mechanical Engineering at the University of Alberta. The OSIM is essentially a human mouth model with a single dental arch containing 14 teeth, to which brackets can be bonded and wires ligated. The OSIM can measure the forces applied by orthodontic appliances on every tooth in the dental arch. The developed software generates real-time three-dimensional displays of the forces acting on every tooth simultaneously. Below is a detailed description of this apparatus.

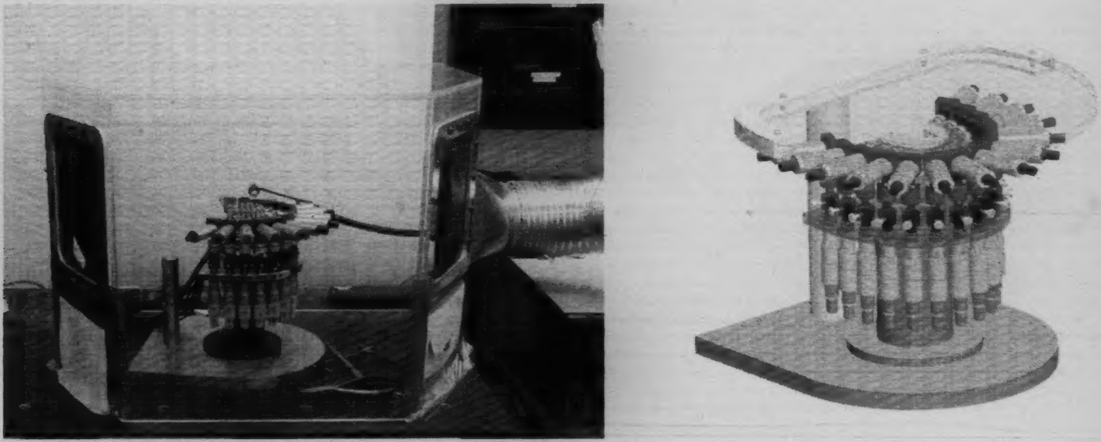

Figure 4-1: Orthodontic Simulator (OSIM) in a temperature chamber

4.2 Hardware:

4.2.1 Force/torque transducers

ATI Industrial Automation Nano17® force transducers (Apex, NC) were used to measure the three force and three moment components of the applied loads. The Nano17 transducer is a compact, rugged, monolithic structure that converts force and torque into analog electrical signals, commonly used as a wrist sensor mounted between a robot and a robot end-effector. The compact transducer is the smallest commercially available 3D load cell that uses silicon strain gauges to sense forces (Figure 4-2).

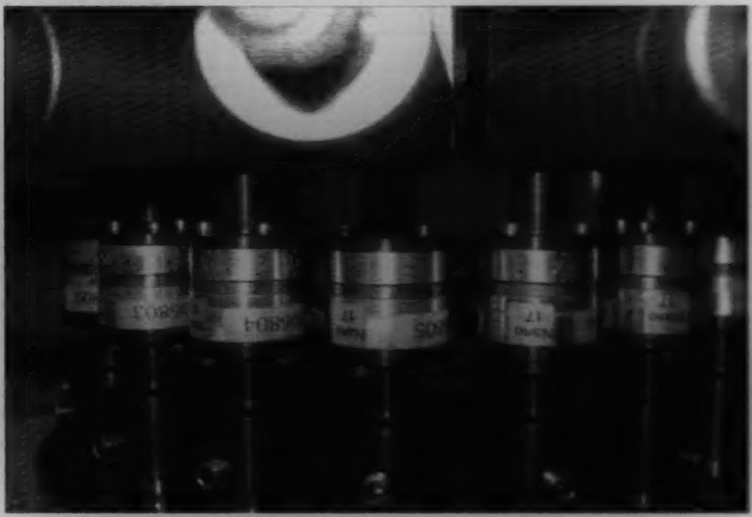

Figure 4-2: Nano 17 force sensors

The force applied to the transducer flexes three symmetrically placed beams machined from a solid piece of metal. Semiconductor strain gauges are attached to the beams. The resistance of the strain gauge changes as a function of the applied strain. The transducer's silicon strain gauges provide high noise immunity and allow high overload protection. The electronic hardware detects the change in resistance, and provides six readings in the form of raw voltages relative to ground. The software converts these voltages to force and moment data using transducer specific calibration curves. Table 4-1 shows the manufacturer-provided error and resolution of measurement for the Nano 17 force sensor.

	Cal	Fx	Fy	Fz	Tx	Ty	Tz
Nano17	SI-59-0.5	1.50%	1.50%	2.00%	1.50%	1.75%	2.00%
Sensing ranges		+/- 50 N	+/- 50 N	+/- 70 N	+/- 500 Nmm	+/- 500 Nmm	+/- 500 Nmm
Resolution DAQ card (N)		1/1280	1/1280	1/1280	1/256	1/256	1/256

Table 4-1: Maximum full-scale measurement uncertainties for Nano 17 transducer (error) (provided by the manufacturer, ATI automation, NC)

The sensor's strain gauges are optimally placed to share information between the forces and torques applied to the sensor. Because of this sharing, it is possible to saturate the transducer with a complex load that has components below the rated load of the sensor. However, this arrangement allows a greater sensing range and resolution. Graphs in Figure 4-3 are used to estimate a sensor's range under complex loading. The sample graph (top graph) shows how operating ranges can change with complex loading. The labels indicate the following regions:

A. Normal operating region. Rated accuracy is expected to be achieved in this region.

B. Saturation region. Any load in this region will report a gauge saturation condition.

C. Extended operating region. In this region, the sensor will operate correctly, but the full-scale accuracy is not guaranteed.

The middle graph represents combinations of forces in the x and/or y directions with torques about the z-axis. The bottom graph represents combinations of z-axis forces with x- and/or y-axis torques. The graphs contain several different calibrations, we used the highest calibration the Nano17 SI-50-0.5.

We chose the Nano17 SI-50-0.5 calibration to make sure that our experimental loads are within the area A on the graphs, which provides the rated accuracy. Our experiments are carried out in the body temperature environment, therefore sensitivity changes due to temperature is an important consideration, Table 4-2 shows that a modest change in sensitivity of less than 0.5% results from placing the transducer in the body temperature environment.

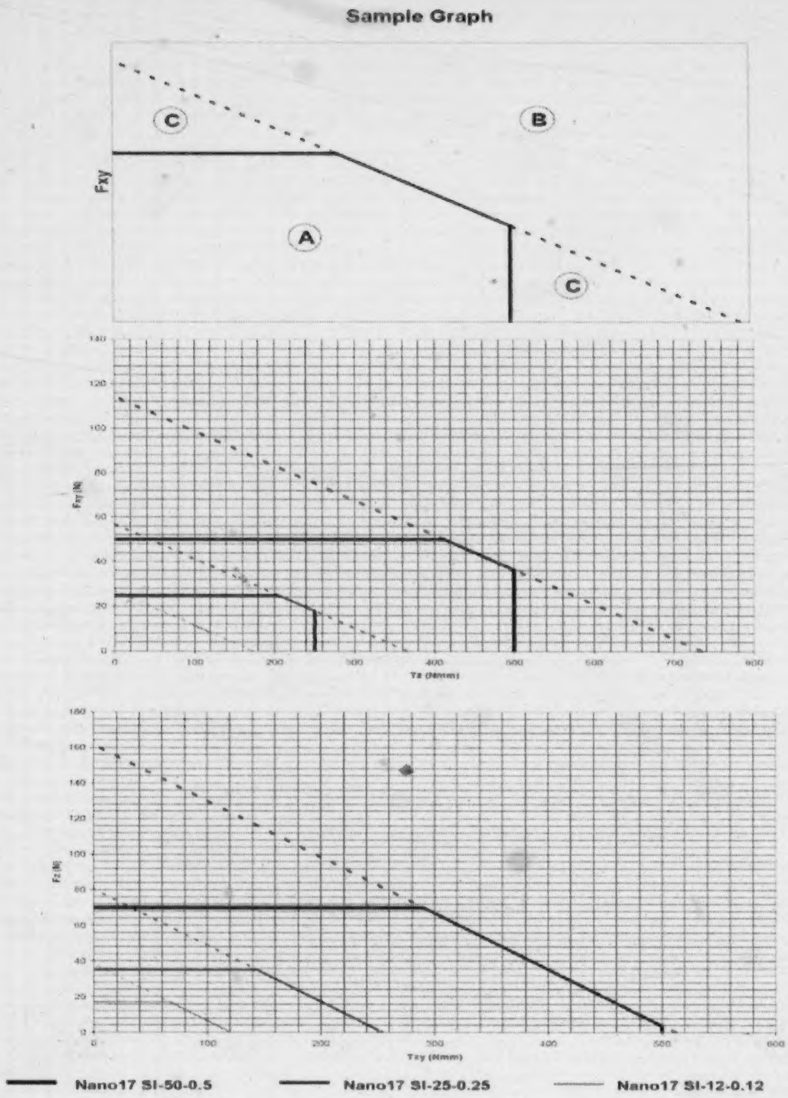

Figure 4-3: Compound Loading Range of Nano17 transducer

Deviation from 22°C	Change in Sensitivity
± 5°C	0.1%
± 15°C	0.5%
± 25°C	1%
± 50°C	5%

Table 4-2: sensitivity change sure to temperature change for the Nano17 (ATI Automation, NC)

4.2.2 Temperature chamber

A temperature chamber (Figure 4-4) was constructed out of plexiglass, in order to simulate the oral environment's temperature. The temperature is monitored using a temperature controller, which controls a heat source. The temperature is maintained at 35-37°C.

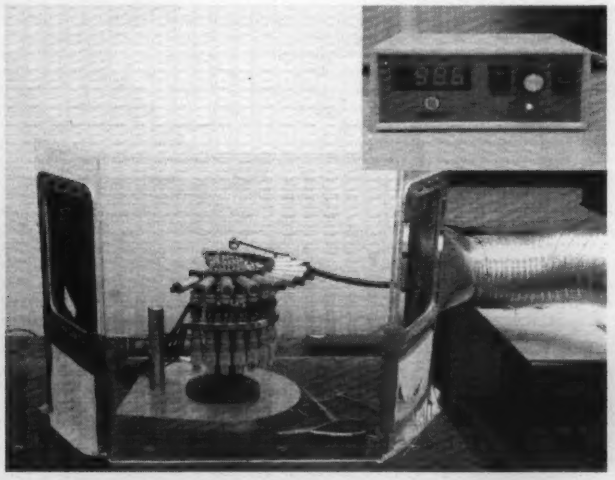

Figure 4-4: temperature chamber and temperature controller

4.2.3 OSIM Device

The Nano17 transducer is 17mm in diameter, human teeth range from 5-11mm in diameter. In order to build a dental arch containing 14 teeth, and connect each tooth to a Nano17 transducer, a special connector was designed for each tooth. The OSIM device (Figure 4-5, Figure 4-6 and Figure 4-7) was built to connect each tooth in a dental arch to its corresponding Nano17 multi-axis force transducers.

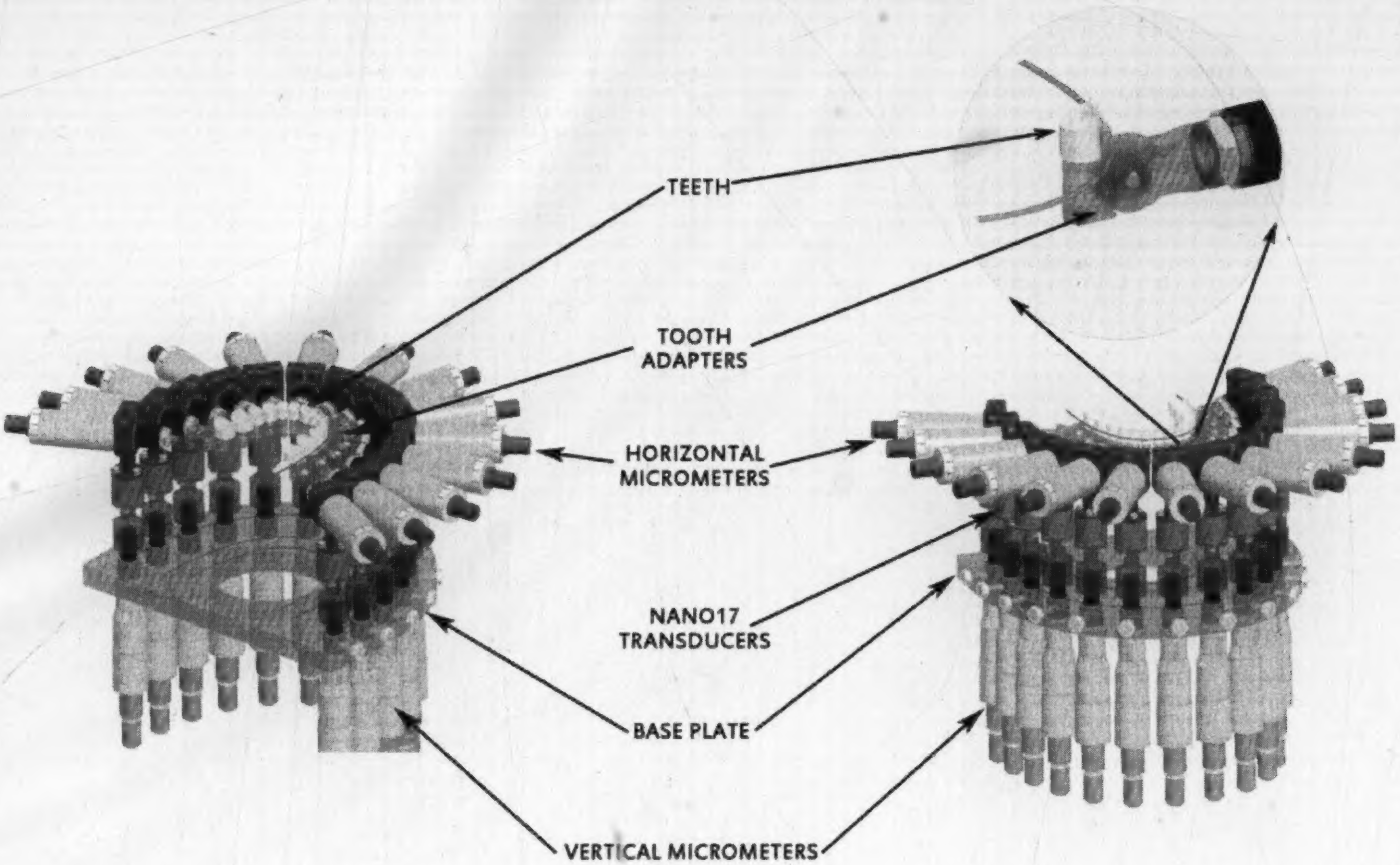

Figure 4-5: OSIM major components

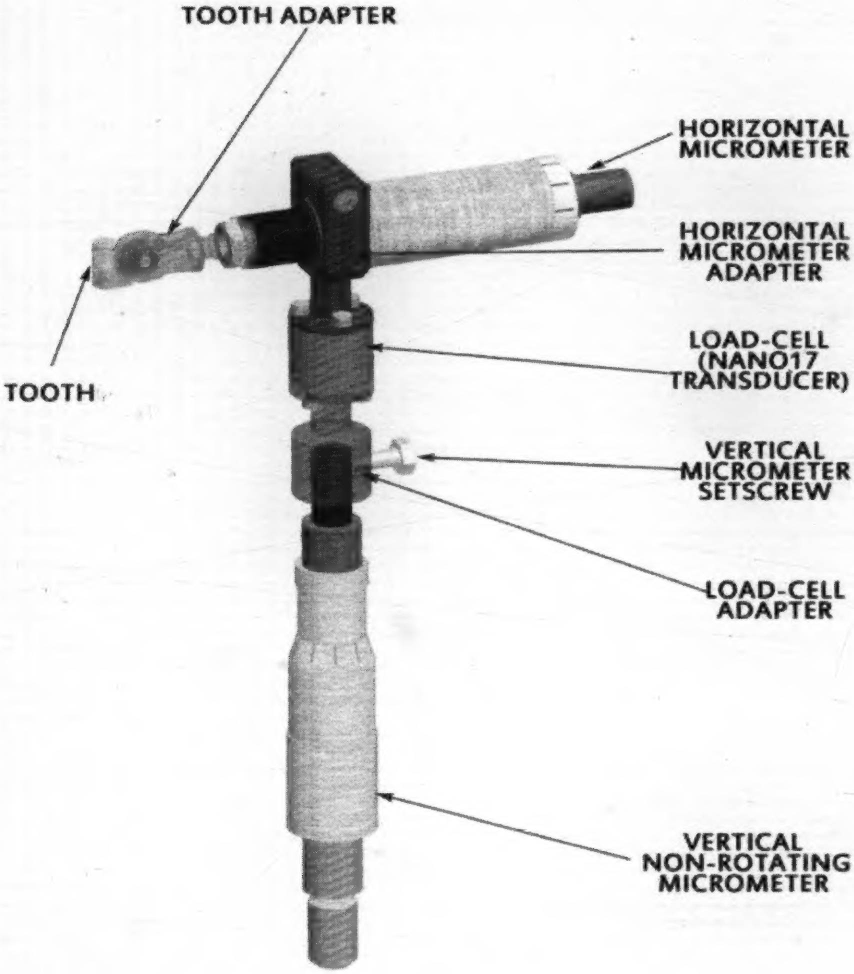
TOOTH ADAPTER
HORIZONTAL MICROMETER
HORIZONTAL MICROMETER ADAPTER
LOAD-CELL (NANO17 TRANSDUCER)
TOOTH
VERTICAL MICROMETER SETSCREW
LOAD-CELL ADAPTER
VERTICAL NON-ROTATING MICROMETER

Figure 4-6: OSIM tooth connector

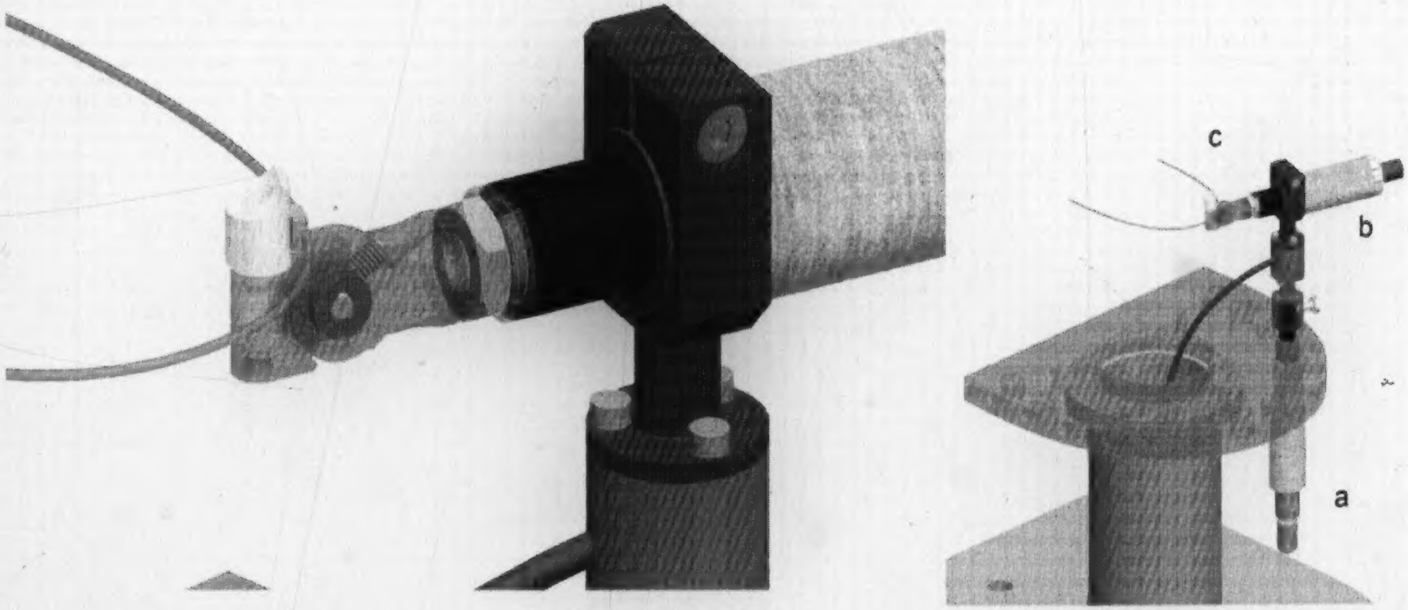

Figure 4-7: load-cell to tooth connector, (a) Vertical micrometer (b) Horizontal micrometer (c) Tooth adapter

We used tooth connectors that incorporated vertical (MTI-153203, MIC 0-25MM Head, Mitutoyo, Japan, figure 6) and horizontal (M-631.00 PI, Germany, figure 4b) micrometer heads with non-rotating spindles. Turning the horizontal micrometers produces horizontal tooth movement, while turning the vertical micrometers produces vertical tooth movement. Complete engineering drawings were made, the Department of Mechanical Engineering machine shop was used to manufacture the different components of the OSIM model. The major components were made of aluminum because of its lightweight, stiffness, and ease of machining. Smaller components were made out of stainless steel and brass.

The Model contains a base plate (Figure 4-5) that holds the 14 vertical micrometers. The load cells are mounted on top of the vertical micrometer spindles using a load-cell adapter, placing the sensing end of the loadcell at the top. Another adapter was mounted on top of the load cell to hold the horizontal micrometer. The spindle of the horizontal micrometer was replaced with a custom-made tooth adapter that holds a platform on which artificial teeth with brackets were mounted. Three types of Aluminum artificial teeth were prepared, on which metal brackets were bonded using epoxy resin (Loctite, E-20HP):

a. Aluminum cylinders 5 mm in diameter with a flat surface to allow accurate orientation of the teeth, with no tooth to tooth contacts.
b. Aluminum cylinders with diameters equal to the widths of natural teeth with a flat surface to allow accurate orientation of the teeth, with tooth to tooth contacts.

c. Anatomically correct Aluminum teeth machined in a multi-axis CNC machine.

Three basic dental arch forms have been described by many clinicians. These include Tapered, Ovoid and Square archforms ([134]), In order to mount the teeth on the OSIM in the default position of natural dentition, the ovoid archform of the MBT archform template (3M, Unitek) was used. This ovoid archform was chosen as the baseline reference for default positioning of the artificial teeth. The following steps were performed to mount the teeth.

1. A placement jig (Figure 4-8) was made to hold the artificial teeth, the jig was made of PVS rubber impression material. This jig holds the teeth such that the flat surfaces of the teeth are parallel to each other.

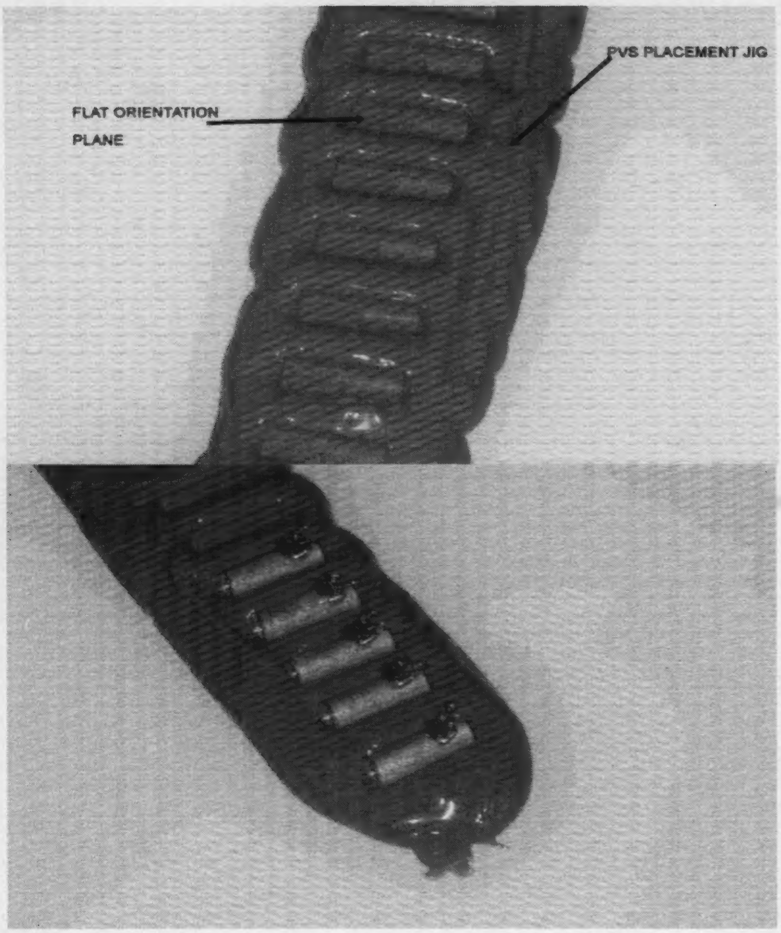

Figure 4-8: bracket-mounting jig

2. A 0.021”X0.025” Stainless Steel straight wire was used to position the brackets. The brackets were attached to the wire using figure-eight elastomeric ligature ties.
3. Epoxy resin was used to glue the brackets onto the artificial teeth. All the brackets were glued at once, while they are ligated to the wire, this ensures that the bracket slots are parallel and that any tip, torque, rotation or in/out prescription in the brackets is eliminated, and that the

brackets are mounted to the teeth with zero prescription and perfect bracket slot alignment between adjacent teeth.

4. An archform template (Figure 4-9) was prepared out of the 3M ovoid archform template. A second archform was drawn on the template, using the measured in/out dimension from the archwire slot to the bracket pad, and the buccoligual dimension of the teeth. This archform was used to locate the midpoints of the teeth as accurately as possible using the data from Table 4-3. This method allowed us to locate the points of application on the ovoid archform.

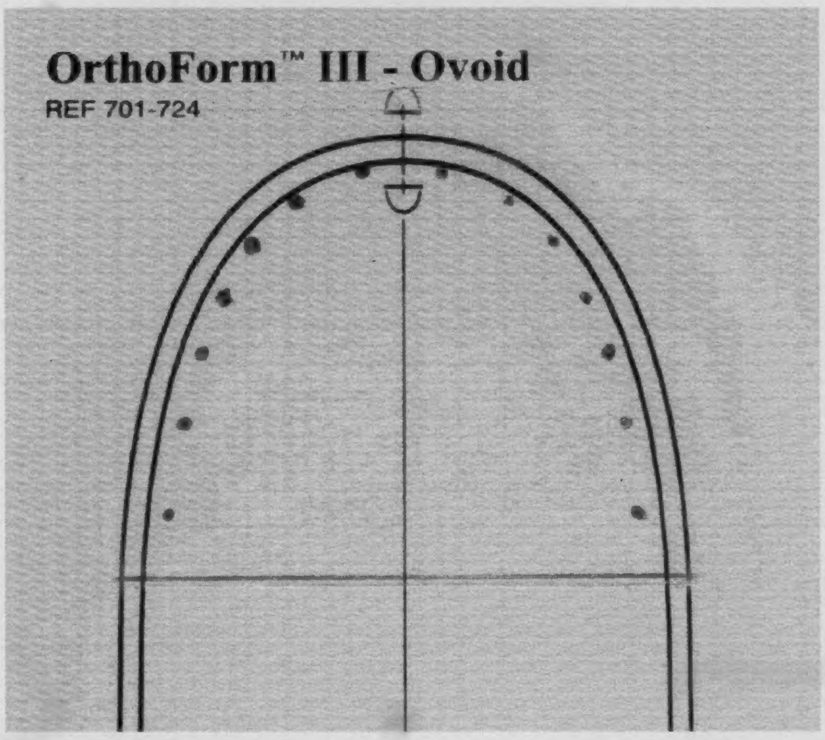

Figure 4-9: tooth-mounting guide

	Mesio-distal dimension	midpoint to midpoint distances	Bucco-lingual dimension	crown Height	root length
upper central	8.7	*4.35	7	10.5	13
upper lateral	6.5	7.6	6	9	13
upper cuspid	7.6	7.05	8	10	17
upper first bicuspid	7	7.3	9	8.5	14.5
upper second bicuspid	6.8	6.9	9	8.5	14
upper first molar	10.5	8.65	11	7.5	12.5
upper second molar	9.8	10.15	11	7	11.5
lower central incisor	5.3	*2.65	6	9	12.5
lower lateral incisor	5.8	5.55	6.5	9.5	14
lower cuspid	6.8	6.3	7.5	11	15.5
lower first bicuspid	7	6.9	7.5	8.5	14
lower second bi	7.1	7.05	8	8	14.5
lower first molar	11	9.05	10	7.5	14
lower second molar	10.6	10.8	9.8	7	12
*: distance measured from midpoint of archform to					

Table 4-3: Tooth sizes (Burlington growth study) used for locating the application points in the OSIM device

5. The teeth were glued to the template according to the reference points drawn.
6. A transfer template was used to transfer the positions of those teeth to the OSIM (Figure 4-10)

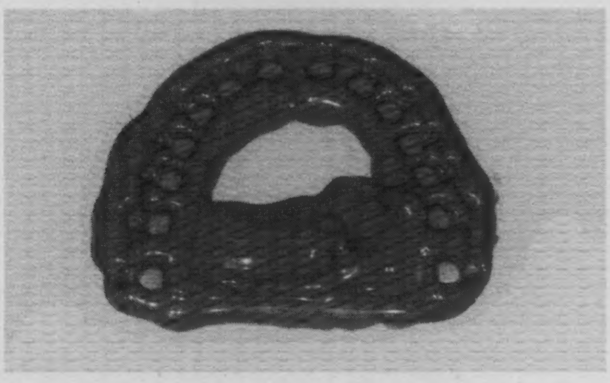

Figure 4-10: transfer template

7. The OSIM tooth platforms were kept horizontal and the vertical micrometers were set.
8. The tooth mounting holes on the tooth platform was positioned to coincide with the artificial teeth threaded holes. The horizontal micrometers were positioned so that the readings of all the teeth are as symmetrical as possible.
9. The readings from the sensors were used for the final positioning of the teeth, using a 0.021"X0.025" Nickel Titanium ovoid archform wire ligated to all teeth. Near zero reading on all the teeth, means that the archwire slots are near perfect parallelism.
10. Two different sets of brackets were prepared using the above method. Damon Mx self-ligating orthodontic brackets and GAC InOvation self-ligating orthodontic brackets were used. The X-Y coordinates of the midpoint of the brackets were measured using a coordinate measurement machine, relative to the OSIM global point of origin, the points are listed in Table 4-4.

tooth number	X coordinate	Y coordinate	Zcoordinate
1	-15.148	24.85	88.8
2	-4.487	23.641	88.8
3	4.122	22.243	88.8
4	10.689	20.038	88.8
5	17.65	17.039	88.8
6	23.062	12.44	88.8
7	26.676	5.535	88.8
8	26.713	-3.336	88.8
9	23.562	-10.876	88.8
10	17.981	-15.97	88.8
11	11.683	-19.503	88.8
12	5.113	-21.966	88.8
13	-3.519	-24.421	88.8
14	-14.574	-26.249	88.8

Table 4-4: X, Y and Z coordinates of the points of application for maxillary arch relative to the OSIM global point of origin

4.2.4 Data acquisition Hardware

A data acquisition device (DAQ) that measures voltages and converts them to digital readings by using Analog to Digital converters (ADCs) was used to automate the measurement process. The DAQ card used (NI PCI-6259, M Series DAQ, 32 Analog Inputs, 48 Digital I/O, 4 Analog Outputs, with NI–DAQmx driver software, National Instruments, Austin, TX) has a sampling rate of 1.25 million samples per second with a 16 bit resolution.

Each load-cell consists of 6 channels, the 14 load-cells take up 84 channels of the DAQ. A PCI expansion card was used to link the load cells to a single DAQ card. Each of the load cells requires a D.C. current of 400mA (at 5V), the manufacturer recommends using a low-noise, low-drift voltage source, therefore an external precision power supply (0 to 18V, 0 to 5A Digital display power supply, model # 1621A, BK Precision, Yorba Linda, CA) was used to power all the load cells. Figure 4-11 is a schematic diagram of the DAQ system hardware.

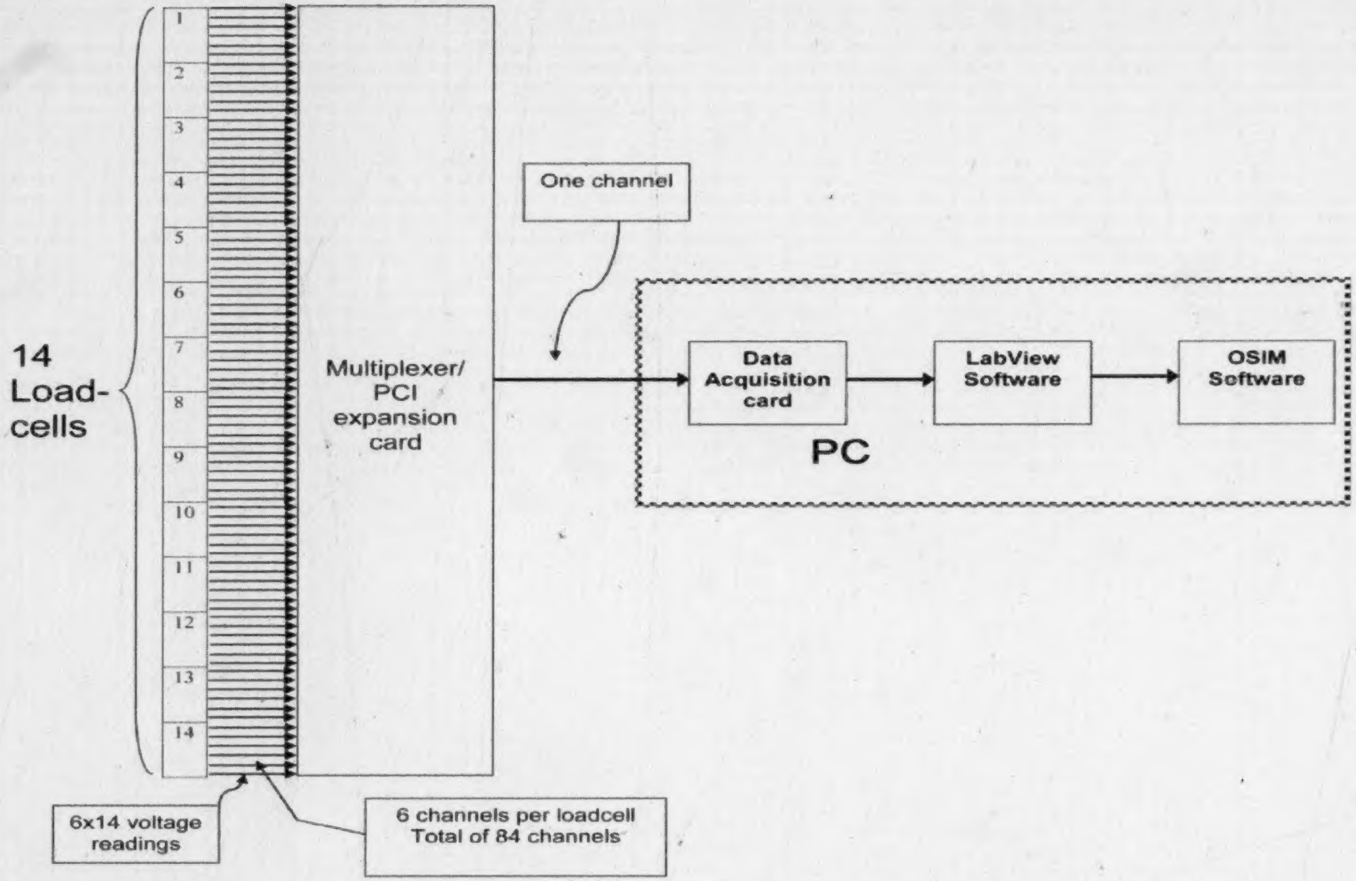

Figure 4-11: data acquisition hardware

4.2.5 Coordinate measurement

The sensors were connected to teeth via custom-made connectors, meaning that the loads are being measured at a point other than the point of load application. Therefore, force system transformations were necessary to transform the force system from the load cell coordinate system to the tooth coordinate system. This process consists of a number of matrix multiplications. In order to perform those transformations, the X, Y and Z coordinates and orientation of the tooth in relation to its corresponding load cell is necessary. FaroArm coordinate measurement machine (Platinum 4ft FaroArm, Lake Mary, FL) was used to accurately measure the position of each tooth relative to its corresponding load cell. This positional data is provided to custom-made Matlab™ software that carries out the force system transformations. Those mathematical transformations are performed in real-time as data is being gathered from the fourteen transducers.

4.2.5.1 Global point of origin and coordinate system determination

In order to carry out the transformations a number of measurements were performed on the OSIM. The middle of the OSIM base-plate contains a cylinder, the centre of which was considered the global point of origin for measurement purposes (Figure 4-12). The following measurements were made using the Faro Arm to construct this point of origin for every transducer/tooth:

1. The upper surface (X-Y surface) of the base plate was measured by recording the coordinates of four points on the surface to construct a plane
2. The back surface (Y-Z surface) of the base plate was measured
3. The circle in the middle of the base plate was constructed by measuring the cylinder and projecting it on the upper surface (X-Y surface). The centre of this circle constituted the global point of origin
4. An orientation line was constructed from the intersection of the two measured planes (the upper and back surfaces of the OSIM base plate, this line was used to orient the global point of origin coordinate system.

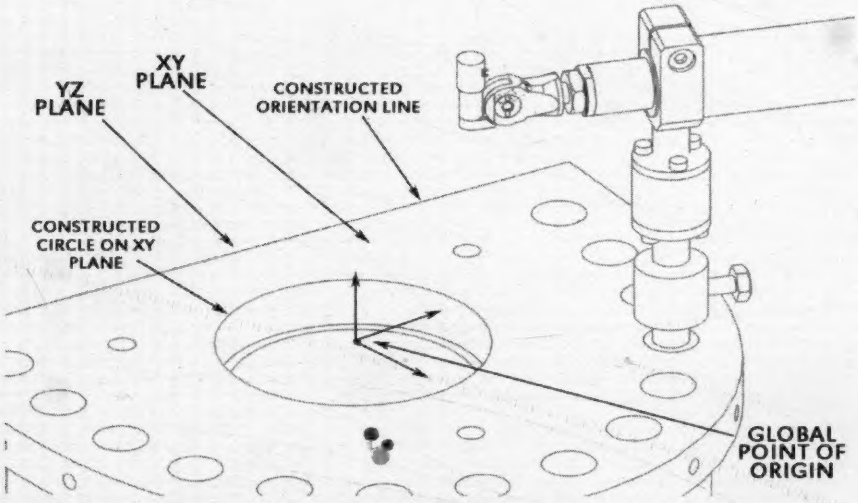

Figure 4-12: Global point of origin determination

4.2.5.2 Transducer point of origin and coordinate system construction

The following measurements were made using the Faro Arm to construct the transducer coordinate system relative to the global point of origin (Figure 4-13):

1. The transducer X-Y plane was measured on the top of the horizontal micrometer adapter
2. The transducer circle was measured and projected at a set distance from the transducer plane. The centre of this circle was considered the point of origin for the transducer plane
3. The transducer orientation plane was measured and a normal to this plane was used to orient the transducer coordinate system. This normal was considered the X-axis of the transducer coordinate system.

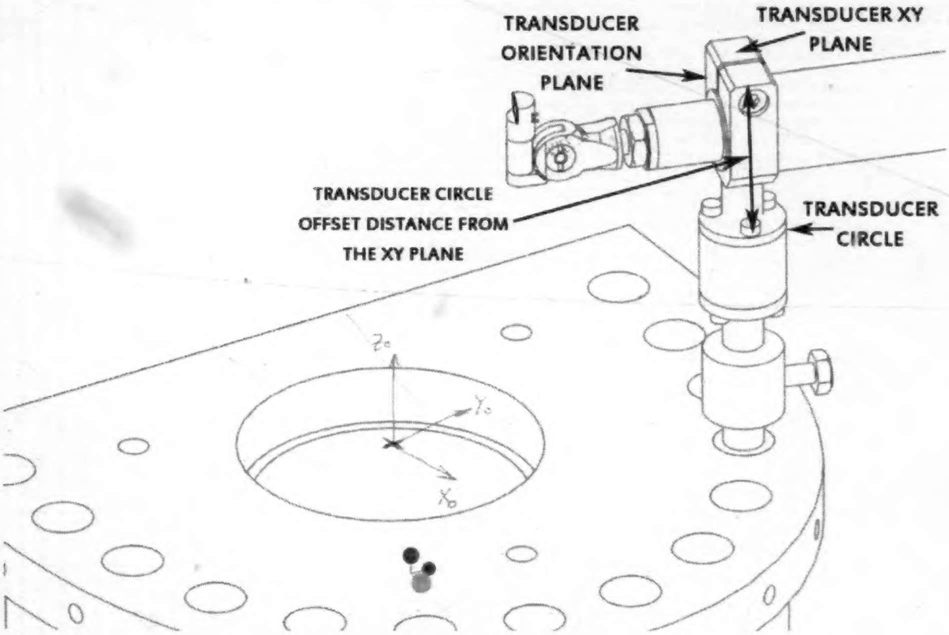
TRANSDUCER ORIENTATION PLANE
TRANSDUCER XY PLANE
TRANSDUCER CIRCLE OFFSET DISTANCE FROM THE XY PLANE
TRANSDUCER CIRCLE
Zo
Yo
Xo

Figure 4-13: Transducer point of origin determination

4.2.5.3 Tooth point of origin and coordinate system construction

The following measurements were made using the Faro Arm to construct the tooth coordinate system relative to the global point of origin (Figure 4-14):

1. The tooth X-Y plane was measured
2. The tooth circle was measured and projected on the tooth X-Y plane, the centre of this circle is the tooth point of origin
3. The tooth orientation plane was measured, a normal to this plane was used for orientation of the tooth coordinate system, this normal was considered the Y-axis of the tooth coordinate system.

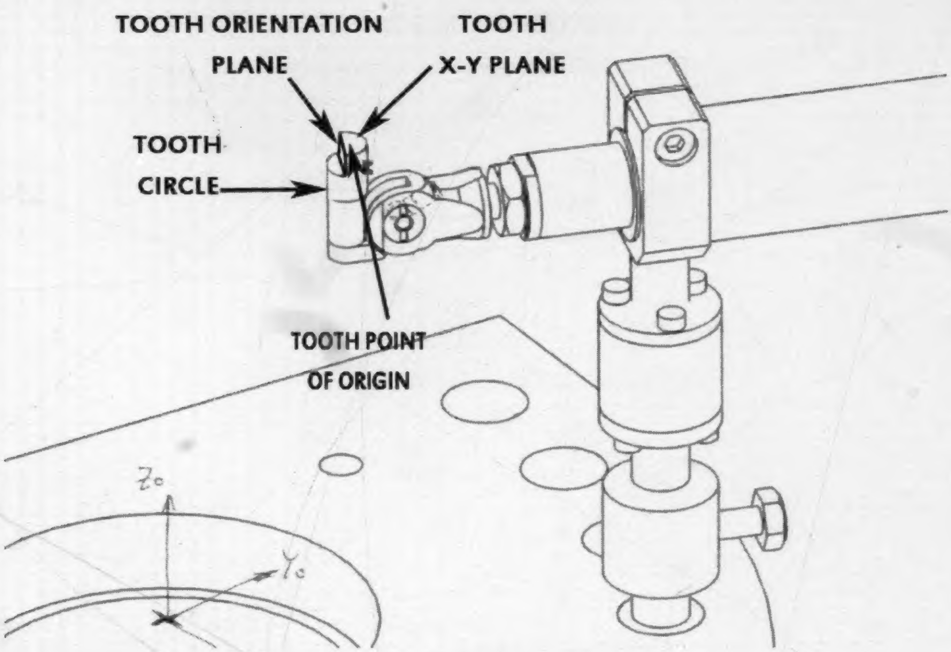

Figure 4-14: the tooth point of origin determination

4.2.5.4 Bracket coordinate system construction

The following measurements were made using a caliper to construct the bracket coordinate system relative to the tooth point of origin (Figure 4-15):

1. The vertical distance from the bracket slot to the X-Y tooth surface was measured.
2. The horizontal distance from the bracket slot to the tooth point of origin was measured.

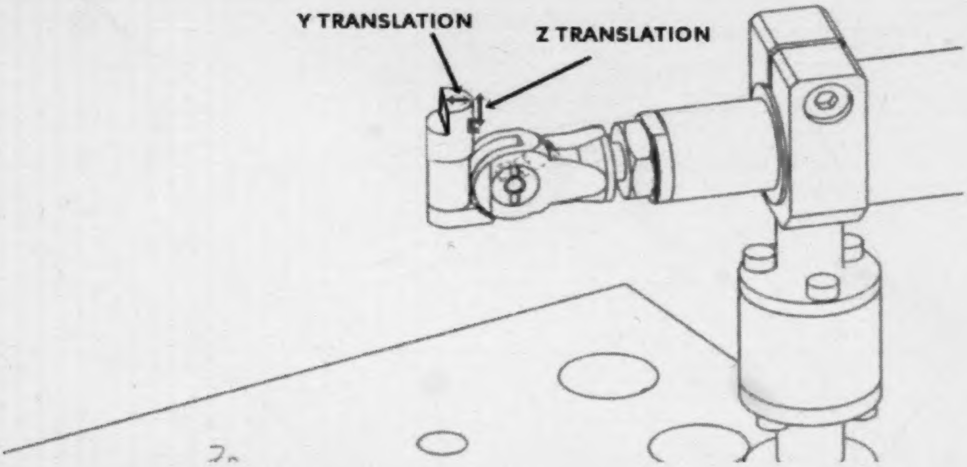

Figure 4-15: the bracket point of origin determination

All of the previous measurements are performed in preparation to construct a bracket coordinate system relative to the global point of origin for one tooth, the same measurements were performed twice for each of the 14 teeth, once using the Damon Mx brackets and another time using the InOvation brackets.

4.2.6 Transformations

4.2.6.1 Positional Transformations

The transducer readings obtained are the forces and moments that are acting at the top of the transducer (the transducer coordinate system). Since the force and moment measurements at the bracket midpoints are required, the force and moment readings are transformed from the transducer to the brackets' coordinate systems. To that effect, exact teeth and load cells positions and orientations in space are required, which allows us to create a homogeneous transformation matrix (T4) that will go from the transducer to the bracket coordinate system (Figure 4-16). The transformation will then be used to create the Jacobian matrix required for the force system transformations. Using the Jacobian transformation matrix, the force and moment readings applied to the bracket midpoint can be calculated from the force and moment readings at the top of the transducers.

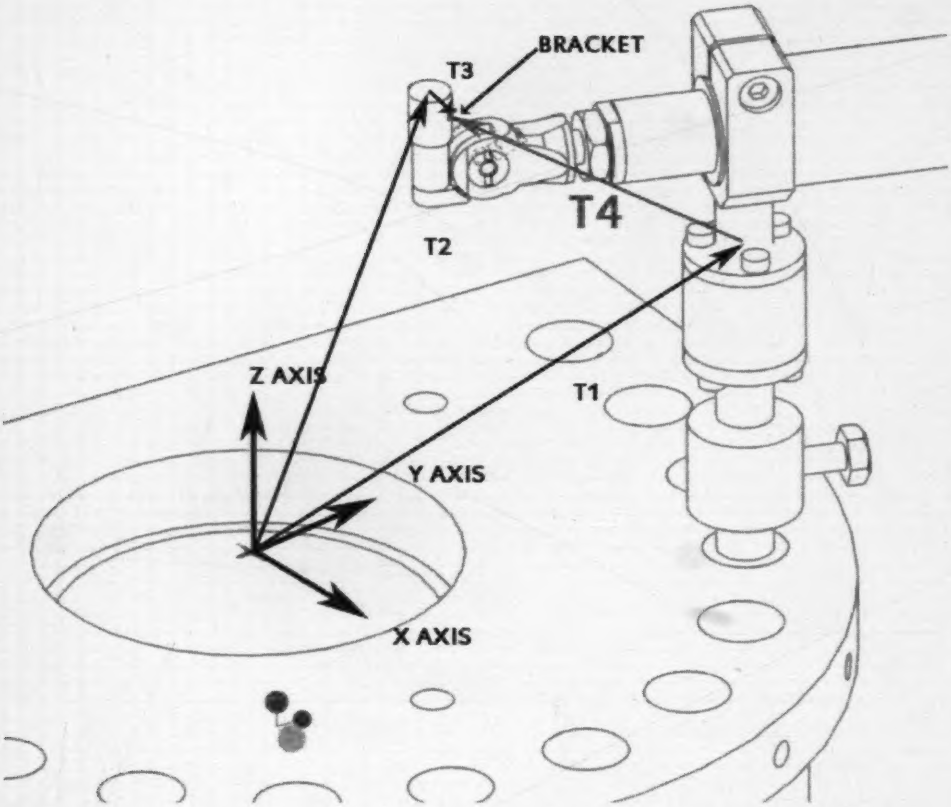

Figure 4-16: Positional transformations T1, T2 and T3 are required to calculate T4 required for the force system transformation from the load-cell coordinate system to the tooth coordinate system.

The homogeneous transformation is a way to represent a coordinate system using a 4x4 matrix. We can label the entries in the 4x4 matrix as follows:

$$\begin{bmatrix} n_x & o_x & a_x & p_x \\ n_y & o_y & a_y & p_y \\ n_z & o_z & a_z & p_z \\ 0 & 0 & 0 & 1 \end{bmatrix}$$

Where p_x, p_y, p_z represent a translation in the x, y, and z axes respectively, relative to some reference coordinate system. n_x, n_y, n_z are the components of the unit vector that represents the direction of the X axis, relative to the reference coordinate system. o_x, o_y, o_z are components of the unit vector that represents the direction of the Y axis, relative to the reference coordinate system. a_x, a_y, a_z are the components of the unit vector that represents the direction of the Z axis of the new coordinate system, relative to the reference coordinate system (Figure 4-17). The four entries on the bottom row of the matrix should always be {0 0 0 1}, in that order. Notice that if we know two of the three vector columns n, o and a, we can calculate the third since they are perpendicular to each other.

$$\begin{array}{cc} & \begin{array}{cccc}\text{X-axis unit vector} & \text{Y-axis unit vector} & \text{Z-axis unit vector} & \text{Translation in x, y, and z}\end{array} \\ T = & \left[\begin{array}{cccc} \boxed{n_x} & \boxed{o_x} & \boxed{a_x} & \boxed{p_x} \\ n_y & o_y & a_y & p_y \\ n_z & o_z & a_z & p_z \\ 0 & 0 & 0 & 1 \end{array}\right]\end{array}$$

Figure 4-17: Typical positional transformation matrix

After determining the position and orientation of the transducer coordinate system in relation to the global point of origin, a homogenous transformation T1 was generated (Figure 4-16). A second homogenous transformation T2 was generated for the position and orientation of the tooth coordinate system and a third transformation T3 was generated for the bracket coordinate system. Using those three transformations the fourth transformation T4 from the transducer coordinate system to the bracket coordinate system was constructed. The T4 transformation is a homogenous 4x4 matrix and it was used to build the Jacobian transformation, required for the force system transformation from the transducer coordinate system to the bracket coordinate system.

4.2.6.2 Jacobian Transformations

When forces and moments are applied to a rigid body at a certain point, it is possible to compute forces and moments that act at a different point on the rigid body (Figure 4-18). This can be performed by simply moving the forces, and finding the equivalent moments using the moment equation (M=F*D). This becomes more complicated when the force system is moved to a differently oriented coordinate system, and even more complicated in 3D than it is for 2D transformations.

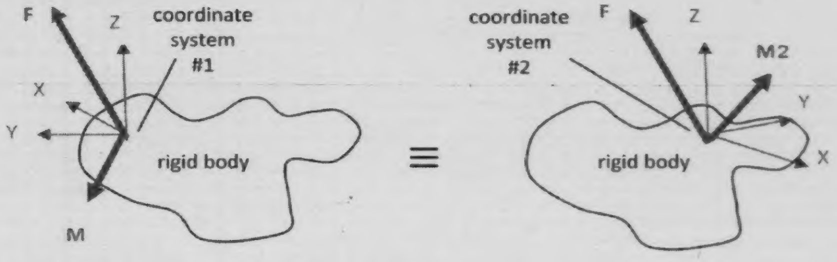

Figure 4-18: force system transformation

The Jacobian transformation is a simplified way to perform these operations, and is used extensively in the field of robotics. It requires the positional transformation (described in the previous section) that describes the path from the coordinate at which we know the forces and moments, to where we would like to find the equivalent forces and moments.

The Jacobian (J) is a 6x6 matrix that is a function of that homogeneous positional transformation.

$$[J] = \begin{bmatrix} n_x & n_y & n_z & 0 & 0 & 0 \\ o_x & o_y & o_z & 0 & 0 & 0 \\ a_x & a_y & a_z & 0 & 0 & 0 \\ (p \times n)_x & (p \times n)_y & (p \times n)_z & n_x & n_y & n_z \\ (p \times o)_x & (p \times o)_y & (p \times o)_z & o_x & o_y & o_z \\ (p \times a)_x & (p \times a)_y & (p \times a)_z & a_x & a_y & a_z \end{bmatrix}$$

After obtaining the Jacobian, we simply perform matrix multiplication of the 6x6 Jacobian by the 3 force components and 3 moment components stored in one 6x1 matrix, to obtain another 6x1 matrix, which is the forces and moments at the required point.

The jacobian transformation generated from the T4 positional homogenous transformation was used to transform the force system from the transducer coordinate system to the bracket coordinate system as shown below.

$$\begin{bmatrix} F_{x\ bracket} \\ F_{y\ bracket} \\ F_{z\ bracket} \\ M_{x\ bracket} \\ M_{y\ bracket} \\ M_{y\ bracket} \end{bmatrix} = \begin{bmatrix} n_x & n_y & n_z & 0 & 0 & 0 \\ o_x & o_y & o_z & 0 & 0 & 0 \\ a_x & a_y & a_z & 0 & 0 & 0 \\ (p \times n)_x & (p \times n)_y & (p \times n)_z & n_x & n_y & n_z \\ (p \times o)_x & (p \times o)_y & (p \times o)_z & o_x & o_y & o_z \\ (p \times a)_x & (p \times a)_y & (p \times a)_z & a_x & a_y & a_z \end{bmatrix} \times \begin{bmatrix} F_{x\ transducer} \\ F_{y\ transducer} \\ F_{z\ transducer} \\ M_{x\ transducer} \\ M_{y\ transducer} \\ M_{y\ transducer} \end{bmatrix}$$

4.3 Software

The OSIM device has 14 transducers, each transducer is producing a large amount of information at a very rapid rate. Real-time three dimensional force system display is necessary to interpret this amount of data. The load-cell manufacturer provides its own software for calibration that can be integrated into common programming environments. The LabView program written for this project is designed to perform several operations. It controls the sampling of the 84 channels by controlling the multiplexer and the DAQ card. After receiving raw voltage readings, calibrations are performed (Figure 4-19). The software provides a text-based display of all voltage readings and all Force/Torque readings in the transducer coordinate system (there are 14 teeth with 6 readings for each tooth, a total 84 readings). Then the software combines all readings into one array, and sends that data to the interface between LabView and the OSIM Software Package. Figure 4-20 shows the data-flow of the OSIM setup.

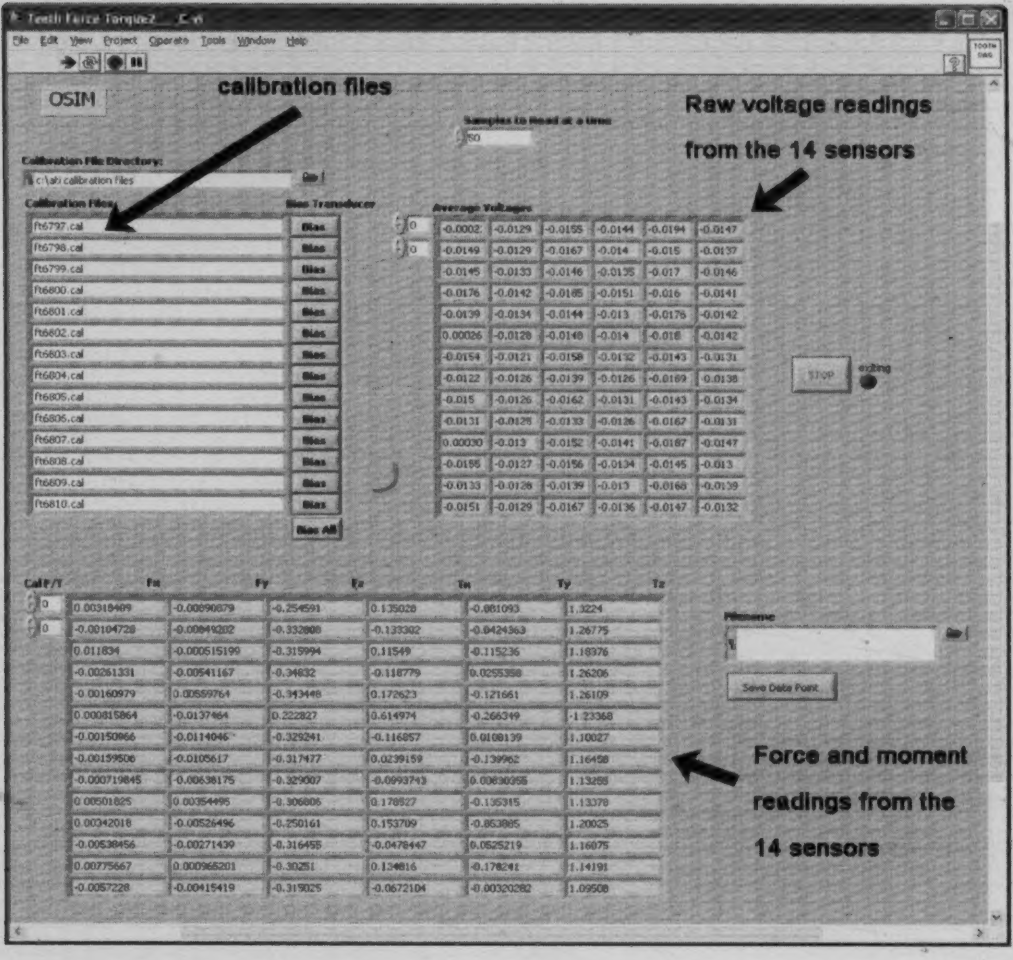

-0.0002	-0.0129	-0.0155	-0.0144	-0.0194	-0.0147
-0.0149	-0.0129	-0.0167	-0.014	-0.015	-0.0137
-0.0145	-0.0133	-0.0146	-0.0135	-0.017	-0.0146
-0.0176	-0.0142	-0.0185	-0.0151	-0.016	-0.0141
-0.0139	-0.0134	-0.0144	-0.013	-0.0176	-0.0142
0.00026	-0.0128	-0.0148	-0.014	-0.018	-0.0142
-0.0154	-0.0121	-0.0158	-0.0132	-0.0143	-0.0131
-0.0122	-0.0126	-0.0139	-0.0126	-0.0169	-0.0138
-0.015	-0.0126	-0.0162	-0.0131	-0.0143	-0.0134
-0.0131	-0.0128	-0.0133	-0.0126	-0.0167	-0.0131
0.00030	-0.013	-0.0152	-0.0141	-0.0187	-0.0147
-0.0155	-0.0127	-0.0156	-0.0134	-0.0145	-0.013
-0.0133	-0.0128	-0.0139	-0.013	-0.0168	-0.0139
-0.0151	-0.0129	-0.0167	-0.0136	-0.0147	-0.0132

Fx	Fy	Fz	Tx	Ty	Tz
0.00318409	-0.00890879	-0.254591	0.135028	-0.881093	1.3224
-0.00104728	-0.00849202	-0.332808	-0.133302	-0.0424363	1.26775
0.011834	-0.000515199	-0.315994	0.11549	-0.115236	1.18376
-0.00261331	-0.00541167	-0.34832	-0.118779	0.0255358	1.26206
-0.00160979	0.00599764	-0.343448	0.172623	-0.121661	1.26109
0.000815864	-0.0137464	0.222827	0.614974	-0.266349	-1.23368
-0.00150966	-0.0114046	-0.329241	-0.116857	0.0108139	1.10027
-0.00159506	-0.0105617	-0.317477	0.0239159	-0.139962	1.16458
-0.000719845	-0.00638175	-0.329007	-0.0993743	0.00830355	1.13288
0.00501825	0.00354495	-0.306806	0.178527	-0.135315	1.13378
0.00342018	-0.00526496	-0.250161	0.153709	-0.853885	1.20025
-0.00538456	-0.00271439	-0.316455	-0.0478447	0.0525219	1.16075
0.00775667	0.000965201	-0.30251	0.134816	-0.178241	1.14191
-0.0057228	-0.00415419	-0.315025	-0.0672104	-0.00320282	1.09508

Figure 4-19: LabView control panel

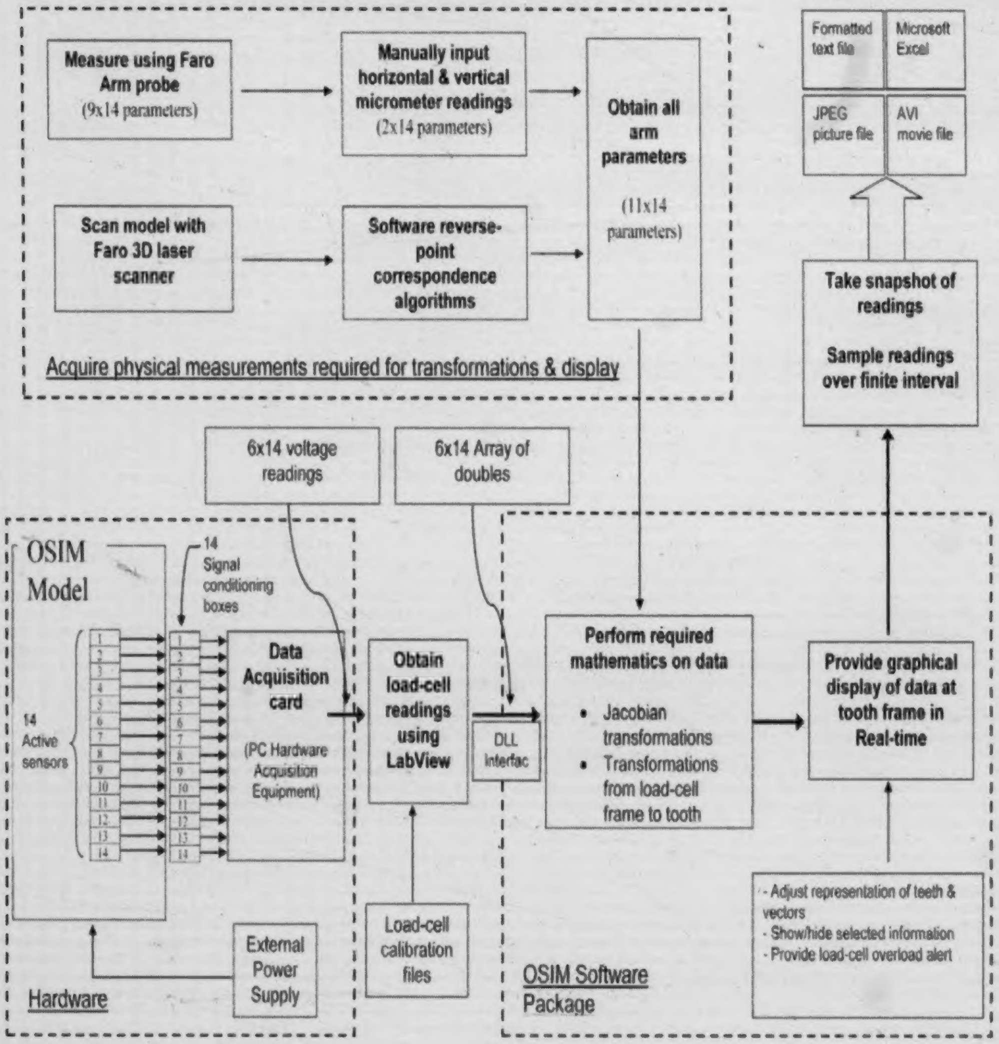
Measure using Faro Arm probe (9x14 parameters)
Manually input horizontal & vertical micrometer readings (2x14 parameters)
Obtain all arm parameters (11x14 parameters)
Scan model with Faro 3D laser scanner
Software reverse-point correspondence algorithms
Acquire physical measurements required for transformations & display
Formatted text file
Microsoft Excel
JPEG picture file
AVI movie file
Take snapshot of readings
Sample readings over finite interval
6x14 voltage readings
6x14 Array of doubles
OSIM Model
14 Signal conditioning boxes
14 Active sensors
1
2
3
4
5
6
7
8
9
10
11
12
13
14
Data Acquisition card
(PC Hardware Acquisition Equipment)
Obtain load-cell readings using LabView
DLL Interfac
Perform required mathematics on data
• Jacobian transformations
• Transformations from load-cell frame to tooth
Provide graphical display of data at tooth frame in Real-time
- Adjust representation of teeth & vectors
- Show/hide selected information
- Provide load-cell overload alert
External Power Supply
Load-cell calibration files
Hardware
OSIM Software Package

Figure 4-20: OSIM dataflow

The OSIM software package was written using MATLAB programming environment and provides functionality to gather and display data. This software was required to provide graphical display of the forces and moments for each load-cell/ tooth (Figure 4-21).

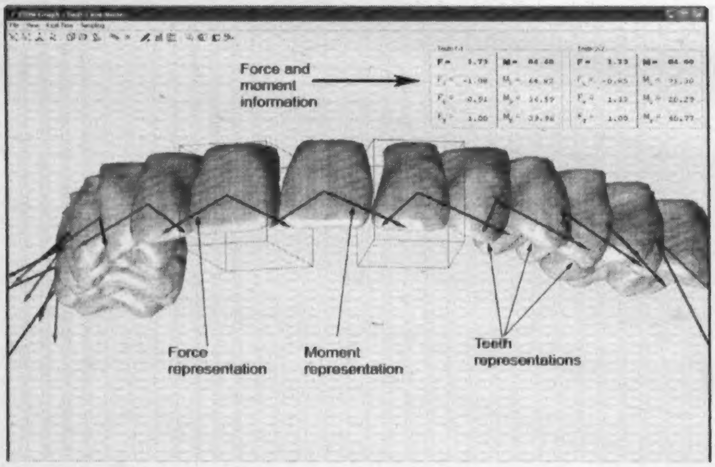

Figure 4-21: OSIM display

These forces and moments are represented by two scaled arrows one for the force and the other for the moment projected on 3D images of the teeth (Figure 4-22). The OSIM software package provides several functions:

- Acquire force and moment data in the transducer coordinate system and apply the Jacobian transformation (discussed above), to produce the force and moment data in the bracket coordinate system. This calculation is performed on every data set collected for each of the 14 transducers.
- The transformations are calculated based on the previously made measurements (discussed in the previous section). The three sets of transformations (world-loadcell, world-tooth and tooth-bracket) can be loaded in the OSIM software (Figure 4-23, Figure 4-24, Figure 4-25) and this information is used for the force and moment calculations.

- Produce 3D graphical representation of the teeth, forces and moments, in real-time (Figure 4-22) and manipulate how information is displayed graphically, using advanced 3D computer graphics techniques.

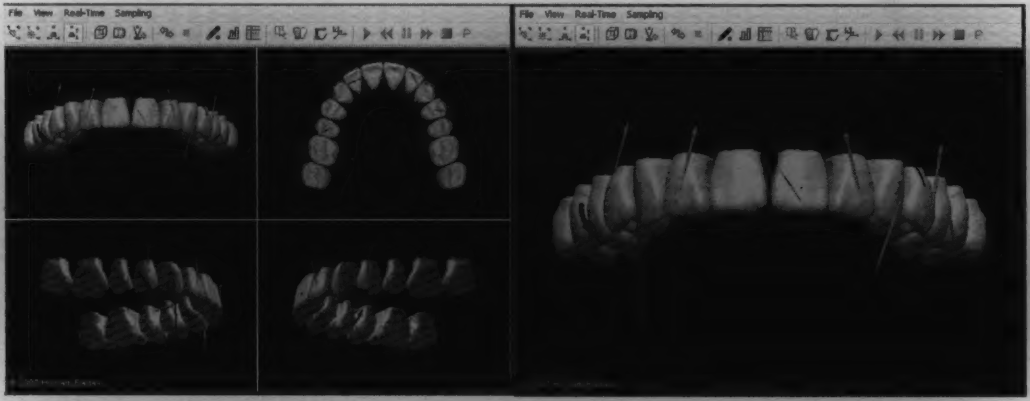

Figure 4-22: OSIM software user interface

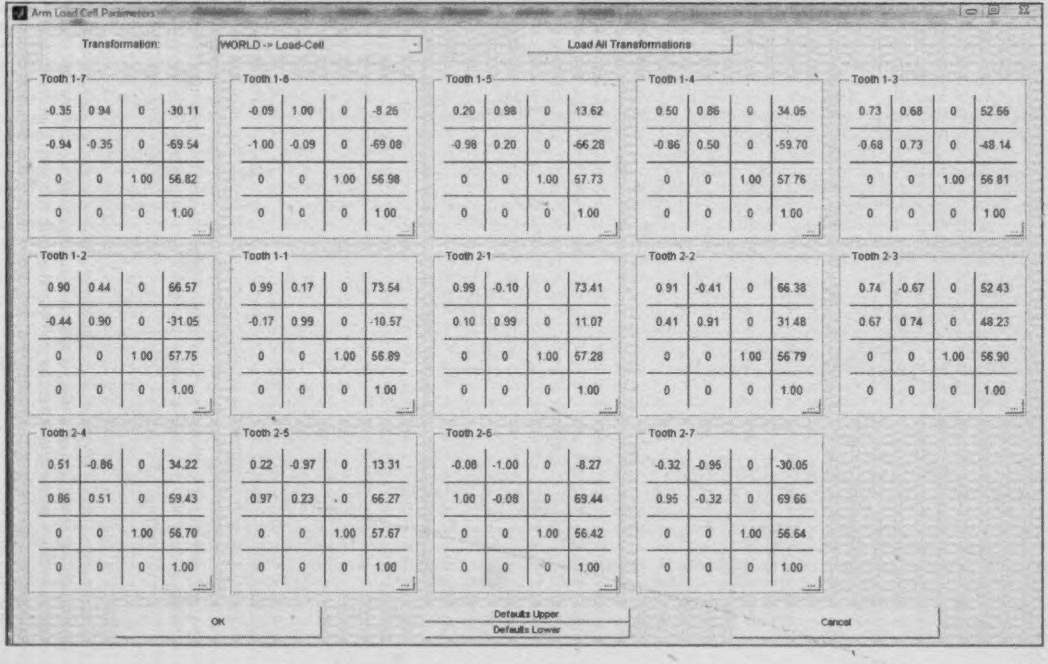

Transformation: WORLD -> Load-Cell

Tooth 1-7

-0.35	0.94	0	-30.11
-0.94	-0.35	0	-69.54
0	0	1.00	56.82
0	0	0	1.00

Tooth 1-6

-0.09	1.00	0	-8.26
-1.00	-0.09	0	-69.08
0	0	1.00	56.98
0	0	0	1.00

Tooth 1-5

0.20	0.98	0	13.62
-0.98	0.20	0	-66.28
0	0	1.00	57.73
0	0	0	1.00

Tooth 1-4

0.50	0.86	0	34.05
-0.86	0.50	0	-59.70
0	0	1.00	57.76
0	0	0	1.00

Tooth 1-3

0.73	0.68	0	52.66
-0.68	0.73	0	-48.14
0	0	1.00	56.81
0	0	0	1.00

Tooth 1-2

0.90	0.44	0	66.57
-0.44	0.90	0	-31.05
0	0	1.00	57.75
0	0	0	1.00

Tooth 1-1

0.99	0.17	0	73.54
-0.17	0.99	0	-10.57
0	0	1.00	56.89
0	0	0	1.00

Tooth 2-1

0.99	-0.10	0	73.41
0.10	0.99	0	11.07
0	0	1.00	57.28
0	0	0	1.00

Tooth 2-2

0.91	-0.41	0	66.38
0.41	0.91	0	31.48
0	0	1.00	56.79
0	0	0	1.00

Tooth 2-3

0.74	-0.67	0	52.43
0.67	0.74	0	48.23
0	0	1.00	56.90
0	0	0	1.00

Tooth 2-4

0.51	-0.86	0	34.22
0.86	0.51	0	59.43
0	0	1.00	56.70
0	0	0	1.00

Tooth 2-5

0.22	-0.97	0	13.31
0.97	0.23	0	66.27
0	0	1.00	57.67
0	0	0	1.00

Tooth 2-6

-0.08	-1.00	0	-8.27
1.00	-0.08	0	69.44
0	0	1.00	56.42
0	0	0	1.00

Tooth 2-7

-0.32	-0.95	0	-30.05
0.95	-0.32	0	69.66
0	0	1.00	56.64
0	0	0	1.00

Figure 4-23: World to load-cell transformation matrices

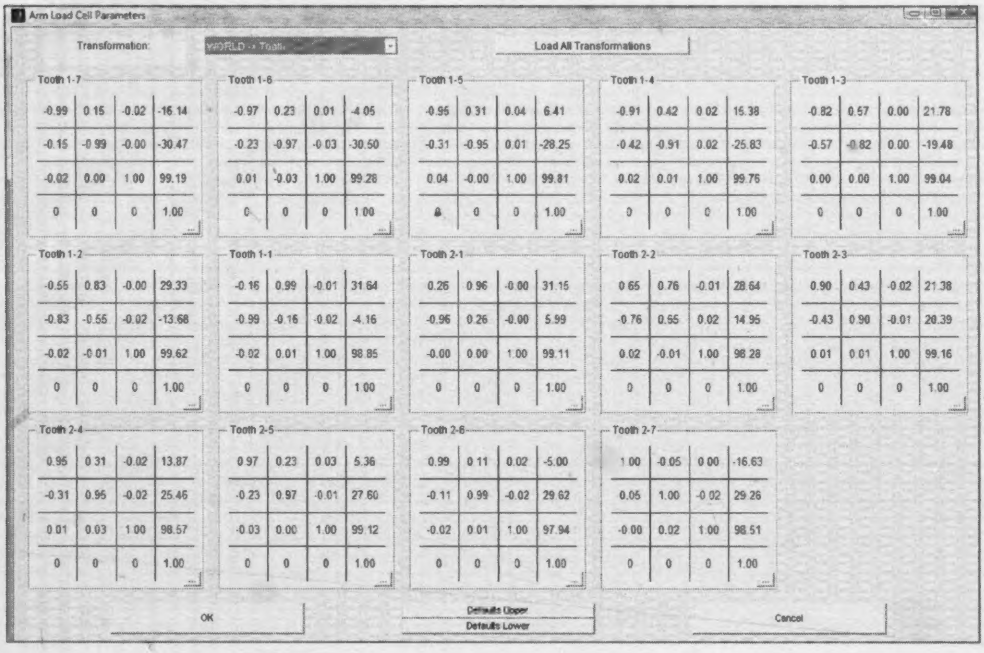

Transformation: WORLD -> Tooth

Tooth 1-7

-0.99	0.15	-0.02	-16.14
-0.15	-0.99	-0.00	-30.47
-0.02	0.00	1.00	99.19
0	0	0	1.00

Tooth 1-6

-0.97	0.23	0.01	-4.05
-0.23	-0.97	-0.03	-30.50
0.01	-0.03	1.00	99.28
0	0	0	1.00

Tooth 1-5

-0.95	0.31	0.04	6.41
-0.31	-0.95	0.01	-28.25
0.04	-0.00	1.00	99.81
0	0	0	1.00

Tooth 1-4

-0.91	0.42	0.02	15.38
-0.42	-0.91	0.02	-25.83
0.02	0.01	1.00	99.76
0	0	0	1.00

Tooth 1-3

-0.82	0.57	0.00	21.78
-0.57	-0.82	0.00	-19.48
0.00	0.00	1.00	99.04
0	0	0	1.00

Tooth 1-2

-0.55	0.83	-0.00	29.33
-0.83	-0.55	-0.02	-13.68
-0.02	-0.01	1.00	99.62
0	0	0	1.00

Tooth 1-1

-0.16	0.99	-0.01	31.64
-0.99	-0.16	-0.02	-4.16
-0.02	0.01	1.00	98.85
0	0	0	1.00

Tooth 2-1

0.26	0.96	-0.00	31.15
-0.96	0.26	-0.00	5.99
-0.00	0.00	1.00	99.11
0	0	0	1.00

Tooth 2-2

0.65	0.76	-0.01	28.64
-0.76	0.65	0.02	14.95
0.02	-0.01	1.00	98.28
0	0	0	1.00

Tooth 2-3

0.90	0.43	-0.02	21.38
-0.43	0.90	-0.01	20.39
0.01	0.01	1.00	99.16
0	0	0	1.00

Tooth 2-4

0.95	0.31	-0.02	13.87
-0.31	0.95	-0.02	25.46
0.01	0.03	1.00	98.57
0	0	0	1.00

Tooth 2-5

0.97	0.23	0.03	5.36
-0.23	0.97	-0.01	27.60
-0.03	0.00	1.00	99.12
0	0	0	1.00

Tooth 2-6

0.99	0.11	0.02	-5.00
-0.11	0.99	-0.02	29.62
-0.02	0.01	1.00	97.94
0	0	0	1.00

Tooth 2-7

1.00	-0.05	0.00	-16.63
0.05	1.00	-0.02	29.26
-0.00	0.02	1.00	98.51
0	0	0	1.00

Figure 4-24: World to tooth transformation matrices

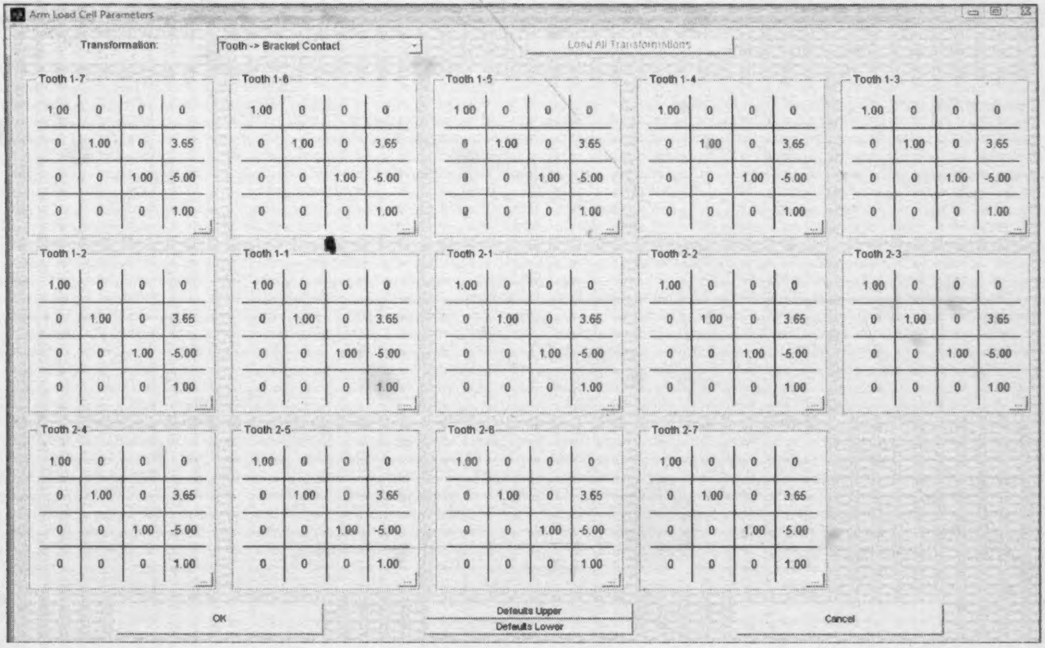

Transformation: Tooth -> Bracket Contact

Tooth 1-7

1.00	0	0	0
0	1.00	0	3.65
0	0	1.00	-5.00
0	0	0	1.00

Tooth 1-6

1.00	0	0	0
0	1.00	0	3.65
0	0	1.00	-5.00
0	0	0	1.00

Tooth 1-5

1.00	0	0	0
0	1.00	0	3.65
0	0	1.00	-5.00
0	0	0	1.00

Tooth 1-4

1.00	0	0	0
0	1.00	0	3.65
0	0	1.00	-5.00
0	0	0	1.00

Tooth 1-3

1.00	0	0	0
0	1.00	0	3.65
0	0	1.00	-5.00
0	0	0	1.00

Tooth 1-2

1.00	0	0	0
0	1.00	0	3.65
0	0	1.00	-5.00
0	0	0	1.00

Tooth 1-1

1.00	0	0	0
0	1.00	0	3.65
0	0	1.00	-5.00
0	0	0	1.00

Tooth 2-1

1.00	0	0	0
0	1.00	0	3.65
0	0	1.00	-5.00
0	0	0	1.00

Tooth 2-2

1.00	0	0	0
0	1.00	0	3.65
0	0	1.00	-5.00
0	0	0	1.00

Tooth 2-3

1.00	0	0	0
0	1.00	0	3.65
0	0	1.00	-5.00
0	0	0	1.00

Tooth 2-4

1.00	0	0	0
0	1.00	0	3.65
0	0	1.00	-5.00
0	0	0	1.00

Tooth 2-5

1.00	0	0	0
0	1.00	0	3.65
0	0	1.00	-5.00
0	0	0	1.00

Tooth 2-6

1.00	0	0	0
0	1.00	0	3.65
0	0	1.00	-5.00
0	0	0	1.00

Tooth 2-7

1.00	0	0	0
0	1.00	0	3.65
0	0	1.00	-5.00
0	0	0	1.00

Figure 4-25: tooth to bracket transformation matrices

- Forces can be represented as one resultant vector (Figure 4-22) or it can be presented using the three components of that force (Figure 4-26). Those vectors are presented in 3D in real-time. The length of the vectors is proportional to the magnitude (Figure 4-27), the scaling of the vector can be modified to preference.

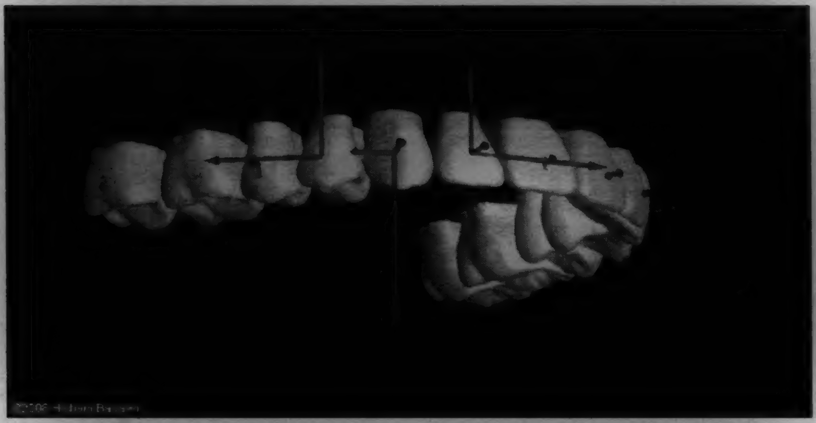

Figure 4-26: X Y and Z component display of force components

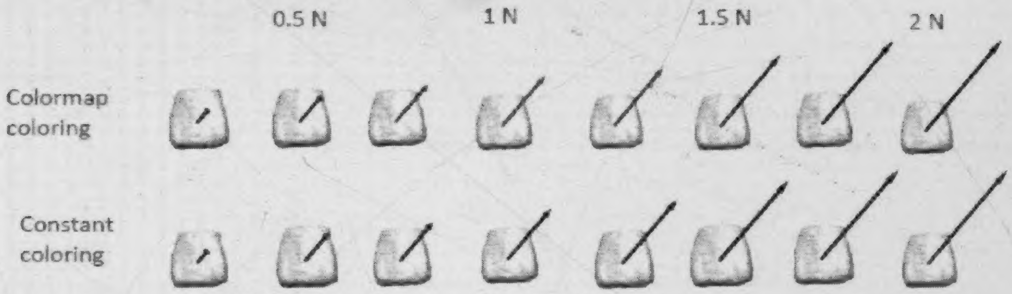

Figure 4-27: Force vector display

- Color indexing of the vectors can be produced according to customized color map that varies the color of the vector depending on the magnitude (Figure 4-28), the colors can be customized to preference.

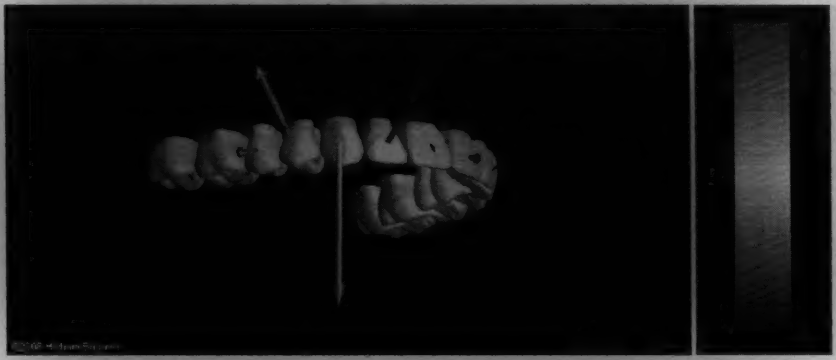

Figure 4-28: color gradient display of force magnitude

- Moments can be displayed using the traditional moment vector display (Figure 4-21) or using an icon that shows the direction of the rotation that would result from the moments (Figure 4-22)
- The OSIM software can record and sample data from the 14 transducers, using either discrete sampling (one sample on command) or timed sampling (take samples for a predetermined length of time at a certain sampling rate (Figure 4-29). Every sample taken has a certain time stamp (Figure 4-30).

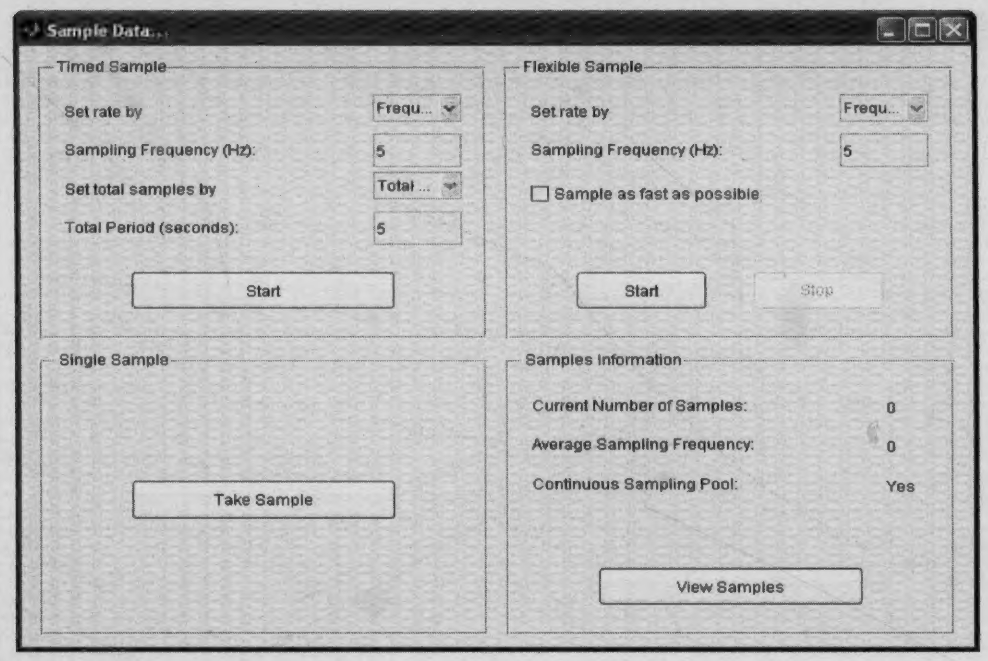

Set rate by Frequ...
Sampling Frequency (Hz): 5
Set total samples by Total ...
Total Period (seconds): 5

Set rate by Frequ...
Sampling Frequency (Hz): 5
☐ Sample as fast as possible

Current Number of Samples: 0
Average Sampling Frequency: 0
Continuous Sampling Pool: Yes

Figure 4-29: sampling window

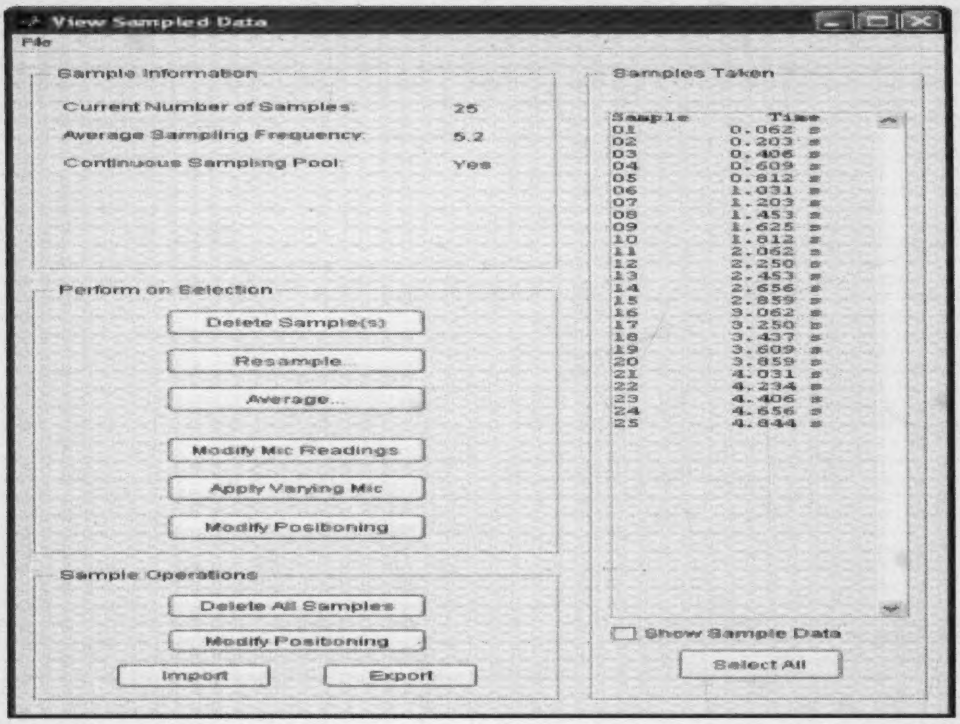

Current Number of Samples: 25
Average Sampling Frequency: 5.2
Continuous Sampling Pool: Yes

```
Sample        Time
01          0.062 s
02          0.203 s
03          0.406 s
04          0.609 s
05          0.812 s
06          1.031 s
07          1.203 s
08          1.453 s
09          1.625 s
10          1.812 s
11          2.062 s
12          2.250 s
13          2.453 s
14          2.656 s
15          2.859 s
16          3.062 s
17          3.250 s
18          3.437 s
19          3.609 s
20          3.859 s
21          4.031 s
22          4.234 s
23          4.406 s
24          4.656 s
25          4.844 s
```

☐ Show Sample Data

Figure 4-30: samples view

- If micrometers settings were changed during data gathering, we can retrospectively change the micrometer settings and this will in turn update and reapply the force system Jacobian transformations to the collected samples
- Samples can be exported in a .samp format readable by the OSIM software in order to replay previously collected samples, the .samp file contains the samples as well as the transformation information
- Samples can be exported in JPEG picture format and AVI video format, useful for scientific presentations

- Samples can be exported into Excel format for statistical analysis, raw untransformed data, as well as tooth-transformed data can be exported. The software can export the micrometer readings as well as all the positional data used for the transformations
- The OSIM can perform error analysis on the transducer readings, for checking the accuracy and precision of each transducer this is described below in more detail (Figure 4-31, Figure 4-32)

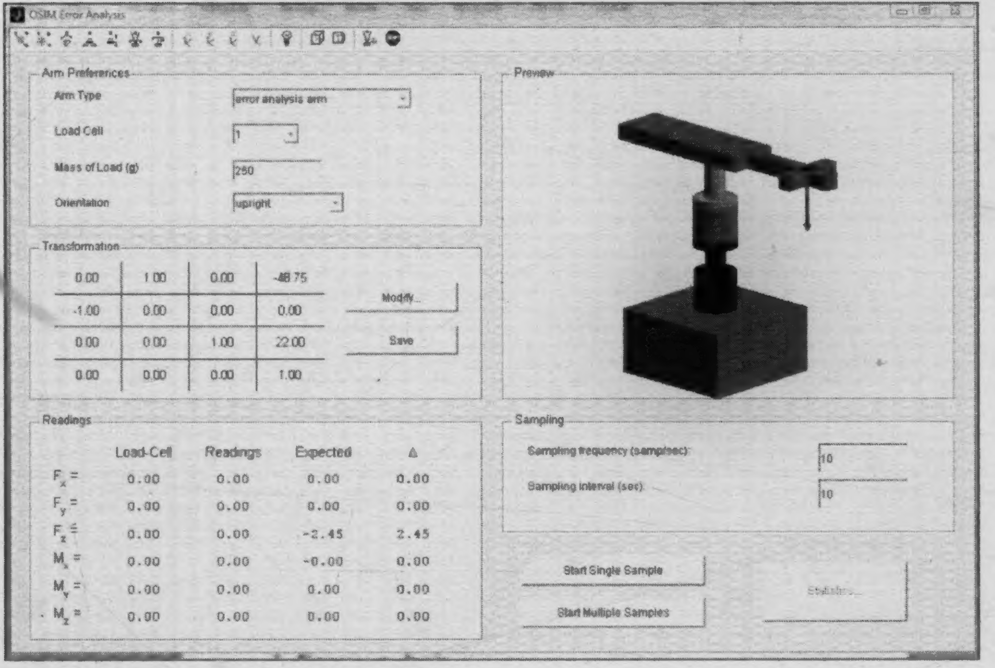

Arm Type: error analysis arm
Load Cell: 1
Mass of Load (g): 250
Orientation: upright

0.00	1.00	0.00	-48.75
-1.00	0.00	0.00	0.00
0.00	0.00	1.00	22.00
0.00	0.00	0.00	1.00

	Load-Cell	Readings	Expected	Δ
F_x =	0.00	0.00	0.00	0.00
F_y =	0.00	0.00	0.00	0.00
F_z =	0.00	0.00	-2.45	2.45
M_x =	0.00	0.00	-0.00	0.00
M_y =	0.00	0.00	0.00	0.00
M_z =	0.00	0.00	0.00	0.00

Sampling frequency (samp/sec): 10
Sampling interval (sec): 10

Figure 4-31: Error analysis window

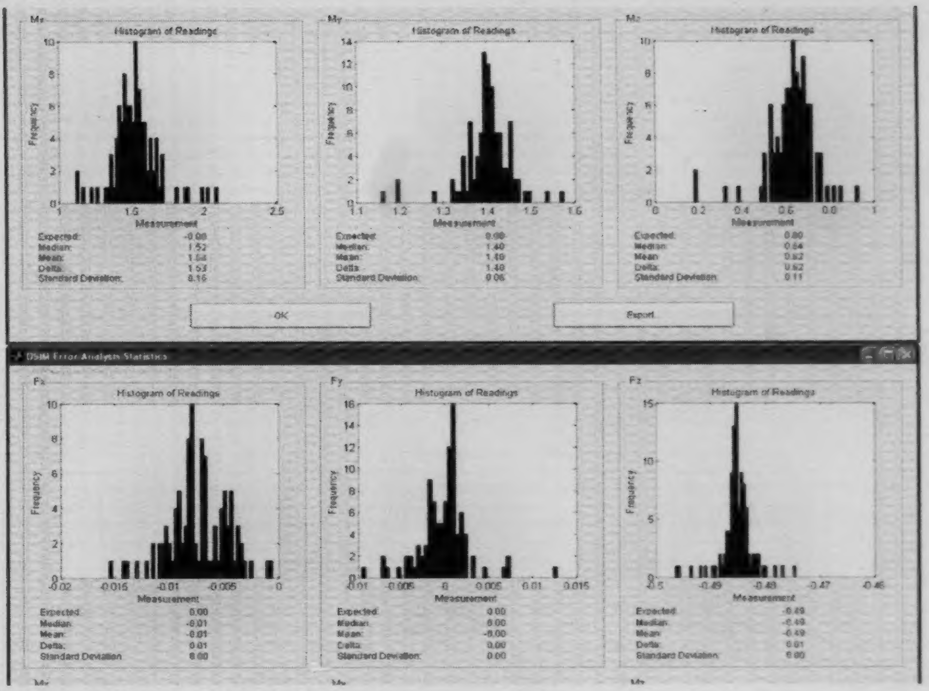

Mx
Expected: -0.00
Median: 1.52
Mean: 1.54
Delta: 1.53
Standard Deviation: 0.16

My
Expected: 0.00
Median: 1.40
Mean: 1.40
Delta: 1.40
Standard Deviation: 0.06

Mz
Expected: 0.00
Median: 0.64
Mean: 0.62
Delta: 0.62
Standard Deviation: 0.11

Fx
Expected: 0.00
Median: -0.01
Mean: -0.01
Delta: 0.01
Standard Deviation: 0.00

Fy
Expected: 0.00
Median: 0.00
Mean: -0.00
Delta: 0.00
Standard Deviation: 0.00

Fz
Expected: -0.49
Median: -0.49
Mean: -0.49
Delta: 0.01
Standard Deviation: 0.00

Figure 4-32: Force and moment error analysis

- As a safety precaution, the OSIM software can monitor all the loads on the transducer and produce a visual and audible alert if a predetermined load level (force or moment overload threshold input window, Figure 4-33) is exceeded on any of the transducers (Figure 4-34).

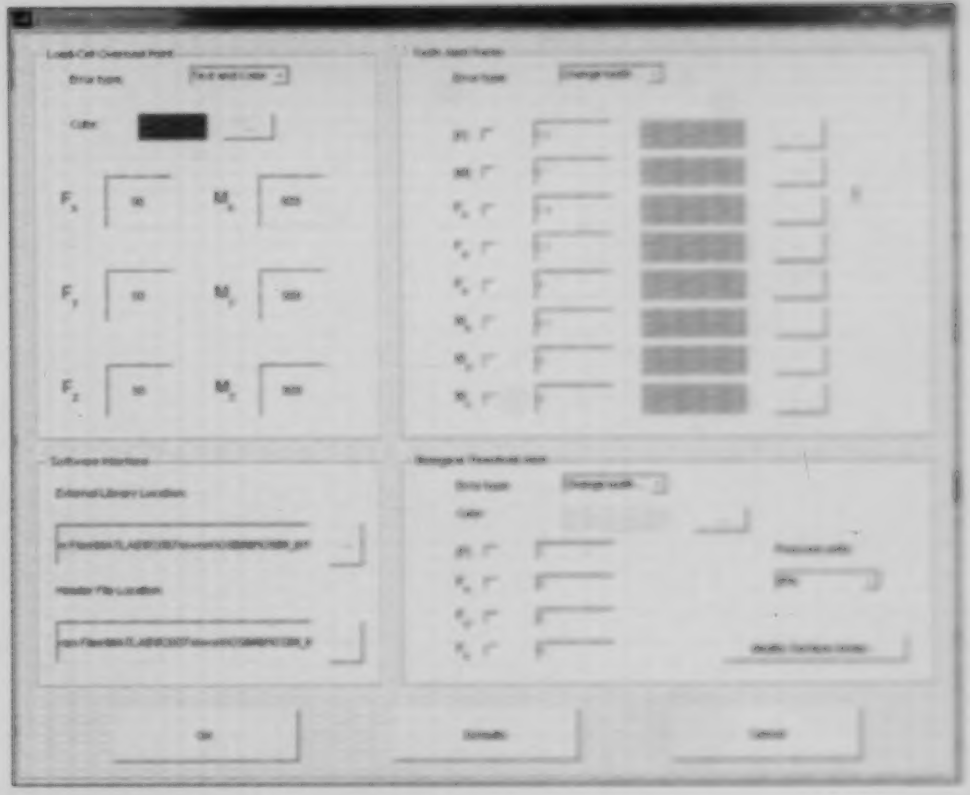

Figure 4-33: Overload protection window, force or moment overload threshold input window

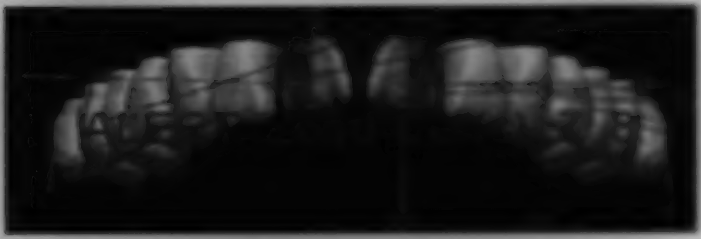

Figure 4-34: Overload alert

- The OSIM can play two or more previously collected samples simultaneously to allow easy visual comparisons between two or more samples (Figure 4-35)

Figure 4-35: Multi-sample Display

- The OSIM can monitor any force or moment on all teeth and provide visual indicator or text alert if the monitored force or moment exceeds a predetermined level (Figure 4-36)

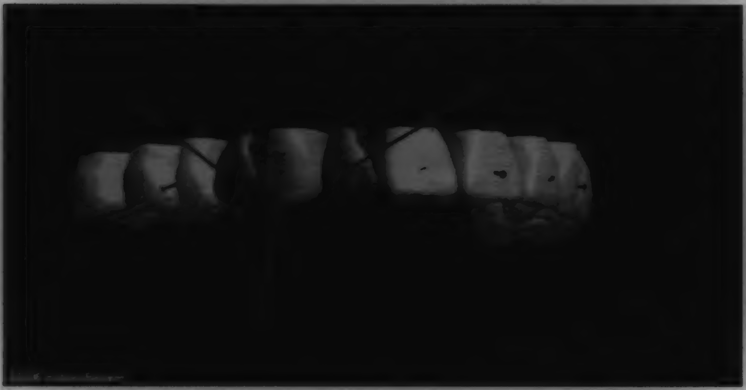

Figure 4-36: tooth alerts of teeth experiencing F_x higher than 0.4N

- The OSIM can play previously collected samples, the playing mode depends on the data gathering mode (discrete or continuous sampling pool) (Figure 4-37).

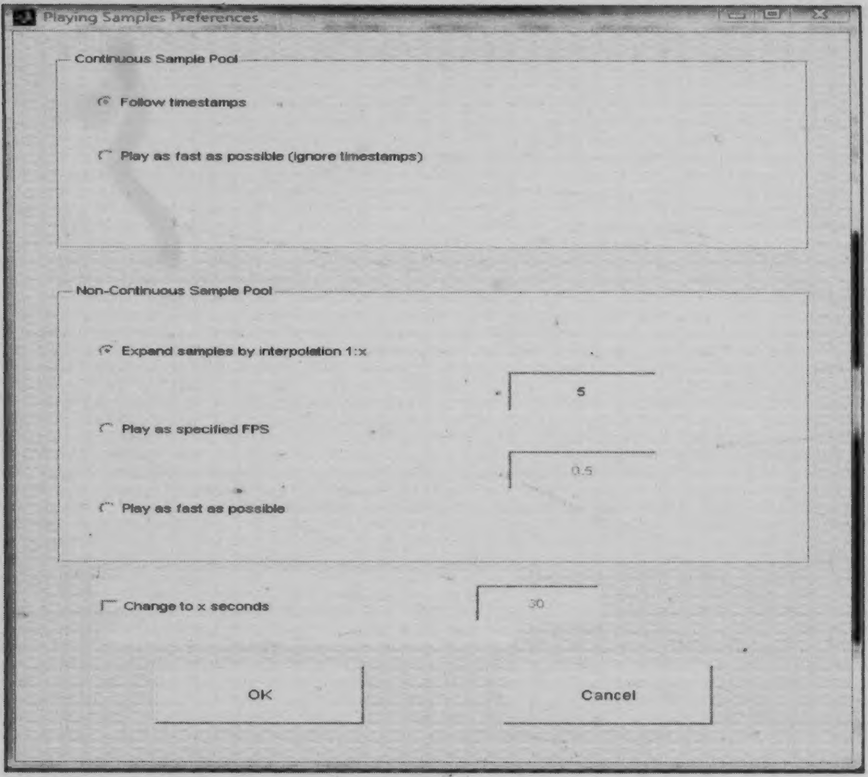

Continuous Sample Pool

● Follow timestamps

○ Play as fast as possible (ignore timestamps)

Non-Continuous Sample Pool

● Expand samples by interpolation 1:x 5

○ Play as specified FPS 0.5

○ Play as fast as possible

☐ Change to x seconds 30

Figure 4-37: OSIM sample playing options

4.3.1 Sign convention

The sign convention used in the OSIM software is presented in Table 4-5, notice that that Fx, My and Mz sign indicates a different direction for the right and left sides of the dental arch.

	Sign	**Right side**	**Left side**
F_x	Positive	Distal	Mesial
	Negative	Mesial	Distal
F_y	Positive	Buccal	Buccal
	Negative	Lingual	Lingual
F_z	Positive	Intrusion	Intrusion (apical)
	Negative	Extrusion	Extrusion (occlusal)
M_x	Positive	Buccal crown torque	Buccal crown torque
	Negative	Lingual crown torque	Lingual crown torque
M_y	Positive	Mesial tip	Distal tip
	Negative	Distal tip	Mesial tip
M_z	Positive	Disto-Buccal rotation	Mesio-Buccal rotation
	Negative	Mesio-Buccal rotation	Disto-Buccal rotation

Table 4-5: Sign convention

4.4 Error analysis

The overall error in this device is the result of the following sources:

1. Error inherent in the load cell raw readings
2. Errors due to inaccuracies in performing the transformations due to metrology errors from the coordinate measurement machine
3. Errors due to the transformations. The transformations magnify the error of the load cell and is generally proportional to the moment arm (the distance from the point of load application to the load-cell)

A calibration arm (Figure 4-38 a) was built to measure the overall error (the error resulting from the three sources listed above). Using the calibration arm, we were able to apply known loads on specific axes using calibrated weights. The loads were applied on one axis at a time and this was done by reorienting the calibration arm and using gravity to apply the loads (Figure 4-38 b, c, d). In order to ascertain that the loads were applied only on one axis at a time, a precision master level (Starrett No. 199 Master Precision Level) was used to make sure that the calibration arm was level and properly oriented, indicating that when a load is applied in F_x the transducer should theoretically give zero readings on all other components. If F_y was loaded the transducer should theoretically give zero readings on all other components.

Error data was collected for each of the 14 transducers. The calibration arm was mounted on each transducer and was loaded from zero to 500gm in 50gm increments. The calibration arm was reoriented to six different positions to allow us to apply loads in +X, -X, +Y, -Y, +Z, -Z. Two hundred samples were gathered for each load, and the average was calculated.

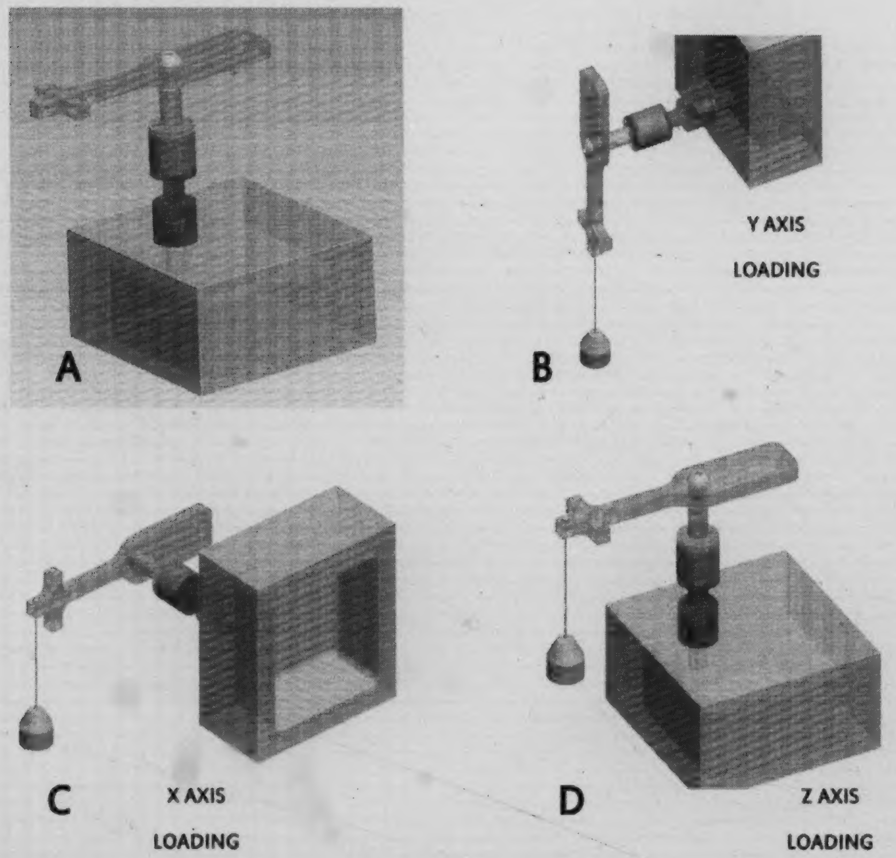

Figure 4-38: (a) Calibration arm (b) Testing weight applied in F_y (c) Testing weight applied in F_x (d) Testing weight applied in F_z

The force error of the loaded axis (e_L) is reported as a percentage by calculating the difference between actual (F_a) and expected (F_e), and dividing it by the expected (Equation 4-1).

$$Errorintheloadedaxis = \frac{expected\ reading\ of theloaded\ axis - actual\ reading\ of theloaded\ axis}{expected\ rea\,ding\ of theloaded\ axis} \times 100\%$$

Equation 4-1: Error in the loaded axis

The force error of the unloaded axis (e_U) (which should have a zero load) is reported as a percentage by dividing the actual reading of the unloaded axis (F_{au}) by the expected reading of the loaded axis (Equation 4-2).

$$e_U = \frac{F_{au}}{F_e} \times 100\%$$

Equation 4-2

The moment errors were derived by factoring in the moment arm for that specific moment, moment arms for M_x M_y and M_z are 53.5mm, 22mm and 48.75mm respectively. In other words, the force that is required to generate the moment is calculated, and then that force value is used for the error calculation by dividing it by the expected force of the loaded axis following Equation 4-1.

Twenty different weights were applied to each transducer in each of the three axes (X, Y and Z). To report the error in F_y (for example) when the X axis is being loaded, we calculated the average error in F_y when the load was being applied in the X axis, and reported it in one percentage number. The same was performed for all six components (F_x, F_y, F_z, M_x, M_y, M_z). The force error data is reported in Table 4-6 and the moment error data is reported in Table 4-7.

When F_x was being loaded, the overall average error is 1.84%. In F_y Loading the overall average error is 1.38%. When F_z was being loaded, the overall average error is 1.75%. The overall average error in the force reading from the 14 transducers is 1.66% (Table 4-6).

When F_x was being loaded, the overall average error in moments is 2.4%. In F_y Loading the overall average error in moments is 1.53%. In Fz loading the overall average errors in moments is 2.59%. The overall average error in the moment reading from the 14 transducers is 2.17% (Table 4-7).

		Fx Load applied			Fy Load applied			Fz Load applied			average error in Fx per loadcell	average error in Fy per loadcell	average error in Fz per loadcell	Overall Force error per loadcell
	Load cell	Fx	Fy	Fz	Fx	Fy	Fz	Fx	Fy	Fz				
average	1	1.49%	2.67%	0.97%	2.20%	0.20%	3.23%	0.43%	0.57%	5.36%	1.37%	1.14%	3.19%	1.90%
SD	1	0.60%	0.94%	0.32%	0.17%	0.13%	0.91%	0.26%	0.44%	2.47%				0.39%
average	2	1.43%	0.62%	1.59%	0.25%	0.48%	1.14%	0.52%	0.61%	2.52%	0.73%	0.57%	1.75%	1.02%
SD	2	0.42%	0.35%	0.63%	0.19%	0.15%	0.71%	0.36%	0.26%	1.64%				0.39%
average	3	2.00%	1.44%	0.46%	0.19%	0.18%	1.11%	0.39%	0.41%	1.74%	0.86%	0.68%	1.11%	0.88%
SD	3	0.47%	0.92%	0.25%	0.04%	0.12%	0.61%	0.33%	0.17%	1.25%				0.36%
average	4	0.69%	1.59%	1.01%	2.24%	1.41%	2.70%	0.64%	1.64%	4.59%	1.19%	1.55%	2.77%	1.83%
SD	4	0.23%	0.26%	0.68%	0.20%	0.47%	0.57%	0.49%	1.25%	1.91%				0.40%
average	5	2.18%	0.88%	1.04%	2.24%	1.41%	2.70%	0.64%	1.64%	4.59%	1.69%	1.31%	2.77%	1.92%
SD	5	0.77%	0.44%	0.69%	0.20%	0.47%	0.57%	0.49%	1.25%	1.91%				0.37%
average	6	0.68%	3.28%	2.07%	1.83%	0.09%	0.86%	0.36%	0.44%	1.51%	0.96%	1.27%	1.48%	1.24%
SD	6	0.38%	0.53%	0.47%	0.07%	0.06%	0.60%	0.17%	0.31%	0.83%				0.12%
average	7	3.08%	0.87%	0.71%	0.73%	0.51%	0.59%	0.81%	0.47%	1.36%	1.54%	0.62%	0.89%	1.01%
SD	7	0.60%	0.27%	0.15%	0.08%	0.27%	0.41%	0.18%	0.43%	0.62%				0.15%
average	8	0.75%	1.63%	4.21%	1.22%	0.61%	2.92%	0.60%	0.81%	4.46%	0.86%	1.02%	3.86%	1.91%
SD	8	0.32%	0.42%	0.42%	0.21%	0.25%	0.83%	0.23%	0.35%	1.68%				0.29%
average	9	7.86%	2.43%	2.36%	2.34%	1.29%	4.57%	0.29%	0.71%	7.72%	3.50%	1.48%	4.88%	3.29%
SD	9	0.74%	1.46%	0.86%	0.10%	0.20%	0.91%	0.09%	0.30%	1.49%				0.29%
average	10	0.48%	4.56%	0.70%	0.13%	0.11%	3.60%	0.52%	0.63%	5.44%	0.38%	1.77%	3.24%	1.80%
SD	10	0.21%	0.31%	0.44%	0.06%	0.09%	1.07%	0.35%	0.29%	1.85%				0.42%
average	11	4.40%	3.84%	1.00%	1.58%	0.75%	2.19%	2.04%	1.89%	2.59%	2.67%	2.16%	1.93%	2.25%
SD	11	0.42%	1.23%	0.62%	0.31%	0.12%	1.30%	0.23%	0.26%	1.42%				0.30%
average	12	3.88%	1.96%	2.08%	1.52%	0.33%	2.79%	1.34%	0.52%	4.70%	2.25%	0.93%	3.19%	2.12%
SD	12	0.60%	0.38%	0.86%	0.14%	0.24%	0.66%	0.39%	0.29%	1.90%				0.49%
average	13	1.28%	0.95%	0.41%	0.82%	0.32%	2.55%	0.60%	0.42%	3.37%	0.90%	0.56%	2.11%	1.19%
SD	13	0.35%	0.58%	0.29%	0.22%	0.22%	0.80%	0.44%	0.32%	2.04%				0.24%
average	14	0.46%	0.48%	0.88%	0.42%	0.11%	1.56%	0.53%	0.21%	2.76%	0.47%	0.27%	1.73%	0.82%
SD	14	0.36%	0.34%	0.80%	0.09%	0.08%	0.60%	0.28%	0.15%	2.22%				0.18%
OSIM Average error per		**2.19%**	**1.94%**	**1.39%**	**1.27%**	**0.56%**	**2.32%**	**0.69%**	**0.78%**	**3.76%**	**1.38%**	**1.09%**	**2.49%**	
Per Axis SD		**2.06%**	**1.26%**	**1.02%**	**0.84%**	**0.48%**	**1.14%**	**0.46%**	**0.53%**	**1.81%**	**0.89%**	**0.53%**	**1.12%**	
OSIM Average force error per loaded axis		**1.84%**			**1.38%**			**1.75%**			**OSIM Overall Force Error**			**1.66%**

Table 4-6: Load cell force errors

		Fx Load applied			Fy Load applied			Fz Load applied			average error in Mx per loadcell	average error in My per loadcell	average error in Mz per loadcell	Overall moment error per loadcell
	Load cell	Mx	My	Mz	Mx	My	Mz	Mx	My	Mz				
average	1	1.40%	2.74%	2.44%	4.82%	0.14%	2.47%	5.76%	3.21%	0.50%	3.99%	2.03%	1.80%	2.61%
SD	1	0.35%	1.69%	0.69%	6.41%	0.11%	0.71%	2.19%	0.12%	0.11%				0.62%
average	2	0.46%	1.39%	0.86%	1.23%	0.09%	1.45%	2.24%	2.52%	0.50%	1.31%	1.33%	0.94%	1.19%
SD	2	0.26%	0.85%	0.26%	0.66%	0.11%	0.25%	1.45%	0.23%	0.19%				0.25%
average	3	1.10%	4.48%	2.00%	1.53%	0.13%	1.04%	1.63%	3.82%	0.27%	1.42%	2.81%	1.10%	1.78%
SD	3	0.71%	1.25%	0.59%	0.69%	0.08%	0.54%	1.02%	0.41%	0.23%				0.44%
average	4	0.72%	2.75%	1.23%	2.22%	0.32%	2.21%	3.73%	3.56%	0.42%	2.22%	2.21%	1.29%	1.91%
SD	4	0.36%	1.28%	0.53%	0.51%	0.22%	0.61%	1.61%	0.68%	0.33%				0.21%
average	5	1.08%	4.84%	2.86%	2.22%	0.32%	2.21%	3.73%	3.56%	0.42%	2.34%	2.91%	1.83%	2.36%
SD	5	0.67%	1.54%	0.61%	0.51%	0.22%	0.61%	1.61%	0.68%	0.33%				0.24%
average	6	0.43%	1.06%	0.61%	0.84%	0.92%	2.03%	1.68%	2.92%	0.23%	0.98%	1.63%	0.95%	1.19%
SD	6	0.29%	0.59%	0.47%	0.54%	0.08%	0.61%	0.93%	0.23%	0.14%				0.28%
average	7	0.71%	5.36%	3.14%	1.56%	0.36%	1.19%	1.39%	4.90%	0.65%	1.22%	3.54%	1.66%	2.14%
SD	7	0.46%	0.96%	0.55%	0.60%	0.12%	0.92%	0.90%	0.19%	0.12%				0.23%
average	8	4.08%	1.22%	0.71%	2.77%	0.14%	1.52%	4.03%	5.45%	0.61%	3.63%	2.27%	0.95%	2.28%
SD	9	0.45%	0.76%	0.33%	0.60%	0.12%	1.18%	1.62%	0.16%	0.09%				0.25%
average	9	1.29%	9.01%	7.52%	4.85%	0.74%	2.57%	7.08%	3.50%	0.14%	4.41%	4.42%	3.41%	4.08%
SD	9	0.37%	1.92%	0.90%	0.73%	0.18%	0.64%	1.53%	0.11%	0.10%				0.17%
average	10	2.39%	3.20%	0.65%	4.03%	0.49%	0.61%	5.33%	3.39%	0.28%	3.92%	2.36%	0.52%	2.26%
SD	11	0.53%	1.07%	0.33%	0.77%	0.15%	0.38%	1.59%	0.98%	0.24%				0.33%
average	11	2.19%	7.68%	4.70%	2.59%	0.41%	1.87%	3.20%	3.96%	0.46%	2.66%	4.02%	2.34%	3.01%
SD	12	0.54%	1.63%	0.74%	1.19%	0.30%	0.71%	1.34%	0.21%	0.10%				0.17%
average	12	1.69%	2.92%	3.63%	2.74%	1.11%	1.73%	4.61%	5.05%	1.28%	3.01%	3.02%	2.21%	2.75%
SD	12	0.87%	1.29%	0.86%	0.45%	0.11%	0.98%	1.73%	0.31%	0.19%				0.45%
average	13	0.71%	0.61%	1.47%	2.54%	0.22%	1.12%	3.29%	2.32%	0.48%	2.18%	1.05%	1.02%	1.42%
SD	13	0.27%	0.38%	0.50%	0.77%	0.22%	0.81%	1.93%	0.33%	0.27%				0.37%
average	14	0.89%	2.08%	0.48%	2.05%	0.21%	0.77%	2.93%	2.81%	0.78%	1.96%	1.70%	0.68%	1.44%
SD	14	0.73%	1.15%	0.34%	0.44%	0.11%	0.66%	2.22%	0.10%	0.14%				0.15%
OSIM Average error per		**1.37%**	**3.52%**	**2.31%**	**2.57%**	**0.40%**	**1.63%**	**3.62%**	**3.64%**	**0.50%**	**2.52%**	**2.52%**	**1.48%**	
Per Axis SD		**0.98%**	**2.51%**	**1.99%**	**1.24%**	**0.32%**	**0.63%**	**1.67%**	**0.94%**	**0.28%**	**1.13%**	**0.99%**	**0.79%**	
OSIM Average moment error per loaded axis		**2.40%**			**1.53%**			**2.59%**			**OSIM Overall Moment Error**			**2.17%**

Table 4-7: Load cell moment error

4.5 Simulating a high upper cuspid

The OSIM was set up to simulate a malocclusion with a high upper right cuspid (Figure 4-39). Indirect bracket placement using a full-sized archwire tied to all brackets was used to insure all brackets were in the zero default position (Zero torque, zero tip and perfect alignment of all teeth). In the first experiment, Damon Mx 0.022" brackets (ORMCO, Orange CA) were used with three types of NiTi wires (0.014", 0.018" and 0.014" x 0.025" Damon Copper NiTi wires, ORMCO, Orange CA). In the second experiment, InOvation 0.022" (GAC International, Bohemia NY) brackets were used with the three types of NiTi wires (0.014", 0.018" and 0.014"x 0.025" Damon Copper NiTi wires). In the third experiment, the three types of NiTi wires (0.014", 0.018" and 0.014"x 0.025" Damon Copper NiTi wires) were ligated with elastomeric ties into Damon Mx 0.022" brackets. The wires were ligated with all brackets in the start (zero) position.

The upper right cuspid was moved from the default position to the apical position then back to the default position, in 0.1 mm increments. The cuspid was moved 4 mm apically then back to the zero position with the 0.014" and the 0.018"wires, and it was moved 3mm apically then back to the zero position with the 0.014" x 0.025" wire. This allowed us to gather the force/moment data during the loading and the unloading of the wires. The same experiment was repeated five times for each ligation method, using a new wire each time. The objective of this experiment was to compare the force systems resulting from passive self-ligation, active ligation and conventional elastic ligation in a high cuspid situation. 3D force and moment data was collected for all the teeth every 0.1 mm of the cuspid movement. The temperature of the OSIM was controlled at 35-36°C throughout the experiment.

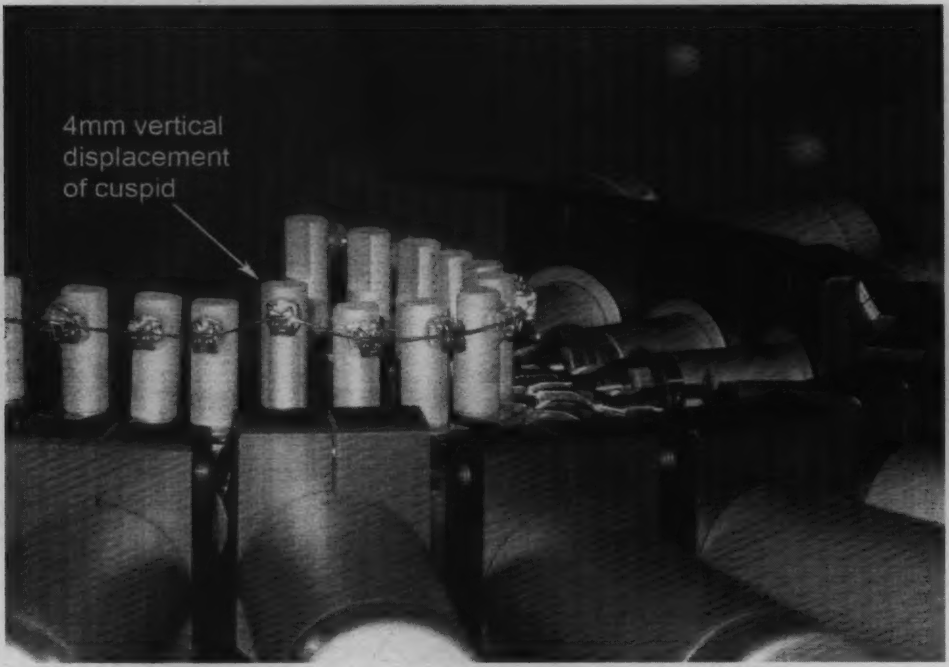

Figure 4-39: Simulated high upper right cuspid

5 Chapter five: Results

5.1 Overview

This experiment yielded a large amount of data that is best assessed on a computer screen with 3D playback of the collected samples, however in this thesis we can only present this data graphically. We will describe the force system by analyzing each of the six components of the force system for the three ligation methods used in our experiments. The data for each force system component for the ten teeth of interest (the upper right second bicuspid #15, to the upper left second bicuspid #25) is presented using graphs, as well as data tables showing the component values at 1mm increments. We will supplement that with graphs of individual teeth that would help to highlight some of our findings. We will attempt to explain some of the findings if plausible explanations are available.

We used two sets of brackets, DamonMx and InOvation brackets. A number of facts need to be kept in mind while reading the results description:

- We are interested in comparing the different ligation methods, however we do not have a sample. We have one set of brackets for each ligation method to use with the OSIM device. Mounting bracket sets on the OSIM is a very long process, therefore a sample size of more than 1 is not possible at this time. We plan to create a faster reproducible method to mount the brackets with future OSIM modifications.
- The data is presented graphically in sections, each section includes graphical display of each force system component using 2D graphs showing the 95% confidence intervals (CI) for the six components of

the force system acting on the ten teeth from tooth #15 to tooth #25, the sample graph in Figure 5-2 outlines the components of the 2D CI graphs. Then we will present the force system component for each ligation method in separate 3D graphs. Graphs for individual teeth will be presented to highlight some of our findings, the sample graph (Figure 5-3) outlines the components of the 3D graphs. And finally JPEG exports of the OSIM display at 1mm intervals will be presented for visual examination of the force system in the Appendix section.

- The graphs will be supplemented with data tables of the components' values at 1mm increments.
- The data is used for qualitative assessment of the force systems. The graphs will be described in relative terms. We will try to identify patterns in the force systems.
- When we consider the moment readings, it is important to recognize that the errors in moments are much larger than the errors in force readings.
- We will try to present the most plausible explanation for the identified patterns. We will not have an explanation for every pattern identified.
- This data will most likely lead to more specific research questions that need to be answered with more experiments.
- The force system is presented at the mid-point of each bracket. However, in most situations the forces are being applied on different points within the brackets, this relatively small discrepancy between the point of application and the force system coordinate frame is bound

to produce some moment readings acting in mid-bracket coordinate system.

- The sign convention will depend on the position of the tooth in the dental arch, below is Table 5-1 which shows the sign convention for both sides of the dental arch.

- A number of terms will be used throughout this section:
    - EL: Elastic ligation
    - SL: Self-ligation
    - PSL: Passive self-ligation
    - ASL: Active self-ligation
    - Reversal point: the point at which maximum displacement is achieved, and the tooth movement is reversed to move the cuspid back to the default/start position.

	Sign	**Right side**	**Left side**
F_x	Positive	Distal	Mesial
	Negative	Mesial	Distal
F_y	Positive	Buccal	Buccal
	Negative	Lingual	Lingual
F_z	Positive	Gingival	Gingival
	Negative	Occlusal	Occlusal
M_x	Positive	Buccal crown torque	Buccal crown torque
	Negative	Lingual crown torque	Lingual crown torque
M_y	Positive	Mesial tip	Distal tip
	Negative	Distal tip	Mesial tip
M_z	Positive	Disto-Buccal rotation	Mesio-Buccal rotation
	Negative	Mesio-Buccal rotation	Disto-Buccal rotation

Table 5-1: Sign convention

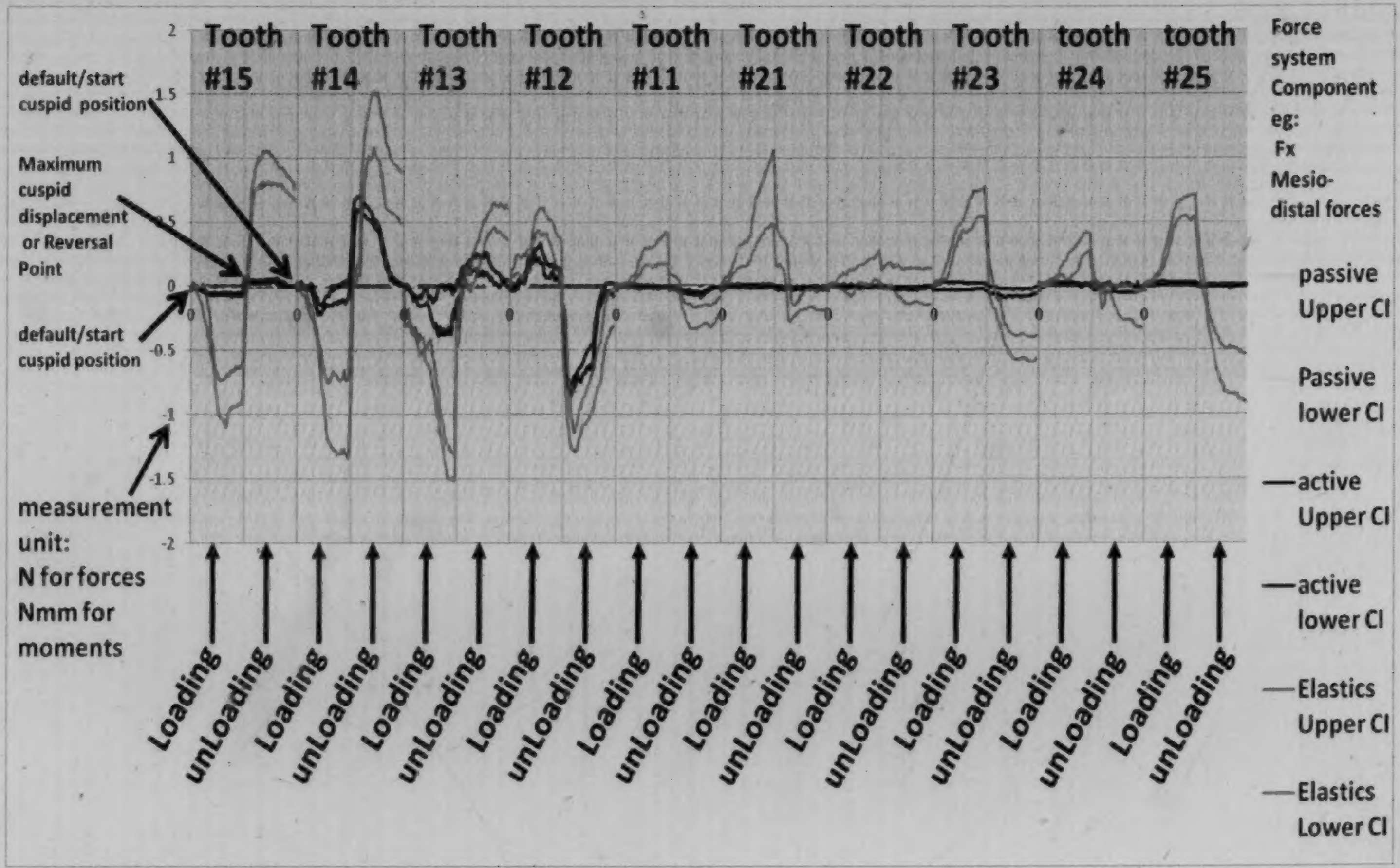

Figure 5-1: Sample 2D graph showing the different graph components

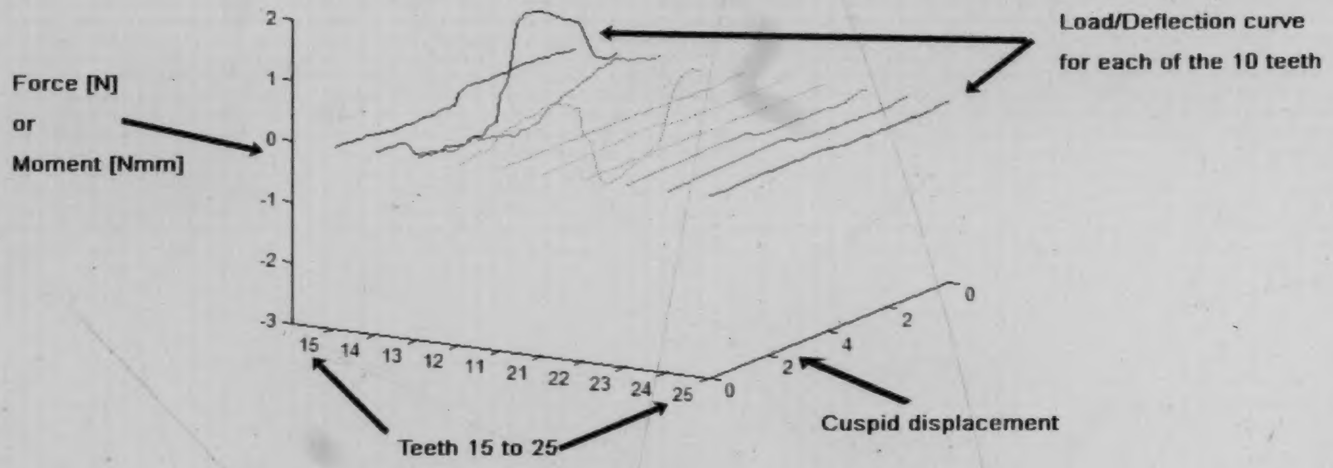

Figure 5-2: Sample 3D graph showing the different graph components

5.2 0.014" NiTi wire results

5.2.1 Mesio-distal forces (F_x)

Different ligation methods produce different levels of resistance to sliding, which seems to affect the force system produced. When we examine the Fx graphs and table (Figure 5-4, Figure 5-6, Table 5-2) of the 10 teeth, we notice Fx forces are generated as the cuspid is moved from the default position to the displaced position and then back to the default position. On the teeth distal to the 13 (tooth#14 and #15) the Fx force is in a mesial direction during loading and in distal direction during unloading. On the teeth mesial of the 13, tooth #12 and #11, Fx force is in a distal direction during loading and in a mesial direction during unloading, and for teeth #21, #22, #23, #24 and #25 Fx is in a mesial direction during loading and in distal direction during unloading. It is noticed that for both types of self-ligation the #14, 13 and 12 are the only teeth with Fx forces. Whereas with EL all ligated teeth, experience high levels of Fx forces.

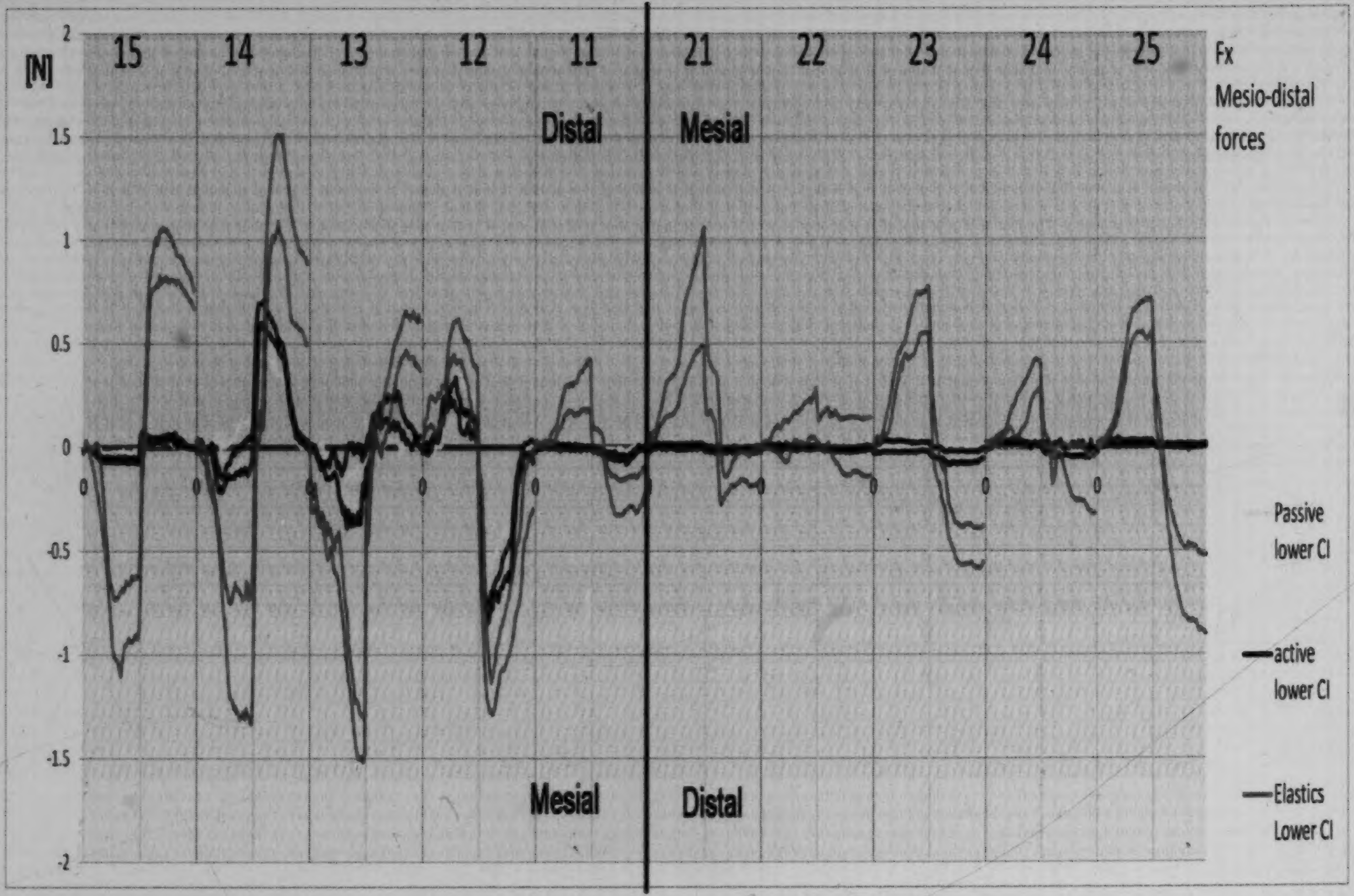

Figure 5-3: 0.014" NiTi, Fx Mesio-distal forces 95% confidence intervals

014 Fx		Displacement mm						
		1 mm	2 mm	3 mm	4 mm	3 mm	2 mm	1 mm
Tooth	Ligation	Force N						
15	Passive	-0.01	-0.04	-0.03	-0.03	0.03	0.03	0.00
	Active	-0.04	-0.06	-0.06	-0.06	0.03	0.05	0.03
	Elastics	-0.10	-0.77	-0.82	-0.75	0.85	0.93	0.86
14	Passive	0.00	-0.04	0.00	0.04	0.46	0.43	0.09
	Active	0.00	-0.16	-0.06	0.00	0.62	0.49	0.13
	Elastics	-0.18	-0.71	-0.98	-1.00	0.71	1.27	0.83
13	Passive	-0.03	-0.15	-0.20	-0.21	0.01	0.07	0.03
	Active	-0.08	-0.12	-0.19	-0.14	0.16	0.17	0.07
	Elastics	-0.37	-0.53	-1.13	-1.40	0.05	0.34	0.56
12	Passive	0.01	0.19	0.20	0.15	-0.67	-0.48	-0.10
	Active	0.05	0.26	0.12	0.07	-0.74	-0.57	-0.11
	Elastics	0.15	0.47	0.44	0.17	-1.21	-0.93	-0.59
11	Passive	0.01	0.01	0.01	0.01	-0.02	-0.01	-0.01
	Active	0.00	0.01	0.00	0.00	-0.03	-0.05	-0.04
	Elastics	0.02	0.19	0.24	0.29	-0.05	-0.24	-0.22
21	Passive	0.01	0.01	0.01	0.00	0.00	0.00	0.00
	Active	0.00	0.00	0.01	0.01	0.00	-0.01	-0.01
	Elastics	0.16	0.27	0.58	0.77	0.16	-0.14	-0.09
22	Passive	0.00	0.00	0.00	0.00	0.00	0.00	0.00
	Active	0.00	0.00	0.00	0.00	-0.01	-0.01	-0.01
	Elastics	0.03	0.03	0.11	0.16	0.07	0.00	0.01
23	Passive	0.00	0.00	0.00	0.00	0.00	0.00	0.00
	Active	0.01	0.00	0.00	0.00	-0.03	-0.05	-0.05
	Elastics	0.12	0.44	0.58	0.66	-0.18	-0.45	-0.47
24	Passive	0.00	0.00	0.00	0.00	-0.01	-0.01	-0.01
	Active	0.02	0.02	0.01	0.01	-0.01	-0.02	-0.02
	Elastics	0.04	0.13	0.22	0.34	-0.11	-0.09	-0.13
25	Passive	0.00	0.00	0.00	0.00	-0.01	-0.01	-0.01
	Active	0.02	0.02	0.02	0.02	0.01	0.00	0.00
	Elastics	0.08	0.37	0.61	0.62	-0.22	-0.59	-0.66
Sign convention		R			L			
	Positive	Distal			Mesial			
	Negative	Mesial			Distal			

Table 5-2: 0.014" wire Fx Force data at 1mm increments

5.2.1.1 Tooth #13:

In advance of the experiment, we anticipated that there would be no mesial or distal forces to acting on tooth #13, however we recorded a mesial force during loading and a distal force during unloading with all ligation methods. This pattern of mesial force on loading and distal force on unloading can be explained by the cumulative resistance to sliding produced by teeth located mesial of tooth #13 as opposed to distal of tooth #13. This will favour sliding of the wire through tooth #13 bracket in a mesial direction during loading, and in a distal direction during unloading, this sliding generates the Fx forces. We notice the immediate reversal of the force at the reversal point for the PSL compared to the more gradual reversal for EL and ASL (Figure 5-5). It is apparent that the force magnitude is highest for elastics during loading and unloading. When we compare the two self-ligating methods, there is no appreciable difference between ASL and PSL during loading, however during unloading PSL shows somewhat less resistance to sliding than ASL.

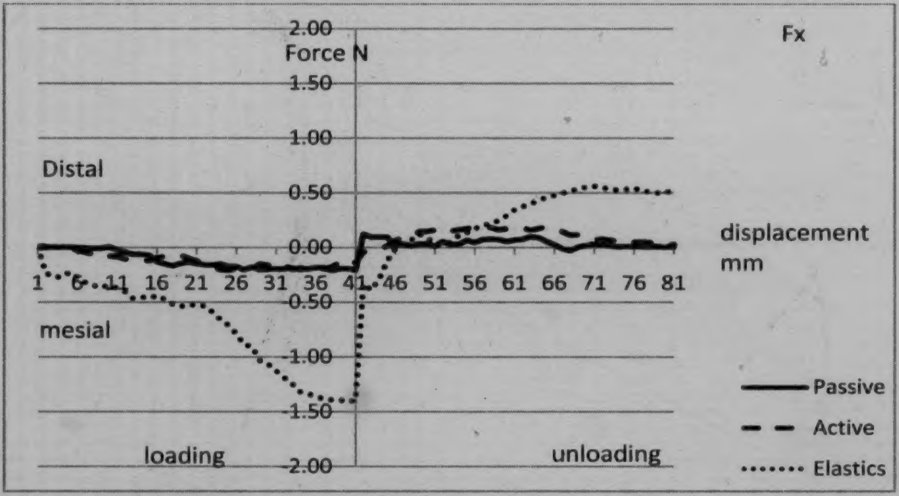

Figure 5-4: 0.014" Fx force on tooth #13

5.2.1.2 Teeth distal to the cuspid:

The teeth distal to the cuspid experience mesial force on loading and distal force on unloading, again this can be explained by the direction of the archwire sliding, EL shows much higher force levels compared to SL brackets. On tooth #14 in spite of the presence of binding due to contact between the wire and the bracket walls, it is clear that the ligation method still plays a major role in producing the resistance to sliding as evidenced by the much higher Fx levels with EL. When the two SL methods on tooth #14 are compared, the only difference exists during unloading with slightly lower resistance to sliding with PSL compared to ASL. On tooth #15 there is very small amount of resistance to sliding for SL, during loading and unloading. EL showed mesial forces during loading and distal forces during unloading which were much larger than for SL, however, with the magnitude being slightly less than that for tooth #14.

5.2.1.3 Teeth mesial to the cuspid:

With EL the resistance to sliding continues to be present throughout the dental arch all the way to tooth #25. The highest levels of Fx forces seem to skip certain teeth. Teeth # 21, #23 and #25 seem to experience much higher Fx forces than # 11, #22 and #24. This phenomena needs to be investigated further as no logical explanation can be presented at this point. The most interesting finding in this graph is the fact that the resistance to sliding continues throughout the dental arch when elastic ligation is used.

With SL brackets tooth #12 is the only tooth mesial to the cuspid experiencing measureable high levels of Fx. This can be explained by the presence of relatively heavy contact between the wire and the bracket, this contact generates a normal force, which produces friction, this phenomena is known as binding in orthodontics. Similar to our finding for the #14, EL produced higher resistance to sliding than SL. However, the difference is smaller for tooth #12 than it is for tooth #14, this can be explained by the smaller interbracket distance distal of the 12 compared to that mesial of the 14, which causes a higher normal force to be acting on the wire.

Another interesting finding on these graphs, is the fact that with EL the force levels start at zero for every tooth but never end at zero, unlike the SL brackets. There are significant residual Fx forces with EL, acting on all teeth even when the cuspid is back in the default position at the end of the unloading curve, this can be caused by the elasticity of the ligation method.

On average it seems that the difference between the two SL brackets is relatively small with PSL producing slightly less resistance to sliding than ASL. The most apparent difference lies between the EL and the SL brackets.

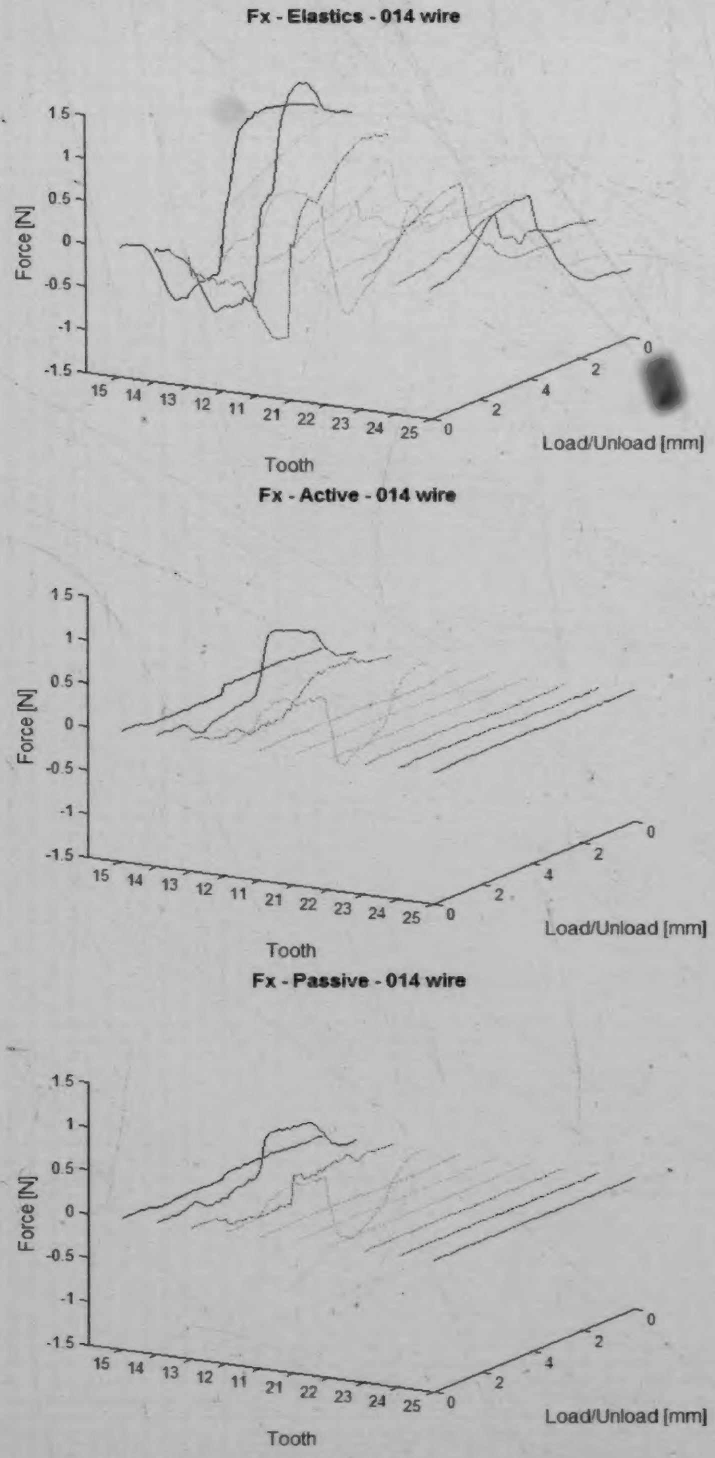

Figure 5-5: 3D 0.014" Fx graphs means EL, ASL and PSL brackets

5.2.2 Fy Bucco-lingual forces

In this simulated clinical situation, we would ideally prefer no Fy forces on any of the teeth. However, on examining the Fy graphs (Figure 5-7, Table 5-3) it is apparent that there are significant levels of bucco-lingual forces on all the teeth with EL. With ASL, the levels of Fy are much lower than EL but only slightly higher than PSL. There is large CI range for Fy forces with EL. It appears that the behavior of the interaction between the elastic ligation and the wire is complex and quite variable.

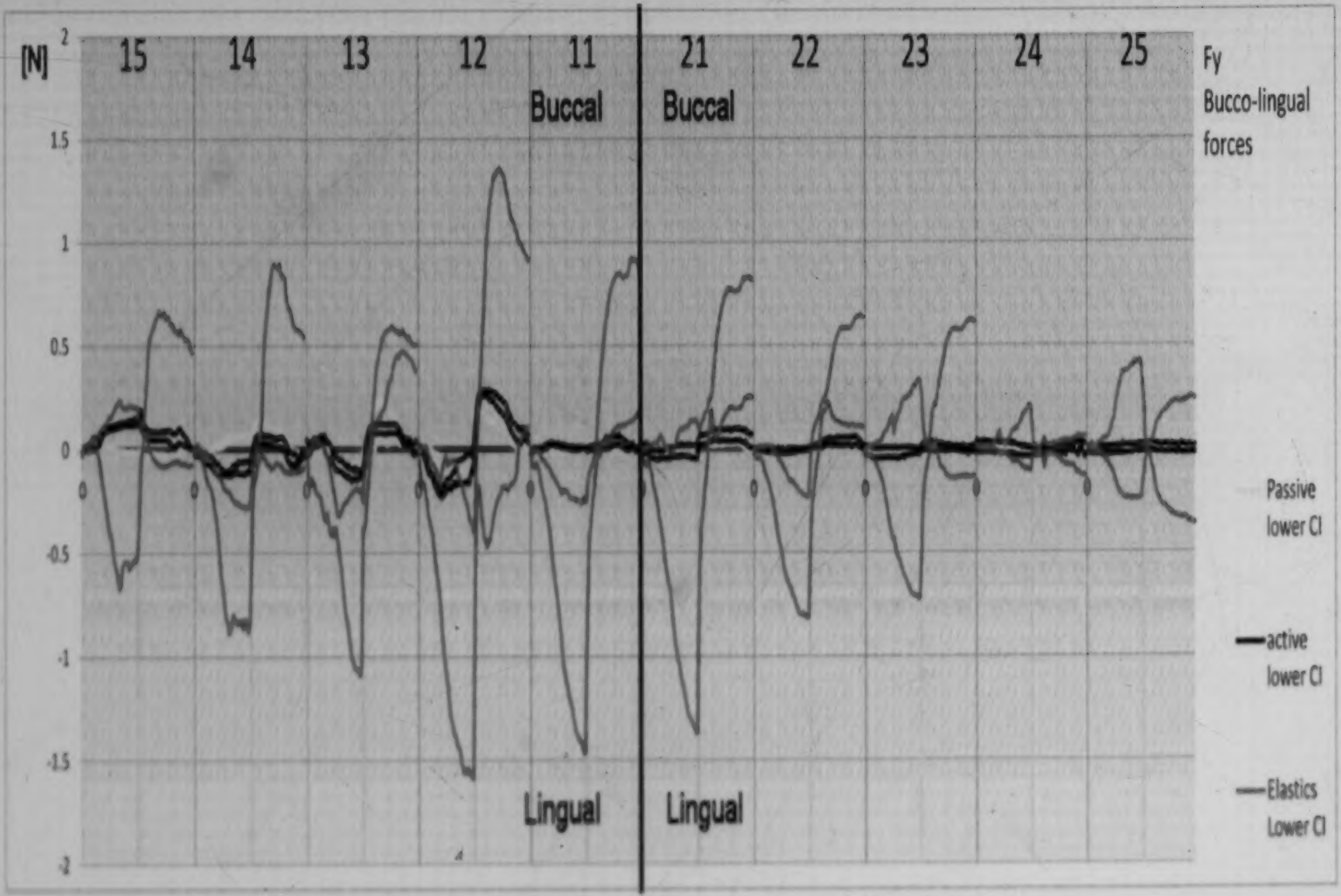

Figure 5-6: 0.014" Fy Bucco-lingual forces 95% confidence intervals

014 Fy		Displacement mm						
		1 mm	2 mm	3 mm	4 mm	3 mm	2 mm	1 mm
Tooth	Ligation	Force N						
15	Passive	0.00	0.01	-0.01	-0.01	-0.03	-0.02	-0.01
	Active	0.04	0.11	0.13	0.13	0.07	0.07	0.07
	Elastics	0.02	-0.13	-0.17	-0.16	0.27	0.29	0.25
14	Passive	0.00	0.03	0.06	0.07	0.10	0.08	0.03
	Active	-0.05	-0.11	-0.09	-0.08	0.05	0.04	-0.04
	Elastics	-0.10	-0.41	-0.56	-0.56	0.17	0.41	0.28
13	Passive	0.00	-0.08	-0.10	-0.10	0.09	0.12	0.05
	Active	0.05	-0.05	-0.11	-0.11	0.10	0.10	0.05
	Elastics	-0.10	-0.31	-0.55	-0.62	0.21	0.45	0.32
12	Passive	-0.02	-0.08	-0.08	-0.06	0.18	0.13	0.03
	Active	-0.13	-0.18	-0.11	-0.06	0.27	0.21	0.09
	Elastics	-0.24	-0.55	-0.81	-0.99	0.27	0.57	0.47
11	Passive	0.00	0.00	0.00	0.00	-0.01	-0.01	-0.01
	Active	0.01	0.02	0.01	0.01	0.00	0.03	0.02
	Elastics	-0.15	-0.47	-0.74	-0.86	0.11	0.46	0.48
21	Passive	-0.01	0.00	0.01	0.01	0.02	0.02	0.03
	Active	-0.03	-0.02	-0.01	-0.02	0.06	0.07	0.07
	Elastics	-0.10	-0.35	-0.53	-0.62	0.21	0.44	0.46
22	Passive	0.00	0.00	0.00	0.00	0.00	0.00	0.00
	Active	-0.01	-0.02	-0.01	0.00	0.02	0.03	0.03
	Elastics	-0.07	-0.28	-0.45	-0.52	0.19	0.32	0.35
23	Passive	0.00	0.00	0.00	0.00	0.01	0.00	0.00
	Active	-0.02	-0.02	-0.01	-0.01	0.01	0.04	0.06
	Elastics	-0.04	-0.14	-0.20	-0.19	0.11	0.19	0.12
24	Passive	0.00	-0.01	-0.02	-0.02	-0.01	0.00	0.01
	Active	0.01	0.00	-0.01	-0.02	-0.01	-0.01	0.00
	Elastics	0.00	0.01	0.02	0.05	-0.03	-0.01	-0.02
25	Passive	0.00	0.01	0.01	0.02	0.01	0.00	0.00
	Active	-0.01	-0.01	0.00	0.00	0.00	0.00	0.00
	Elastics	0.00	0.01	0.07	0.08	-0.04	-0.05	-0.06
Sign convention		R			L			
	Positive	Buccal			Buccal			
	Negative	Lingual			Lingual			

Table 5-3: 0.014" wire Fy force data at 1mm increments

5.2.2.1 Cuspid:

We would expect no Fy forces to act on the 13, however there is a lingual force on loading and buccal force on unloading for all ligation methods, highest forces are with EL while both SL brackets delivered similar levels of Fy forces to # 13. This pattern is most likely related to the curvature of the arch and we might not see this if the brackets were arranged in a straight line.

5.2.2.2 Teeth distal to #13:

On tooth #14 with PSL there is a relatively small buccal force throughout the loading and unloading, this can be explained by the fact that the 14 bracket is sliding (relative to the wire) to a wider part of the archwire, which would apply a buccally directed force. This is different from the pattern of ASL and EL. El produced a substantial lingual force during loading and buccal force during unloading, ASL produced the same pattern with much lower force magnitudes. This could be related to the mesial and distal forces acting on a curved archwire.

On tooth 15 PSL shows no buccal forces while ASL shows a buccal force during loading and unloading almost identical to the force acting on tooth #14 with PSL. One plausible explanation to this phenomenon is the presence of the molar tube distal to the 15 that does not apply a force restricting the wire bucco-lingually, the same pattern was seen on the 14 with PSL, the 15 PSL bracket causes the saem phenomenon that the molar tube cause with ASL.

5.2.2.3 Teeth mesial to #13:

Tooth #12 shows a lingual force on loading and a buccal force on unloading for all ligation methods, the highest Fy force levels were recorded on the 12 bracket with EL. PSL shows marginally lower Fy forces compared to ASL. The rest of the teeth mesial of the 13 show high Fy forces with EL, and very low Fy force with SL.

There is a large amount of variation with EL, this is expected of elastomeric ties. On examining the 3D graphs, it is apparent that EL produces the highest Fy forces. With SL brackets, the Fy forces are generally limited to the teeth 14, 13 and 12, ASL on tooth # 15 shows relatively high buccal force compared to PSL.

When we examine the Fy graphs of all the teeth we notice in general the presence of a lingual force on loading and a buccal force on unloading. For self-ligation this pattern was generally not present on teeth of the left side. For EL this pattern was generally present on all teeth except the 24 and 25.

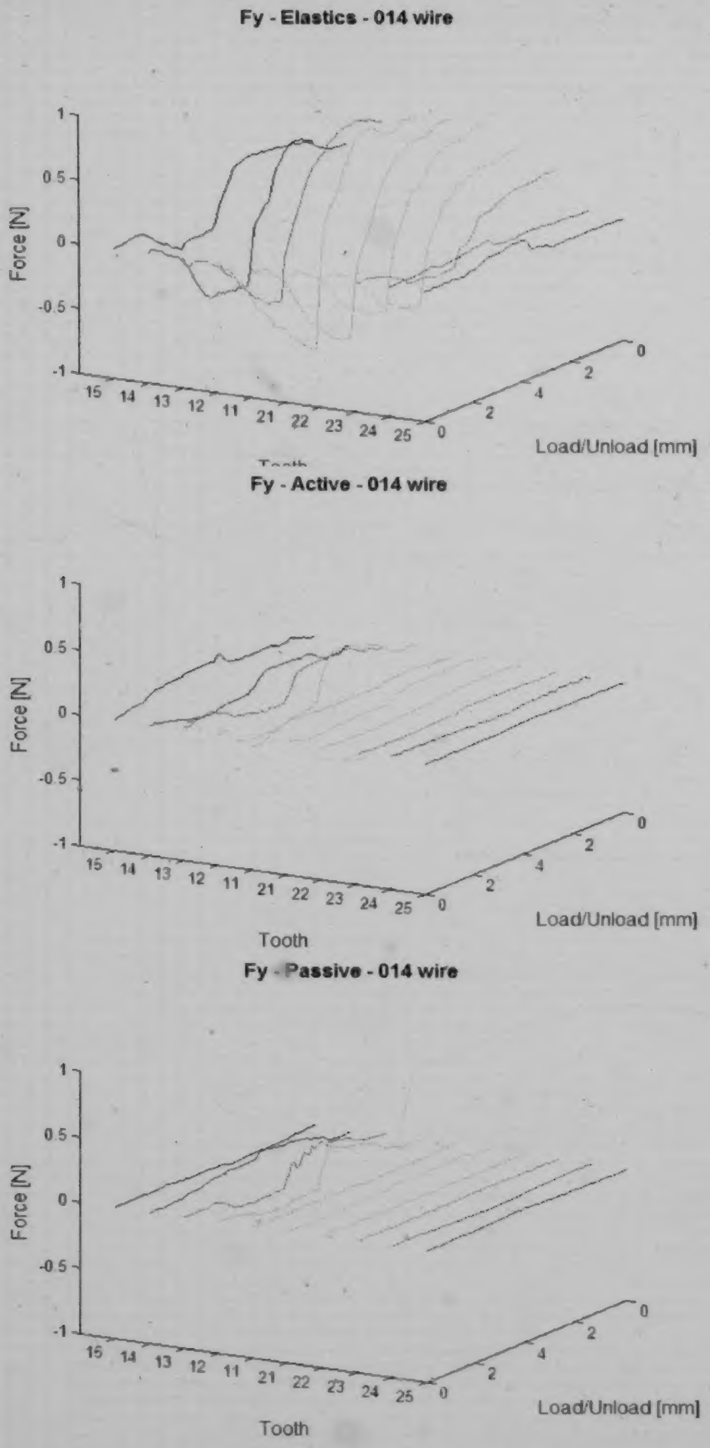

Figure 5-7: 3D 0.014” Fy graphs means EL, ASL and PSL brackets

5.2.3 Fz Occluso-gingival forces

In this simulated clinical situation, we would expect an extrusive force on #13 and two reciprocal intrusive forces on the #12 and #14, during loading and unloading. On examining the Fz graphs (Figure 5-9, Table 5-4) we notice the intrusive forces on the #12, #14 and the extrusive force on the #13. An interesting finding is that the #15 and the #11 have a very similar low magnitude Fz "W" pattern (Figure 5-10), despite of its low magnitude it is worth mentioning since we see the same pattern with the 0.018" and 0.014" x 0.025" wires. This could be related to the angulation of the wire relative to those two teeth as the canine displacement is produced. Another interesting finding is that the typical flat load deflection curves of the NiTi wire are only seen with self-ligating brackets, there are no flat load deflection curves on loading with EL brackets, while during unloading those flat load-deflection curves are distorted relative to those of SL brackets.

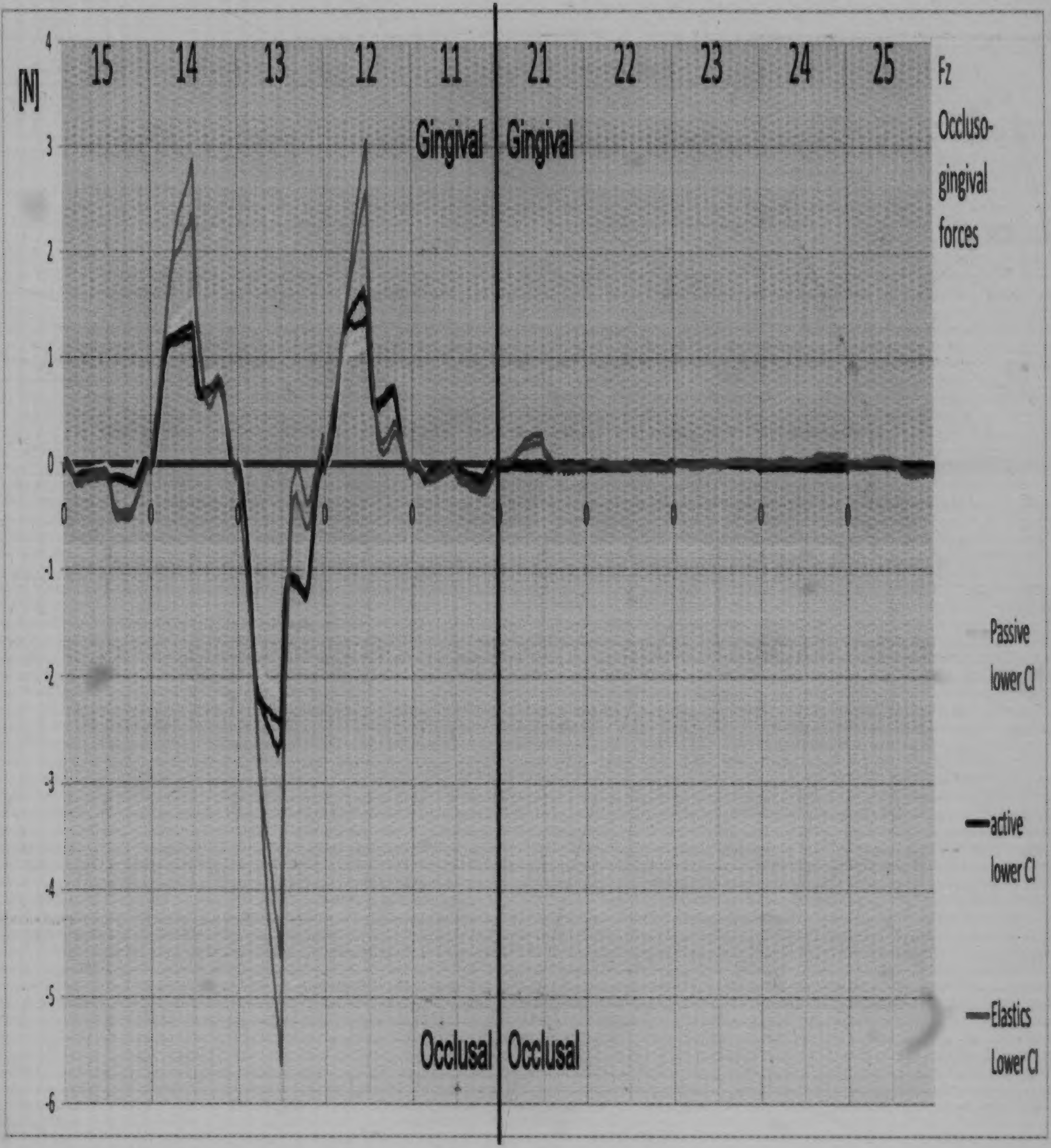

Figure 5-8: 0.014"Fz Occluso-gingival 95% confidence intervals

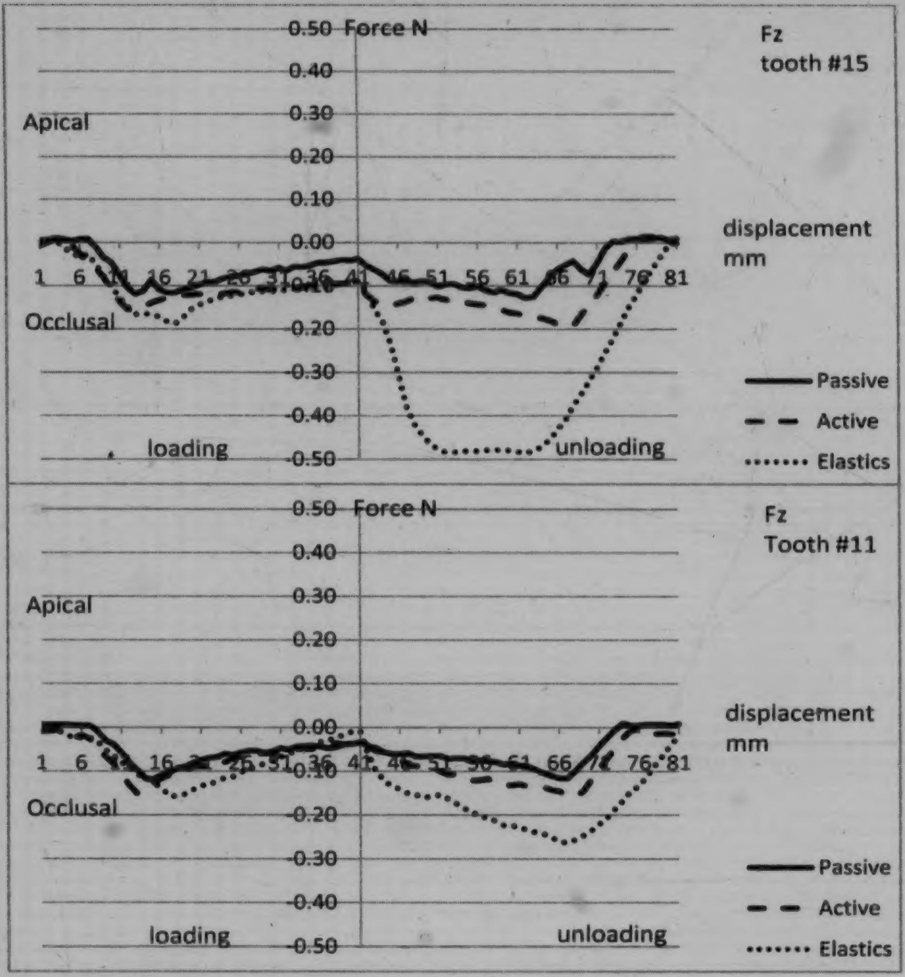

Figure 5-9: 0.014" Fz load deflection of tooth #15 and #11 showing the "W" pattern

014 Fz		Displacement mm						
		1 mm	2 mm	3 mm	4 mm	3 mm	2 mm	1 mm
Tooth	ligation	Force N						
15	Passive	-0.08	-0.10	-0.06	-0.04	-0.10	-0.12	-0.05
	Active	-0.14	-0.12	-0.11	-0.10	-0.13	-0.16	-0.12
	Elastics	-0.13	-0.14	-0.11	-0.09	-0.48	-0.48	-0.29
14	Passive	0.49	1.27	1.37	1.42	0.78	0.86	0.36
	Active	0.67	1.16	1.21	1.25	0.66	0.74	0.54
	Elastics	0.86	1.84	2.27	2.59	0.73	0.70	0.52
13	Passive	-0.63	-1.92	-2.23	-2.37	-1.09	-1.17	-0.50
	Active	-0.92	-2.21	-2.42	-2.55	-1.09	-1.19	-0.73
	Elastics	-1.28	-2.90	-4.12	-5.11	-0.48	-0.32	-0.32
12	Passive	0.32	1.00	1.16	1.22	0.54	0.61	0.27
	Active	0.46	1.29	1.42	1.46	0.56	0.66	0.35
	Elastics	0.66	1.44	2.18	2.80	0.28	0.22	0.24
11	Passive	-0.06	-0.07	-0.05	-0.03	-0.07	-0.09	-0.04
	Active	-0.11	-0.09	-0.06	-0.03	-0.10	-0.13	-0.10
	Elastics	-0.08	-0.13	-0.07	-0.01	-0.15	-0.23	-0.22
21	Passive	0.00	0.00	0.00	0.00	0.00	0.00	0.00
	Active	-0.01	-0.02	-0.02	-0.02	-0.02	-0.02	-0.03
	Elastics	0.03	0.14	0.21	0.24	0.00	-0.03	-0.03
22	Passive	0.00	0.00	0.00	0.00	0.00	0.00	0.00
	Active	-0.01	-0.02	-0.02	-0.03	-0.02	-0.01	-0.02
	Elastics	0.01	0.00	-0.01	-0.01	-0.02	-0.04	-0.04
23	Passive	0.00	0.01	0.00	0.00	0.00	0.00	0.00
	Active	0.00	0.00	0.00	0.01	0.00	0.00	-0.01
	Elastics	0.00	-0.02	-0.01	0.00	0.01	0.02	0.02
24	Passive	0.00	0.00	0.01	0.01	0.01	0.01	0.00
	Active	-0.01	-0.01	-0.01	-0.01	-0.02	-0.02	-0.01
	Elastics	0.00	0.02	0.02	0.00	0.04	0.06	0.07
25	Passive	0.00	0.00	0.00	0.00	0.00	0.00	0.00
	Active	0.00	-0.01	-0.01	-0.01	-0.01	-0.01	-0.01
	Elastics	0.00	0.01	0.03	0.03	-0.04	-0.09	-0.09
Sign convention		R			L			
	Positive	Gingival			Gingival			
	Negative	Occlusal			Occlusal			

Table 5-4: 0.014" wire Fz force data at 1mm increments

5.2.3.1 Cuspid:

During loading, the cuspid experiences highest Fz forces with EL and lowest with PSL, with very little difference between PSL and ASL (Figure 5-11). During unloading ASL shows marginally higher Fz force than PSL, and EL showing the lowest Fz magnitude. There is a very large difference in the Fz magnitude between loading and unloading, especially for EL brackets.

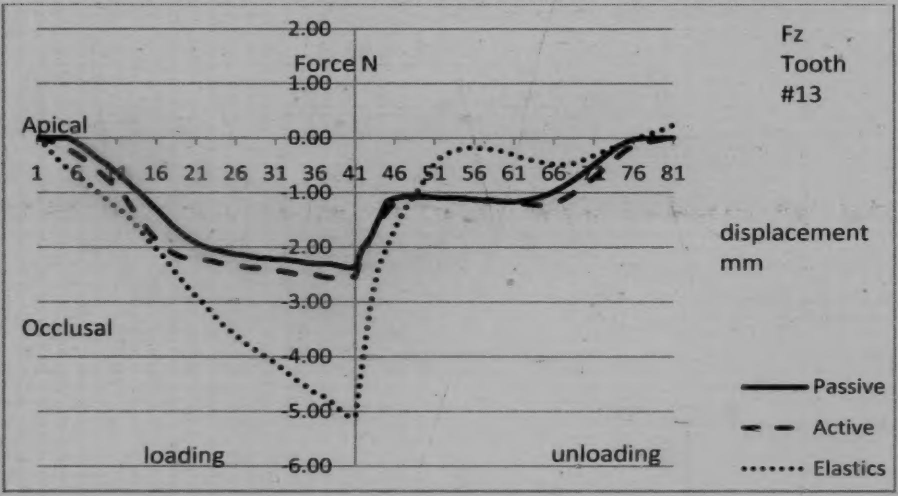

Figure 5-10: 0.014" Fz force on tooth #13

5.2.3.2 Teeth distal to #13:

All ligation methods produce similar patterns of Fz with different magnitudes. On tooth #14 the EL brackets produce the highest intrusive force during loading and ASL produced slightly lower Fz than PSL. During unloading, there is very little difference between the three ligation methods. Tooth #15 shows a "W" pattern of extrusive force throughout the loading and unloading declining to zero at the reversal point (Figure 5-10). This can be explained by the angulation of the wire relative to the 14 bracket slot during loading and unloading. At the start of the loading, the 14 bracket acts as a lever point for the wire as the cuspid is intruded, this causes the wire to apply an extrusive force on #15. When the wire bends mesial of the 14 as the cuspid is further intruded, this extrusive force disappears since the wire becomes parallel to the 14 bracket slot. EL produced the largest extrusive force on tooth #15, while PSL produced a slightly lower extrusive force than ASL.

5.2.3.3 Teeth mesial to #13:

All ligation methods produce similar patterns of Fz with different magnitudes. On tooth #12 the EL brackets produce the highest gingival force during loading and PSL produced slightly lower Fz than ASL (the opposite of #14 pattern). During unloading, there is no difference between the SL brackets, while EL produced very low Fz that increases as unloading progresses. Tooth #11 shows a "W" pattern of occlusal force (Figure 5-10) similar to that of #15, throughout the loading and unloading declining to zero at the reversal point.
When we examine teeth #12, 11 and 21, despite the low force magnitude, we notice a very interesting pattern of gingival force on 12, occlusal force on 11 and gingival force on 21.
On examining the 3D graphs in Figure 5-12, we notice that SL brackets [illegible]ver the load-deflection curve expected of NiTi wires, characterized by flat loading and unloading curves, and the loading curves exhibiting higher force magnitudes compared to the unloading curves.

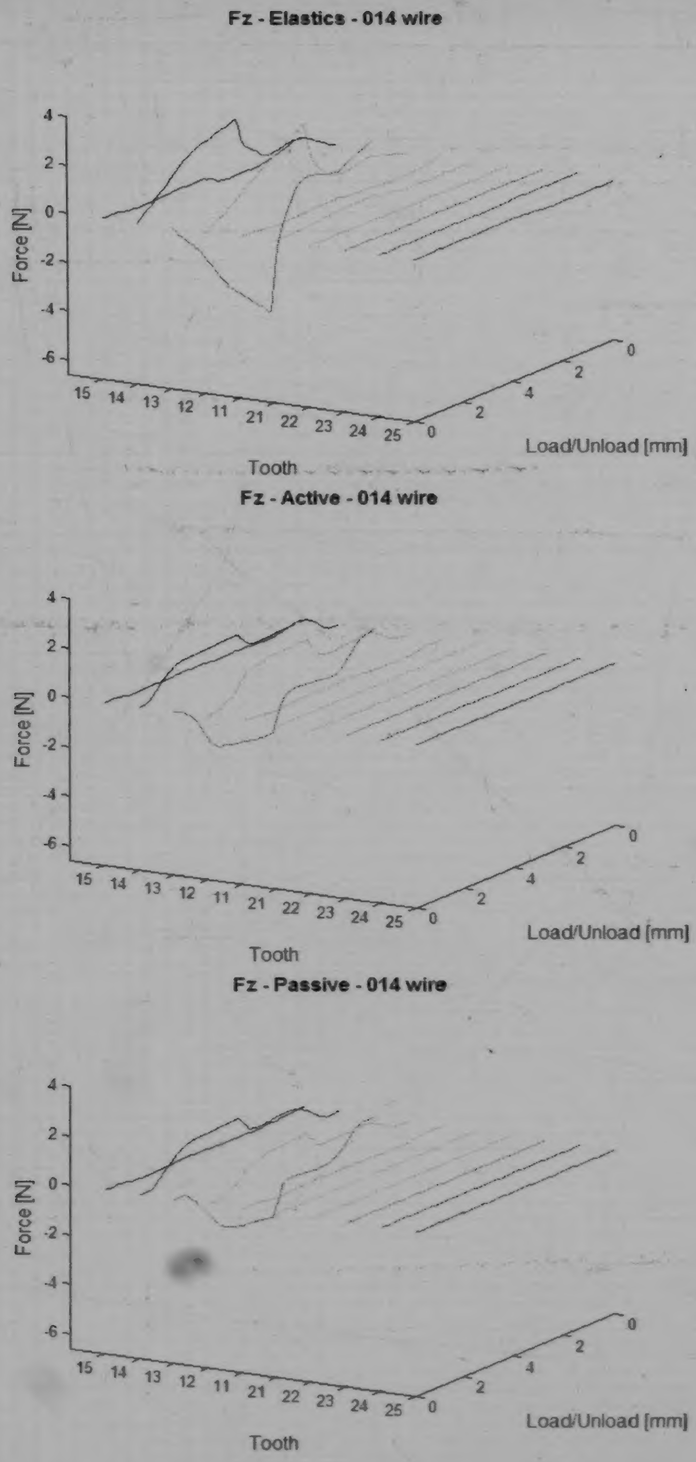

Figure 5-11: 3D 0.014" Fz graphs, means EL, ASL and PSL brackets

5.2.4 Mx Moments (Bucco-Lingual Moments)

We would expect no Mx moments on any of the teeth, however the largest moments were detected when elastic ligation (EL) was used specifically on teeth # 13, 12, 11, 21, 22 and 23. These moments are in a buccal crown torque direction on loading and a lingual crown torque on unloading (Figure 5-13, Figure 5-14, Table 5-5). The Mx moments seen here can be caused by one of the following:

a) Fy acting on the bracket at an occluso-gingival distance from the bracket coordinate system.

b) Fz acting on the bracket at a bucco-lingual distance from the bracket coordinate system

c) A force couple

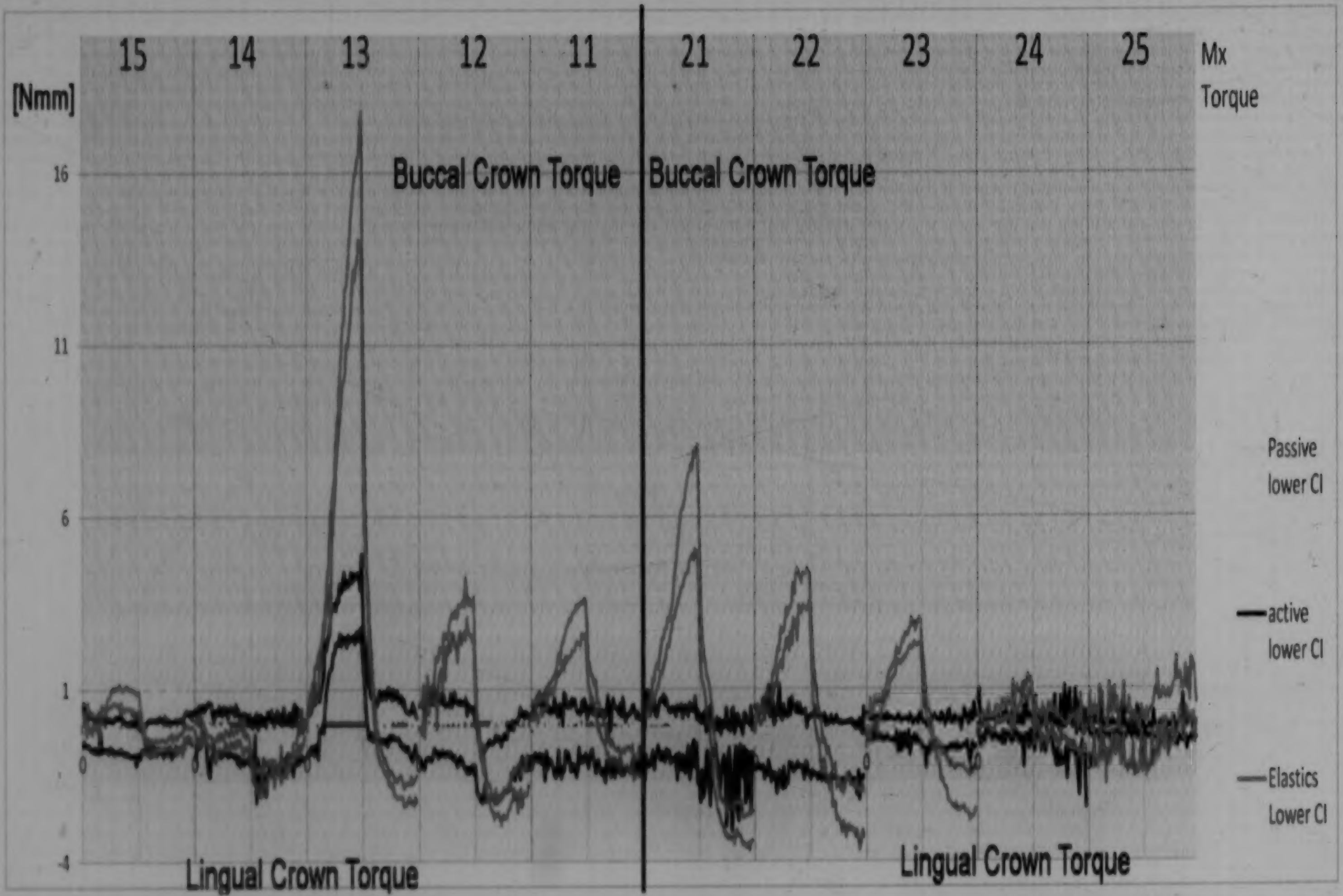

Figure 5-12: 0.014" Mx Bucco-lingual crown torque, 95% confidence intervals

014 Mx		Displacement mm						
		1 mm	2 mm	3 mm	4 mm	3 mm	2 mm	1 mm
Tooth	ligation	Moment Nmm						
15	Passive	0.34	0.37	0.40	0.53	0.03	0.49	0.21
	Active	-0.34	-0.25	-0.36	-0.45	-0.20	-0.26	-0.31
	Elastics	0.05	0.65	0.71	0.62	-0.65	-0.59	-0.58
14	Passive	-0.01	-0.29	-0.46	-0.44	-0.39	-0.32	-0.04
	Active	-0.40	-0.32	-0.16	-0.46	-0.43	-0.43	-0.46
	Elastics	-0.44	-0.58	-0.29	-0.70	-1.63	-1.30	-1.02
13	Passive	0.61	2.73	3.39	3.57	0.18	0.07	0.52
	Active	0.37	2.76	3.29	3.66	0.11	0.34	-0.07
	Elastics	2.05	6.75	12.06	15.82	0.10	-1.61	-1.94
12	Passive	0.38	0.43	0.24	0.32	-0.65	-0.44	0.26
	Active	-0.18	-0.14	-0.14	-0.50	-1.39	-1.36	-0.79
	Elastics	0.91	2.37	3.04	3.04	-2.00	-2.56	-1.79
11	Passive	0.37	0.33	0.56	0.54	0.47	0.21	0.35
	Active	-0.48	-0.29	-0.30	-0.16	-0.45	-0.24	-0.53
	Elastics	0.60	1.71	2.62	3.05	0.22	-0.83	-0.98
21	Passive	0.17	0.17	0.10	0.06	0.14	0.05	0.11
	Active	-0.34	-0.40	-0.46	-0.68	-0.29	-0.76	-1.30
	Elastics	1.38	2.83	5.27	6.52	-0.08	-2.80	-2.79
22	Passive	0.21	0.11	0.13	0.11	0.10	0.07	0.13
	Active	-0.01	-0.89	-0.48	-0.65	-0.73	-0.73	-0.76
	Elastics	0.60	2.11	3.67	3.93	-0.83	-2.31	-2.42
23	Passive	0.10	0.17	0.09	0.19	0.17	0.12	0.13
	Active	-0.15	-0.18	-0.27	-0.13	-0.20	-0.24	-0.44
	Elastics	0.40	1.54	2.30	[illegible]	-0.69	-1.63	-1.85
24	Passive	0.10	0.19	0.19	0.29	0.39	0.42	0.33
	Active	-0.16	-0.21	-0.24	-0.06	-0.36	-0.71	-0.47
	Elastics	-0.01	0.32	0.65	0.86	-0.27	-0.26	-0.30
25	Passive	0.08	0.08	-0.03	0.15	0.24	0.12	0.14
	Active	0.15	-0.16	-0.18	-0.23	-0.23	-0.17	0.12
	Elastics	-0.10	-0.33	-0.22	-0.57	-0.07	-0.01	0.30
Sign convention		R			L			
	Positive	Buccal crown torque			Buccal crown torque			
	Negative	Lingual crown torque			Lingual crown torque			

Table 5-5: 0.014" wire Mx moment data at 1mm increments

5.2.4.1 Cuspid:

The cuspid experiences a very large buccal crown torque (moment) during loading and a relatively smaller lingual crown torque on unloading. SL brackets produce similar levels and patterns of Mx moments with larger variation for ASL compared to PSL. It is not possible to present a complete explanation for this moment however two plausible explanations can be presented. One explanation for such a moment of EL is that the Fy force acting on the cuspid in a lingual direction during loading and buccal direction during unloading, are being applied at a point within the bracket slot superior (gingival) to the mid-bracket coordinate system. It seems that the elastics cause the wire to apply the Fy force on a point superior (gingival) to the mid-bracket coordinate system of #13 bracket, since these moments are of less magnitude with PSL brackets in spite of the fact that EL and PSL are the same bracket set. However, this moment cannot possibly account to the large magnitude of the Mx moment acting on #13 due to the very small moment arm from the point of application to the mid-bracket coordinate system. Another explanation for such a moment is the development of a force couple within the bracket slot due to archwire contacting the bracket slot at three points (one gingival and two occlusal points). SL brackets produce a Mz moment of similar pattern to that of Fx, with flat loading and unloading curves which leads us to believe that a portion of the Mz moment is caused by the Fx force acting at a distance from the midbracket coordinate system.

5.2.4.2 Teeth distal to #13:

Tooth #14 experiences lingual crown torque on loading and slightly higher lingual crown torque during unloading with EL. On tooth #15 there is a small buccal crown torque on loading and a small lingual crown torque on unloading. There is no discernable pattern for SL brackets on teeth #14 and #15. Those moments are of very small magnitude and can be considered negligible when errors in moments are taken into consideration.

5.2.4.3 Teeth mesial to #13:

El brackets produce large buccal crown torque moments on loading and lingual crown torque moments on unloading for teeth 12, 11, 21, 22 and 23. The highest moment is experienced by tooth #21. SL brackets produce no specific pattern on those teeth, however the ASL produce larger variation than PSL.

It seems that the addition of elastic ligation, produces complex Mx loading pattern (on teeth 12, 11, 21, 22 and 23) that does not exist with SL brackets.

Mx - Elastics - 014 wire

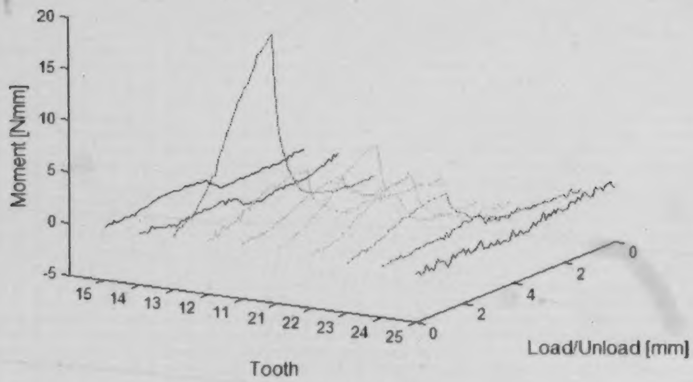

Mx - Active - 014 wire

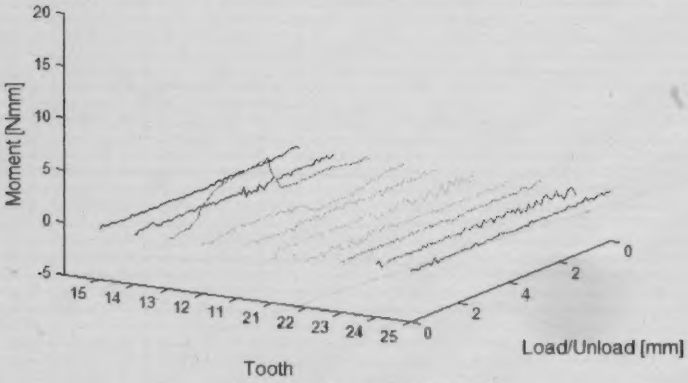

Mx - Passive - 014 wire

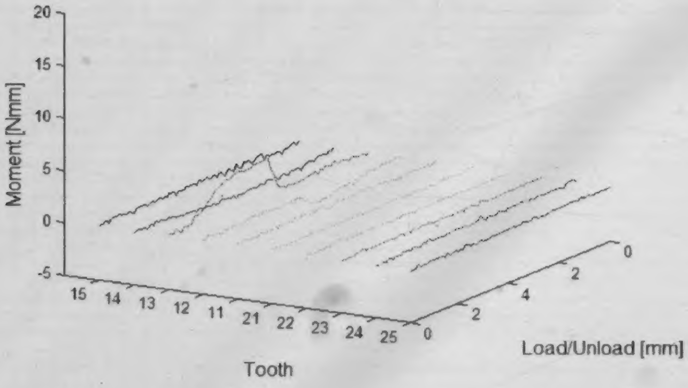

Figure 5-13: 3D 0.014" Mx Bucco-lingual crown torque graphs, means EL, ASL and PSL brackets

5.2.5 My Moments (Mesio-Distal Moments)

We would expect My moments on teeth 12 and 14 only. EL again produces the highest My moments compared to the SL brackets (Figure 5-15, Figure 5-16 , Table 5-6). The My moments seen here can be caused by one of the following:

a) Fx acting on the bracket at an occluso-gingival distance from the bracket coordinate system.

b) Fz acting on the bracket at a mesio-distal distance from the bracket coordinate system

c) A force couple

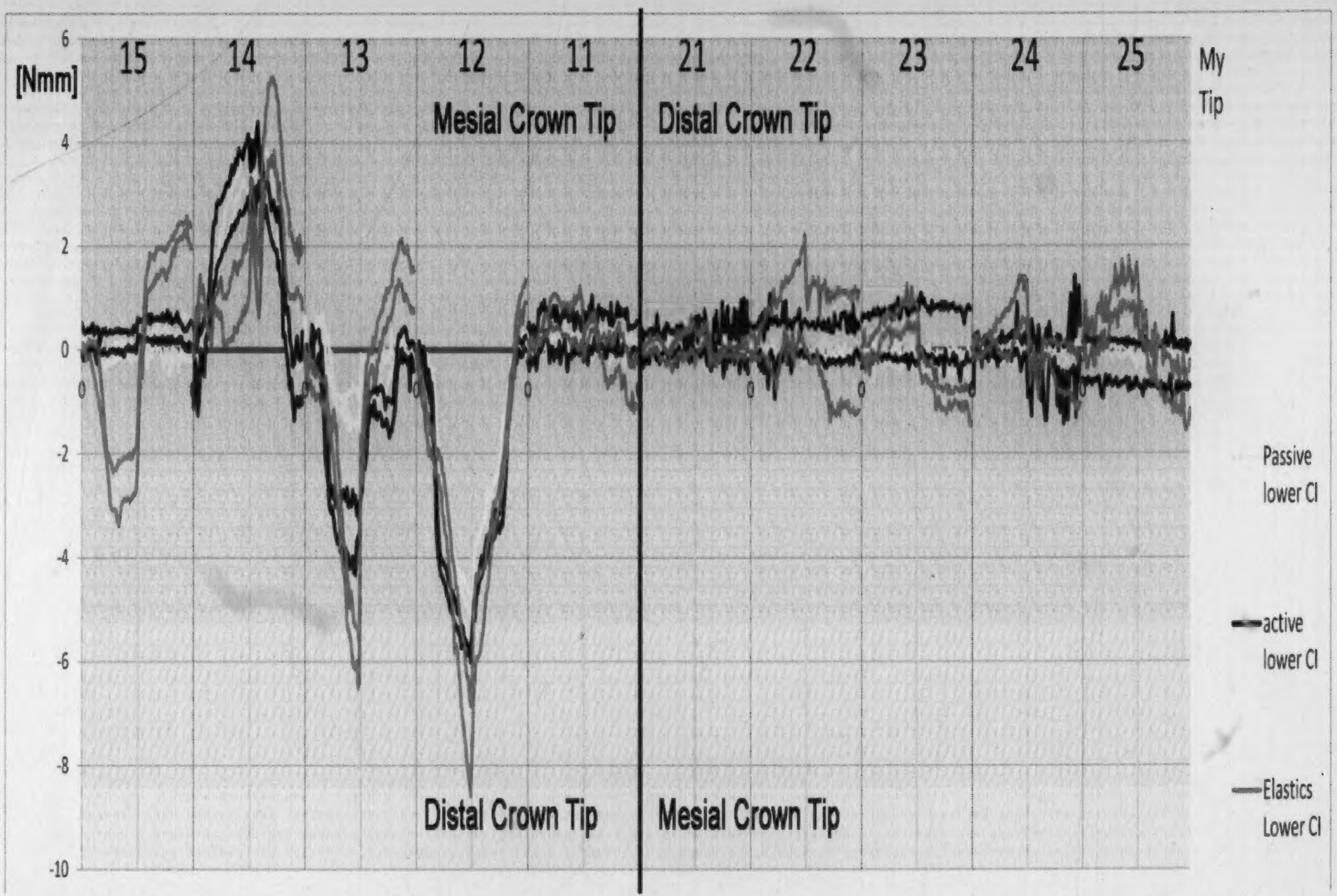

Figure 5-14: 0.014” My mesio-distal crown tip, 95% confidence intervals

014 My		Displacement mm						
		1 mm	2 mm	3 mm	4 mm	3 mm	2 mm	1 mm
Tooth	ligation	Moment Nmm						
15	Passive	0.04	-0.11	0.04	-0.04	0.15	0.01	0.13
	Active	0.11	0.15	0.14	0.16	0.35	0.35	0.45
	Elastics	-0.24	-2.41	-2.52	-2.29	1.51	1.75	2.27
14	Passive	0.37	2.03	2.92	3.51	3.40	2.38	0.31
	Active	0.56	2.31	2.90	3.54	3.17	2.26	0.02
	Elastics	0.55	1.05	1.05	1.58	2.73	4.22	1.85
13	Passive	0.37	-0.70	-1.20	-1.20	-0.51	-0.36	-0.03
	Active	0.14	-2.93	-3.53	-3.48	-1.04	-1.17	0.05
	Elastics	-0.66	-1.76	-4.29	-5.99	-0.05	0.80	1.69
12	Passive	-0.43	-3.17	-4.33	-4.92	-3.80	-2.70	-0.33
	Active	-0.83	-4.30	-5.21	-5.91	-4.01	-3.30	-0.70
	Elastics	-1.76	-2.82	-5.19	-7.71	-4.67	-2.92	-0.68
11	Passive	0.06	0.15	0.21	0.13	0.17	0.05	-0.07
	Active	0.44	0.25	0.22	0.26	0.32	0.36	0.43
	Elastics	0.26	0.73	0.51	0.51	0.39	-0.13	-0.11
21	Passive	0.01	0.00	-0.01	-0.03	-0.13	-0.06	-0.06
	Active	0.19	0.22	0.15	0.20	-0.11	0.00	0.26
	Elastics	0.07	-0.17	0.15	0.22	0.31	-0.09	-0.02
22	Passive	-0.06	-0.06	-0.08	-0.09	-0.03	-0.07	-0.07
	Active	-0.12	0.12	0.00	0.26	0.24	0.09	0.25
	Elastics	0.23	0.26	0.62	1.13	0.59	0.03	0.03
23	Passive	-0.04	-0.19	-0.21	-0.21	-0.14	-0.24	-0.17
	Active	0.27	0.31	0.32	0.24	0.25	0.37	0.30
	Elastics	0.10	0.54	0.64	0.71	-0.45	-0.98	-0.88
24	Passive	-0.03	0.01	-0.12	-0.08	-0.01	-0.01	-0.05
	Active	-0.04	0.07	0.20	0.00	-0.30	-0.13	-0.20
	Elastics	0.09	0.26	0.52	0.91	-0.52	-0.16	-0.40
25	Passive	0.02	0.03	-0.01	-0.13	0.05	0.04	0.05
	Active	-0.22	-0.19	-0.23	-0.24	-0.30	-0.28	-0.29
	Elastics	0.32	0.68	1.24	1.22	-0.13	-0.58	-0.84
Sign convention		R			L			
	Positive	Mesial crown tip			Distal crown tip			
	Negative	Distal crown tip			Mesial crown tip			

Table 5-6: 0.014" wire My data at 1mm increments

5.2.5.1 Cuspid:

The 13 experiences distal crown tip on loading and unloading with SL brackets, PSL producing lower My moments than ASL during both phases. The 13 experiences distal crown tip on loading and mesial crown tip on unloading with EL brackets. This moment can be produced by:

a. The Fz occlusal force being more concentrated on the mesial side of the #13 bracket, this is confirmed by noticing the pattern of My which is similar to the pattern of Fz on #13

b. The Fx force on the #13 acting on the gingival aspect of the bracket slot, more superior to the mid-bracket coordinate system.

5.2.5.2 Teeth distal to #13:

Tooth #14 shows a mesial crown tip on the loading and unloading and this is expected considering the angulation of the wire relative to the bracket slot. SL brackets produces higher My than EL during loading, while EL produces higher My during unloading. This My is directly related to the binding developed on the 14 bracket. The 15 on the other hand shows small My moments with SL brackets, while EL produces a relatively high distal crown tip on loading and a mesial crown tip on unloading, this could be related to the Fx force acting on the gingival slot wall of the 15 bracket on loading and unloading.

5.2.5.3 Teeth mesial to #13:

Tooth #12 shows a large distal crown tip for all ligation methods throughout loading and unloading, EL produces the highest moments and PSL produces the lowest moments.

On examining the 3D graphs (Figure 5-16) we notice that EL produces the most unwanted My moments while SL produces the least unwanted My moments.

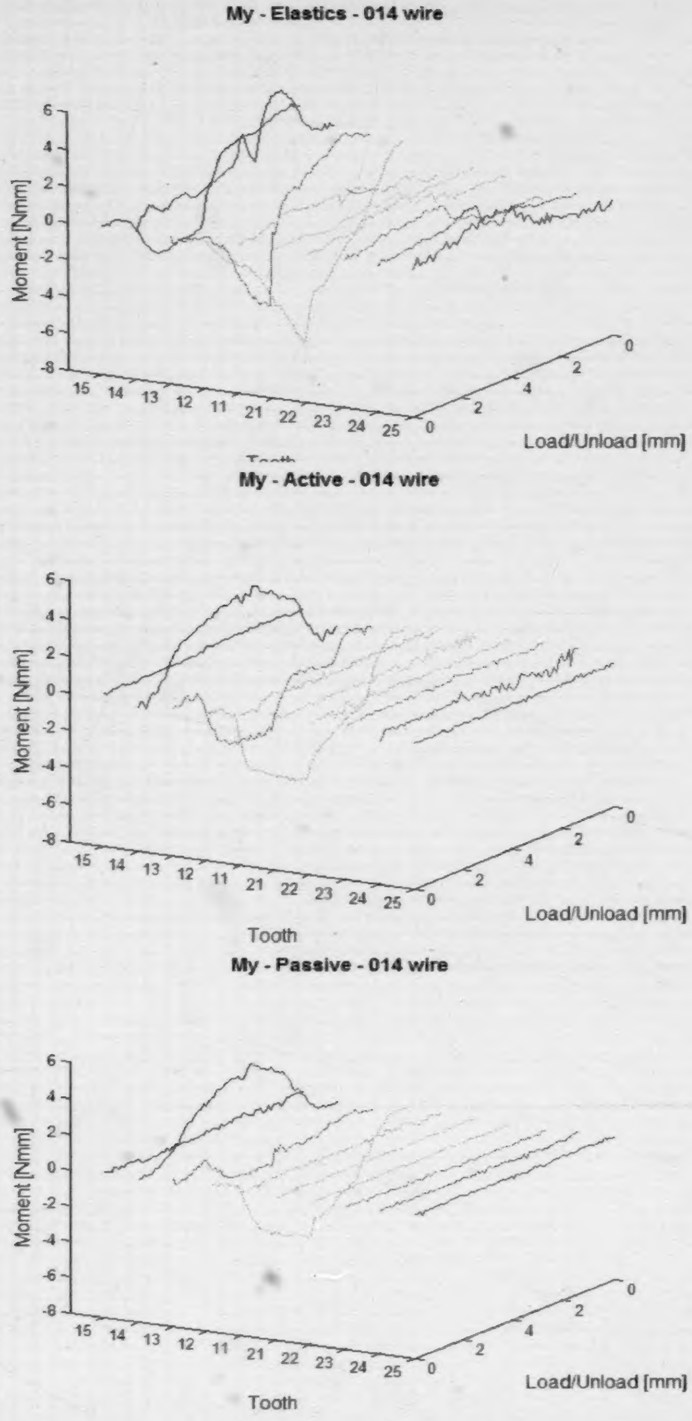

Figure 5-15: 3D 0.014" My mesio-distal crown tip, graphs, means EL, ASL and PSL brackets

5.2.6 Mz Moments (Disto-Buccal/Mesio-Buccal Moments)

We would expect no Mz moments on any of the teeth, however the largest moments were detected when elastic ligation (EL) was used (Figure 5-17, Figure 5-18, Table 5-7). The Mz moments seen here can be caused by one of the following:

a) Fx acting on the bracket at a distance from the bracket coordinate system, (ie an Fx acting more buccal relative to the mid-bracket coordinate system).

b) Fy acting on the bracket at a distance from the bracket coordinate system (ie an Fy acting more mesial or distal relative to the mid-bracket coordinate system).

c) A force couple

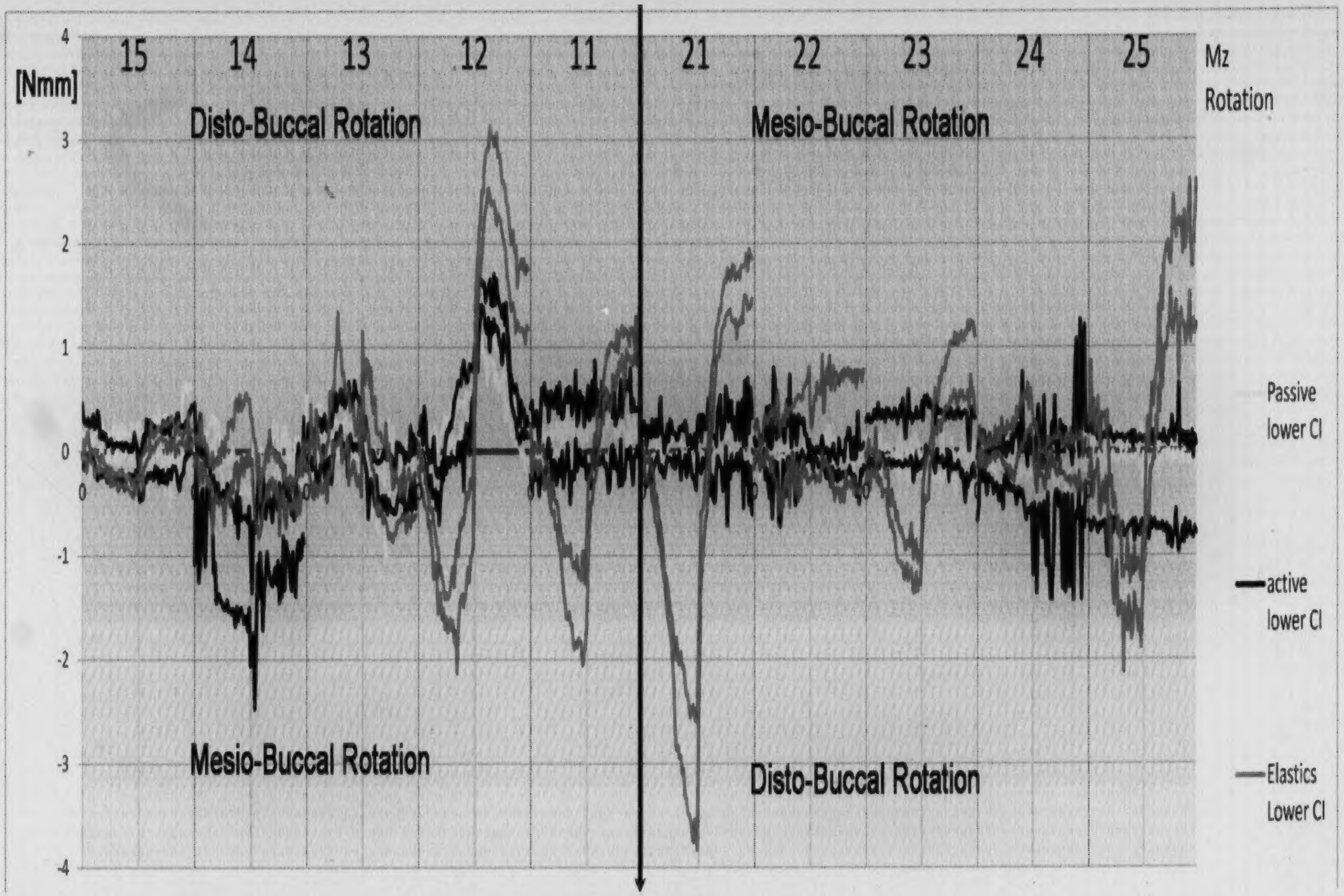

Figure 5-16: 0.014” Mz rotation around the long axis, 95% confidence intervals

014 Mz		Displacement mm						
		1 mm	2 mm	3 mm	4 mm	3 mm	2 mm	1 mm
Tooth	ligation	Moment Nmm						
15	Passive	0.05	0.07	0.12	0.04	0.07	-0.02	0.13
	Active	0.03	-0.06	-0.14	-0.14	-0.01	-0.05	0.03
	Elastics	-0.08	-0.26	-0.27	-0.32	0.13	0.20	0.18
14	Passive	0.11	-0.08	-0.23	-0.26	-0.09	0.07	-0.07
	Active	-0.21	-0.93	-1.17	-1.02	-0.94	-0.88	-0.84
	Elastics	-0.18	-0.20	0.17	0.25	-0.35	-0.27	-0.37
13	Passive	0.07	0.19	0.08	0.07	-0.26	-0.05	-0.30
	Active	0.09	0.23	0.15	0.24	-0.29	-0.24	-0.23
	Elastics	-0.13	0.30	0.37	-0.19	0.09	-0.39	-0.47
12	Passive	0.01	0.16	0.27	0.41	0.97	0.76	0.32
	Active	-0.27	-0.03	0.28	0.59	1.35	1.19	0.45
	Elastics	-0.76	-1.48	-1.08	-0.56	2.67	2.47	1.63
11	Passive	0.02	0.06	0.15	0.12	0.15	-0.04	-0.03
	Active	0.22	0.08	0.08	0.17	0.14	0.19	0.31
	Elastics	-0.21	-0.70	-1.36	-1.58	0.25	0.87	1.06
21	Passive	0.00	0.01	0.01	-0.02	-0.08	0.01	0.01
	Active	0.11	0.11	0.04	0.09	-0.15	-0.06	0.14
	Elastics	-0.56	-1.64	-2.56	-3.21	0.34	1.43	1.47
22	Passive	0.01	-0.02	-0.03	-0.05	0.02	-0.04	0.00
	Active	-0.12	-0.16	-0.18	0.05	0.02	-0.14	0.02
	Elastics	0.10	-0.07	0.05	0.26	0.45	0.20	0.20
23	Passive	-0.01	-0.11	-0.15	-0.11	-0.02	-0.15	-0.08
	Active	0.10	0.12	0.10	0.09	0.14	0.18	0.04
	Elastics	-0.17	-0.65	-0.98	-1.13	0.31	0.66	0.84
24	Passive	-0.03	0.00	-0.12	-0.09	0.05	0.08	0.03
	Active	-0.18	-0.12	-0.06	-0.28	-0.46	-0.28	-0.28
	Elastics	-0.01	0.04	0.14	0.31	-0.21	-0.03	-0.11
25	Passive	-0.01	0.03	0.01	-0.09	0.08	0.08	0.07
	Active	-0.29	-0.27	-0.29	-0.29	-0.30	-0.29	-0.28
	Elastics	0.00	-0.89	-1.27	-1.21	0.56	1.54	1.57
Sign convention		R			L			
	Positive	Disto-Buccal rotation			Mesio-Buccal rotation			
	Negative	Mesio-Buccal rotation			Disto-Buccal rotation			

Table 5-7: 0.014" wire Mz data at 1mm increments

5.2.6.1 Cuspid:

On examining the graph, we notice a pattern of disto-buccal rotation on loading and mesio-buccal rotation on unloading. There is little difference between the three ligation methods. This pattern can be related to Fx forces which is mesial on loading and distal on unloading.

5.2.6.2 Teeth distal to #13:

On tooth #14 we notice a relatively large mesio-buccal rotation on loading and unloading with ASL brackets, which is not present with either PSL or EL. This could be caused by the interaction between the active spring of the ASL bracket and the wire, applying a buccal Fy on the mesial aspect of the bracket during loading and a lingual Fy on the distal aspect of the bracket during unloading. This moment is unlikely to be caused by the Fx force, which would cause different patterns during loading and unloading.

5.2.6.3 Teeth mesial to #13:

The #12 and #11 shows a high mesio–buccal rotation on loading and a disto-buccal rotation on unloading with elastics, as well as a disto-buccal moment on loading followed by a mesio-buccal moment on unloading for teeth 21, 23 and 25. These moments are most likely related to the Fx forces. We notice tooth # 22 and #24 have low Mz moments, which is consistent with the Fx pattern.

SL brackets produces low Mz moments, however there is more variation with ASL when compared to PSL.

On examining the 3D graphs (Figure 5-18) it is apparent that PSL produces the least unwanted Mz moments while EL produces the most unwanted Mz moments.

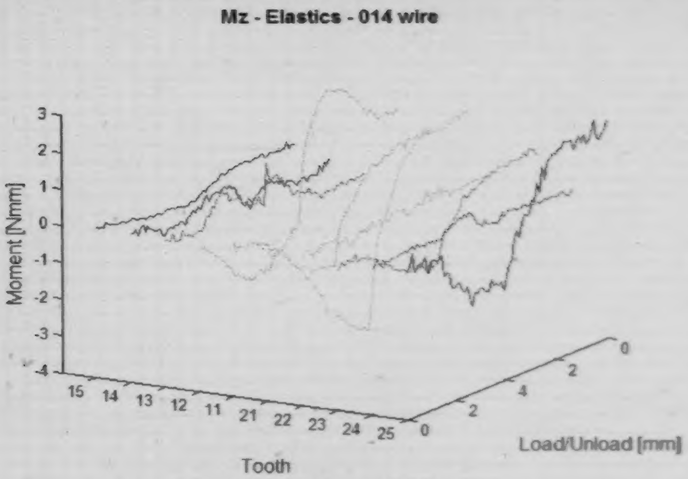

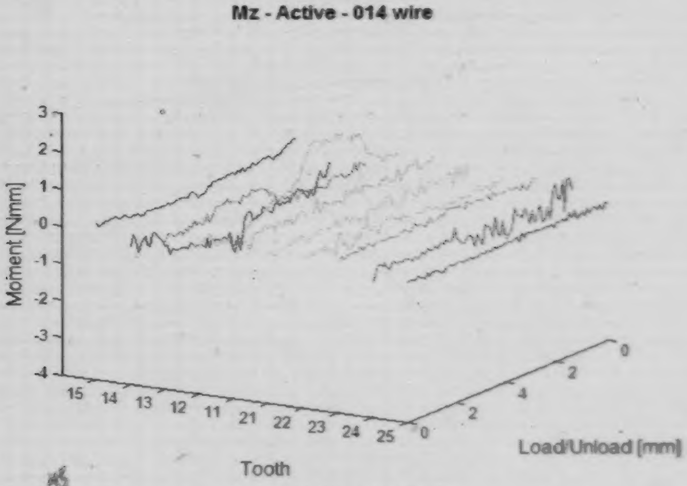

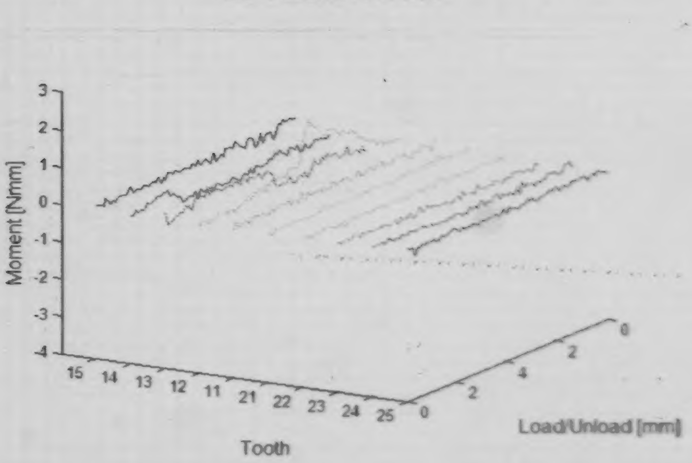

Figure 5-17: 3D 0.014" Mz rotation around the long axis graphs, means EL, ASL and PSL brackets

5.3 0.018" NiTi wire

5.3.1 Mesio-distal forces (Fx)

Different ligation methods produce different levels of resistance to sliding, which seems to affect the force system produced. When we examine the Fx graph (Figure 5-19, Figure 5-21, Table 5-8) of the 10 teeth, we notice Fx forces are generated as the cuspid is moved from the default position to the displaced position and then back to the default position. On the teeth distal to the 13 (tooth#14 and #15) the Fx force is in a mesial direction during loading and in distal direction during unloading, which would be expected. On the teeth mesial of the 13 (tooth #12, #11,) Fx force is in a distal direction during loading and in a mesial direction during unloading, and for teeth #21, #23, #24 and #25 Fx is in a mesial direction during loading and in distal direction during unloading.

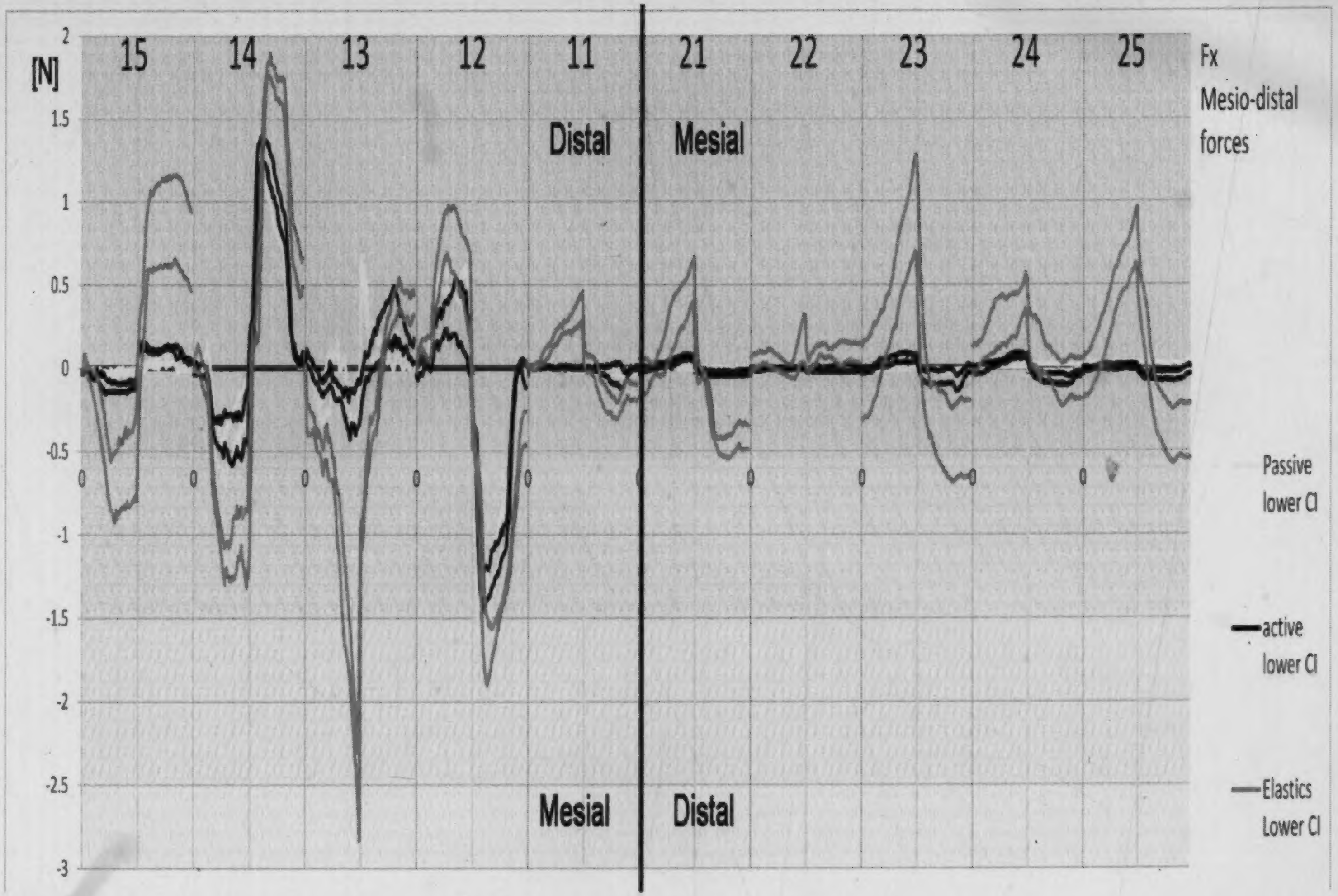

Figure 5-18: 0.018" NiTi, Fx Mesio-distal forces 95% confidence intervals

018 Fx		Displacement mm						
		1 mm	2 mm	3 mm	4 mm	3 mm	2 mm	1 mm
Tooth	ligation	Force N						
15	Passive	-0.04	-0.05	-0.02	-0.01	0.03	0.05	-0.01
	Active	-0.04	-0.10	-0.11	-0.10	0.11	0.12	0.10
	Elastics	-0.14	-0.66	-0.64	-0.52	0.83	0.87	0.89
14	Passive	0.05	-0.51	-0.35	-0.22	1.30	0.96	0.36
	Active	-0.06	-0.41	-0.42	-0.28	1.32	1.06	0.47
	Elastics	-0.13	-1.02	-1.07	-1.05	1.25	1.69	1.08
13	Passive	-0.20	-0.04	-0.14	-0.31	0.15	0.11	0.09
	Active	-0.08	-0.10	-0.22	-0.21	0.11	0.28	0.22
	Elastics	-0.44	-0.60	-1.46	-2.23	-0.35	0.21	0.43
12	Passive	0.10	0.54	0.47	0.51	-1.47	-1.08	-0.37
	Active	0.02	0.30	0.33	0.11	-1.33	-1.13	-0.36
	Elastics	0.12	0.79	0.70	0.25	-1.58	-1.51	-1.03
11	Passive	0.02	0.00	-0.01	-0.01	-0.02	-0.02	-0.04
	Active	0.00	0.00	0.00	0.00	0.00	-0.03	-0.07
	Elastics	0.05	0.18	0.26	0.31	-0.03	-0.20	-0.16
21	Passive	0.01	0.01	0.01	0.01	0.00	0.00	0.00
	Active	0.00	0.03	0.06	0.06	-0.03	-0.03	-0.03
	Elastics	-0.01	0.14	0.36	0.49	-0.12	-0.47	-0.43
22	Passive	0.00	0.00	0.00	0.00	0.00	0.00	0.00
	Active	-0.01	0.00	0.00	0.00	-0.01	-0.01	0.00
	Elastics	0.06	0.03	-0.02	0.16	0.10	0.08	0.09
23	Passive	0.00	0.00	0.00	0.00	-0.02	-0.02	-0.02
	Active	0.01	0.04	0.06	0.06	-0.06	-0.06	-0.09
	Elastics	0.04	0.29	0.68	0.98	-0.25	-0.37	-0.44
24	Passive	0.01	0.01	0.01	0.02	0.00	0.00	0.00
	Active	0.00	0.03	0.07	0.07	-0.05	-0.07	-0.08
	Elastics	0.15	0.27	0.32	0.44	0.09	-0.02	-0.07
25	Passive	0.02	0.02	0.02	0.02	0.00	0.00	0.00
	Active	0.00	0.01	0.01	0.01	-0.05	-0.05	-0.05
	Elastics	0.07	0.33	0.59	0.78	-0.02	-0.32	-0.39
Sign convention		R			L			
	Positive	Distal			Mesial			
	Negative	Mesial			Distal			

Table 5-8: 0.018" wire Fx force data at 1mm increments

5.3.1.1 Tooth #13:

In advance of the experiment, we anticipated that there would be no mesial or distal forces acting on tooth #13, however we recorded a mesial force during loading and a distal force during unloading with all ligation methods. This pattern of mesial force on loading and distal force on unloading, can be explained by the cumulative resistance to sliding produced by teeth located mesial of tooth #13 as opposed to distal of tooth #13. This will favour sliding of the wire through tooth #13 bracket in a mesial direction during loading, and in a distal direction during unloading, this sliding generates the Fx forces. We notice the immediate reversal of the force at the reversal point for the PSL compared to the more gradual reversal for EL and ASL (Figure 5-20), this is most likely due to the resilience of the ligation method of EL and ASL. It is apparent that the force magnitude is highest for elastics during loading and unloading. When we compare the two self-ligating methods, there is no appreciable difference between ASL and PSL during loading, however during unloading PSL shows somewhat less resistance to sliding than ASL except at the reversal point. This pattern is remarkably similar to the pattern seen with the 0.014”wire.

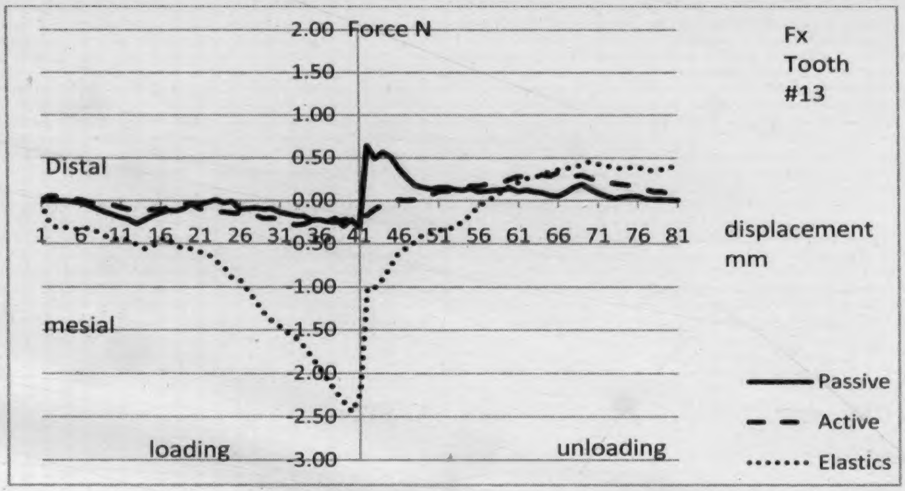

Figure 5-19: 0.018" Fx force on tooth #13

5.3.1.2 Teeth distal to the cuspid:

The teeth distal to the cuspid experience mesial force on loading and distal force on unloading, this pattern is consistent with what be the expected wire sliding. EL shows much higher force levels compared to SL brackets. On tooth #14 in spite of the presence of binding due to contact between the wire and the bracket walls, it is clear that the ligation method still plays a major role in producing the resistance to sliding as evidenced by the much higher Fx levels with EL. There is no difference between the SL brackets on tooth #14. On tooth #15, EL shows mesial forces during loading and distal forces during unloading which are much larger than those for SL, with the magnitude being slightly less than that for tooth #14. PSL produces less resistance to sliding than ASL on tooth #15 during loading and unloading.

5.3.1.3 Teeth mesial to the cuspid:

With EL, the resistance to sliding continues to be present throughout the dental arch all the way to tooth #25. The highest levels of Fx forces seem to skip certain teeth. Teeth # 21, #23 and #25 seem to experience much higher Fx forces than # 11, #22 and #24. This phenomena needs to be investigated further as no logical explanation can be presented at this point, the same observation was identified with the 0.014" wire. The most interesting finding in this graph is the fact that the resistance to sliding continues throughout the dental arch when elastic ligation is used.

With SL brackets tooth #12 is the only tooth mesial to the cuspid experiencing measureable high levels of Fx. This can be explained by the presence of relatively heavy contact between the wire and the bracket, this contact generates a normal force, which produces friction, this phenomenon is known as binding in orthodontics. Similar to our finding for the #14, EL produced higher resistance to sliding than SL, however the difference is smaller for tooth #12 than it is for tooth #14, and again the same pattern was identified with the 0.014"wire.

Another interesting finding on these graphs, is the fact that with EL the force levels start at zero for every tooth but never end at zero, unlike the SL brackets. There are significant residual Fx forces with EL, acting on all teeth even when the cuspid is back in the default position at the end of the unloading curve. Certain teeth (#21,23, 24 and 25) show higher resistance to sliding with ASL when compared to PSL.

On examining the 3D graphs in Figure 5-21, it seems that the difference between the two SL brackets is relatively small with PSL producing slightly less resistance to sliding than ASL on teeth #15, # 23 and #24. The most apparent difference lies between the EL and the SL brackets.

Fx - Elastics - 018 wire

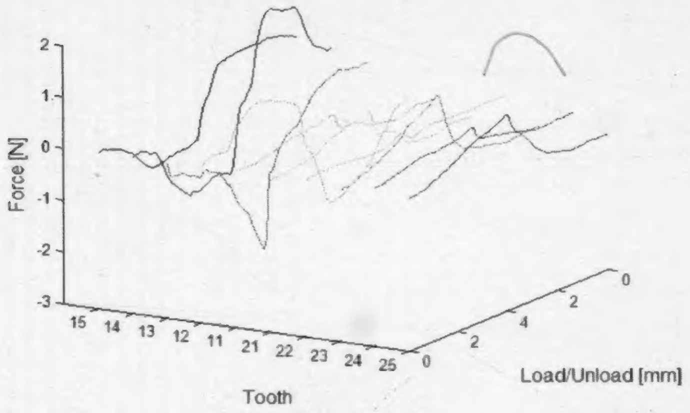

Fx - Active - 018 wire

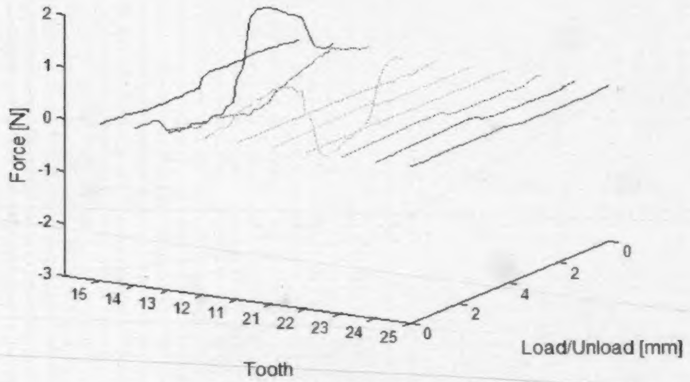

Fx - Passive - 018 wire

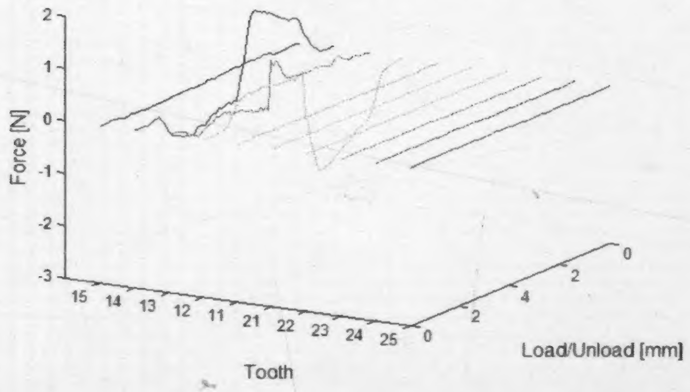

Figure 5-20: 3D 0.018” Fx graphs means EL, ASL and PSL brackets

5.3.2 Fy Bucco-lingual forces

In this simulated clinical situation, we would ideally prefer no Fy forces on any of the teeth. However, on examining the Fy graphs (Figure 5-22, Figure 5-23, Table 5-9) it is apparent that there are significant levels of bucco-lingual forces on all the teeth with all ligation methods. With ASL, the levels of Fy are lower than EL but higher than PSL, the same differences were found with 0.014" wire however these differences are more pronounced with the 0.018"wire. There is large CI range for Fy forces with EL and PSL brackets.

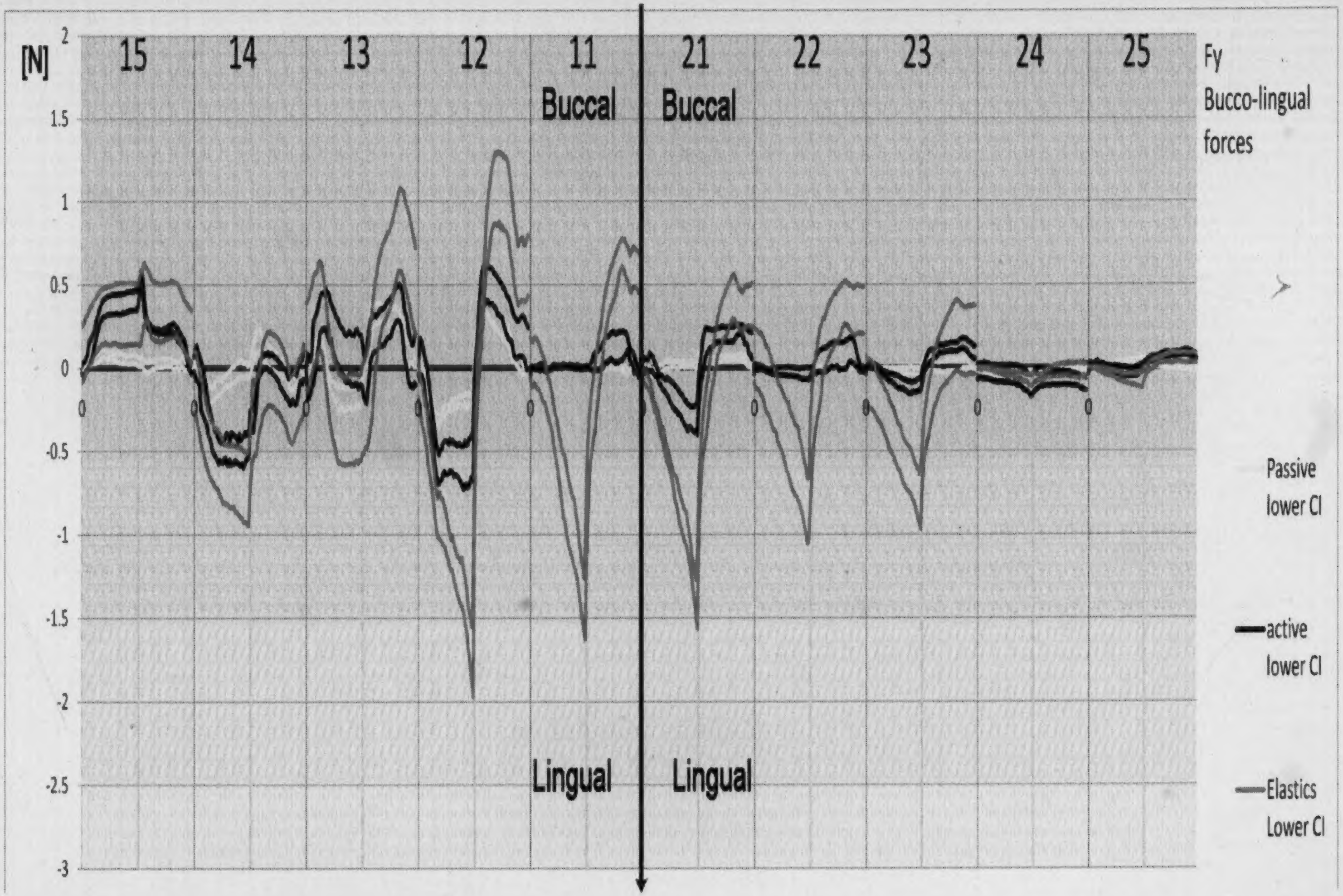

Figure 5-21: 0.018" Fy Bucco-lingual forces 95% confidence intervals

018 Fy		Displacement mm						
		1 mm	2 mm	3 mm	4 mm	3 mm	2 mm	1 mm
Tooth	ligation	Force N						
15	Passive	0.05	0.08	0.06	0.05	0.01	0.03	0.02
	Active	0.22	0.38	0.39	0.40	0.24	0.22	0.20
	Elastics	0.26	0.32	0.33	0.33	0.39	0.33	0.35
14	Passive	-0.13	-0.11	-0.03	-0.02	0.12	0.03	-0.10
	Active	-0.29	-0.51	-0.48	-0.47	0.03	0.00	-0.13
	Elastics	-0.43	-0.60	-0.66	-0.71	-0.08	-0.03	-0.24
13	Passive	0.17	-0.13	-0.18	-0.17	0.33	0.31	0.25
	Active	0.32	0.22	0.06	0.05	0.21	0.30	0.34
	Elastics	0.38	-0.20	-0.31	-0.29	0.22	0.57	0.82
12	Passive	-0.21	-0.25	-0.19	-0.21	0.37	0.26	0.06
	Active	-0.34	-0.54	-0.56	-0.53	0.51	0.41	0.19
	Elastics	-0.61	-0.98	-1.28	-1.60	0.78	1.07	0.70
11	Passive	0.01	0.00	0.00	0.00	0.00	0.00	-0.01
	Active	0.00	0.00	0.00	0.00	0.05	0.13	0.15
	Elastics	-0.08	-0.48	-0.94	-1.38	0.03	0.50	0.64
21	Passive	-0.03	0.02	0.02	0.02	0.04	0.06	0.06
	Active	-0.01	-0.14	-0.26	-0.31	0.18	0.20	0.23
	Elastics	-0.25	-0.57	-0.93	-1.35	-0.04	0.31	0.37
22	Passive	0.00	0.00	0.00	0.00	0.00	0.00	0.00
	Active	-0.02	-0.02	-0.03	-0.04	0.04	0.08	0.11
	Elastics	-0.08	-0.31	-0.55	-0.84	0.12	0.30	0.36
23	Passive	-0.01	-0.02	-0.02	-0.02	0.01	0.01	0.02
	Active	-0.01	-0.07	-0.11	-0.10	0.08	0.12	0.14
	Elastics	-0.19	-0.38	-0.60	-0.78	-0.07	0.11	0.17
24	Passive	-0.02	-0.04	-0.05	-0.06	-0.04	-0.03	-0.03
	Active	-0.03	-0.04	-0.05	-0.11	-0.06	-0.07	-0.07
	Elastics	-0.01	-0.03	-0.05	-0.08	-0.04	-0.02	-0.01
25	Passive	0.00	0.02	0.03	0.04	0.02	0.01	0.00
	Active	0.00	-0.01	-0.03	-0.01	0.06	0.08	0.09
	Elastics	-0.02	-0.04	-0.07	-0.07	0.03	0.05	0.06
Sign convention		R			L			
	Positive	Buccal			Buccal			
	Negative	Lingual			Lingual			

Table 5-9: 0.018" wire Fy force data at 1mm increments

5.3.2.1 Cuspid:

We would expect no Fy forces to act on tooth #13, however there is a lingual force on loading and buccal force on unloading for EL and PSL. ASL produce a buccal force throughout loading and unloading. Highest forces are recorded with EL. These Fy forces are most likely related to the curvature of the arch and we might not see this if the brackets were arranged in a straight line. EL produce the most variability and PSL produce the least amount of variability.

5.3.2.2 Teeth distal to #13:

On tooth #14 there is a relatively large lingual force on loading for EL and ASL, PSL produce a much smaller lingual force during loading when compared to EL and ASL. During unloading there is no difference between the ligation methods, they all produce a lingual force. EL produce the largest variability and PSL produce the least variability.

On tooth 15 PSL shows no Fy forces while ASL and EL shows a relatively large buccal force during loading and unloading, with much larger variation for EL than ASL. It seems that the elastics and active ligation methods (elastics and spring clip) tend to apply a buccal force on the bracket during archwire sliding.

5.3.2.3 Teeth mesial to #13:

Tooth #12 shows a lingual force on loading and a buccal force on unloading for all ligation methods, the highest Fy force levels were recorded on the #12 bracket with EL. PSL shows lower Fy forces compared to ASL. The rest of the teeth mesial of the 13 show high Fy forces (lingual on loading, buccal on unloading) with EL except teeth #24 and #25. SL shows lower Fy forces compared to EL, with ASL producing higher Fy forces than PSL specifically on teeth # 11, 21, 22 and 23.

There is a large amount of variation with EL, this is expected of elastomeric ties. On examining the 3D graphs (Figure 5-23) it is apparent that EL produces the highest Fy forces and PSL produces the lowest Fy forces. With PSL brackets the Fy forces are generally limited to the teeth 14, 13 and 12. ASL on teeth #15, 11, 21, 22 and 23 shows relatively high buccal force compared to PSL.

When we examine the Fy graphs of all the teeth we notice in general the presence of a lingual force on loading and a buccal force on unloading. For PSL this pattern was generally not present on teeth of the left side. For EL this pattern was generally present on all teeth except the 24 and 25, which is very similar to the pattern seen with the 0.014" wire. ASL shows similar pattern of Fy forces to that of EL, but with lower magnitudes.

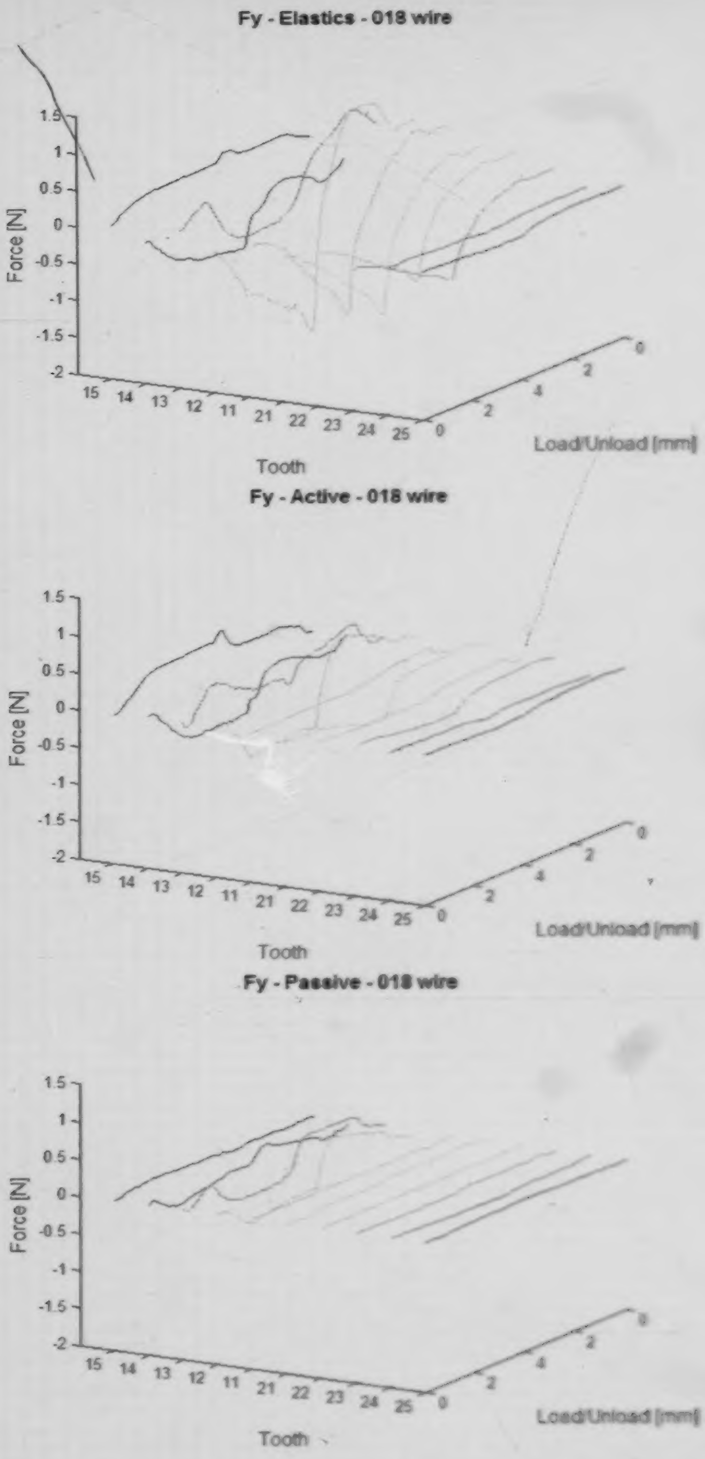

Figure 5-22: 3D 0.018" Fy graphs. Means EL, ASL and PSL brackets

5.3.3 Fz Occluso-gingival forces

In this simulated clinical situation, we would expect an extrusive force on 13 and two reciprocal intrusive forces on the 12 and 14, during loading and unloading. On examining the Fz graphs (Figure 5-24, Figure 5-27, Table 5-10) we notice the intrusive forces on the 12 and 14, and the extrusive force on the 13. An interesting finding is that the 15 and the 11 have a very similar Fz "W" pattern (Figure 5-25), this could be related to the angulation of the wire relative to those two teeth as the canine displacement is produced.

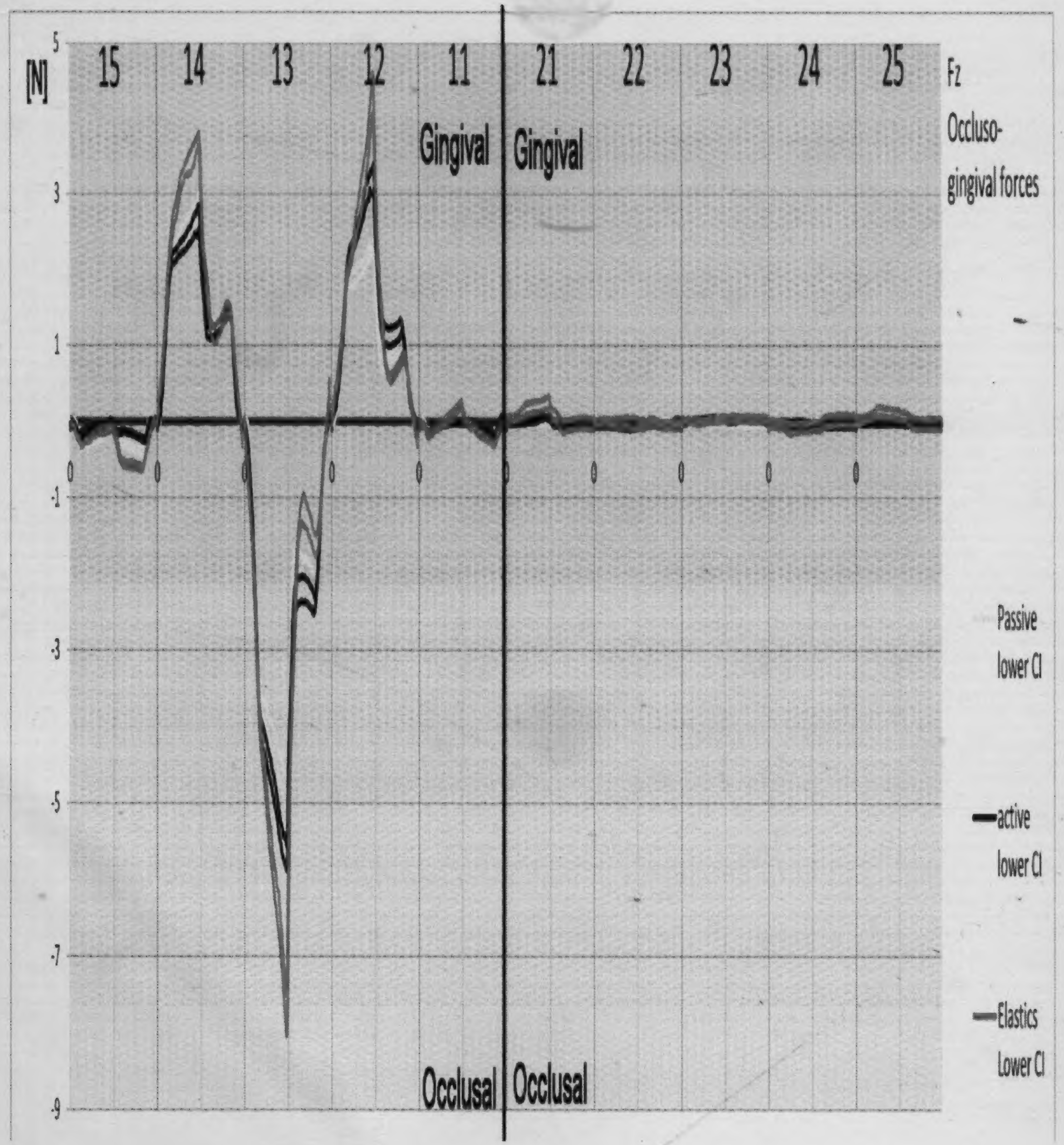

Figure 5-23: 0.018” Fz Occluso-gingival 95% confidence intervals

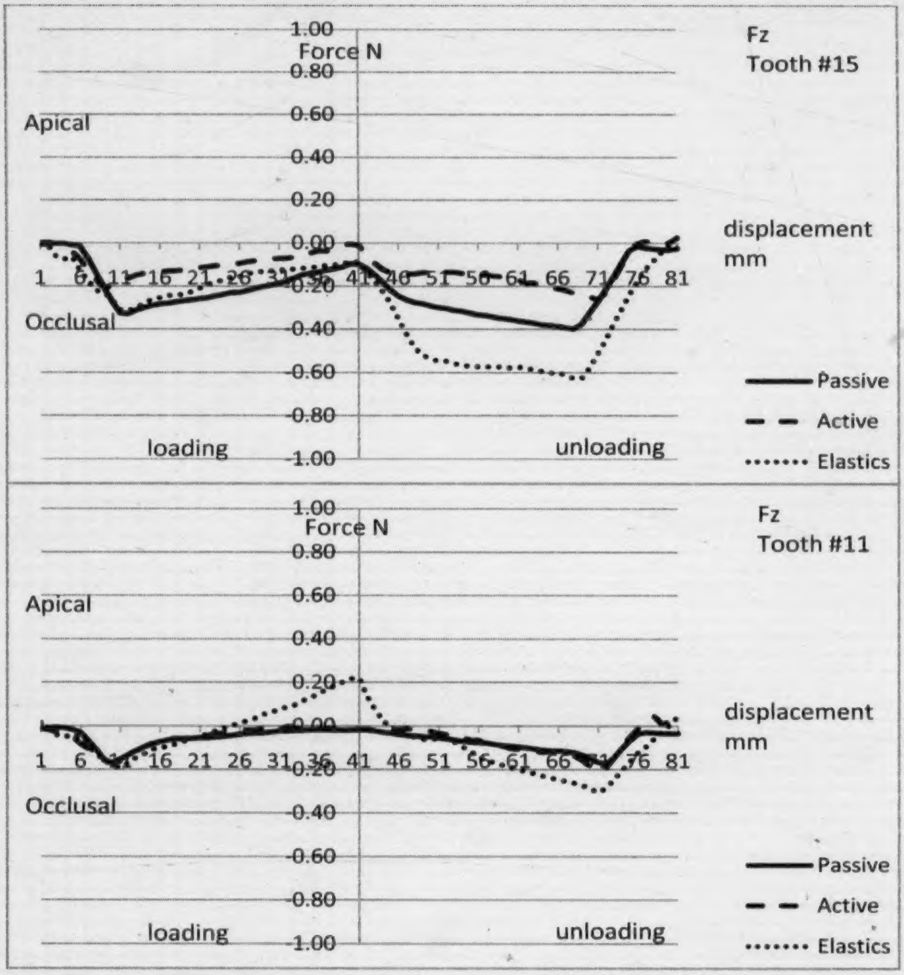

Figure 5-24: 0.018” Fz load deflection of tooth #15 and #11showing the “W” pattern

018 Fz		Displacement mm						
		1 mm	2 mm	3 mm	4 mm	3 mm	2 mm	1 mm
Tooth	ligation	Force N						
15	Passive	-0.33	-0.26	-0.19	-0.10	-0.30	-0.36	-0.27
	Active	-0.18	-0.12	-0.07	-0.01	-0.13	-0.17	-0.26
	Elastics	-0.31	-0.21	-0.13	-0.09	-0.55	-0.58	-0.51
14	Passive	1.54	2.37	2.58	2.84	1.23	1.33	1.15
	Active	1.65	2.25	2.44	2.68	1.16	1.29	1.28
	Elastics	1.87	2.95	3.40	3.68	1.29	1.28	1.33
13	Passive	-2.12	-3.86	-4.34	-4.98	-1.83	-1.98	-1.71
	Active	-2.40	-4.30	-5.03	-5.74	-2.23	-2.26	-1.65
	Elastics	-2.53	-4.82	-6.26	-7.68	-1.61	-1.34	-1.39
12	Passive	1.02	1.88	2.05	2.38	0.76	0.92	0.87
	Active	1.08	2.30	2.81	3.22	1.13	1.15	0.76
	Elastics	1.19	2.28	3.18	4.25	0.81	0.66	0.72
11	Passive	-0.15	-0.06	-0.02	-0.02	-0.06	-0.10	-0.17
	Active	-0.16	-0.05	-0.01	-0.01	-0.04	-0.11	-0.21
	Elastics	-0.19	-0.05	0.07	0.22	-0.06	-0.20	-0.31
21	Passive	0.00	-0.02	-0.02	-0.01	-0.02	-0.03	-0.03
	Active	-0.02	-0.01	0.03	0.05	-0.05	-0.04	-0.03
	Elastics	0.06	0.17	0.20	0.24	-0.02	-0.04	-0.02
22	Passive	-0.02	-0.02	-0.02	-0.02	-0.02	-0.03	-0.03
	Active	-0.03	-0.04	-0.06	-0.06	-0.03	-0.03	-0.05
	Elastics	0.00	-0.01	-0.01	-0.03	-0.03	-0.03	-0.05
23	Passive	-0.02	-0.01	-0.01	-0.01	-0.02	-0.02	-0.02
	Active	0.00	0.02	0.03	0.02	0.02	0.03	0.03
	Elastics	0.00	-0.01	0.01	0.04	0.05	0.03	0.03
24	Passive	-0.01	-0.01	-0.02	-0.02	-0.02	-0.03	-0.03
	Active	-0.03	-0.02	-0.03	-0.03	-0.04	-0.04	-0.05
	Elastics	-0.03	-0.10	-0.08	-0.07	-0.03	0.02	0.02
25	Passive	-0.01	-0.01	-0.01	-0.02	-0.02	-0.02	-0.02
	Active	-0.01	-0.01	-0.01	-0.01	-0.02	-0.02	-0.03
	Elastics	0.05	0.13	0.11	0.11	0.02	-0.03	-0.03
Sign convention		R			L			
	Positive	Gingival			Gingival			
	Negative	Occlusal			Occlusal			

Table 5-10: 0.018” wire Fz force data at 1mm increments

5.3.3.1 Cuspid:

During loading, the cuspid experiences highest Fz forces with EL and lowest with PSL, (Figure 5-26). During unloading ASL shows marginally higher Fz force than PSL, and EL showing the lowest Fz magnitude. There is a very large difference in the Fz magnitude between loading and unloading, especially for EL brackets. This pattern is remarkably similar to that of the 0.014" wire.

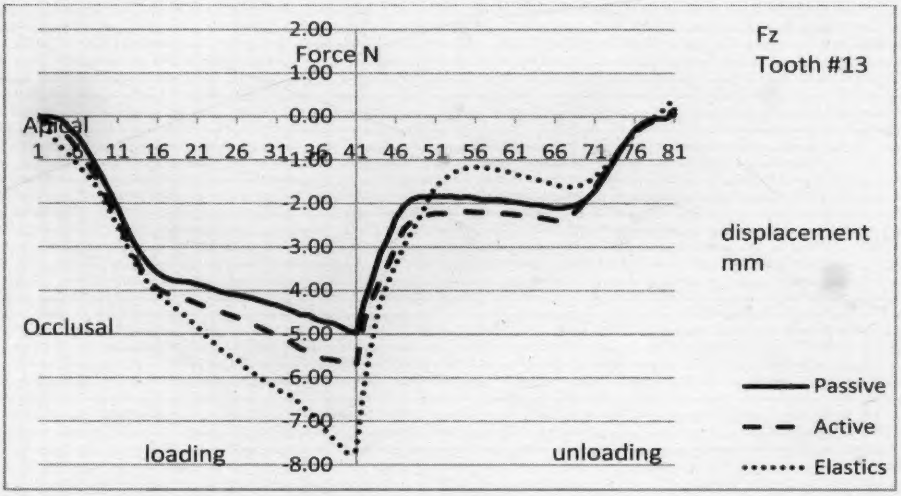

Figure 5-25: 0.018" Fz force on tooth #13

5.3.3.2 Teeth distal to #13:

All ligation methods produce similar patterns of Fz with different magnitudes. On tooth #14 the EL brackets produce the highest intrusive force during loading and ASL produced slightly lower Fz than PSL. During unloading, there is very little difference between the three ligation methods, and again this pattern is very similar to that of 0.014" wire.

Tooth #15 shows a "W" pattern of extrusive force throughout the loading and unloading declining to zero at the reversal point (Figure 5-25). This can be explained by the angulation of the wire relative to the 14 bracket slot during loading and unloading. At the start of the loading, the 14 bracket acts as a lever point for the wire as the cuspid is intruded, this causes the wire to apply an extrusive force on the 15. When the wire bends mesial of the 14 as the cuspid is further intruded, this extrusive force disappears since the wire becomes parallel to the 14 bracket slot. EL produces the largest extrusive force on tooth #15 during unloading, while ASL produced a slightly lower extrusive force than PSL.

5.3.3.3 Teeth mesial to #13:

All ligation methods produce similar patterns of Fz with different magnitudes. On tooth #12 the EL brackets produce the highest intrusive force during loading and PSL produce the lowest Fz force. During unloading ASL produce the highest Fz and EL produce the lowest Fz. ASL produce much higher Fz forces than PSL during loading and unloading. Tooth #11 shows a "W" pattern of occlusal force (Figure 5-25) similar to that of #15, throughout the loading and unloading declining to zero at the reversal point.

On examining the 3D graphs in Figure 5-27, we notice that SL brackets deliver the load-deflection curve expected of NiTi wires, characterized by flat loading and unloading curves, and the loading curves exhibiting higher force magnitudes compared to the unloading curves.

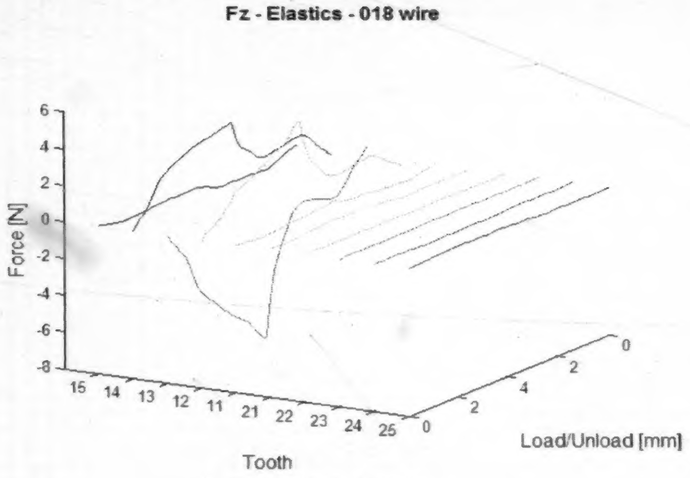
Fz - Elastics - 018 wire

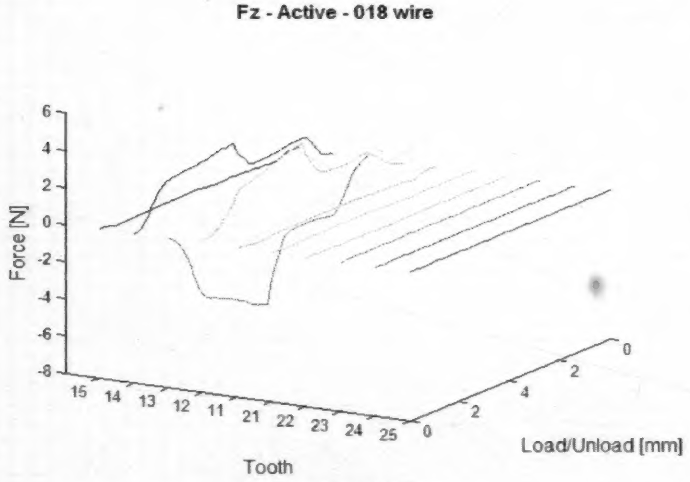
Fz - Active - 018 wire

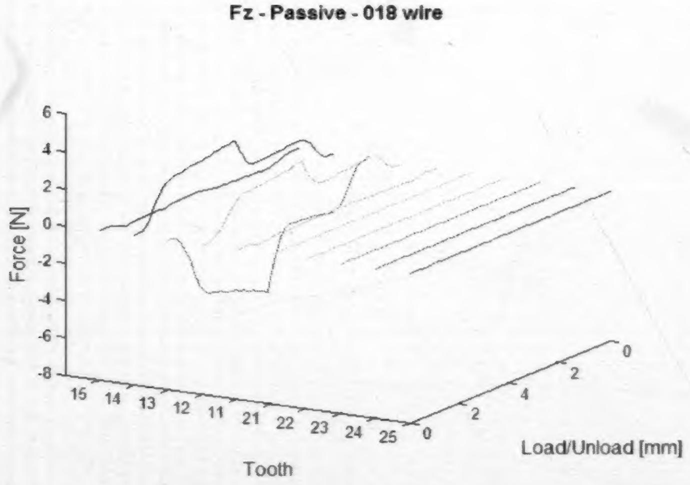
Fz - Passive - 018 wire

Figure 5-26: 3D 0.018" Fz graphs. Means EL, ASL and PSL brackets

5.3.4 Mx Moments (Bucco-Lingual Moments)

We would expect no Mx moments on any of the teeth, however the largest moments were detected when elastic ligation (EL) was used and specifically on the 13, 12, 11, 21, 22 and 23. These moments are in a buccal crown torque direction on loading and a lingual crown torque on unloading (Figure 5-28, Figure 5-29, Table 5-11). The Mx moments seen here can be caused by one of the following:

a) Fy acting on the bracket at a occluso-gingival distance from the bracket coordinate system.

b) Fz acting on the bracket at a bucco-lingual distance from the bracket coordinate system

c) A force couple

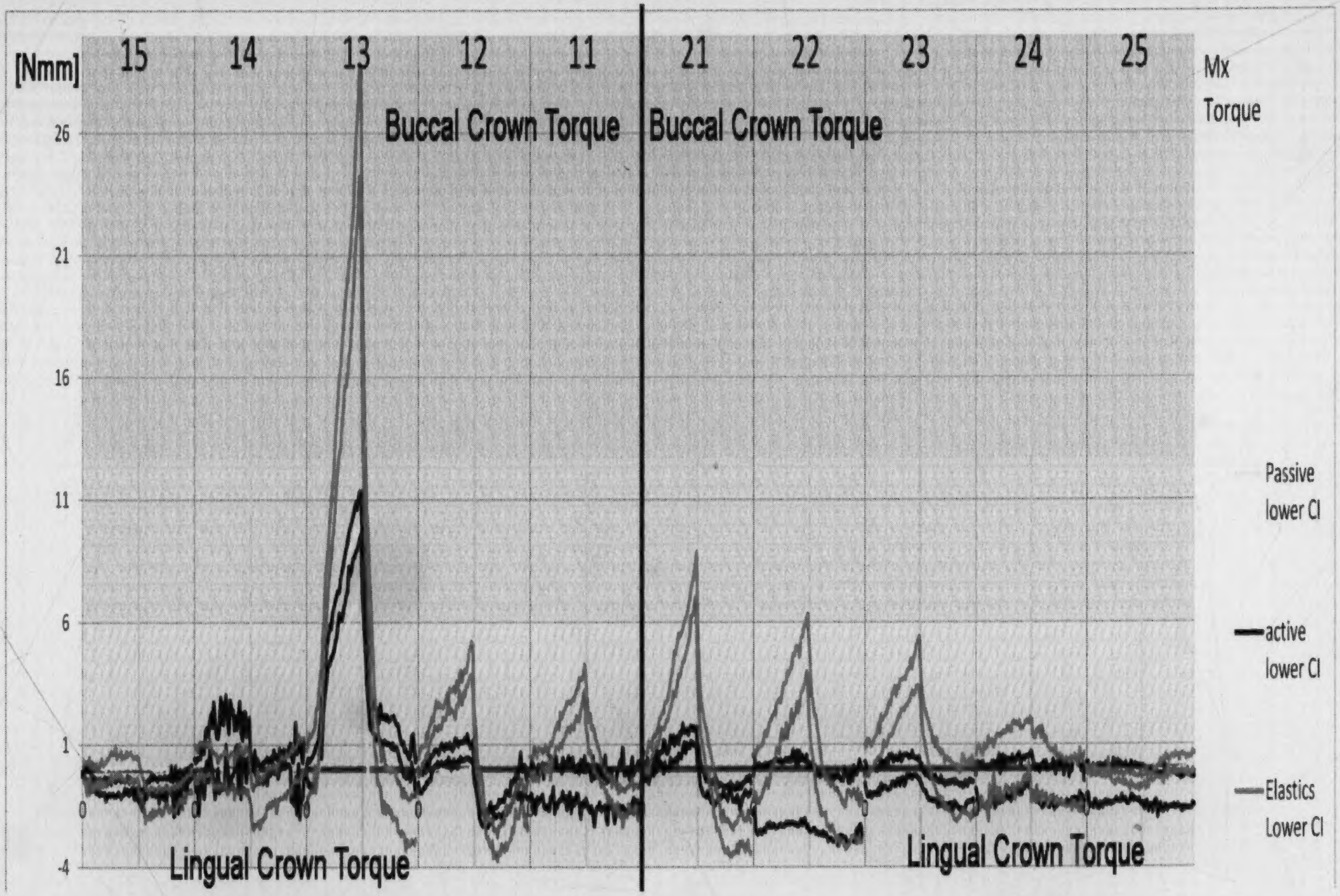

Figure 5-27: 0.018” Mx Bucco-lingual crown torque, 95% confidence intervals

018 Mx		Displacement mm						
		1 mm	2 mm	3 mm	4 mm	3 mm	2 mm	1 mm
Tooth	ligation	Moment Nmm						
15	Passive	-0.52	-0.55	-0.58	-0.54	-0.55	-0.72	-0.66
	Active	-0.69	-0.71	-0.72	-0.77	-0.55	-0.51	-1.03
	Elastics	-0.26	0.14	0.06	0.08	-1.39	-1.16	-1.05
14	Passive	-0.04	-0.30	-0.41	-0.32	-0.65	-0.54	-0.42
	Active	0.47	0.80	1.50	1.01	-0.14	0.30	0.55
	Elastics	0.35	-0.06	-0.16	-0.28	-1.21	-0.94	-0.13
13	Passive	1.21	5.82	7.10	9.09	-0.23	-0.09	-0.03
	Active	1.24	5.73	8.28	10.44	1.97	1.51	0.53
	Elastics	2.49	11.05	18.14	25.26	1.91	-0.81	-1.85
12	Passive	0.12	0.41	0.29	0.57	-1.81	-1.63	-1.06
	Active	0.21	0.66	0.70	0.75	-2.01	-1.60	-0.74
	Elastics	1.72	2.45	3.49	4.14	-2.30	-2.90	-1.94
11	Passive	-0.59	-0.56	-0.73	-0.73	-0.80	-0.96	-1.07
	Active	-0.90	-0.76	-0.85	-0.48	-0.91	-0.86	-0.98
	Elastics	0.43	1.38	2.23	3.71	0.26	-1.00	-1.40
21	Passive	-0.15	-0.37	-0.38	-0.36	-0.48	-0.54	-0.58
	Active	0.07	0.40	1.36	1.32	-0.87	-0.79	-0.84
	Elastics	1.10	2.71	5.06	7.45	-0.02	-2.50	-2.64
22	Passive	-0.64	-0.68	-0.74	-0.78	-0.80	-0.91	-1.00
	Active	-1.07	-0.95	-0.78	-1.09	-1.44	-1.56	-1.77
	Elastics	0.49	2.03	3.36	4.97	-0.75	-1.76	-2.00
23	Passive	-0.38	-0.37	-0.40	-0.43	-0.58	-0.75	-0.88
	Active	-0.42	0.01	0.01	0.03	-0.81	-0.99	-1.16
	Elastics	1.16	2.20	3.11	4.30	0.36	-0.53	-1.06
24	Passive	-0.34	-0.35	-0.36	-0.36	-0.49	-0.67	-0.75
	Active	-0.61	-0.36	-0.26	-0.03	-0.61	-0.68	-0.73
	Elastics	0.17	0.07	0.47	0.86	0.02	-0.36	-0.51
25	Passive	-0.27	-0.42	-0.52	-0.63	-0.58	-0.68	-0.77
	Active	-0.61	-0.51	-0.69	-0.65	-0.79	-0.95	-0.98
	Elastics	-0.15	-0.30	-0.42	-0.38	-0.23	0.01	0.23
Sign convention		R			L			
	Positive	Buccal crown torque			Buccal crown torque			
	Negative	Lingual crown torque			Lingual crown torque			

Table 5-11: 0.018" wire Mx moment data at 1mm increments

5.3.4.1 Cuspid:

The cuspid experiences a very large buccal crown torque moment during loading and a relatively smaller lingual crown torque on unloading. SL brackets produce lower level but similar pattern of Mx moment with larger variation for PSL compared to ASL. One explanation for such a moment of EL is that the Fy forces acting on the cuspid in a lingual direction during loading and buccal direction during unloading, are being applied at a point within the bracket slot superior (gingival) to the mid-bracket coordinate system. another explanation is the development of a force couple with the bracket slot that produces this Mx moment.

5.3.4.2 Teeth distal to #13:

There is no discernable pattern for moments produced by the three ligation methods on teeth #14 and #15. However, we notice the high level of variation.

5.3.4.3 Teeth mesial to #13:

El brackets produce large buccal crown torque moments on loading and lingual crown torque moments on unloading for teeth #12, 11, 21, 22 and 23, which is very similar to the pattern seen with 0.014" wire. Again, the highest moment is experienced by tooth #21. SL brackets produce a lingual crown torque moment on unloading on tooth #12, and no specific pattern on the other teeth, the ASL produce similar variation to PSL.

The 3D graphs (Figure 5-29) show that EL produce the largest amount of Mx moments, with very little difference between ASL and PSL, however PSL seem to produce slightly lower moments than ASL, which is not detectable on the 95% CI graphs. It seems that the addition of elastics produces complex Mx loading which is not seen with the SL brackets.

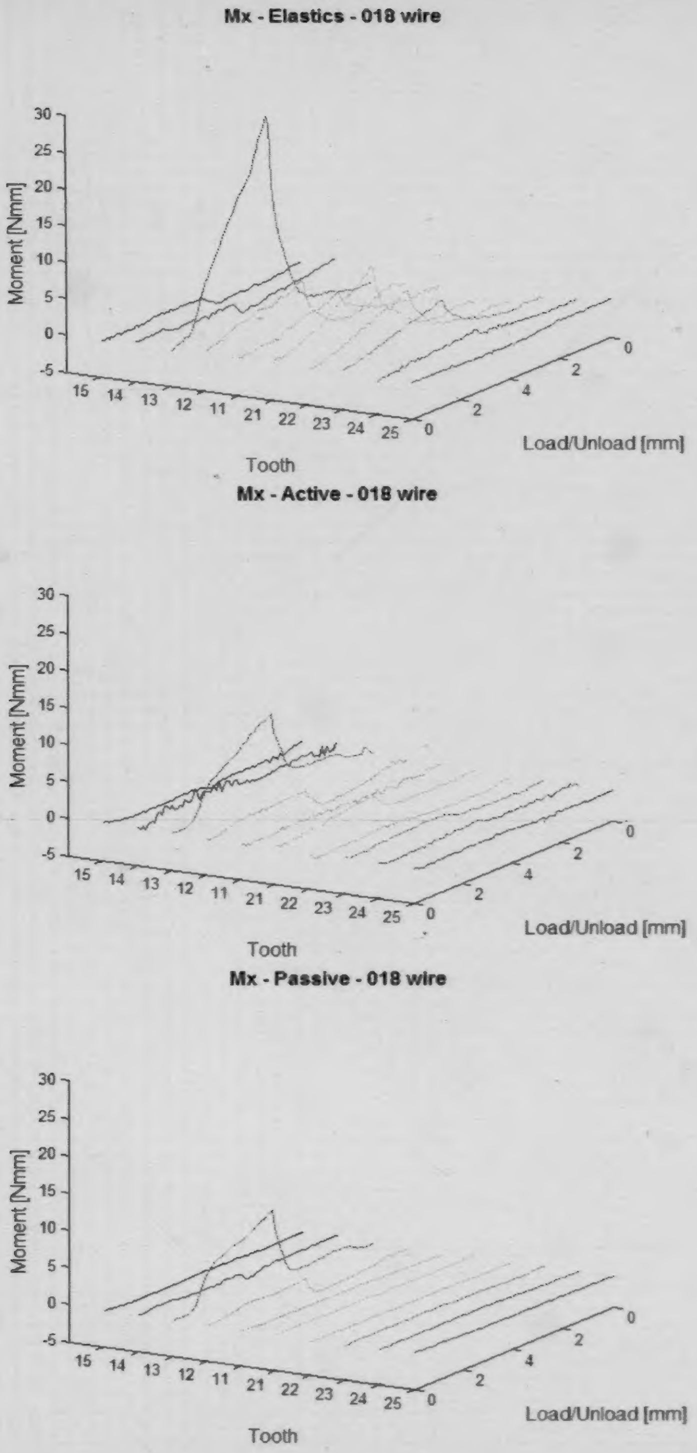

Figure 5-28: 3D 0.018" Mx Bucco-lingual crown torque graphs, means EL, ASL and PSL brackets

5.3.5 My Moments (Mesio-Distal Moments)

We would expect My moments on teeth #12 and 14 only. EL again produces the highest My moments compared to the SL brackets (Figure 5-30, Figure 5-31, Table 5-12). The My moments seen here can be caused by one of the following:

a) Fx acting on the bracket at an occluso-gingival distance from the bracket coordinate system.

b) Fz acting on the bracket at a mesio-distal distance from the bracket coordinate system

c) A force couple

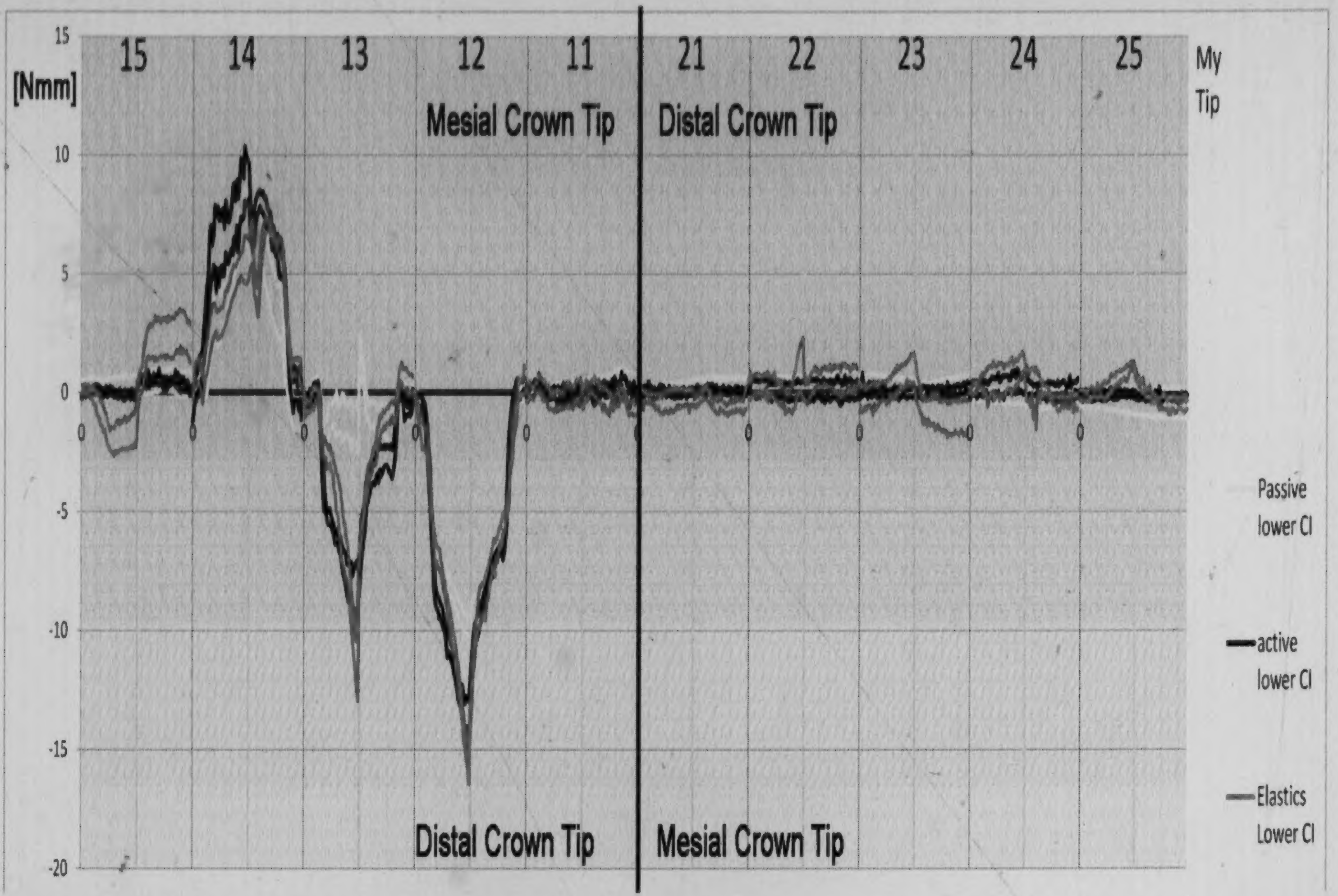

Figure 5-29: 0.018” My mesio-distal crown tip, 95% confidence intervals

018 My		Displacement mm						
		1 mm	2 mm	3 mm	4 mm	3 mm	2 mm	1 mm
Tooth	ligation	Moment Nmm						
15	Passive	0.16	0.17	0.28	0.28	0.47	0.55	0.42
	Active	0.12	-0.03	-0.10	-0.13	0.42	0.37	0.49
	Elastics	-0.20	-1.83	-1.79	-1.44	2.16	2.32	2.53
14	Passive	0.64	3.20	5.47	7.49	6.39	3.89	0.42
	Active	3.65	6.42	7.66	8.89	8.03	6.21	2.02
	Elastics	1.39	2.97	4.68	5.60	5.86	6.37	2.47
13	Passive	0.25	-0.99	-1.15	-1.64	-0.92	-1.29	-0.50
	Active	0.23	-5.33	-7.26	-8.50	-3.29	-2.70	0.24
	Elastics	0.00	-2.92	-6.53	-10.54	-3.04	-1.12	0.59
12	Passive	-2.80	-7.36	-8.83	-9.94	-8.59	-6.75	-2.92
	Active	-3.02	-9.32	-11.76	-13.74	-8.97	-6.89	-1.64
	Elastics	-2.92	-7.57	-11.12	-15.50	-8.76	-6.48	-3.06
11	Passive	0.25	0.10	0.11	0.12	0.18	0.21	0.31
	Active	0.47	0.11	0.01	-0.13	-0.17	0.13	0.58
	Elastics	0.33	-0.33	-0.07	0.14	0.27	-0.36	-0.06
21	Passive	0.07	0.11	0.08	0.17	0.18	0.14	0.17
	Active	0.12	0.07	-0.04	0.07	0.16	0.08	0.05
	Elastics	-0.23	-0.39	-0.20	-0.19	0.01	-0.59	-0.47
22	Passive	0.24	0.25	0.26	0.26	0.27	0.32	0.37
	Active	0.25	0.09	0.05	0.25	0.23	0.11	0.10
	Elastics	0.34	0.07	-0.38	1.03	0.55	0.71	0.59
23	Passive	0.31	0.29	0.27	0.25	0.21	0.30	0.36
	Active	0.04	-0.05	0.06	0.04	0.14	0.11	0.15
	Elastics	-0.23	0.02	0.68	1.04	-0.85	-0.91	-1.00
24	Passive	-0.10	-0.14	-0.16	-0.14	-0.24	-0.23	-0.20
	Active	0.13	0.32	0.35	0.34	0.09	0.13	0.12
	Elastics	0.27	0.54	0.73	1.21	0.39	-0.16	-0.40
25	Passive	-0.23	-0.27	-0.33	-0.35	-0.42	-0.43	-0.44
	Active	-0.04	-0.13	-0.02	-0.09	-0.13	-0.17	-0.16
	Elastics	-0.04	0.11	0.68	1.11	-0.04	-0.41	-0.47
Sign convention		R			L			
	Positive	Mesial crown tip			Distal crown tip			
	Negative	Distal crown tip			Mesial crown tip			

Table 5-12: 0.018" wire My moment data at 1mm increments

5.3.5.1 Cuspid:

The 13 experiences distal crown tip on loading and unloading with ASL and EL, PSL produces much lower My moments than ASL and EL during both phases. This moment can be produced by:

a. The Fz occlusal force being more concentrated on the mesial side of the #13 bracket, this is confirmed by noticing the pattern of My which is similar to the pattern of Fz on #13

b. The Fx force on the #13 acting on the gingival aspect of the bracket slot, more superior to the mid-bracket coordinate system, which can be caused by the ligating mechanism.

5.3.5.2 Teeth distal to #13:

Tooth #14 shows a mesial crown tip on the loading and unloading and this is expected considering the angulation of the wire relative to the bracket slot. ASL brackets produce higher My than EL and PSL during loading, while ASL and EL produce higher My than PSL during unloading. This My is directly related to the binding developed on the 14 bracket. The 15 on the other hand shows small My moments with SL brackets, while EL produces a relatively high distal crown tip on loading and a mesial crown tip on unloading, this could be related to the Fx force acting on the gingival slot wall of the 15 bracket on loading and unloading, the same pattern was identified with the 0.014" wire.

5.3.5.3 Teeth mesial to #13:

Tooth #12 shows a large distal crown tip for all ligation methods throughout loading and unloading, EL and ASL produce the highest moments and PSL produces the lowest moments.

On examining the 3D graphs (Figure 5-31) we notice that EL produces the most unwanted My moments while PSL produces the least unwanted My moments.

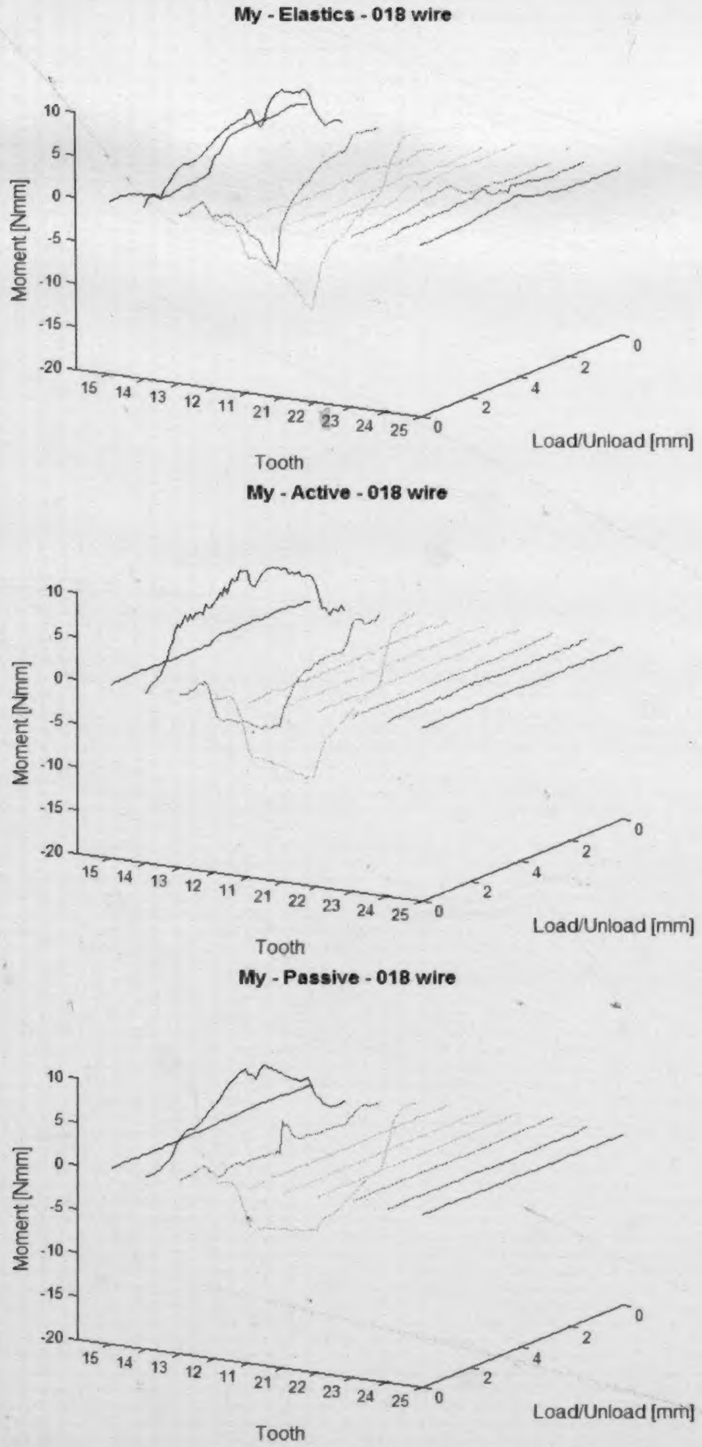

Figure 5-30: 3D 0.018" My mesio-distal crown tip, graphs, means EL, ASL and PSL brackets

5.3.6 Mz Moments (Disto-Buccal/Mesio-Buccal Moments)

We would expect no Mz moments on any of the teeth, however the largest moments were detected when elastic ligation (EL) was used (Figure 5-32, Figure 5-33, Table 5-13). The Mz moments seen here can be caused by one of the following:

a) Fx acting on the bracket at a distance from the bracket coordinate system, (ie an Fx acting more buccal relative to the mid-bracket coordinate system).

b) Fy acting on the bracket at a distance from the bracket coordinate system (ie an Fy acting more mesial or distal relative to the mid-bracket coordinate system).

c) A force couple

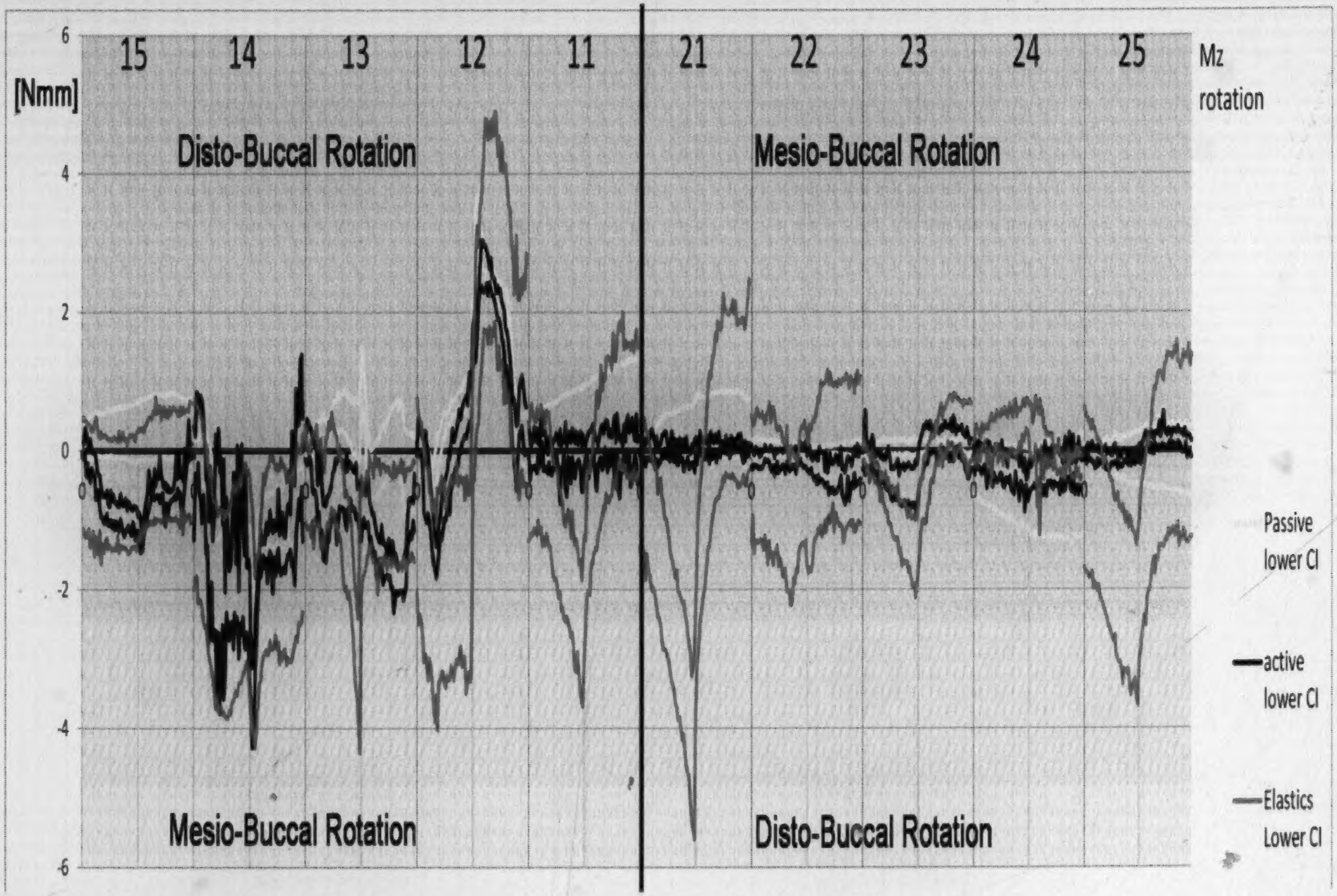

Figure 5-31: 0.018" Mz rotation around the long axis, 95% confidence intervals

018 Mz		Displacement mm						
		1 mm	2 mm	3 mm	4 mm	3 mm	2 mm	1 mm
Tooth	ligation	Moment Nmm						
15	Passive	0.25	0.24	0.26	0.27	0.33	0.35	0.33
	Active	-0.39	-0.93	-0.97	-1.02	-0.67	-0.70	-0.47
	Elastics	-0.38	-0.61	-0.57	-0.58	-0.27	-0.17	-0.25
14	Passive	-0.19	-0.92	-1.05	-1.33	-1.06	-0.94	-0.80
	Active	-0.89	-1.53	-1.45	-2.12	-1.52	-1.46	-1.15
	Elastics	-1.46	-2.29	-2.06	-1.71	-1.90	-1.46	-1.73
13	Passive	0.24	0.52	0.52	0.29	-0.29	0.01	0.16
	Active	-0.61	-0.60	-0.59	-0.87	-1.18	-1.64	-1.84
	Elastics	-0.50	-0.26	-1.27	-2.54	-0.99	-0.97	-0.88
12	Passive	-0.18	0.36	0.74	0.82	2.73	2.28	1.11
	Active	-0.87	-0.72	0.13	0.77	2.64	2.09	0.36
	Elastics	-1.86	-1.90	-1.77	-1.42	3.25	3.01	1.43
11	Passive	0.26	0.27	0.34	0.38	0.47	0.53	0.55
	Active	0.18	0.13	0.02	-0.18	-0.19	0.04	0.16
	Elastics	-0.39	-1.05	-1.74	-2.61	-0.29	0.32	0.59
21	Passive	0.05	0.22	0.23	0.27	0.37	0.39	0.39
	Active	0.08	0.03	-0.06	-0.07	0.07	0.07	0.12
	Elastics	-1.10	-2.02	-3.05	-4.23	-0.25	0.65	0.87
22	Passive	0.04	0.02	0.02	0.00	0.00	0.02	0.03
	Active	-0.02	-0.15	-0.11	-0.05	-0.20	-0.36	-0.44
	Elastics	-0.42	-0.66	-1.09	-0.51	-0.24	0.08	-0.01
23	Passive	0.02	0.05	0.05	0.05	0.05	0.08	0.08
	Active	-0.20	-0.36	-0.47	-0.52	0.20	0.19	0.19
	Elastics	-0.31	-0.80	-1.16	-1.47	-0.18	0.27	0.36
24	Passive	-0.34	-0.42	-0.48	-0.54	-0.57	-0.57	-0.57
	Active	-0.20	-0.16	-0.32	-0.55	-0.34	-0.22	-0.22
	Elastics	0.07	0.25	0.31	0.50	0.28	-0.10	-0.19
25	Passive	-0.09	-0.10	-0.11	-0.12	-0.07	-0.04	-0.10
	Active	-0.04	-0.14	-0.08	-0.13	0.17	0.19	0.22
	Elastics	-0.93	-1.53	-2.06	-2.42	-0.69	-0.07	0.11
Sign convention		R			L			
	Positive	Disto-Buccal rotation			Mesio-Buccal rotation			
	Negative	Mesio-Buccal rotation			Disto-Buccal rotation			

Table 5-13: 0.018" wire Mz moment data at 1mm increments

5.3.6.1 Cuspid:

On examining the graph, we notice a mesio-buccal rotation on loading and unloading for ASL and EL, and a smaller magnitude disto-buccal rotation on loading and unloading for PSL. There is however little difference between the three ligation methods.

5.3.6.2 Teeth distal to #13:

On tooth #14 we notice a mesio-buccal rotation on loading and unloading with all ligation methods, with higher variation for ASL and EL than for PSL. This could be caused by the interaction between the ligation method and the wire, applying a lingual Fy on the distal aspect of the bracket and/or buccal Fy on the mesial aspect of the bracket during loading and unloading. This moment is unlikely to be caused by the Fx force which would cause different patterns during loading and unloading.

5.3.6.3 Teeth mesial to #13:

The 12 and 11 shows a high mesio –buccal rotation on loading and a disto-buccal rotation on unloading with EL, as well as a disto-buccal moment on loading followed by a mesio-buccal moment on unloading for teeth 21, 23 and 25, which is similar to the pattern seen with 0.014" wire. These moments are most likely related to the Fx forces. We notice tooth # 22 and #24 have low Mz moments, which is consistent with the Fx pattern.

SL brackets produce low Mz moments, however there is more variation with PSL when compared to ASL.

On examining the 3D graphs (Figure 5-33) it is apparent that PSL produces the least unwanted Mz moments while EL produces the most unwanted Mz moments.

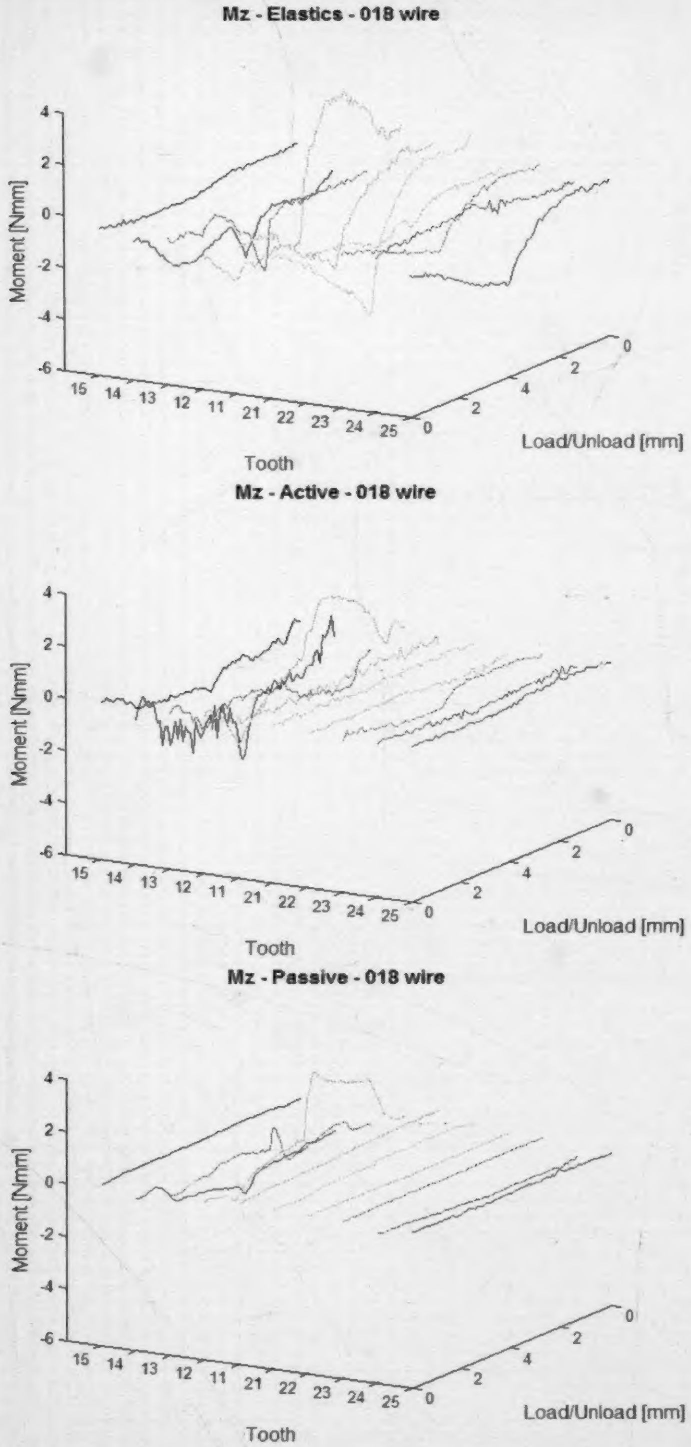

Figure 5-32: 3D 0.018" Mz rotation around the long axis graphs, means EL, ASL and PSL brackets

5.4 0.014" x 0.025" NiTi wire

5.4.1 Mesio-distal forces (Fx)

Resistance to sliding seems to affect the force system produced, when we examine the Fx graph (Figure 5-34, Figure 5-36, Table 5-14) of the 10 teeth, we notice that Fx forces are generated as the cuspid is moved from the default position to the displaced position and then back to the default position. On the teeth distal to the 13 (tooth#14 and #15) the Fx force is in a mesial direction during loading and in distal direction during unloading. On the teeth mesial of the 13 (tooth #12, #11,) Fx force is in a distal direction during loading and in a mesial direction during unloading. It is noticed that unlike the 0.014" and 0.018" wires, all teeth experience certain levels of resistance to sliding with all ligation methods.

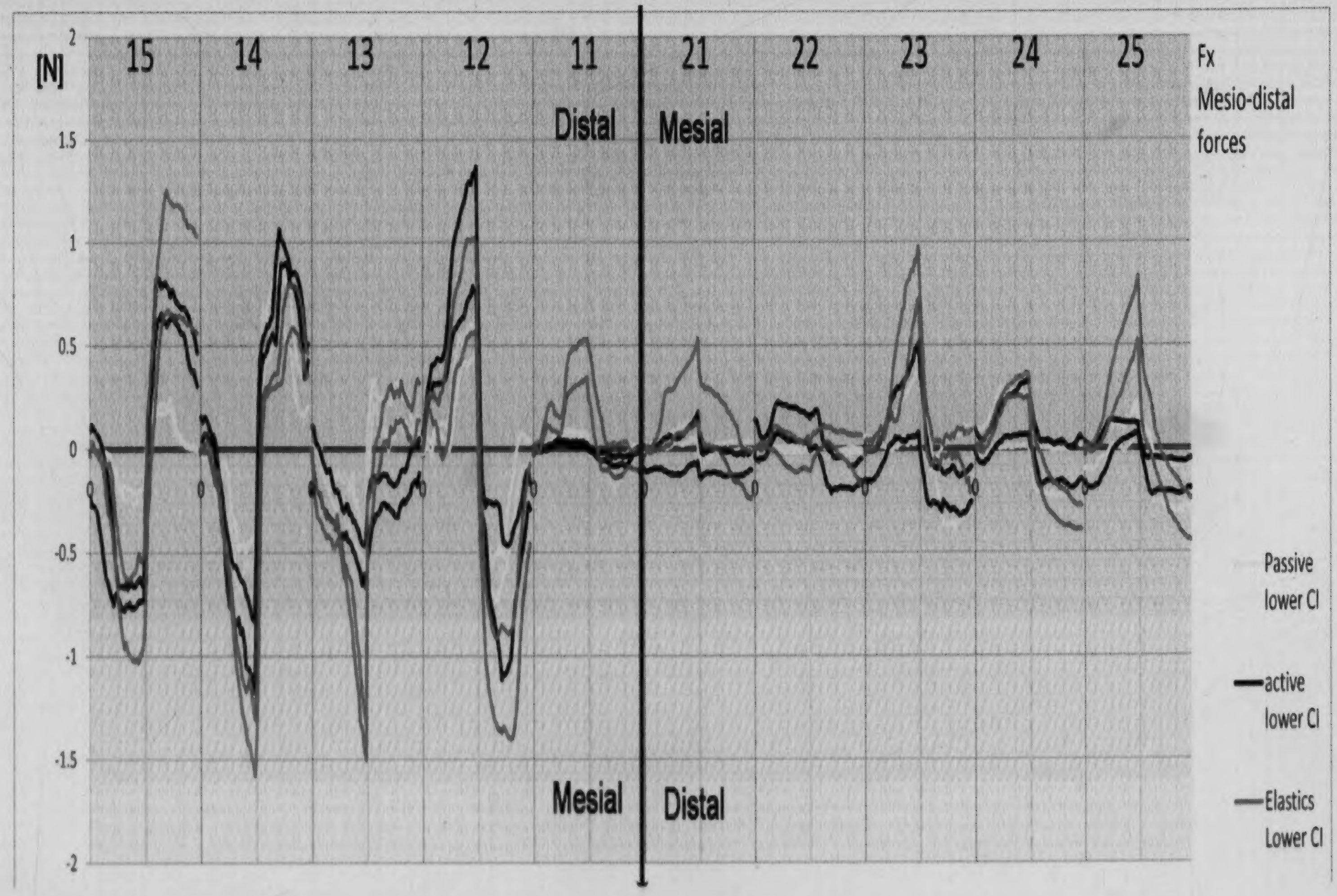

Figure 5-33: 0.014"x 0.025" NiTi, Fx Mesio-distal forces 95% confidence intervals

14x25 Fx		Displacement mm				
		1 mm	2 mm	3 mm	2 mm	1 mm
Tooth	ligation	Force N				
15	Passive	-0.05	-0.21	-0.23	0.19	0.06
	Active	-0.39	-0.70	-0.70	0.72	0.64
	Elastics	-0.19	-0.78	-0.72	0.82	0.91
14	Passive	-0.21	-0.54	-0.52	0.63	0.62
	Active	-0.16	-0.71	-0.99	0.60	0.84
	Elastics	-0.19	-1.01	-1.44	0.32	0.68
13	Passive	-0.18	-0.25	-0.44	0.18	0.19
	Active	-0.21	-0.36	-0.56	-0.19	-0.18
	Elastics	-0.39	-0.66	-1.42	0.13	0.24
12	Passive	0.10	0.43	0.52	-0.60	-0.29
	Active	0.37	0.85	1.07	-0.55	-0.66
	Elastics	0.13	0.60	0.78	-1.10	-1.13
11	Passive	0.03	0.07	0.06	-0.08	-0.10
	Active	0.01	0.02	0.02	-0.04	-0.06
	Elastics	0.16	0.37	0.44	-0.03	-0.05
21	Passive	0.03	0.07	0.07	0.00	0.01
	Active	-0.03	-0.04	0.05	-0.06	-0.08
	Elastics	0.08	0.21	0.33	0.13	-0.01
22	Passive	0.00	0.00	0.00	-0.02	-0.02
	Active	0.09	0.12	0.09	-0.07	-0.12
	Elastics	0.04	-0.01	-0.02	0.07	0.02
23	Passive	0.06	0.11	0.26	-0.10	-0.16
	Active	0.00	0.17	0.29	-0.18	-0.19
	Elastics	0.06	0.42	0.85	-0.01	0.01
24	Passive	0.09	0.14	0.14	-0.11	-0.11
	Active	0.06	0.15	0.20	-0.06	-0.07
	Elastics	0.10	0.28	0.30	-0.19	-0.29
25	Passive	0.02	0.06	0.09	-0.16	-0.19
	Active	-0.03	0.08	0.10	-0.13	-0.13
	Elastics	0.08	0.40	0.68	-0.02	-0.23
Sign convention		R			L	
	Positive	Distal			Mesial	
	Negative	Mesial			Distal	

Table 5-14: 0.014" x 0.025" wire Fx force data at 1mm increments

5.4.1.1 Tooth #13:

In advance of the experiment, we anticipated that there would be no mesial or distal forces to acting on tooth #13. However, similar to the patterns seen with 0.014" and 0.018 wires, we recorded a mesial force during loading and a distal force during unloading with EL and PSL ligation methods, while there was a mesial force during loading and unloading for ASL. This pattern of mesial force on loading and distal force on unloading with EL and PSL, can be explained by the cumulative resistance to sliding produced by teeth located mesial of tooth #13 as opposed to distal of tooth #13. This will favour sliding of the wire through tooth #13 bracket in a mesial direction during loading, and in a distal direction during unloading, this sliding generates the Fx forces. We notice the immediate reversal of the force at the reversal point for the PSL compared to the more gradual reversal for EL and ASL (Figure 5-35). It is apparent that the force magnitude is highest for elastics during loading and unloading. When we compare the two self-ligating methods, there is no appreciable difference between ASL and PSL during loading, however during unloading PSL produces a distal force while ASL produces a mesial force of slightly higher magnitude.

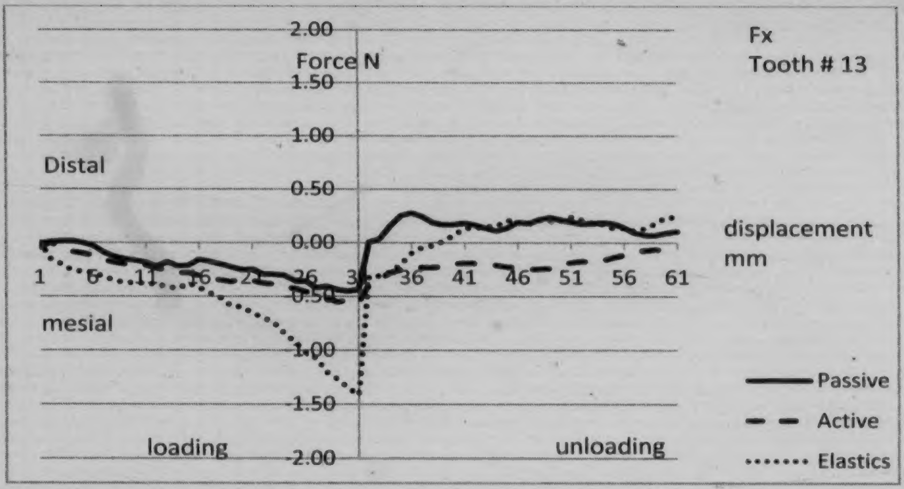

Figure 5-34: 0.014" x 0.025" Fx force on tooth #13

5.4.1.2 Teeth distal to the cuspid:

The teeth distal to the cuspid experience mesial force on loading and distal force on unloading, EL and ASL show much higher force levels compared to PSL especially on #15. On tooth #14 in spite of the presence of binding due to contact between the wire and the bracket walls, it is clear that the ligation method still plays a major role in producing the resistance to sliding as evidenced by the much higher Fx levels with EL and ASL compared to PSL. When the two SL methods on tooth #14 are compared, PSL produces smaller Fx forces during loading and unloading. On tooth #15 ASL and EL produce equivalent levels of resistance to sliding on loading and unloading, while PSL produce much lower levels of resistance to sliding.

5.4.1.3 Teeth mesial to the cuspid:

The most interesting finding in this graph is the fact that the resistance to sliding continues throughout the dental arch with all ligation methods.

Tooth #12 experiences the highest resistance to sliding with ASL, which is surprisingly higher than that of EL. PSL produces the lower resistance to sliding on tooth #12. On the rest of the teeth EL, produce the highest resistance to sliding while both SL methods show similar levels of resistance to sliding.

Another interesting finding on these graphs, is the fact that with EL and ASL the force levels start at zero for every tooth but never end at zero, unlike the PSL brackets. There are significant residual Fx forces with EL and ASL, acting on all teeth even when the cuspid is back in the default position at the end of the unloading curve.

On average, it seems that the difference between the two SL brackets is much greater than it was with 0.014"and 0.018"wires. With PSL producing the least resistance to sliding, while EL producing the highest resistance to sliding.

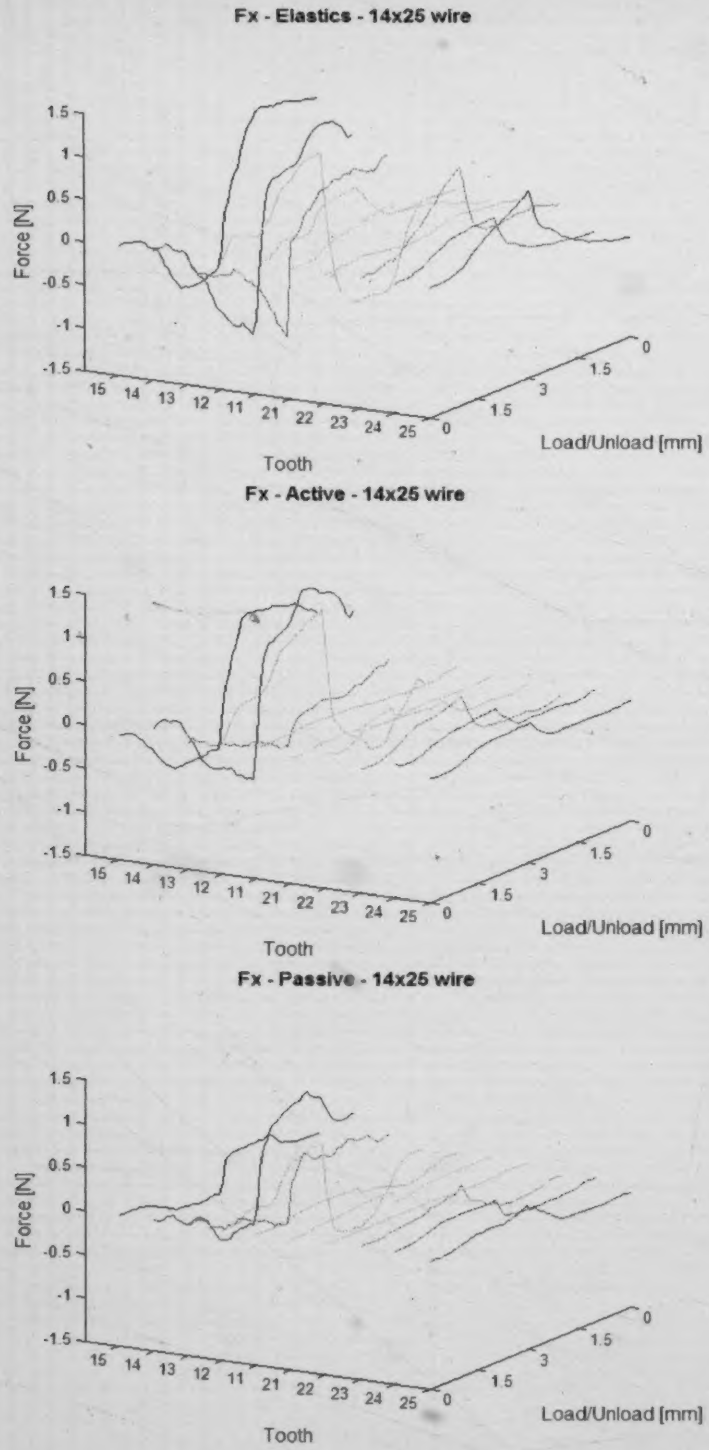

Fx - Elastics - 14x25 wire

Fx - Active - 14x25 wire

Fx - Passive - 14x25 wire

Figure 5-35: 3D 0.014" x 0.025" Fx graphs means EL, ASL and PSL brackets

5.4.2 Fy Bucco-lingual forces

In this simulated clinical situation, we would ideally prefer no Fy forces on any of the teeth. However, on examining the Fy graphs (Figure 5-37, Figure 5-38, Table 5-15) it is apparent that there are significant levels of bucco-lingual forces on all the teeth with all ligation methods.

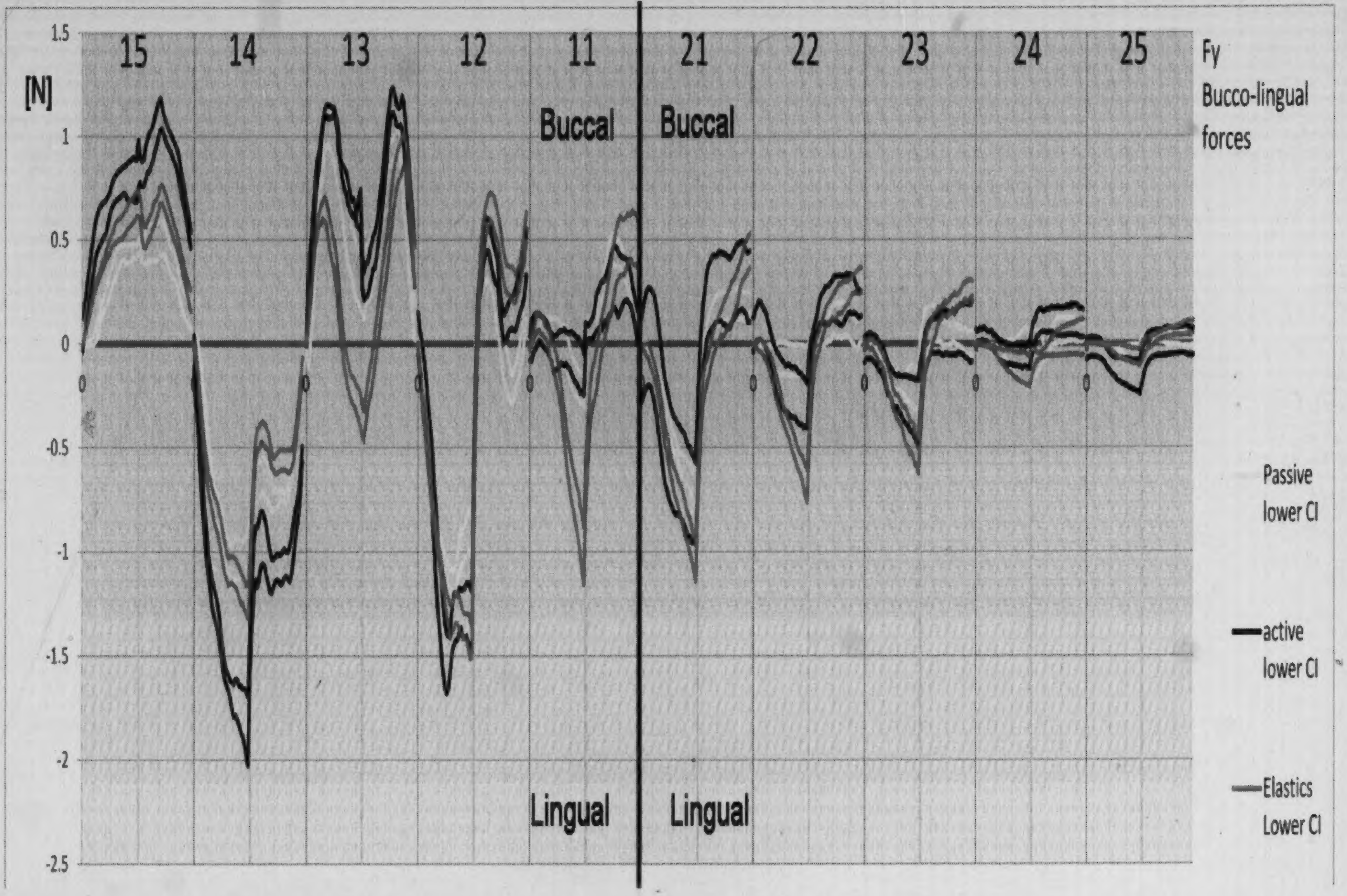

Figure 5-36: 0.014”x 0.025” Fy Bucco-lingual forces 95% confidence intervals

14x25 Fy		Displacement mm				
		1 mm	2 mm	3 mm	2 mm	1 mm
Tooth	ligation	Force N				
15	Passive	0.13	0.41	0.44	0.49	0.39
	Active	0.57	0.77	0.79	1.00	0.94
	Elastics	0.34	0.55	0.67	0.63	0.56
14	Passive	-0.70	-1.05	-1.03	-0.66	-0.74
	Active	-1.20	-1.66	-1.86	-1.00	-1.06
	Elastics	-0.75	-1.09	-1.24	-0.45	-0.56
13	Passive	1.00	0.75	0.29	0.55	0.98
	Active	1.11	0.83	0.65	0.57	1.11
	Elastics	0.65	0.04	-0.32	0.11	0.83
12	Passive	-0.83	-1.14	-0.89	0.38	-0.16
	Active	-0.96	-1.32	-1.33	0.48	0.13
	Elastics	-0.90	-1.29	-1.43	0.66	0.31
11	Passive	0.05	-0.04	-0.24	0.26	0.43
	Active	0.02	-0.02	-0.15	0.19	0.29
	Elastics	0.03	-0.47	-1.02	0.05	0.47
21	Passive	-0.19	-0.53	-0.70	0.13	0.19
	Active	-0.21	-0.60	-0.77	0.25	0.26
	Elastics	-0.26	-0.70	-1.05	0.01	0.20
22	Passive	-0.05	-0.08	-0.08	0.05	0.12
	Active	-0.04	-0.22	-0.30	0.18	0.21
	Elastics	-0.11	-0.42	-0.68	0.12	0.23
23	Passive	-0.06	-0.19	-0.23	0.08	0.05
	Active	-0.09	-0.25	-0.34	0.04	0.05
	Elastics	-0.08	-0.33	-0.54	0.11	0.19
24	Passive	-0.02	-0.05	-0.07	-0.02	0.07
	Active	0.00	-0.06	-0.07	0.11	0.11
	Elastics	-0.02	-0.09	-0.13	-0.03	0.02
25	Passive	-0.01	-0.03	-0.05	0.04	0.03
	Active	-0.05	-0.13	-0.16	0.00	0.01
	Elastics	-0.01	-0.04	-0.07	0.03	0.06
Sign convention		R			L	
	Positive	Buccal			Buccal	
	Negative	Lingual			Lingual	

Table 5-15: 0.014" x 0.025" wire Fy force data at 1mm increments

5.4.2.1 Cuspid:

We would expect no Fy forces to act on the 13, however there is a buccal force on loading and unloading for all ligation methods, highest forces are with ASL while EL produced the lowest levels of Fy forces to # 13. This is most likely related to fact that the elastic ligation is not able to maintain full engagement of the wire as it stretches during loading, which was observed during the experiment. All ligation methods produced a very interesting "M" shaped load deflection curve which at the moment cannot be explained.

5.4.2.2 Teeth distal to #13:

On tooth #14 there is a lingual force on loading and unloading for all ligation methods. This lingual force is highest with ASL during loading and unloading. EL and PSL produce similar levels during loading, while EL produces a lower lingual force during unloading. No plausible explanation for this lingual force on tooth #14 can be presented at this time.

On tooth #15 all ligation methods produce a buccal force on loading and unloading, with ASL producing the highest force and PSL producing the lowest force.

5.4.2.3 Teeth mesial to #13:

Tooth #12 shows a lingual force on loading and a buccal force on unloading for all ligation methods, the highest Fy force levels were recorded on the 12 bracket with ASL during loading and with EL during unloading. PSL shows lower Fy forces compared to ASL and EL. The rest of the teeth mesial of the

13 show high Fy forces with all ligation methods, ASL produce higher Fy forces than PSL on teeth # 22, 24, 25. EL, produce higher Fy forces than SL on tooth #11. All ligation methods show similar Fy forces on 21 and 23.

There is a large amount of variation with all ligation methods. On examining the 3D graphs (Figure 5-38) is apparent that all ligation methods produce relatively high Fy.

When we examine the Fy graphs of all the teeth we notice in general the presence of a lingual force on loading and a buccal force on unloading. This pattern was generally present on all teeth, this could be related to the Fx forces on the curved archform.

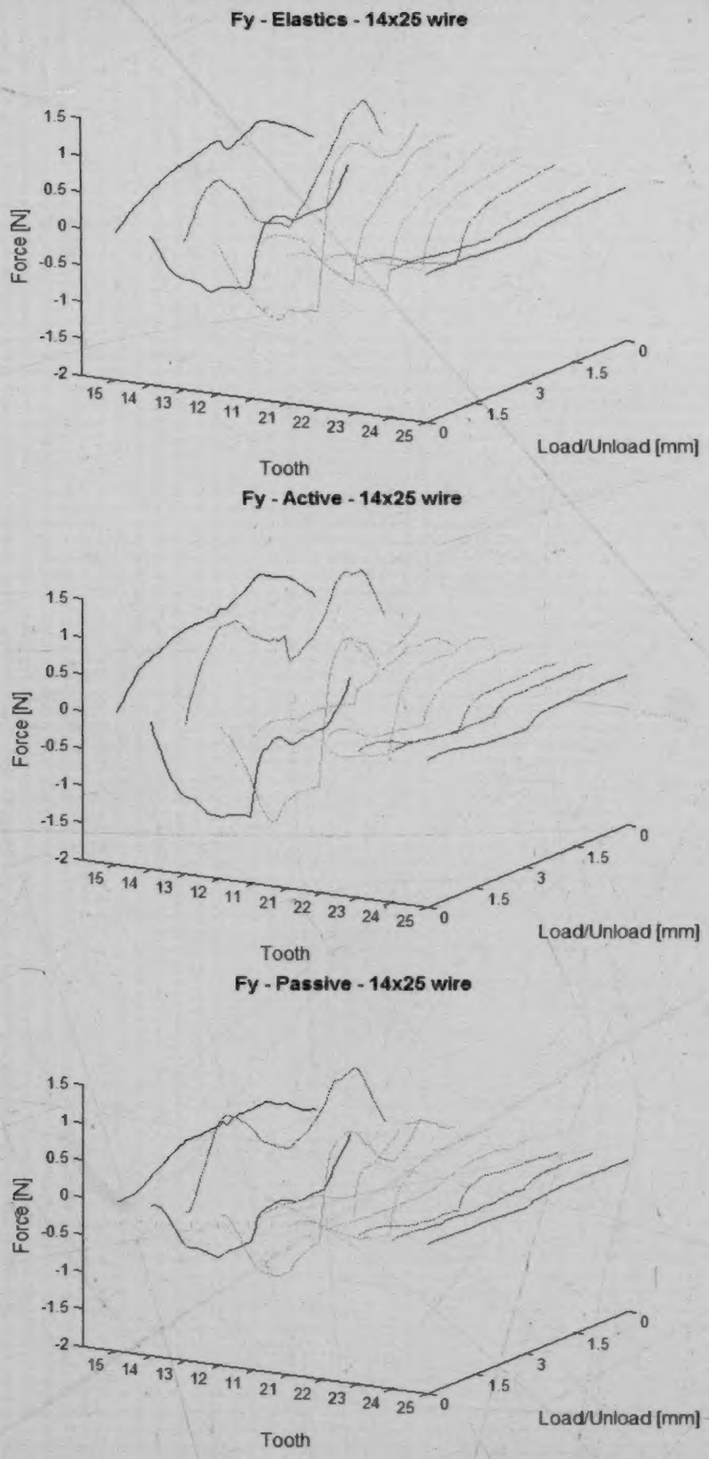

Figure 5-37: 3D 0.014" x 0.025" Fy graphs means EL, ASL and PSL brackets

5.4.3 Fz Occluso-gingival forces

In this simulated clinical situation, we would expect an extrusive force on 13 and two reciprocal intrusive forces on the 12 and 14, during loading and unloading. On examining the Fz graphs (Figure 5-39, Figure 5-40, Table 5-16) we notice the intrusive forces on the 12, 14 and the extrusive force on the 13. An interesting finding is that the 15 and the 11 have a very similar Fz "W" pattern (Figure 5-40), this could be related to the angulation of the wire relative to those two teeth as the canine displacement is produced. This pattern is similar to the one seen with 0.014"and 0.018"wires.

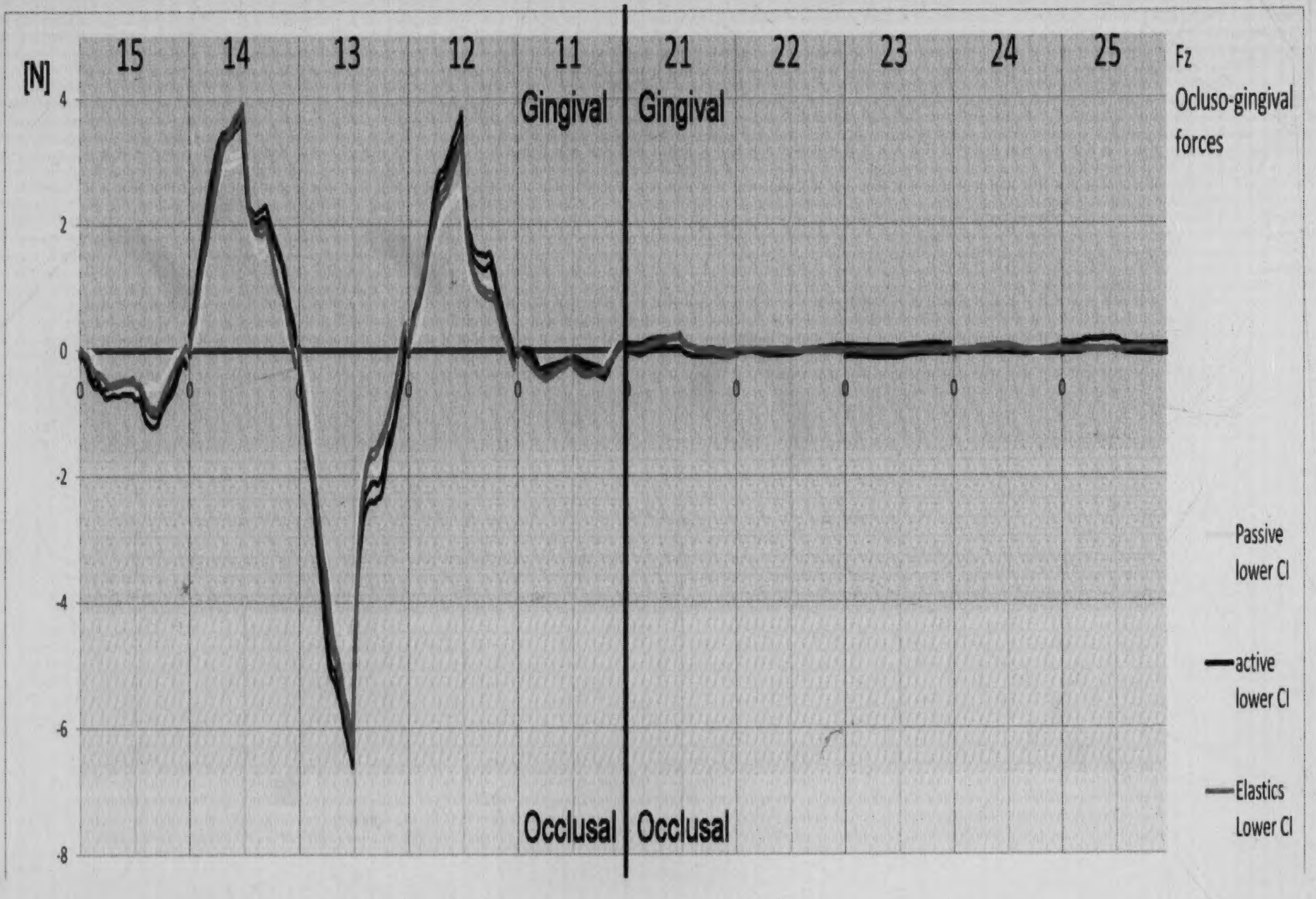

Figure 5-38: 0.014” x 0.025” Fz Occluso-gingival 95% confidence intervals

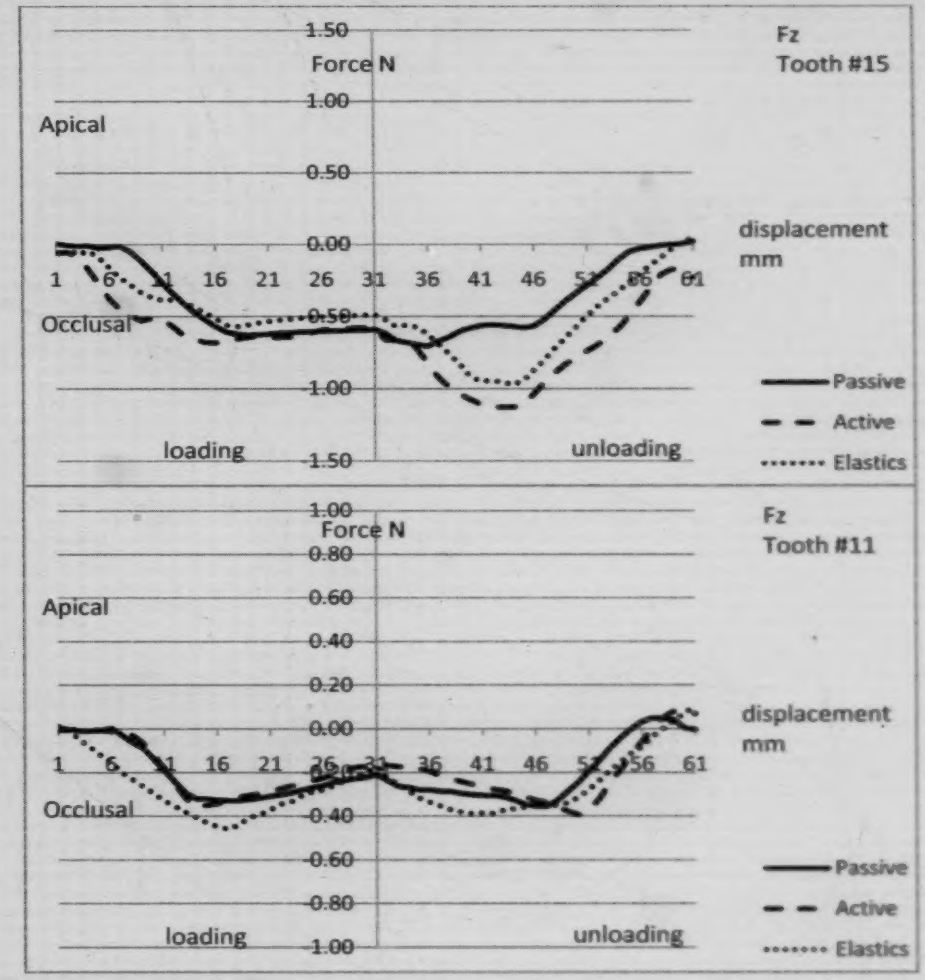

Figure 5-39: 0.014"x 0.025" Fz load deflection of tooth #15 and #11showing the "W" pattern

14x25 Fz		Displacement mm				
		1 mm	2 mm	3 mm	2 mm	1 mm
Tooth	ligation	Force N				
15	Passive	-0.27	-0.62	-0.59	-0.56	-0.29
	Active	-0.52	-0.64	-0.58	-1.11	-0.74
	Elastics	-0.39	-0.54	-0.49	-0.95	-0.50
14	Passive	1.66	3.01	3.12	1.57	1.20
	Active	2.26	3.39	3.70	2.14	1.59
	Elastics	1.76	3.33	3.84	1.90	1.08
13	Passive	-2.19	-4.22	-4.74	-1.75	-1.49
	Active	-2.94	-5.17	-6.37	-2.29	-1.55
	Elastics	-2.41	-4.77	-6.29	-1.69	-1.34
12	Passive	1.02	2.21	2.57	0.97	0.77
	Active	1.39	2.81	3.61	1.44	0.98
	Elastics	1.40	2.47	3.35	1.01	0.73
11	Passive	-0.19	-0.31	-0.21	-0.31	-0.19
	Active	-0.18	-0.29	-0.15	-0.26	-0.17
	Elastics	-0.33	-0.37	-0.17	-0.39	-0.38
21	Passive	0.01	0.07	0.08	-0.01	-0.03
	Active	0.04	0.11	0.11	-0.04	-0.04
	Elastics	0.04	0.14	0.22	0.01	-0.03
22	Passive	0.01	0.00	0.00	0.00	-0.01
	Active	-0.01	-0.04	-0.04	0.00	0.00
	Elastics	0.01	0.00	0.00	-0.01	-0.01
23	Passive	0.00	-0.03	-0.04	0.02	0.04
	Active	-0.02	-0.04	-0.04	0.00	0.01
	Elastics	-0.01	-0.02	-0.02	-0.02	-0.01
24	Passive	0.01	0.04	0.04	-0.02	-0.03
	Active	-0.01	0.00	0.01	-0.03	-0.04
	Elastics	0.00	0.03	0.04	0.00	-0.01
25	Passive	-0.01	0.01	0.02	-0.01	-0.02
	Active	0.04	0.08	0.09	0.01	0.00
	Elastics	0.01	0.00	0.01	0.01	0.01
Sign convention		R			L	
	Positive	Gingival			Gingival	
	Negative	Occlusal			Occlusal	

Table 5-16: 0.014" x 0.025" wire Fz force data at 1mm increments

5.4.3.1 *Cuspid:*

During loading, the cuspid experiences highest Fz forces with EL and ASL and lowest with PSL, with very little difference between ASL and EL (Figure 5-41). During unloading ASL shows higher Fz force than PSL and EL. There is a very large difference in the Fz magnitude between loading and unloading for all brackets, these differences are expected of NiTi wires.

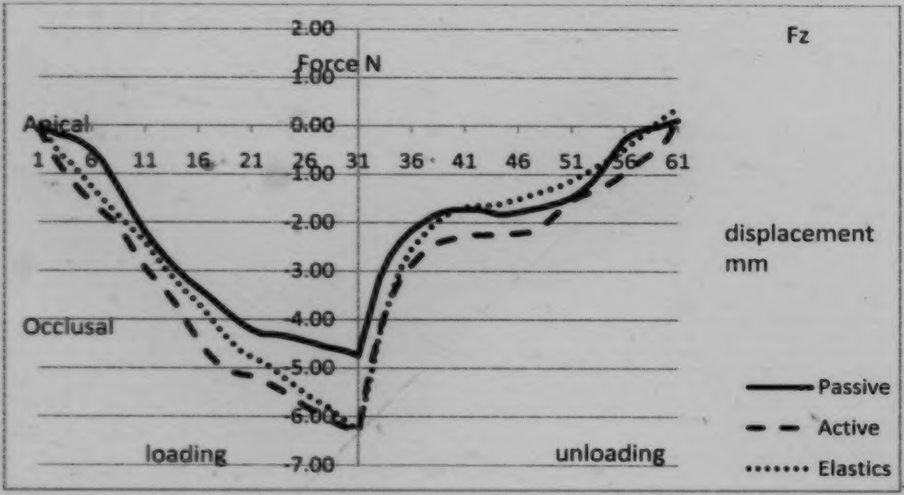

Figure 5-40: 14"x25" Fz force on tooth #13

5.4.3.2 *Teeth distal to #13:*

All ligation methods produce similar patterns of Fz with different magnitudes. On tooth #14 the EL and ASL brackets produce the highest intrusive force during loading and PSL produced lower Fz than ASL. During unloading, ASL produce the highest intrusive force, while PSL produce the lowest intrusive force. Tooth #15 shows a "W" pattern of extrusive force throughout the loading and unloading (Figure 5-40). Similar to the 0.014"and 0.018"wires, this phenomenon can be explained by the angulation of the wire relative to the 14 bracket slot during loading and unloading. At the start of the loading, the 14 bracket acts as a lever point for the wire as the cuspid is intruded, this causes the wire to apply an extrusive force on the 15. When the wire bends mesial of the 14 as the cuspid is further intruded, this extrusive force declines since the wire becomes more or less parallel to the #14 bracket slot. ASL and EL produce a slightly larger extrusive force on tooth #15 during unloading.

5.4.3.3 Teeth mesial to #13:

All ligation methods produce similar patterns of Fz with different magnitudes. On tooth #12 the ASL brackets produce the highest intrusive force during loading and PSL produce slightly lower Fz than EL especially during loading. Tooth #11 shows a "W" pattern of occlusal force (Figure 5-40) similar to that of #15, throughout the loading and unloading declining to zero at the reversal point.

On examining the 3D graphs in Figure 5-42, we notice that all ligation methods brackets deliver the load-deflection curve expected of NiTi wires, characterized by flat loading and unloading curves, and the loading curves exhibiting higher force magnitudes compared to the unloading curves.

Fz - Elastics - 14x25 wire

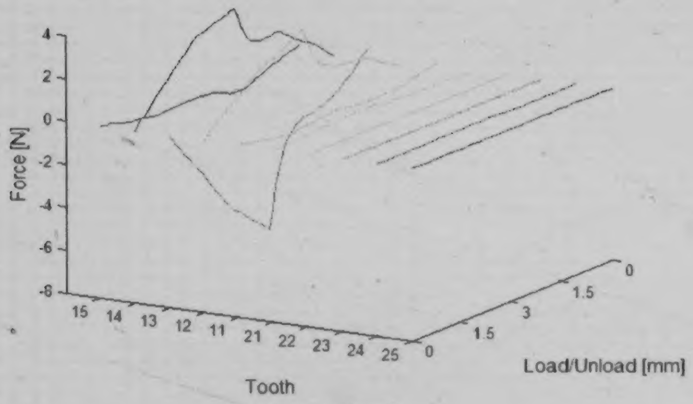

Fz - Active - 14x25 wire

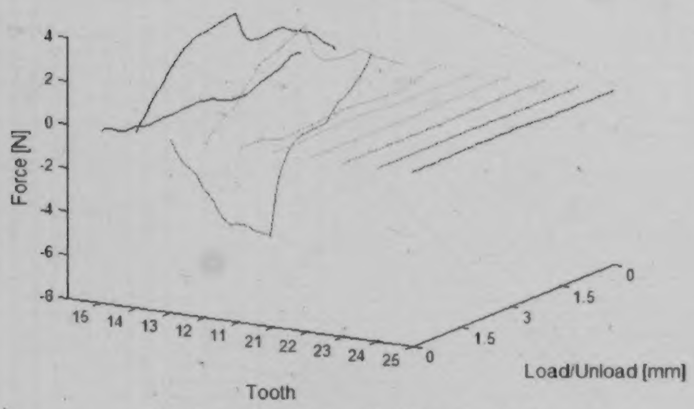

Fz - Passive - 14x25 wire

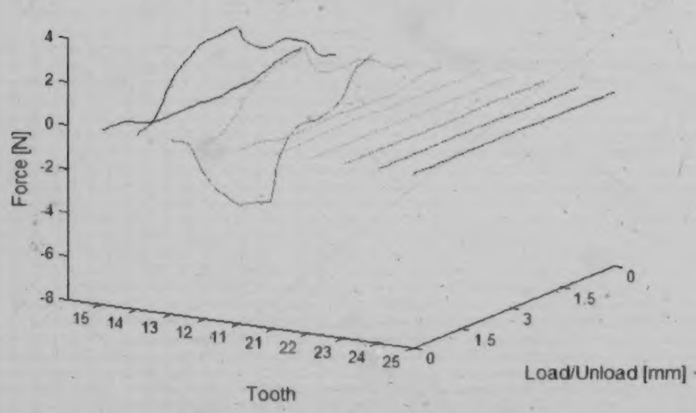

Figure 5-41: 3D 0.014"x 0.025" Fz graphs, means EL, ASL and PSL brackets

5.4.4 Mx Moments (Bucco-Lingual Moments)

We would expect no Mx moments on any of the teeth, however the largest moments were detected when elastic ligation (EL) was used however those were only slightly higher than the SL brackets. These moments are in a buccal crown torque direction on loading and a lingual crown torque on unloading (Figure 5-43, Figure 5-44, Table 5-17). The Mx moments seen here can be caused by one of the following:

a) Fy acting on the bracket at an occluso-gingival distance from the bracket coordinate system.

b) Fz acting on the bracket at a bucco-lingual distance from the bracket coordinate system

c) A force couple

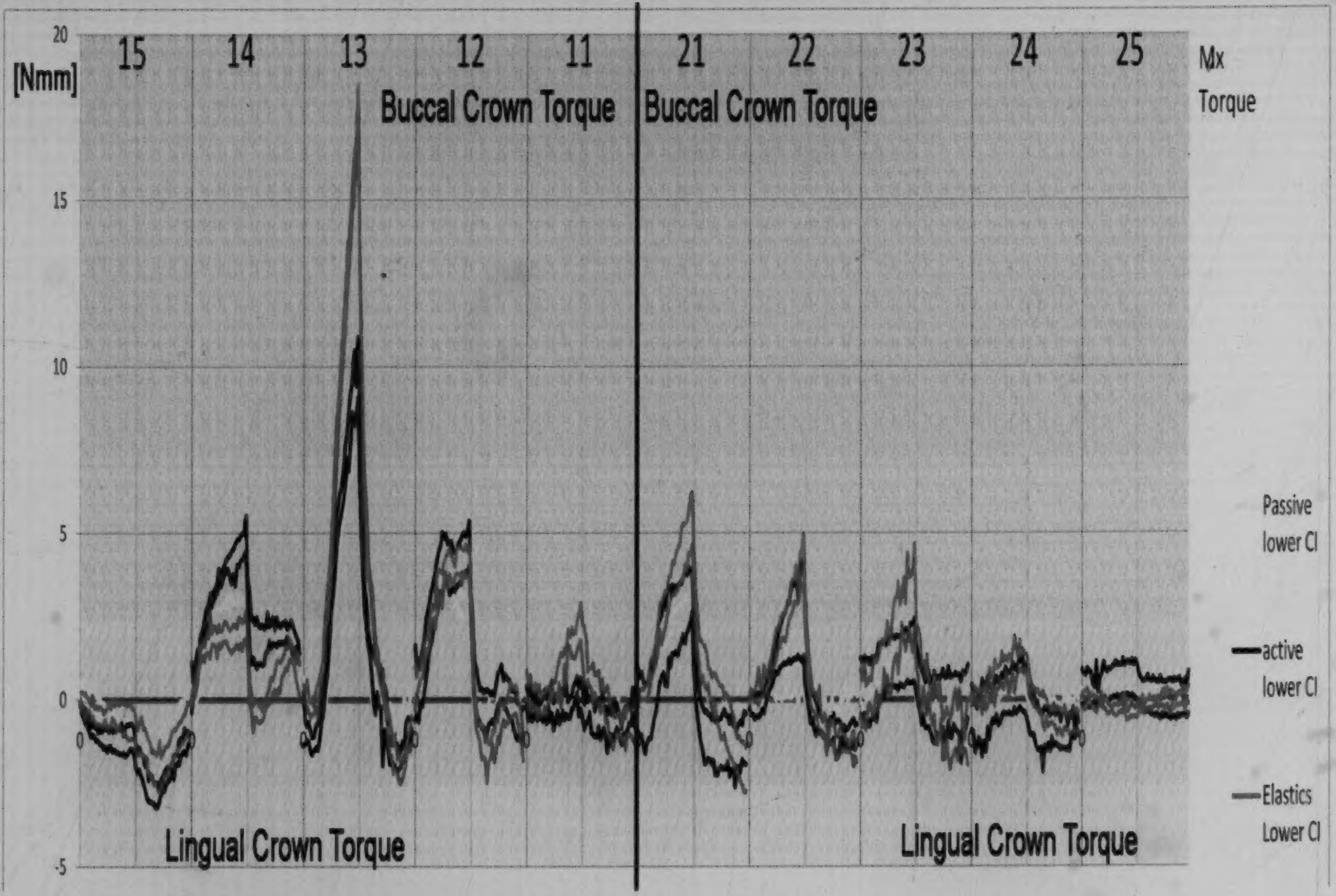

Figure 5-42: 0.014"x 0.025" Mx Bucco-lingual crown torque, 95% confidence intervals

14x25 Mx		Displacement mm				
		1 mm	2 mm	3 mm	2 mm	1 mm
Tooth	ligation	Moment Nmm				
15	Passive	-0.16	-0.79	-1.08	-1.15	-0.56
	Active	-1.10	-1.18	-1.24	-2.67	-2.13
	Elastics	-0.49	-0.51	-0.73	-1.97	-1.55
14	Passive	2.09	2.61	2.70	1.18	1.78
	Active	2.98	4.09	4.97	1.61	2.01
	Elastics	1.97	1.91	2.25	-0.25	0.95
13	Passive	-1.04	4.89	8.99	0.07	-1.93
	Active	-0.20	5.77	9.97	0.36	-1.56
	Elastics	0.73	9.18	17.83	1.60	-1.77
12	Passive	2.60	3.27	2.77	-0.87	0.98
	Active	2.77	4.00	4.69	-0.34	0.25
	Elastics	2.56	3.95	4.14	-1.78	-0.50
11	Passive	0.06	0.32	0.84	-0.30	-0.53
	Active	-0.01	-0.06	0.17	-0.40	-0.48
	Elastics	-0.01	0.69	2.33	0.38	-0.77
21	Passive	1.13	2.76	3.83	-0.49	-0.65
	Active	0.65	2.30	3.24	-1.14	-1.18
	Elastics	1.48	3.62	5.42	0.42	-0.71
22	Passive	0.24	0.47	0.61	-0.16	-0.66
	Active	0.32	1.85	2.75	-0.73	-1.07
	Elastics	0.57	2.21	4.24	-0.76	-1.31
23	Passive	0.16	0.76	1.14	-1.00	-0.37
	Active	0.79	1.14	1.47	-0.37	-0.23
	Elastics	0.55	2.19	3.40	-0.36	-1.35
24	Passive	0.24	0.78	1.07	-0.36	-0.61
	Active	-0.41	0.17	0.31	-1.30	-1.08
	Elastics	0.54	0.95	1.12	-0.28	-0.64
25	Passive	-0.08	-0.11	-0.31	0.08	0.08
	Active	0.24	0.56	0.57	0.08	-0.02
	Elastics	-0.07	-0.34	-0.40	-0.15	-0.08
Sign convention		R			L	
	Positive	Buccal crown torque			Buccal crown torque	
	Negative	Lingual crown torque			Lingual crown torque	

Table 5-17: 0.014” x 0.025” wire Mx Moment data at 1mm increments

5.4.4.1 Cuspid:

The cuspid experiences a very large buccal crown torque moment during loading and a relatively smaller lingual crown torque on unloading. SL brackets produce similar levels and patterns of Mx moments. One explanation for such a moment is that the Fy forces acting on the cuspid in a lingual direction during loading and buccal direction during unloading, are being applied at a point within the bracket slot superior (gingival) to the mid-bracket coordinate system. Another explanation for the development of this moment is the presence of a force couple within the 13 bracket.

5.4.4.2 Teeth distal to #13:

Tooth #14 experiences buccal crown torque on loading and unloading with all ligation methods, with ASL producing the highest moments during loading and EL producing the lowest moments during unloading. This buccal crown torque is expected to develop as the cuspid is displaced. On tooth #15 there is a very small lingual crown torque on loading and unloading. Again, ASL produced the highest moment with little difference between PSL and EL.

5.4.4.3 Teeth mesial to #13:

All brackets produce buccal crown torque moments on loading and small lingual crown torque moments on unloading for teeth 12, 21, 22, 23 and 24. ASL and EL produce larger moments on teeth #22 and #23.

On average, there is little difference between the three ligation methods in the Mx moments generated. However, ASL produced the highest moments on the teeth distal to the 13, and EL produced the highest moments on teeth mesial to the 13.

Mx - Elastics - 14x25 wire

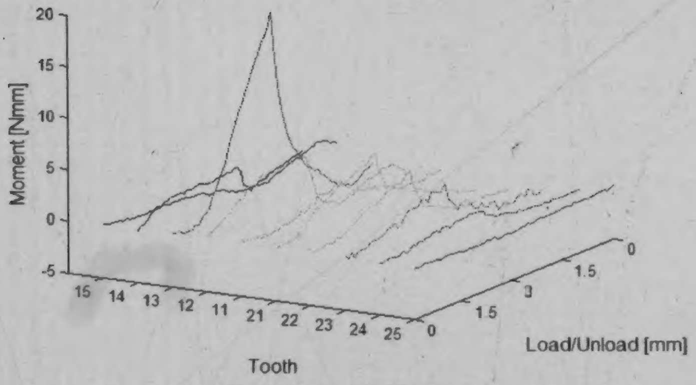

Mx - Active - 14x25 wire

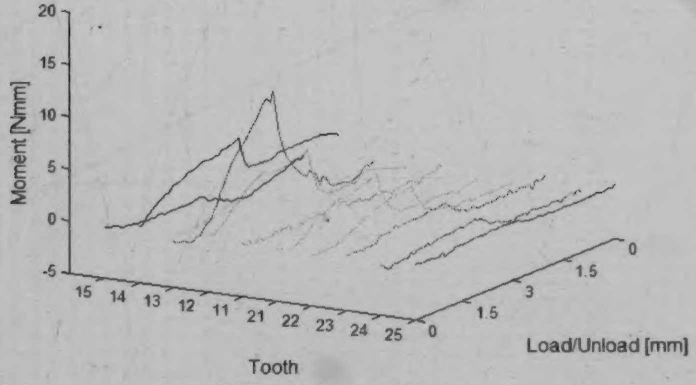

Mx - Passive - 14x25 wire

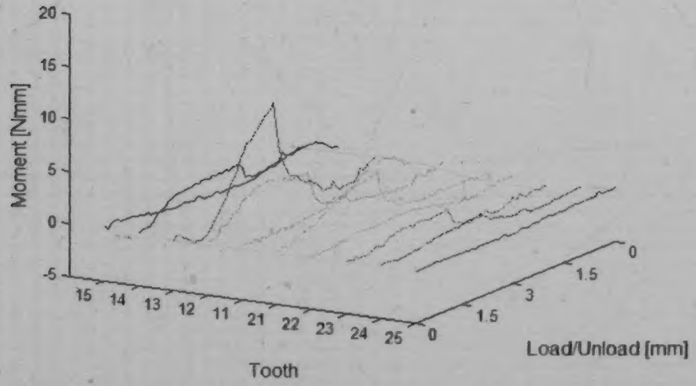

Figure 5-43: 3D 0.014"x 0.025" Mx Bucco-lingual crown torque graphs, means EL, ASL and PSL brackets

5.4.5 My Moments (Mesio-Distal Moments)

We would expect My moments on teeth 12 and 14 only. ASL produces the highest My moments (Figure 5-45, Figure 5-46, Table 5-18). The My moments seen here can be caused by one of the following:

a) Fx acting on the bracket at an occluso-gingival distance from the bracket coordinate system.

b) Fz acting on the bracket at a mesio-distal distance from the bracket coordinate system

c) A force couple

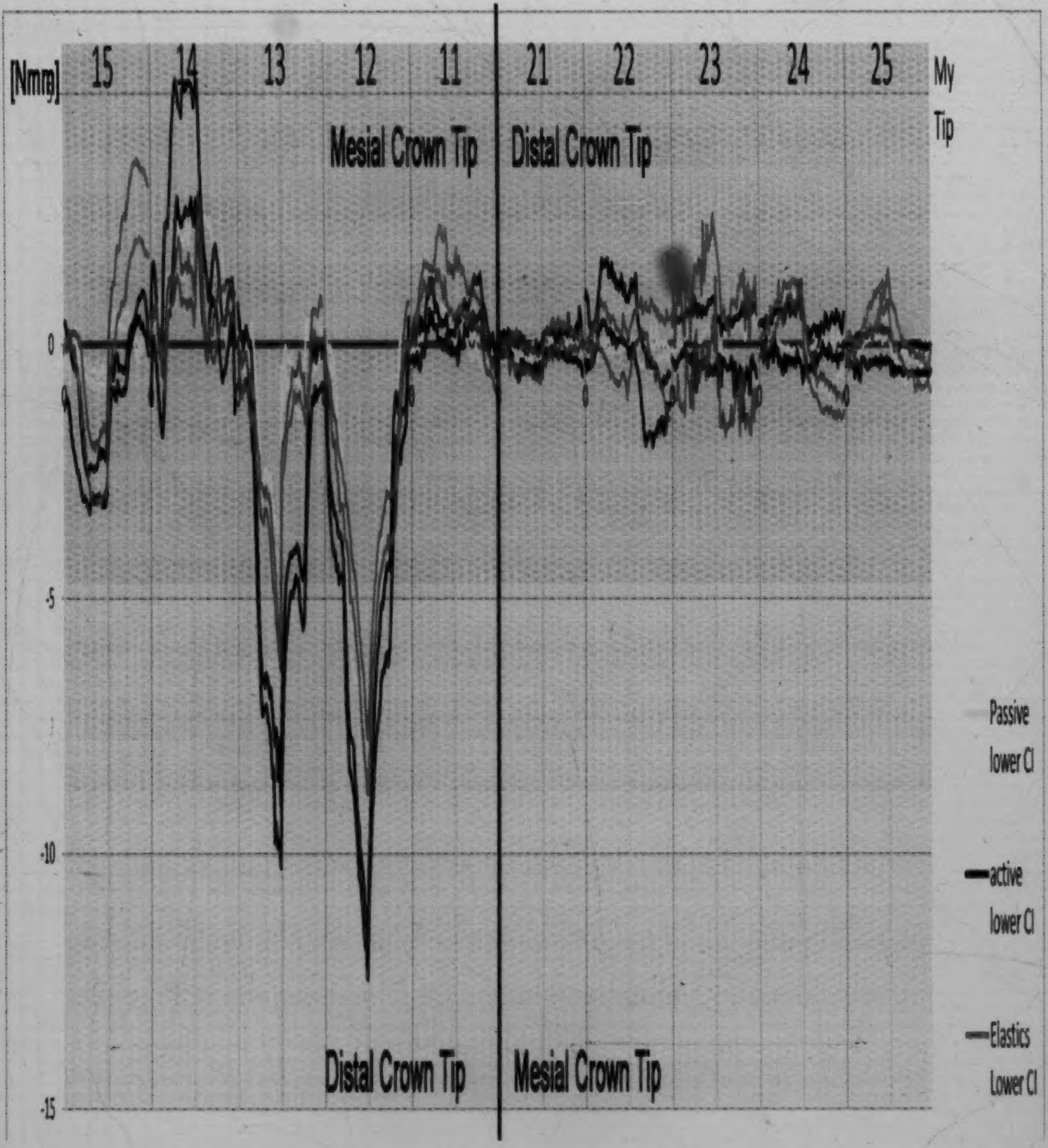

Figure 5-44: 0.014"x 0.025" My mesio-distal crown tip, 95% confidence intervals

14x25 My		Displacement mm				
		1 mm	2 mm	3 mm	2 mm	1 mm
Tooth	ligation	Moment Nmm				
15	Passive	-0.25	-0.60	-0.72	0.49	0.09
	Active	-1.58	-2.71	-2.63	-0.68	0.40
	Elastics	-0.26	-2.48	-2.24	1.29	2.78
14	Passive	0.90	1.87	2.10	1.83	1.25
	Active	1.00	3.66	3.81	0.51	0.17
	Elastics	-0.35	1.69	1.06	-0.03	0.71
13	Passive	0.31	-2.91	-4.15	-0.86	-0.46
	Active	-1.10	-6.80	-9.64	-4.42	-2.07
	Elastics	-1.24	-3.05	-6.12	-0.76	-1.12
12	Passive	-1.91	-6.14	-7.62	-4.36	-1.64
	Active	-4.22	-8.35	-12.07	-5.86	-1.47
	Elastics	-2.53	-4.84	-8.27	-4.09	-3.06
11	Passive	0.24	0.60	0.41	0.23	-0.20
	Active	0.37	0.24	0.04	0.46	0.86
	Elastics	1.36	1.90	0.93	0.73	0.34
21	Passive	-0.19	-0.13	-0.05	0.05	0.10
	Active	-0.07	-0.21	-0.20	0.07	0.14
	Elastics	-0.04	-0.29	-0.43	0.21	0.18
22	Passive	-0.01	0.03	-0.02	-0.24	-0.23
	Active	0.71	0.74	0.44	-0.51	-1.09
	Elastics	0.34	-0.06	-0.39	0.60	0.01
23	Passive	-0.04	-0.09	0.25	-0.05	-0.23
	Active	0.23	0.11	0.24	0.03	-0.34
	Elastics	0.61	0.56	1.06	-0.70	0.36
24	Passive	0.33	0.50	0.27	-0.41	-0.60
	Active	0.18	0.31	0.05	0.09	0.16
	Elastics	0.46	1.04	1.10	-0.75	-1.10
25	Passive	0.05	0.26	0.37	-0.44	-0.30
	Active	-0.30	-0.02	-0.02	-0.27	-0.26
	Elastics	0.08	0.66	1.16	-0.09	-0.55
Sign convention		R			L	
	Positive	Mesial crown tip			Distal crown tip	
	Negative	Distal crown tip			Mesial crown tip	

Table 5-18: 0.014" x 0.025" wire My moment data at 1mm increments

5.4.5.1 Cuspid:

The 13 experiences distal crown tip on loading and unloading with all brackets, PSL producing the lowest My moments and ASL produce the highest My moments during loading and unloading. These moments can be produced by:

a) The Fz occlusal force being more concentrated on the mesial side of the #13 bracket, this is confirmed by noticing the pattern of My which is similar to the pattern of Fz on #13

b) The Fx force acting on the #13 acting on the gingival aspect of the bracket slot, more superior to the mid-bracket coordinate system.

5.4.5.2 Teeth distal to #13:

Tooth #14 shows a mesial crown tip on loading and unloading and this is expected considering the angulation of the wire relative to the bracket slot. ASL brackets produces higher My than PSL and EL during loading, while all brackets produce similar levels of My during unloading. This My is directly related to the binding developed on the 14 bracket.

The 15 on the other hand shows a distal crown tip on loading with all ligation methods, with EL and ASL showing much higher My moment than PSL. During unloading EL brackets produce a high mesial crown tip, ASL produces a distal crown tip that changes to a mesial crown tip. And PSL shows the lowest My moment of mesial crown tip.

These moments could be related to the Fx forces acting on the 15 bracket on loading and unloading.

5.4.5.3 Teeth mesial to #13:

Tooth #12 shows a large distal crown tip for all ligation methods throughout loading and unloading, ASL produces the highest moments and PSL produces the lowest moments. An interesting finding is the presence of distal crown tip on loading and a mesial crown tip on unloading for teeth #22, 23 and 24. This finding could be explained by the elastic ligation pushing the wire against the gingival slot wall, which causes the Fx forces to produce those moments, those moments tend to follow the same pattern of Fx forces.

On examining the 3D graphs (Figure 5-46) we notice that ASL produces the most unwanted My moments while PSL produces the least unwanted My moments.

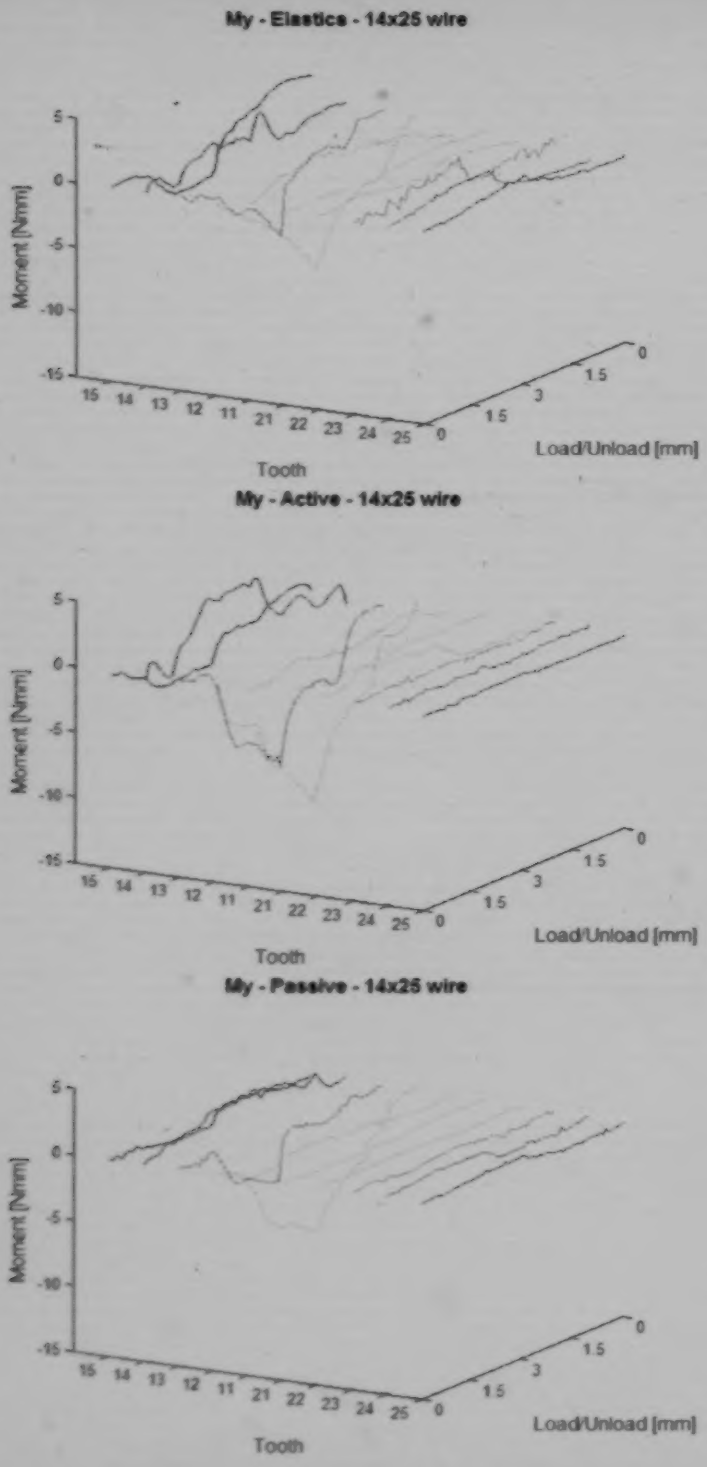

Figure 5-45: 3D 0.014"x 0.025" My mesio-distal crown tip, graphs, means EL, ASL and PSL brackets

5.4.6 Mz Moments (Disto-Buccal/Mesio-Buccal Moments)

We would expect no Mz moments on any of the teeth, however the largest moments were detected with ASL (Figure 5-47, Figure 5-48, Table 5-19). The Mz moments seen here can be caused by one of the following:

a) Fx acting on the bracket at a distance from the bracket coordinate system, (ie an Fx acting more buccal relative to the mid-bracket coordinate system).

b) Fy acting on the bracket at a distance from the bracket coordinate system (ie an Fy acting more mesial or distal relative to the mid-bracket coordinate system).

c) A force couple

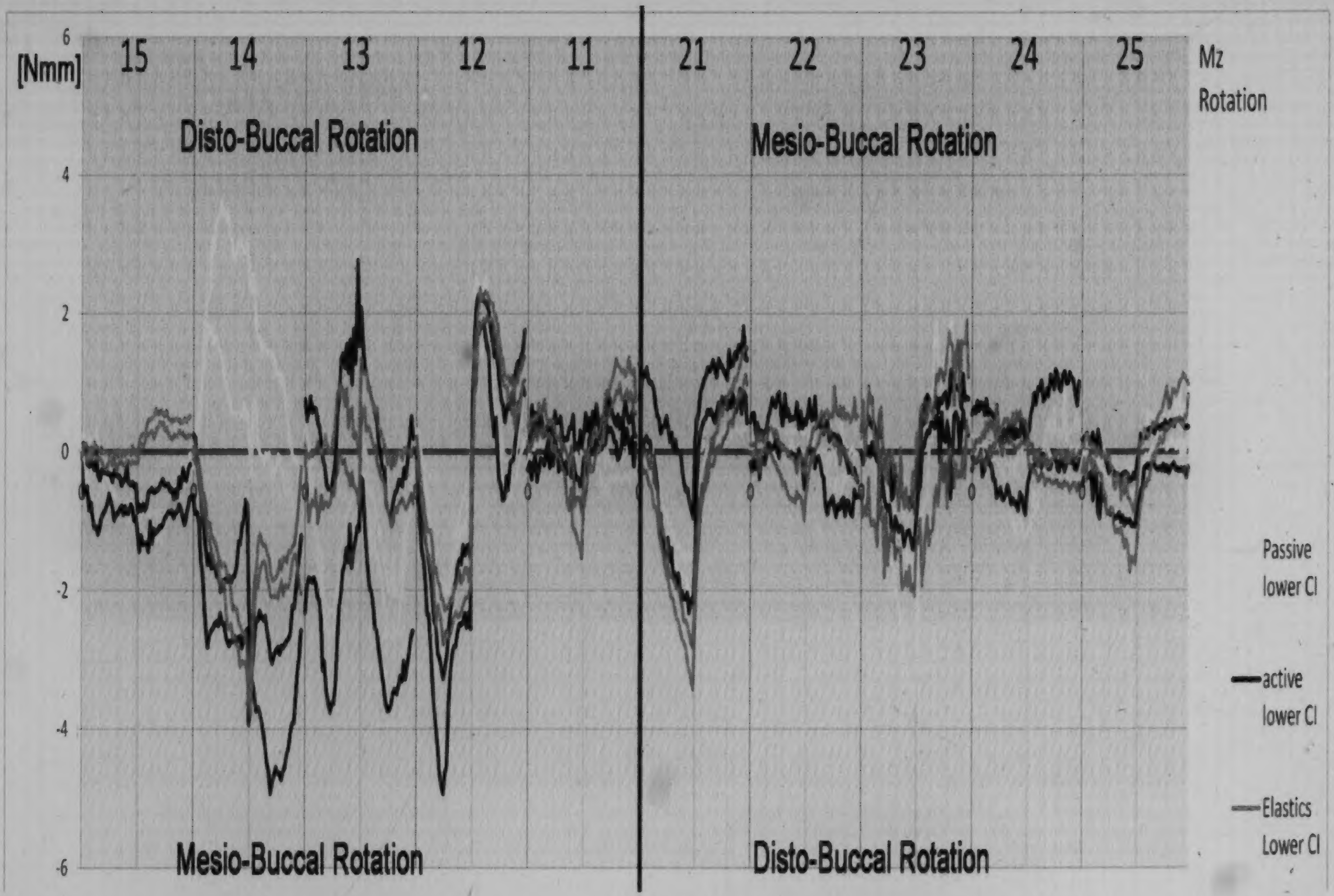

Figure 5-46: 0.014"x 0.025" Mz rotation around the long axis, 95% confidence intervals

14x25 Mz		Displacement mm				
		1 mm	2 mm	3 mm	2 mm	1 mm
Tooth	ligation	Moment Nmm				
15	Passive	-0.36	-0.81	-0.99	-1.05	-0.72
	Active	-0.75	-0.62	-0.72	-0.85	-0.70
	Elastics	-0.04	-0.13	-0.10	0.37	0.31
14	Passive	2.46	1.95	1.77	0.72	0.34
	Active	-2.13	-2.30	-1.67	-3.31	-3.71
	Elastics	-1.35	-2.18	-2.96	-1.47	-1.80
13	Passive	-1.94	-1.59	-0.78	-1.25	-2.40
	Active	-1.63	-0.37	0.20	-1.08	-2.02
	Elastics	-0.39	0.44	-0.42	0.23	-0.51
12	Passive	-2.31	-2.05	-0.62	1.73	-0.40
	Active	-3.05	-2.53	-2.05	1.74	0.12
	Elastics	-1.90	-2.32	-1.86	2.06	1.00
11	Passive	-0.06	0.07	0.11	-0.11	-0.25
	Active	0.18	-0.04	-0.18	0.12	0.21
	Elastics	0.40	-0.09	-1.20	0.17	1.06
21	Passive	-0.63	-1.42	-1.79	0.33	0.46
	Active	0.03	-0.79	-1.55	0.90	1.09
	Elastics	-0.72	-2.09	-3.12	0.00	0.64
22	Passive	0.05	0.14	0.13	-0.20	-0.33
	Active	0.32	0.27	-0.04	0.08	-0.32
	Elastics	0.15	-0.28	-0.64	0.45	0.24
23	Passive	-0.40	-1.57	-2.62	0.59	1.17
	Active	0.10	-0.72	-1.08	0.50	0.25
	Elastics	0.31	-0.93	-1.48	-0.30	0.83
24	Passive	0.00	-0.39	-0.64	-0.24	-0.06
	Active	0.21	-0.09	-0.39	0.35	0.42
	Elastics	0.27	0.34	0.29	-0.22	-0.28
25	Passive	-0.05	-0.39	-0.44	0.19	0.39
	Active	-0.40	-0.63	-0.73	0.07	0.10
	Elastics	-0.16	-0.73	-1.22	0.18	0.54
Sign convention		R			L	
	Positive	Disto-Buccal rotation			Mesio-Buccal rotation	
	Negative	Mesio-Buccal rotation			Disto-Buccal rotation	

Table 5-19: 0.014"x 0.025" wire Mz moment data at 1mm increments

5.4.6.1 Cuspid:

On examining the graph, it is very difficult to identify a specific pattern, however, we notice the wider variation with ASL compared to EL and PSL.

5.4.6.2 Teeth distal to #13:

On tooth #14 we notice a relatively large mesio-buccal rotation on loading and unloading with ASL and EL brackets. This could be caused by the interaction between the active spring and the elastic with the wire, applying a lingual Fy on the distal aspect of the bracket and/or buccal Fy on the mesial aspect of the bracket during loading and unloading. PSL applies a disto-buccal rotation which can be explained by the archwire sliding.

On tooth #15 elastic ligation produces no rotation on loading and a small disto-buccal rotation on unloading. PSL and ASL produce similar levels of mesio-buccal rotation during loading and unloading. this could be related to the Fx force or the Fy forces applied on the tooth #15.

5.4.6.3 Teeth mesial to #13:

The 12 shows a high mesio-buccal rotation on loading and a disto-buccal rotation on unloading with all ligation methods, as well as a disto-buccal moment on loading followed by a mesio-buccal moment on unloading for teeth 21, 23 and 25. These moments are most likely related to the Fx forces. We notice tooth # 22 and #24 have lower Mz moments, which is consistent with the Fx pattern. It seems that ASL produces the largest variation. Tooth #

23 experiences a relatively high disto-buccal rotation with PSL on loading only.

On examining the 3D graphs (Figure 5-48), it is apparent that all ligation methods produce equivalent patterns of Mz moments.

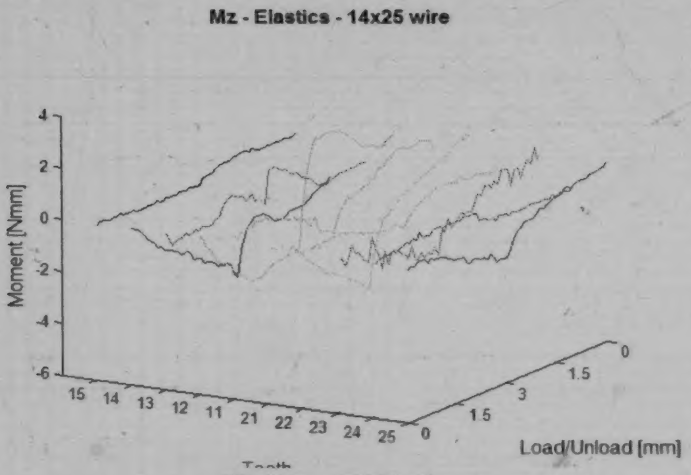
Mz - Elastics - 14x25 wire

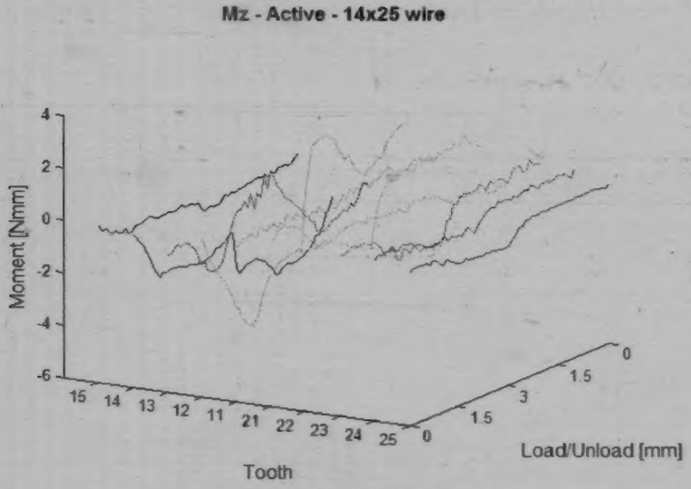
Mz - Active - 14x25 wire

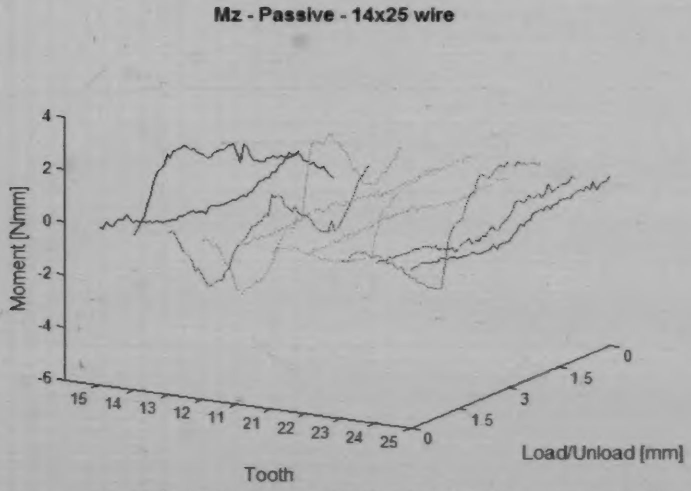
Mz - Passive - 14x25 wire

Figure 5-47: 3D 0.014"x 0.025" Mz rotation around the long axis graphs, means EL, ASL and PSL brackets

5.5 Summary of Results

In our experiment, we attempted to explore the effect of the ligation method on the resultant orthodontic force system. Three identical malocclusions were simulated, in one instance passive self-ligating brackets were used and in another instance conventional ligation was used and in a third instance active self-ligation was used. A high upper right cuspid was created on the OSIM, 0.014", 0.018" and 0.014"× 0.025" Nickel Titanium wire were consecutively tied to all brackets the experiments were repeated 5 times with each wire, a new wire was used every time. Three dimensional force and moment data was collected as the cuspid was moved 4mm (3mm in the 0.014"× 0.025" experiment) occlusally then back to the default position. Data on all the teeth in the dental arch was presented. In this high cuspid situation, the ideal force system is one with an extrusive force on the cuspid, intrusive reciprocal forces on the premolar and lateral, while all other components are best kept at a minimum. In the previous section, we have described each of the components of the force systems, and we identified a number of patterns and differences between the three ligation methods. In this section, we will attempt to analyze and present some of the possible explanations for those patterns and differences. A number of facts need to be highlighted:

- We are interested in comparing the different ligation methods, however we do not have a sample. We have one set of brackets for each ligation method to use with the OSIM device.

- The data is presented graphically in sections, each section describes each of the six components of the force system acting on the ten teeth (tooth #15 - #25).
- The data is used for a qualitative assessment of the force systems.
- The graphs will be described in relative terms.
- We tried to identify patterns in the force system. For the patterns identified, we will try to present the most plausible explanation.
- We will not have an explanation for every pattern identified.
- This data will most likely lead to more specific research questions that need answers.

On examining the 3D force data it is not surprising that the main difference between the three ligation methods lies in the resistance to sliding recorded on the lateral incisor the first premolar and the second premolar. However, this increased resistance to sliding (Fx force) considerably affected the other five components of the force system acting on the rest of the dentition. The force system produced by the same wire can vary considerably according to which ligation method is used.

5.6 Forces produced by 0.014" wire

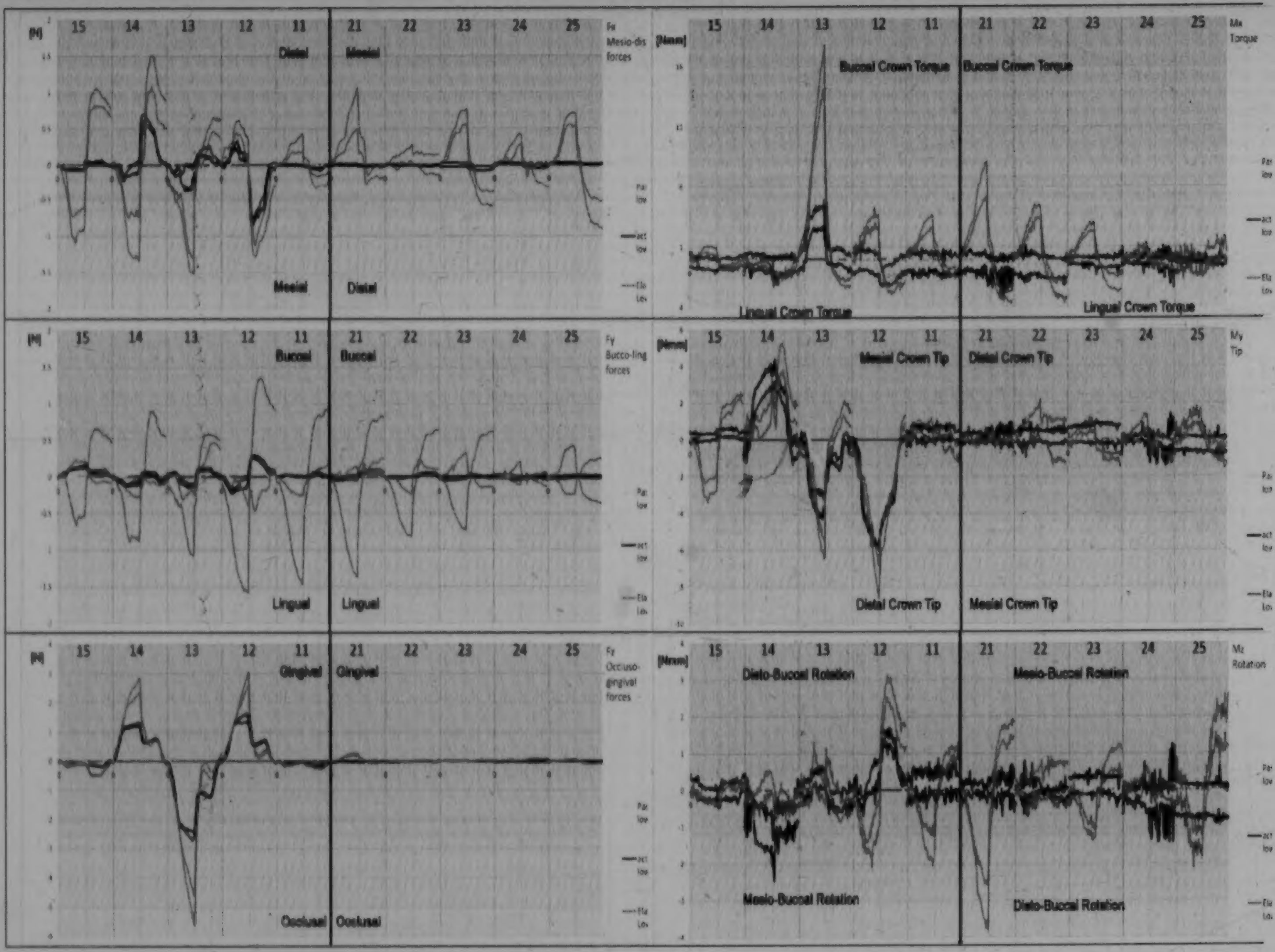

Figure 5-48: 0.014" wire, Fx, Fy, Fz, Mx, My and Mz graphs

The graphs in Figure 5-49, show that the SL brackets behave in remarkably similar patterns while there is a considerable difference between the SL brackets and the EL brackets. With SL the teeth # 12, 13, 14 (and to a lesser degree #15 and #23 with ASL) are the only teeth with Fx forces, while with EL all teeth in the dental arch without exception have Fx forces acting on them. Some of the interesting observations are:

- The variation resulting from the EL brackets is considerably larger than the variation resulting from the SL brackets. This variation is expected however, the magnitude of this variation was not, the variation on tooth #21 for example was as high as 0.6 N at the end of the loading phase of the experiment.
- Another interesting finding is the fact that all ligation methods start with zero Fx and Fy readings, however at the end of the experiment, EL brackets almost always have a residual Fx and Fy forces while SL brackets do not. This can be explained by the elasticity of the EL, which continues to apply a mesial or distal force in spite of all the teeth being in the default zero position at the end of the experiment.
- The high Fx forces seem to skip every other tooth on the left side of the dental arch with EL. Teeth #21, 23 and 25 have considerably higher Fx forces than teeth #11, 22 and 24. This same pattern is seen in the Mz graph.
- The Fy graph shows considerable difference between SL and EL. There are considerable lingual forces on loading and buccal forces on unloading for all the teeth in the dental arch with EL brackets.

Whereas with SL, those Bucco-lingual forces were restricted to teeth # 12, 13, 14 and 15 (and to a lesser degree on tooth #11 and 21 with ASL). Those buccal and lingual forces are a direct result of the Fx forces which cause those Bucco-lingual forces because of the curvature of the dental arch. Had the brackets been arranged in a straight line, minimum Bucco-lingual forces would be recorded.

- Again the variation in the Fy forces was much higher with EL compared to SL.
- The Fz graph shows the effective force intended to align this type of malocclusion in a clinical setting, and this graph shows that although the difference between the SL and EL brackets is less pronounced than in the other five components, a difference nevertheless exists. Fz load deflection curves are supposed to have flat segments (the load does not increase with deflection, a characteristic of NiTi alloy). the NiTi wires are manufactured to deliver constant forces regardless of the deflection, with SL those wires do perform in this manner however with EL we notice the larger magnitude and the absence of the flat segment on loading, and the low magnitude on unloading compared to SL.
- We notice small extrusive forces acting on tooth # 15 and 11 with all ligation methods. And an intrusive force on tooth # 21 with EL on loading. This is caused by the fact that when the wire is deflected a wave of extrusive and intrusive forces propagate past the immediate point of deflection to affect adjacent teeth.

- The Mx graph shows an unexpected high buccal crown torque moment on loading and a small lingual crown torque moment on unloading. the moments are represented on the mid-bracket coordinate system (a point in the slot base in the middle of the bracket). Fy buccal or lingual force can produce this type of Mx moment if a buccal force is acting occlusal to this point or a lingual force is acting gingival to this point. Another way this moment can develop is when the wire is bent in the #13 bracket it contacts the gingival slot wall in the middle of the bracket and it contacts the occlusal slot wall at the periphery of the bracket slot. This contact pattern can produce two non-collinear forces causing a couple which is measured as Mx.
- The Mx graph shows a high degree of variation with ASL when compared to PSL. This is most likely due to the interaction between the active ligation spring clip with the wire.
- The My graph shows expected crown tip on the #12 distally and the #14 mesially, however it shows a distal crown tip of the #13 distally which was not expected especially when we consider the mesial Fx force developing on the 13 due to arch wire sliding. This My moment can be explained by relating the My graph to the Fx graph. A Fx force acting on the mesial side of the #13 bracket will produce this distal crown tip, this is plausible since the interbracket distance between the cuspid and the lateral incisor is smaller than that between the cuspid and first premolar. This explains the higher Fx force on the 12 when

compared to that on the 14, and it would suggest that the Fz on the cuspid is actually being applied on the mesial aspect of its bracket which causes this My moment.

- Tooth # 15 shows a distal crown tip on loading and a mesial crown tip on unloading, the same curve pattern is seen in the Fx graph, which suggests that this My is caused by the Fx force. In order for this Fx force to cause such a My it would have to be acting gingival to the 15 bracket coordinate system, this can be explained by the wire being restrained by the elastic on the gingival aspect of the bracket slot.
- The Mz moment graph seems to show the same pattern seen in the Fx graph, we notice that teeth # 22 and 24 have low Mz moments similar to the Fx graph.
- One interesting finding in the Mz graph is the presence of the unusual large mesio-buccal rotation on the #14 with ASL. It is most likely due to the fact that in this clinical situation, the wire will tend to slide through the 14 bracket and the 15 bracket more than any other bracket in the dental arch. The wire would slide through the 15 with no significant resistance to sliding, however the active clip bracket has a clip that invades the bracket slot in the gingival aspect of it. This is where the wire will tend to be deflected as the cuspid is displaced in our experiment, this will generate a mesio-buccal rotation higher than that seen in the PSL brackets.

When we consider all the aspects of the 0.014" NiTi wire force system, it seems that active self-ligation and passive self-ligation produce remarkably similar forces and moments, that are quite different from those of elastic ligation. No ligation method delivers the ideal force system but self-ligation delivers the force system with the least unwanted components.

5.7 Forces produced by 0.018" wire

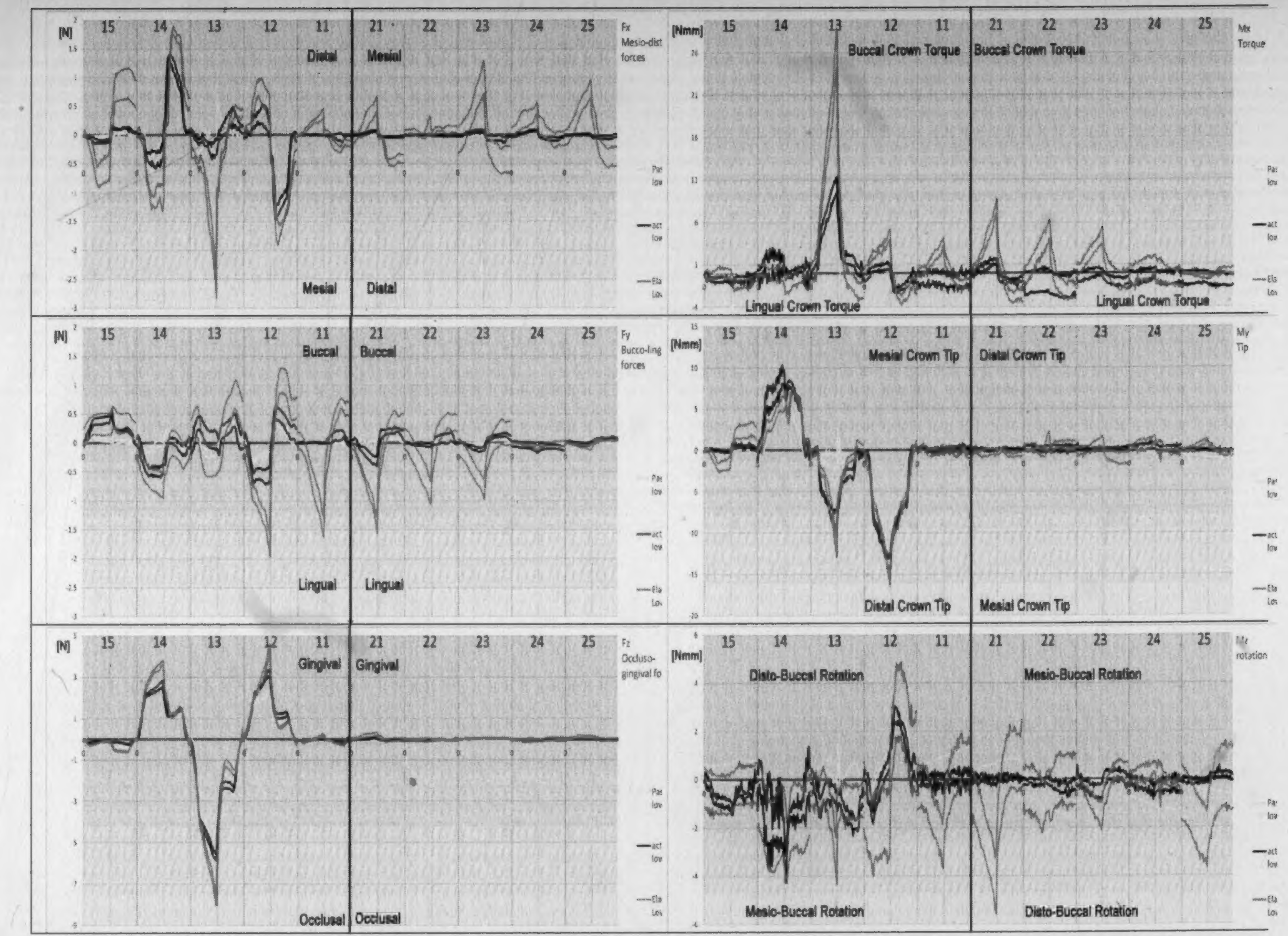

Figure 5-49: 0.018"wire, Fx, Fy, Fz, Mx, My and Mz graphs

The graphs in Figure 5-50, show that although SL brackets with 0.018"wire behave in similar patterns, we start to see differences between the PSL and ASL that were less pronounced with the 0.014" wire. Again similar to 0.014" wire, there is a considerable difference between the SL brackets and the EL brackets. With SL the teeth # 12, 13, 14 (and to a lesser degree #15, #23 and #24 with ASL) are the only teeth with Fx forces, while with EL all teeth in the dental arch without exception have Fx forces acting on them. Some of the interesting observations are:

- The variation resulting from the EL brackets is considerably larger than the variation resulting from the SL brackets. This variation is expected however, the magnitude of this variation was not, the variation in Fx on tooth #15 for example was as high as 0.5 N during the loading and unloading phases of the experiment.
- Again, similar to the pattern seen in 0.014" wire, all ligation methods start with zero Fx and Fy readings, however at the end of the experiment, EL brackets almost always have a residual Fx and Fy forces while SL brackets do not. This can be explained by the elasticity of the EL, which continues to apply a mesial or distal force in spite of all the teeth being in the default zero position at the end of the experiment.
- Again, we are seeing the same pattern as 0.014" wire where the high Fx forces seem to skip certain teeth on the left side of the dental arch with EL. Teeth #21, 23 and 25 have considerably higher Fx forces than teeth #11, 22 and 24.

- The Fy graph shows considerable difference between the three ligation methods, it seems that the most pronounced difference between the PSL and ASL exists in the Fy component of the 0.018"wire, this difference did not exist in the 0.014" wire. There are considerable lingual forces on loading and buccal forces on unloading for all the teeth in the dental arch with EL brackets. Unlike the 0.014" wire, with the 0.018" wire graphs show that with ASL there are considerable Fy forces on all the teeth that mirror those forces of EL however of lesser magnitude. Whereas, those Bucco-lingual forces were restricted to teeth # 12, 13, and 14 with PSL. Those buccal and lingual forces are a direct result of the Fx forces which cause those Bucco-lingual forces because of the curvature of the dental arch. Had the brackets been arranged in a straight line, we suspect minimum Bucco-lingual forces would have been recorded.
- In the 0.018"wire the variations in the Fy forces are much higher with EL and ASL compared to PSL. The overall magnitude of the Fy forces were highest for EL and lowest for PSL with ASL being somewhere in the middle. This change in the behavior of the ASL brackets is not surprising since those brackets are designed with a lumen size of 0.018", which means that a 0.018"wire completely fills the bracket slot and starts to interact with the bracket clip. Whereas the PSL brackets have a rectangular lumen of 0.022"x0.027" which means that a 0.018"wire can lie passively in this lumen.

- What is surprising however is that this extra interaction between the wire and the clip in the ASL brackets produced no difference in Fx forces compared to the PSL brackets, however it produced disproportionately higher Fy forces.
- The Fz graph shows the effective force intended to align this type of malocclusion in a clinical setting, this graph shows that the difference between the three ligation methods is more defined than it was with the 0.014" wire. The differences between the three types of ligation are less pronounced than in the other five components, a difference nevertheless exists. We notice that the Fz load deflection curves have more defined flat segments, a characteristic of NiTi alloy, which are manufactured to deliver constant forces regardless of the deflection. However, the load within these flat segments tends to increase during unloading as the canine displacement decreases, it seems that PSL brackets are the only brackets that do not alter the behavior of those wires, the EL brackets produce higher Fz force on loading and ASL produce higher Fz force on unloading.
- Similar to what we saw with the 0.014" wire, we notice small extrusive force acting on tooth # 15 and to a lesser degree on tooth #11 with all ligation methods. This is caused by the fact that when the wire is deflected a wave of extrusive and intrusive forces propagates past the immediate point of deflection to affect adjacent teeth.
- In the Mx graph we see another resemblance to that of the 0.014" wire, an unexpected high buccal crown torque moment on loading and

a small lingual crown torque moment on unloading on almost all teeth exept tooth #14. The moments are represented on the mid-bracket coordinate system (a point in the slot base in the middle of the bracket). Fy buccal or lingual force can produce this type of Mx moment if a buccal force is acting occlusal to this point or a lingual force is acting gingival to this point. It seems that the Fy force are producing those moments. another way this moment can develop is when the wire is bent in the #13 bracket it contacts the gingival slot wall in the middle of the bracket and it contacts the occlusal slot wall at the periphery of the bracket slot. This contact pattern can produce two non-collinear forces causing a couple which is measured as Mx, this would be the only explanation for tooth #13 having a much larger Mx moment than the rest of the teeth.

- Tooth # 14 has a very distinctive buccal crown torque moments that is consistent with the Fy load on that tooth.
- The My graph shows expected crown tip of the #12 distally and the #14 mesially, however it shows a distal crown tip of the #13, which was not expected especially when we consider the mesial Fx force developing on the 13 due to arch wire sliding. This My moment can be explained by relating the My graph to the Fz graph. A Fz force acting on the mesial side of the #13 bracket, will produce this distal crown tip, this is plausible since the interbracket distance between the cuspid and the lateral incisor is smaller than that between the cuspid and first premolar. This explains the higher Fz force on the 12 when compared to that on the 14, and it would suggest that the Fz on the

cuspid is actually being applied on the mesial aspect of its bracket, which causes this My moment.

- Tooth # 15 shows a distal crown tip on loading and a mesial crown tip on unloading, (similar to what was seen with the 0.014" wire) the same curve pattern is seen in the Fx graph. This suggests that this My is caused by the Fx force, in order for this Fx force to cause such a My it would have to be acting gingival to the 15 bracket coordinate system, this can be explained by the wire being restrained by the elastic on the gingival aspect of the bracket slot.
- The My moments on tooth # 12 and #14 are important, these moments will generate the binding in those two brackets. Those two moments were highest with ASL brackets and lowest with EL and PSL brackets.
- The Mz moment graph shows an unidentifiable pattern of Mz moments with large variations. However, the only identifiable difference between the three ligation methods exists on tooth #14 and to a lesser degree #15, which experience a mesio-buccal rotation with all ligation methods more so on EL and ASL than PSL. No clear explanation could be presented at this point.

When we consider all the aspects of the 0.018"NiTi wire force system, it seems that the difference between PSL and ASL is more pronounced in the 0.018"than in the 0.014" wire. No ligation method delivers the ideal force system but passive self-ligation delivers the least unwanted components.

5.8 Forces produced by 0.014”× 0.025” wire

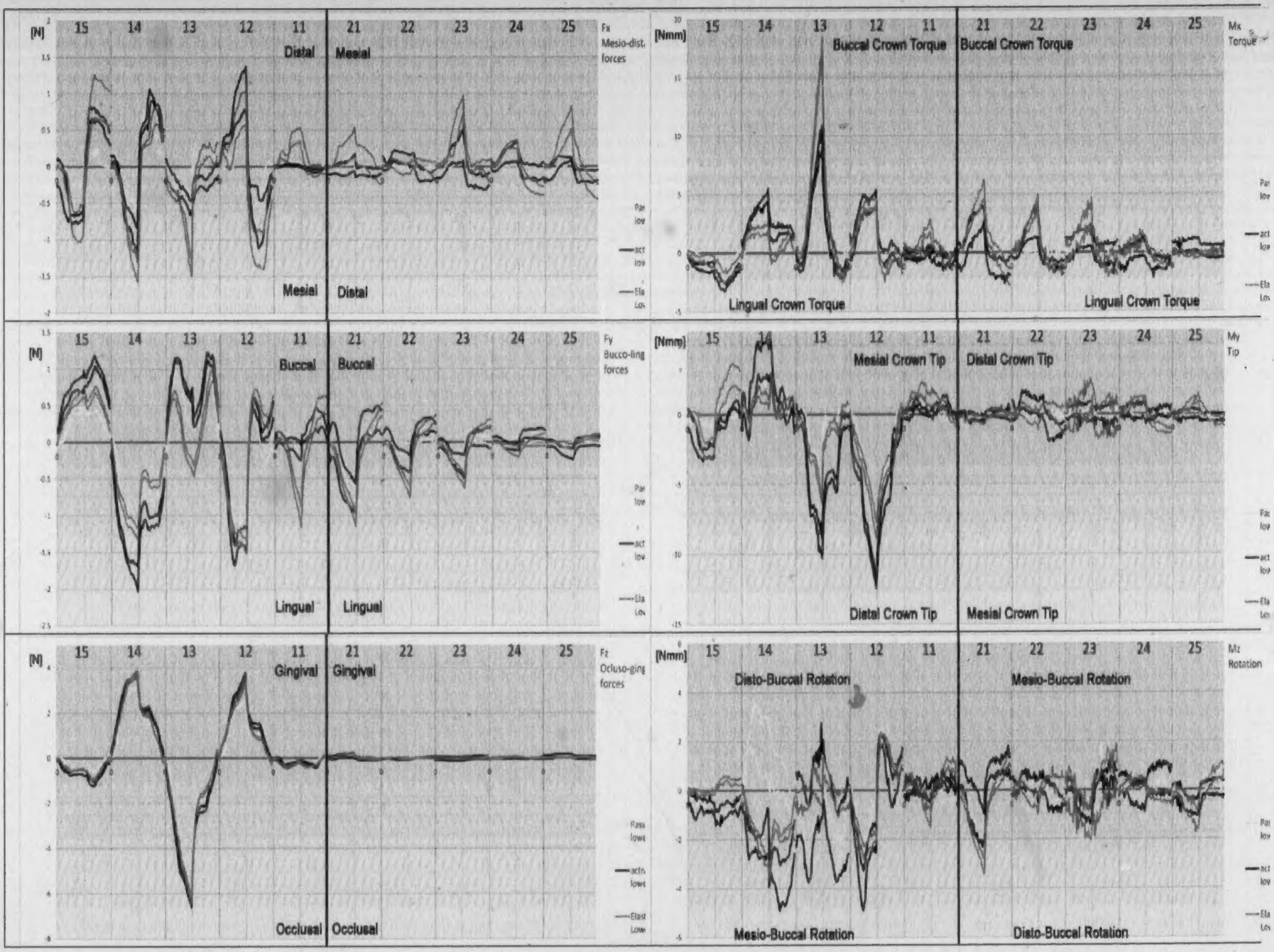

Figure 5-50: 0.014"x 0.025" wire, Fx, Fy, Fz, Mx, My and Mz graphs

The graphs in Figure 5-51 show a different pattern compared to 0.014"and 0.018" wires. Some of the interesting observations are:

- All teeth with all ligation methods experience relatively high levels of Fx forces, PSL brackets show the least amount of variation. PSL brackets as expected produce lower Fx forces than ASL and EL, especially on tooth #15 and to a lesser degree on teeth #14, 13 and 12.
- Another interesting finding is the fact that all ligation methods start with zero Fx readings, however at the end of the experiment, EL and ASL brackets almost always have a residual Fx force while PSL brackets produce this pattern on teeth #14, 13 and 12 only. This can be explained by the elasticity of the EL and ASL ligation methods, which continues to apply a mesial or distal force in spite of all the teeth being in the default zero position at the end of the experiment.
- The high Fx forces similar to what was seen in 0.014" and 0.018" wires, seem to skip every other tooth on the left side of the dental arch. Teeth #21, 23 and 25 have considerably higher Fx forces than teeth #11, 22 and 24.
- The Fy graph shows considerable difference between all ligation methods. There are considerable lingual forces on loading and buccal forces on unloading for all the teeth in the dental arch. These forces decline in magnitude the further we move away from the #13.
- On average it seems that ASL produces the highest Fy forces while PSL produces the lowest Fy forces, except on tooth #13 where EL produces lower Fy forces than PSL, this can be explained by the fact

that the elastic ligation was stretched to the extent that the wire consistently disengaged from the 13 bracket as it was displaced during the experiment. Those buccal and lingual forces are a direct result of the Fx forces which cause those Bucco-lingual forces because of the curvature of the dental arch. Had the brackets been arranged in a straight line, we suspect that minimum bucco-lingual forces would be recorded.

- The variation in the Fy forces was much higher with ASL compared to PSL and EL.
- The Fz graph shows the effective force that is intended to align this type of malocclusion in a clinical setting, and this graph shows that although the differences between the ligation methods are less pronounced than with the other five components, a difference nevertheless exists. Fz load deflection curves are supposed to have flat segments (the load does not increase with deflection, a characteristic of NiTi alloy). The NiTi wires are manufactured to deliver constant forces regardless of the deflection. We notice that the flat segment on loading and unloading are less pronounced when compared to those of 0.018"wire.
- We notice small extrusive force acting on tooth # 15 and 11 with all ligation methods. And an intrusive force on tooth # 21 with EL on loading. This is caused by the fact that when the wire is deflected a wave of extrusive and intrusive forces propagates past the immediate point of deflection to affect adjacent teeth.

- The Mx graph shows an unexpected high buccal crown torque moment on loading and a small lingual crown torque moment on unloading except for teeth #14 and 15. The moments are represented on the mid-bracket coordinate system (a point in the slot base in the middle of the bracket). Fy buccal or lingual force can produce this type of Mx moment if a buccal force is acting occlusal to this point or a lingual force is acting gingival to this point. It seems that the Fy forces are producing those moments. another way this moment can develop is when the wire is bent in the #13 bracket it contacts the gingival slot wall in the middle of the bracket and it contacts the occlusal slot wall at the periphery of the bracket slot. This contact pattern can produce two non-collinear forces causing a couple which is measured as Mx.
- The Mx graph shows a higher degree of variation with ASL when compared to PSL. This is most likely due to the interaction between the active ligation spring clip with the wire.
- The My graph shows expected crown tip of the #12 distally and the #14 mesially, however it shows a distal crown tip of the #13 distally which was not expected especially when we consider the mesial Fx force developing on the 13 due to arch wire sliding. This My moment can be explained by relating the My graph to the Fz graph. A Fz force acting on the mesial side of the #13 bracket will produce this distal crown tip, this is plausible since the interbracket distance between the cuspid and the lateral incisor is smaller than that between the cuspid

and first premolar. This explains the higher Fz force on the 12 when compared to that on the 14, and it would suggest that the Fz on the cuspid is actually being applied on the mesial aspect of its bracket, which causes this My moment.

- Tooth # 15 shows a distal crown tip on loading and a mesial crown tip on unloading, the same curve pattern is seen in the Fx graph, which suggests that this My is caused by the Fx force. In order for this Fx force to cause such an My it would have to be acting gingival to the 15 bracket coordinate system, this can be explained by the wire being restrained by the elastic on the gingival aspect of the bracket slot.
- The My moments on tooth # 12 and #14 are important, these moments will generate the binding in those two brackets. Those two moments were highest with ASL brackets and lowest with EL and PSL brackets.
- The Mz moment graph shows an unidentifiable pattern of Mz moments with large variations. However, the only identifiable difference between the three ligation methods exists on tooth #14, which experiences a mesio-buccal rotation with ASL and EL but a disto-buccal rotation with PSL. The mesio-buccal rotation in the EL and ASL is most likely due to the fact that in this clinical situation, the wire will tend to slide through the 14 bracket and the 15 bracket more than any other bracket in the dental arch. The wire would slide through the 15 with no significant resistance to sliding. However, the active clip on bracket #14 has a clip that invades the bracket slot in the

gingival aspect of it, this is where the wire will be deflected as the cuspid is displaced in our experiment, this will generate a mesio-buccal rotation higher than that seen in the PSL brackets. The disto-buccal rotation with the PSL brackets is most likely due to the Fx force.

When we consider all the aspects of the 0.014" x 0.025" NiTi wire force system , it seems that all ligation methods produce slightly different forces and moments. No ligation method delivers the ideal force system but PSL delivers the force system with slightly less unwanted components.

5.9 The effect of archwire size and dimension on the force system

In our experiment, we used three types of orthodontic wires, 0.014”NiTi, 0.018”NiTi and 0.014” x 0.025” NiTi. It would be of interest to examine the effect of archwire dimension and cross-section on the resultant force system. We will analyze the data by looking at each component of the force systems and comparing the standardized graphs of the three wires.

5.9.1 The effect of the wire size and dimension on Fx

On examining the three Fx graphs in Figure 5-52, we notice that with 0.018”wire, the resistance to sliding increases from the levels seen in the 0.014”wire. This increase is noticed to be present on all teeth with EL, whereas with SL brackets the teeth #14, 13 and 12 are the only teeth exhibiting this increase in Fx forces. This is expected since the 0.018”wire is still a relatively passive wire in both SL brackets and the increase in the size from 0.014” to 0.018” affects the resistance to sliding on teeth mesial and distal to the cuspid. When we examine the 0.014” x 0.025” wire, we notice that with EL there is little increase in the Fx forces compared to 0.018”wire. However, with SL brackets especially ASL, the increase in the resistance to sliding was substantial.

Tooth # 15 is a good example, that tooth is close to the simulated cuspid displacement, the wires slide through the 15 and 14 brackets more than any other bracket, yet the 15 bracket has no binding developing between the bracket and the wire. We notice that with the 0.014" wire the EL is the only ligation method with resistance to sliding, as we move to 0.018"wire, we notice that the resistance to sliding rose only marginally for EL and ASL. However, with 0.014"x 0.025" wire, it is apparent that the gap between the ASL and PSL widens and the resistance to sliding on the ASL bracket approximates that of the EL bracket. This behavior is expected, because the ASL bracket is designed so that 0.018"wire fills the bracket slot fully and any more increase in the wire dimension will cause the ligation method to apply a normal force to the wire, which is what we see in the 0.014"x 0.025" graph.

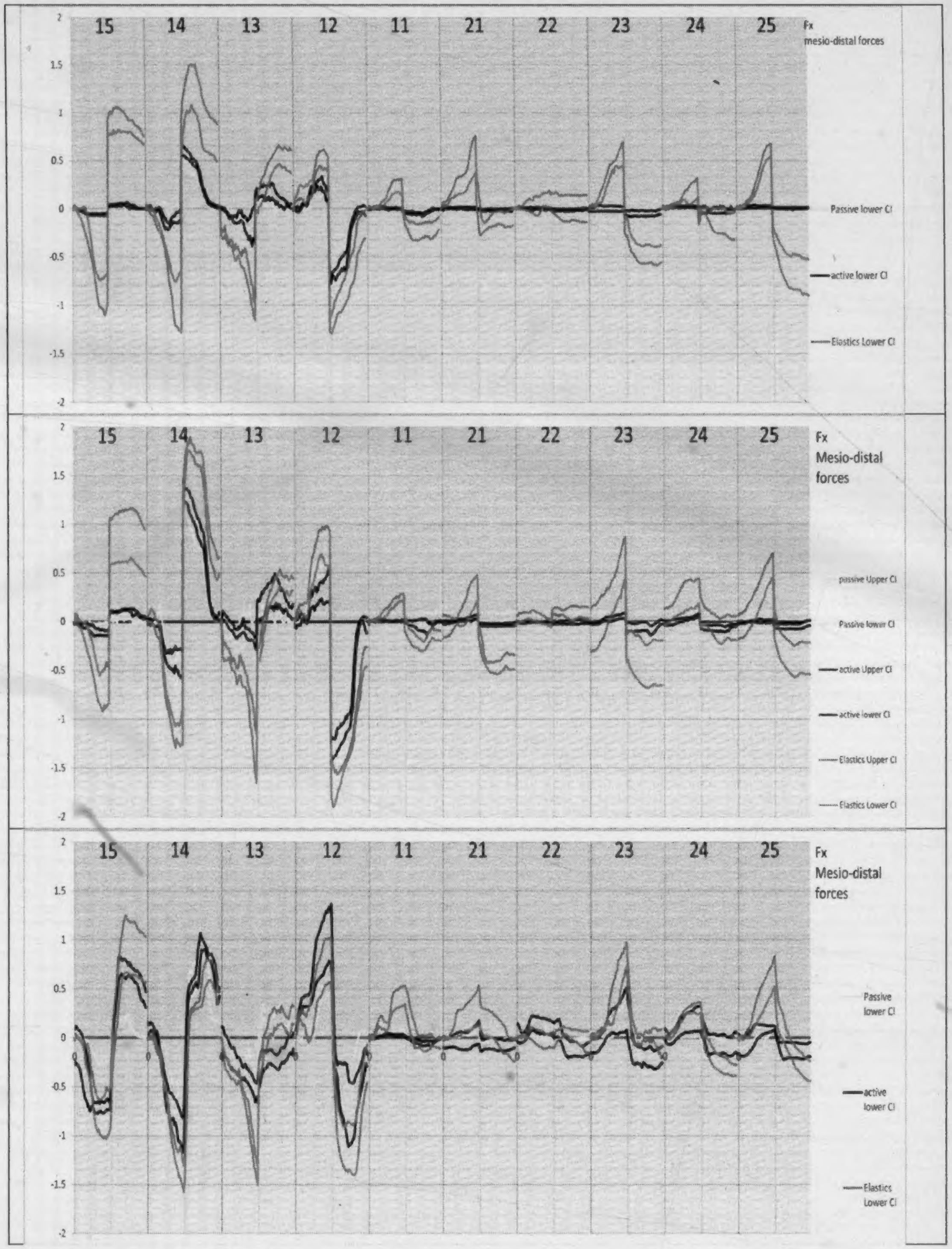

Figure 5-51: Standardized Fx graphs of 0.014", 0.018"and 0.014"x 0.025" NiTi wires

5.9.2 The effect of the wire size and dimension on Fy

On examining the Fy graphs in Figure 5-53, we notice that the graphs of all the wires show somewhat similar patterns, however the magnitudes of the Fy forces tend to increase as the wire size is increased, and the amount of variation tend to decrease as the wire size increases from 0.014" to 0.014" x 0.025". In the 0.014", wire there was a considerable gap between the EL and the SL brackets' behavior. As we increase the wire size the distinction between the two types of SL brackets becomes clearer, ASL brackets consistently produce higher Fy forces with 0.018"wire than PSL brackets. This pattern continues and the gap between the two types of SL brackets widens further as the ASL brackets apply the highest Fy forces in the 0.014"x 0.025" wire on the teeth mesial and distal to the displaced cuspid. Again, this finding is not surprising since with the ASL brackets the spring action of the clip starts to appear as the wire dimension is increased from 0.014" to 0.018" to 0.014" x 0.025", and we would expect this pattern to continue with further increases in archwire dimension.

On tooth #13, we notice a considerable difference in the pattern and magnitude of the forces produced by the 0.014", 0.018" and the 0.014" x 0.025" wires. With the 0.014" x 0.025" wire we notice a buccal force on loading and unloading for all ligation methods, with an interesting "M" shaped load-deflection curve.

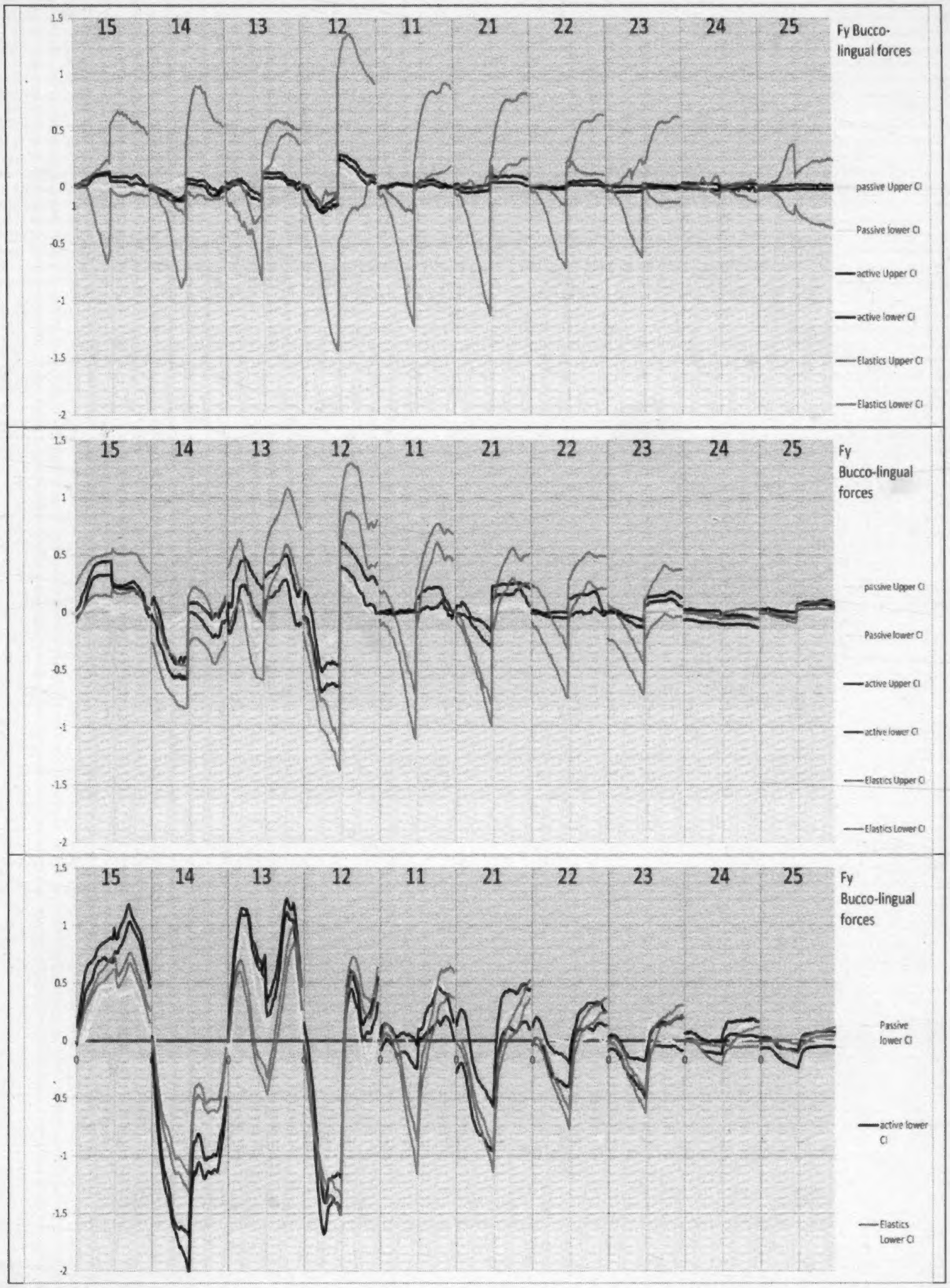

Figure 5-52: Standardized Fy graphs of 0.014", 0.018"and 0.014"x 0.025" NiTi wires

5.9.3 The effect of the wire size and dimension on Fz

On examining the Fz graphs in Figure 5-54, we notice the same pattern seen previously. The Fz forces increase as we move from 0.014"to 0.014"x 0.025" wire. The gap between the SL brackets becomes more apparent as we move from 0.014" to 0.018" to 0.014" x 0.025". With the 0.014" wire the SL brackets apply very similar force levels, as we move to the 0.018" wire the ASL force levels increase and the gap between the two SL brackets further increase as we move to the 0.014" x 0.025" wire.

The Fz force throughout most of the unloading curve on tooth #13 for SL brackets with 0.014"wire, was around 1N, the same portion of the curve with 0.018" wire was around 2N (100% increase) with higher force for ASL than PSL. With the 0.014"x 0.025" wire the same portion of the curve was around 2N, again there is higher force with ASL than PSL.

The 0.014"x 0.025" wire bends as the cuspid is displaced vertically, although the wire cross section is larger than that of the 0.018"wires, this vertical bend is resisted by the 0.014"vertical dimension of the 0.014"x 0.025" wire. Therefore, it seems that the 0.018"wire and the 0.014"x 0.025" wire exhibit almost identical Fz loads when a vertical bend is being produced, however, with a less pronounced flat load deflection curve section with the 0.014" x 0.025" wire. We expect the 0.014"x 0.025" wire would exhibit much higher forces if the cuspid displacement were in the horizontal dimension.

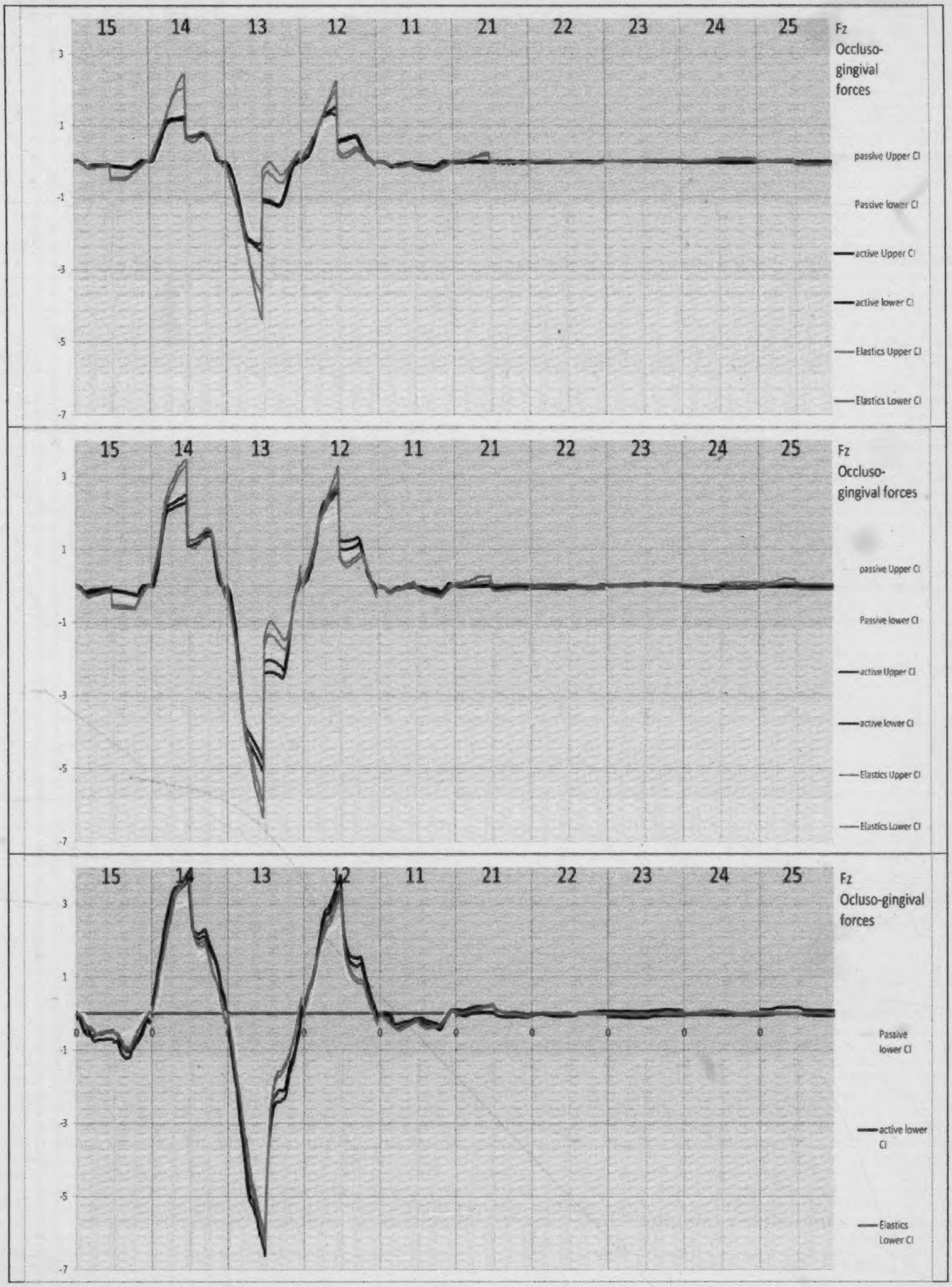

Figure 5-53: Standardized Fz graphs of 0.014”, 0.018”and 0.014”x 0.025” NiTi wires

5.9.4 The effect of the wire size and dimension on Mx

On examining the Mx graphs in Figure 5-55, we notice that there is not much difference in the Mx moments between the three wires except on teeth #13, 14 and 15. The maximum Mx moment for tooth #13 was highest for 0.018”wire and lowest for 0.014”wire, with the 0.014”x 0.025” wire producing slightly less moment than the 0.018”wire.

For teeth # 14 and 15 there was no difference in the Mx moments between the 0.014”and 0.018”wires, however the 0.014”x 0.025” wire applied a much higher Mx moment on those two teeth. This could be caused by torsion of the wire which develops as the cuspid is deflected, this torsion would apply a buccal crown torque on the 14 and a lingual crown torque on the 15.

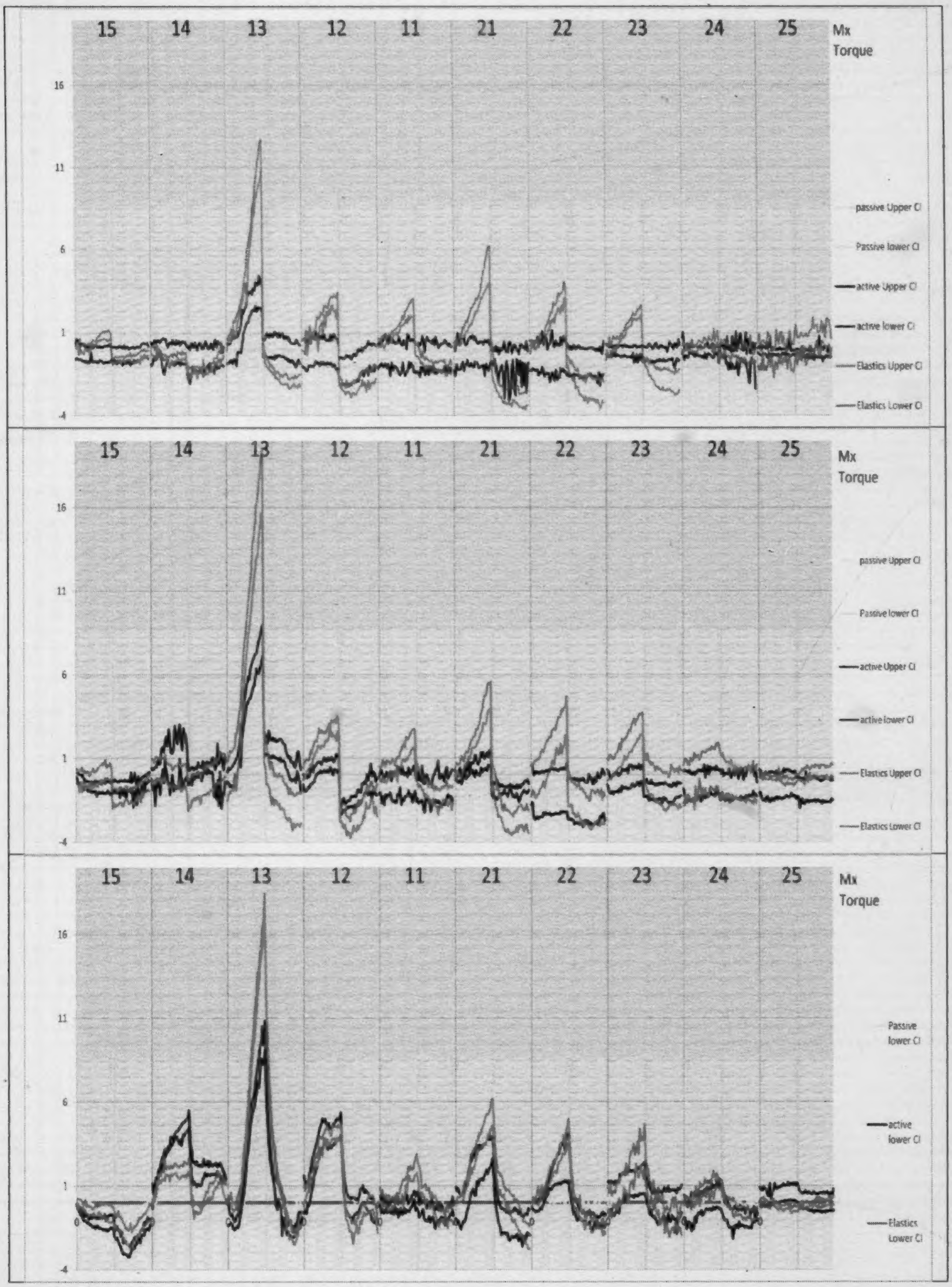

Figure 5-54: Standardized Mx graphs of 0.014, 0.018”and 0.014”x 0.025” NiTi wires

5.9.5 The effect of the wire size and dimension on My

On examining the My graphs in Figure 5-56, we notice that the My moments increase as we move from 0.014”wire to 0.018”wire, however those My moments tend to decrease from the 0.018” levels as we move to the 0.014”x 0.025” wire. This can be explained by the fact that those My moments are partially caused by Fz forces acting on the 12 and 14, and we saw earlier that the Fz forces of the 0.018”and 0.014”x 0.025” were not dissimilar.

The most interesting observation here is the fact that the ASL brackets apply similar My moments to those of EL with the 0.014”and 0.018”wires and applied much higher My moments than PSL or EL with 0.014” x 0.025” wire. PSL brackets applied the lowest amount of My moments with the three wire types.

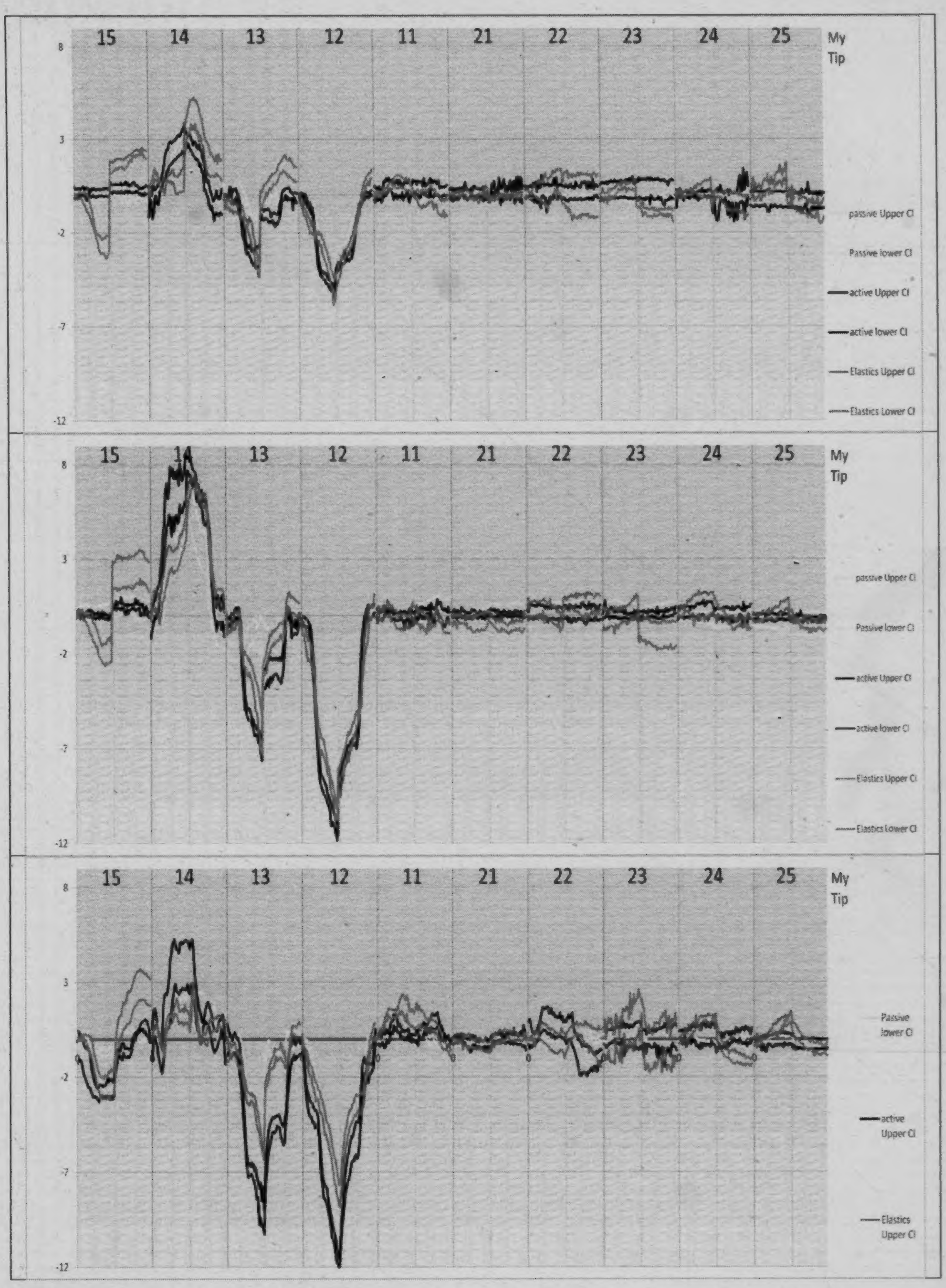

Figure 5-55: Standardized My graphs of 0.014", 018" and 0.014"x 0.025" NiTi wires

5.9.6 The effect of the wire size and dimension on Mz:

On examining the Mz graphs in Figure 5-57, we notice little difference between the three types of wires.

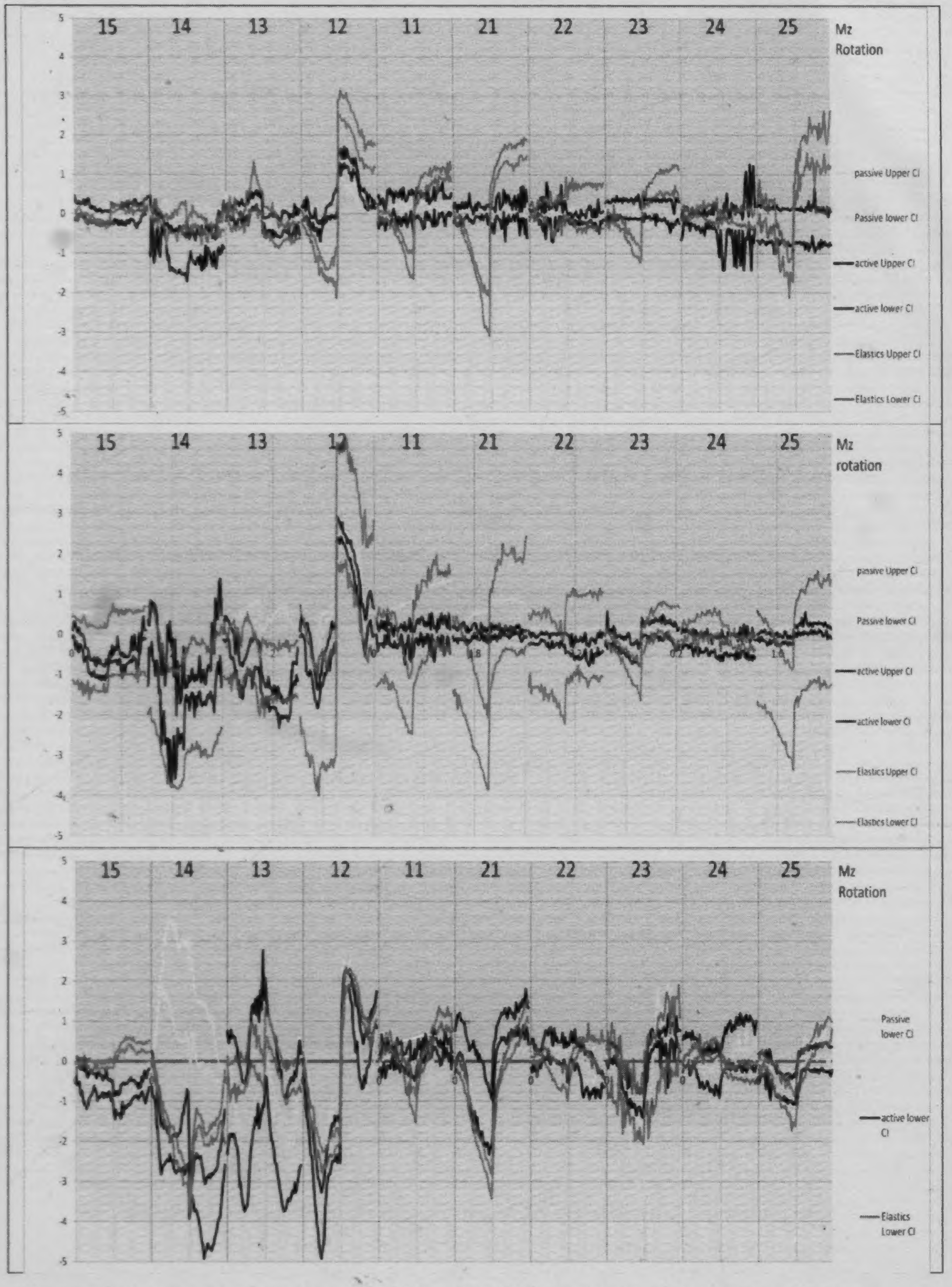

Figure 5-56: Standardized Mz graphs of 0.014", 0.018"and 0.014"x 0.025" NiTi wires

5.10Conclusion

When 0.014" wire was tested it was noticed that the active ligation bracket system produces a remarkably similar force system to that of the passive self-ligation bracket system. As wire dimension is increased from to 0.018"to 0.014"× 0.025" we notice that the difference between the two types of self-ligation becomes more pronounced. In the absence of statistical testing it is very difficult to draw concrete conclusions from this type of dataset, a blinded qualitative assessment of the different aspects of the force systems might be necessary. One way to do so is to have the forces systems qualitatively assessed and rated by a group of orthodontists.

We tried to simulate as closely as possible the oral environment, however elastomeric force decay ([135,136]) is bound to have some effect on the force system, it would be an interesting test to induce force decay and age the elastomeric ties prior to using them and assess how that would affect the resultant force system. The elastomeric ties in this experiment were not changed during the simulated tooth movement, in future studies we will replicate this test but change the elastomeric ties every 1mm of cuspid movement.

We studied the loading and unloading forces applied on the teeth using the three different ligation methods, however it would be interesting to reproduce the same experiment starting from the displaced position, and gather the data of the unloading curves only, this might produce a substantially different force system especially where friction is more pronounced.

When considering the overall force system generated in the high cuspid simulation, we can conclude that based on this in vitro measurements, the passive self-ligation method produced a force system with less unwanted forces and moments. Based on those findings, we might not be able to make definite predictions on the effect of these differences on the actual tooth movement that subsequently takes place. However, it is safe to conclude that different force systems produce different types of tooth movement.

6 Chapter six: Discussion

Orthodontic biomechanics is central to the development of the discipline of orthodontics, however, ironically it is one of the least understood. The study of the biophysics of tooth movement can yield important information, if researchers and clinicians can quantify the force systems applied to the teeth, they can better understand clinical and histologic responses. Therefore, in order to make valid judgments about the tooth response to orthodontic forces, clinicians must first define fully the force systems acting on the teeth.

Orthodontic force systems resulting from contemporary orthodontic applications using full fixed appliances are considered indeterminate, in other words, impossible to analyze and predict. The introduction of the continuous arch technique and the application of new superelastic alloys resulted in force systems that are so complex; we are still to date incapable of modeling or even estimating their components, even with the support of the most powerful computer systems. Developments in the study of orthodontic force systems have been lagging compared to other fields of orthodontic research, partly due to the technical difficulty and financial requirements of such research. Until recently, most of the orthodontic biomechanics literature was restricted to force measurements made on one or two tooth models and to three-dimensional computer modeling where too many assumptions are made, and to material tests in the form of friction studies. Clinicians are not generally interested in knowing the coefficient of friction for a specific type of wire when used with a specific type of bracket, nor are they interested in knowing how much of the resistance to sliding is resulting from friction versus binding. 2D biomechanics studies do not help clinicians in making valid clinical judgments, clinicians need to know the three dimensional forces being applied on the dentition when specific combinations of bracket, wire and ligation method are used in a certain type of malocclusion.

Very little evidence exists in the literature regarding three dimensional experimental measurements and analysis of orthodontic force systems ([2,127,128,129,130,131,132,133]). A large number of variables in orthodontic treatment are not within our control, such as growth and tissue response to appliances, however, the force placed on the tooth should be a controllable variable ([1]), and careful study of the physics underlying our clinical applications, can help is reducing undesirable side effects. Previous studies have attempted to simulate malocclusions ([137]), however we present the most comprehensive method of assessing the orthodontic force system.

In order for us to understand the orthodontic force systems, we need to perform 3D measurements of the forces being applied on every tooth in the dental arch simultaneously. The sensors used for those measurements, must therefore be of small size that can be attached to all teeth in a simulated dental arch. With the very recent technological advances in force/torque sensors technology, data acquisition and data representation using computer graphics, it became possible to measure those forces and reveal the force systems we are applying to the dentition. Three-dimensional force and moment measurement technology is commercially available but not in tooth size dimensions. These 3D sensors are called multi-axis force transducers. Using such sensors in orthodontic research requires complicated engineering designs, micro-machining and specialized software development.

The purpose of this research is to build and validate a laboratory based human mouth model capable of measuring forces and moments in three dimensions on all fourteen teeth in the dental arch simultaneously and in real-time, when orthodontic fixed appliances are used and during simulated tooth movements. We were successful in building this model, which will allow us, for the first time in the history of our profession to determine with high degree of accuracy, the forces acting on orthodontically treated teeth. This research is the first step of a long journey to study the orthodontic force systems, its propagation, and its transformation from one tooth to another along the archwire and its variations in response to changing variables, such as ligation methods and wire types.

6.1 The challenges faced during the development the Orthodontic Simulator (OSIM)

We designed and constructed a torque measurement device (described in chapter 2), which employs a multi-axis force transducer. The torque device was used to measure torque expression of self-ligating brackets. Carrying out this pilot project was necessary in order to understand the complex task of three-dimensional force and moment measurements. Choosing the right force sensor is central to the success of this project, there is a number of commercially available force and moment sensors, some of our requirements were durability, small size, accuracy and precision. The sensor's range of measurable loads needed to be within orthodontic force levels (up to 5N). The range of measurable moments needed to be much higher than what would be applied orthodontically, this is because the sensors would need special connectors to attach them to the teeth, and these connectors create large moments. ATI automation manufactures the smallest multi-axis force transducer, the Nano 17®, this sensor is 17 millimeters in diameter.

Acquiring three-dimensional data from one load-cell is a complex process. Moreover, the challenge was to acquire three-dimensional data from 14 force sensors, simultaneously. Each load-cell has six channels that provide six voltages that are converted to the six force and moment components of the force system. Real-time data for the 84 components of the 14 teeth needed to be acquired. To do so we used a very fast data acquisition card. However, we could not find a data acquisition card that accommodates this number of channels, our solution to this problem is to use an interface device called a multiplexer. This multiplexer acts as a medium through which this large amount of data can be relayed to the data acquisition device, by scanning the 84 channels and providing the data acquisition card with one reading from one channel at a time. This process can slow down the rate of data gathering, which is why we used a very fast data acquisition card to compensate for this slow down caused by the use of the multiplexer. The multiplexer and the data acquisition card are controlled by the LabView program.

Once the data is acquired in LabView, we needed to present it in some meaningful form. Gathering a single dataset from the 14 load-cells produces a 6 × 14 table. Real-time data gathering can produce an infinite number of those matrices with a huge amount of data. Our solution to this problem is to develop custom-made orthodontic force visualization software (the OSIM software package). This software was developed in Matlab programming environment. The main purpose of the OSIM software is to handle the large amount of data produced by the OSIM device and visually represent the force system data in 3D. The OSIM software visualization package is very useful for presenting the data in electronic visual display, more work needs to be done in order to develop a data presentation method that can be used for print publications.

The force sensors were 17mm in diameter, this meant that in order to use those sensors and attach them to every tooth in the dental arch, we had to arrange the sensors on an arch much wider than that of the dental archform. This meant that we had to create a special connector for each tooth in order to attach it to its corresponding sensor. With this arrangement, the load applied on the tooth is being measured in the load-cell at some distance from the tooth. When the load is being measured at a point other than the point of application, transformation of the force system is necessary in order quantify the force system at the point of application. This presented the most significant challenge for the OSIM application, especially when we consider the large amount of data that needed to be transformed. In order to conduct the transformations we needed to measure, with high degree of accuracy, the three dimensional positions of the teeth in relation to their corresponding sensors. We used a highly accurate coordinate measurement machine for those measurements.

We assessed the error in the OSIM system, the errors result from measurement errors of the load-cells, measurement errors of the coordinate measurement machine and the moment error magnification caused by the moment arm of the tooth connectors. As expected the force measurements are very accurate. Errors in moments were in contrast much higher, this is caused by the connectors which act as moment arms, which in turn magnify the errors in the moment measurements. We anticipated this increased moment error and there was very little that can be done about it. There are however two possible future solutions that can be used to reduce those moment errors; using smaller load-cells can help reduce the size of the tooth connector, which in turn can reduce the size of the moment arm, or redesigning the tooth connectors to position the loadcells closer to the teeth. However currently, the Nano 17 is the smallest commercially available multi-axis load-cell. Another solution to this problem can be to calibrate the Nano17 with the connector arm attached. The calibration process is proprietary information that the load-cell supplier is not willing to share. For the time being larger moment errors than force errors are accepted as one limitation to this OSIM device.

6.2 High upper cuspid simulation

Orthodontic knowledge in the field of clinical biomechanics has traditionally been derived from a number of studies that can be categorized in two major types: mechanical testing of orthodontic appliances, which utilizes a few mechanical testing techniques to study specific aspects of orthodontic biomechanics, and computer modeling and finite element analysis (FEA).

Friction has been studied using mechanical testing in a number of ways, in some instances the wires were pulled through one or more brackets (92,99,99,100,138,139,140,141,142,143) in other instances a bracket was slid on a wire (95,113,144,145,146). There is no doubt that friction plays a significant role in orthodontic force systems, as does binding, however distinguishing the effects and importance of one versus the other is a theoretical discussion at best. The sum of friction and binding constitutes what is called resistance to sliding. Resistance to sliding is more clinically relevant but a much more difficult phenomenon to study in a laboratory setup, since it is directly influenced by the ligation method, bracket type, archwire material, and relative positions of the brackets among many other factors.

Orthodontic wires were studied in a number of ways as well (147,148,149,150). Three-point bending was and is still the universally accepted test for orthodontic wires, although it does not incorporate an orthodontic bracket or a ligation method and it is performed on straight sections of the wires. This limits the translation of the test results into clinically useful conclusions, since the tests are usually simplified and designed to look at only one or two variables related to the wires tested. The three-point bend test does produce important information regarding the wire characteristics, however, this information is not clinically relevant in the absence of knowledge about the wire characteristics given a specific bracket/wire interface, and in the presence of an archform. The bracket-wire interface varies significantly according to the ligation mechanism used. Elastomeric ties, stainless steel ligature ties, active self-ligation and passive self-ligation brackets, each might produce distinctly different force systems, all other variables being equal. Interbracket distance is another variable not accounted for when discussing wire properties. Santoro *et. al.* ([52,53]) presented an elaborate two-part review of orthodontic wires, they said:

> *"The cantilever-type test is, at present, the standard, ADA-approved method of testing the mechanical properties of alloy, according to ADA specification number 32. It must be taken into consideration, however, that a single direction deformation induced by unilateral bending tests (including tensile, 1-point, or even 3-point cantilever bending models) ...do not take into consideration the loading effect of the friction generated by the ligatures and are therefore unable to properly reproduce the clinical constraint of the wire in the bracket slot"*

The second area of orthodontic biomechanics research is computer modeling and the use of finite element analysis (FEA). The fast development of computer technologies made it possible for mechanical tests to be simulated instead of performing the actual tests ([151,152,153,154,155]). However in order to accurately perform such simulations, detailed understanding of the components of the object being tested is necessary, and equally important is the way with which those different components interact. The most sophisticated computer modeling and simulation is by definition an approximation to reality, keeping the assumptions in a model to minimum improves its predictions and simulations. The way with which the bracket and the wire interact in varying clinical applications is largely unknown, especially when we consider continuous arch fixed appliance applications. Orthodontic biomechanical force systems with more than two points of applications are considered statically indeterminate, in other words they cannot be theoretically analyzed or directly solved from force balance. We need to measure forces in three dimensions in as many clinical situations as possible, in order to build enough knowledge, and then use this knowledge to construct a robust computer model based on actual experimental studies instead of one that involves many assumptions.

Santoro *et. al.* (52,53) go on to say in their two-part review of orthodontic wires:

> *"To obtain reliable and valuable data, researchers must design experimental models that simulate as closely as possible the orthodontic intraoral clinical setting. The method of ligation of the wire to the brackets should be consistent. The interbracket distance, type of bracket used, and length of the wire specimen should be consistent as well. The results obtained in a laboratory should ultimately be compared with the results of analogous clinical trials"*

For the first time in the history of orthodontics, we have a device that is capable of replicating specific malocclusions and simultaneously producing detailed three-dimensional information regarding orthodontic forces applied on all the teeth in a dental arch. We will use this setup for orthodontic biomechanics testing and orthodontic material testing. We can now substitute the three point bending test with this more accurate method. We began by testing initial aligning wires used on anterior crowding situations.

In our experiment we simulated one of the most common clinical problems, vertical crowding of upper cuspids. The OSIM was set up to simulate the alignment of a high upper right cuspid using three different alignment Nickel

Titanium superelastic heat activated wires. This experiment was repeated three times, using the three different ligation methods, passive ligation, active ligation and conventional elastic ligation. We gathered force system data on all teeth during loading and unloading without untying the wires during the experiment. Our data suggests that none of the three ligation methods produced the ideal force system for this specific malocclusion. However, we noticed that passive self-ligation produced the least unwanted components of the force systems.

Force propagation is the transfer of forces from the teeth adjacent to the displaced tooth to the rest of the teeth in the dental arch during loading and unloading. Force propagation was noticed with all components of the force systems and all ligation methods and wires. However, it was more prominent with conventional ligation and least prominent with passive ligation. Ideally, the only teeth that should experience forces and moments are the displaced tooth and the teeth mesial and distal to it, therefore force propagation is considered a side effect of the force system. The mesiodistal force propagation, which is essentially resistance to archwire sliding, was most prominent for conventional ligation as it was detected on all the teeth including the premolars on the left side of the dental arch, which are distant from the displaced right cuspid. This pattern was seen to a lesser degree with active ligation. With passive self-ligation the mesiodistal forces were recorded on the cuspid and the teeth mesial and distal to it, there was relatively less mesiodistal forces recorded on the rest of the teeth especially with smaller wires.

Force propagation of the buccoligual forces was the most significant of all components, and it followed the same pattern of being most prominent with conventional ligation and least prominent with passive ligation. Force propagation of the vertical forces was less significant than the other components, it still existed past the teeth adjacent to the displaced tooth but to a lesser extent. Load-deflection curves, characteristic of super elastic NiTi wires, were affected by the ligation method, however it seemed that self-ligation had the least effect on those load-deflection curves. Propagation of moments along the archwire to distant teeth was less significant than that of forces. Moments were highest on the displaced tooth and the teeth mesial and distal to it.

On examining our data, we notice that on the reversal point (the point where we stop loading the wire and start unloading it) the force system showed a more immediate change with passive self-ligation than the gradual change of conventional ligation and to a lesser degree of active ligation. This is caused by the resilience of the elastic and active ligation methods.

The main difference between the three types of ligation methods is the friction they produce. Theoretically, Elastic ligation produces the highest friction and passive ligation produces the lowest friction. It is expected to see some differences in the forces and moments generated as a result of this friction, however it was surprising to see the magnitude of those differences especially on the buccolingual forces (Fy). Therefore, we will try to theoretically analyze the development of the resistance to archwire sliding and try to understand its effects in view of the gathered data.

Friction opposes archwire sliding ([140]). The term sliding mechanics has been used to describe the type of orthodontic mechanotherapy that relies on sliding teeth to close spaces or reduce overjet. The term sliding mechanics however is too broad, archwire sliding occurs during every stage of orthodontic treatment. A significant amount of sliding occurs during the initial alignment stage of tooth movement, hence the emergency appointments to cut an archwire that is too long distal of the terminal bracket.

The following is a hypothetical example (Figure 6-1); an initial aligning archwire exerts a certain force (F) to move the displaced middle bracket into alignment. In order for force (F) to move the middle bracket, one of two things should happen:

(a) The archwire will have to slide through the brackets on either side or

(b) If the wire is not free to slide, the two brackets on either side of the displaced bracket will have to move away from it. From a clinical point of view, it is preferable for the wire to be able to slide through the brackets mesial and distal to the misaligned tooth in this example. In order for the wire to slide, a force Fr should act along the long axis of the wire, pushing it laterally through the brackets on each side. Further study and analysis of this Fr is required in order to understand the mechanics of orthodontic tooth alignment.

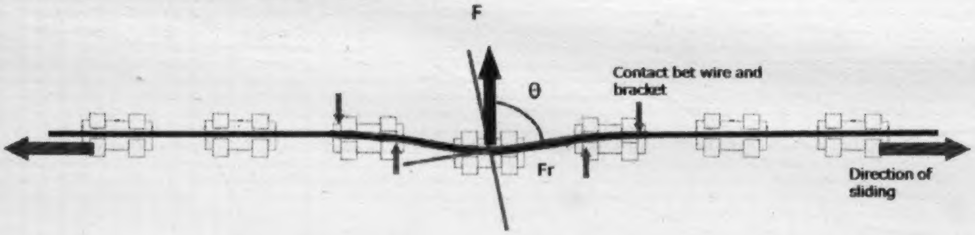

Figure 6-1: Example of five brackets, the middle bracket is out of alignment, aligning force F

When archwire drawing forces are taken into account ([92,104]) a small sliding force is unlikely to overcome the resistance to sliding produced by the ligating mechanism. However, based on what we see in clinical settings, we can assume that in the initial aligning stages, archwire sliding takes place regardless of the type of ligation method, however this sliding is likely to encounter less resistance with low friction mechanics as opposed to high friction mechanics. In our study, we found that high friction mechanics produce a distinctly different force system, which might produce different tooth movements.

As we already know, the ligation mechanism is not the only source of resistance to sliding. Contact between the wire and the bracket's slot walls produces friction, which is known as binding in orthodontics. However, contact between the wire and the bracket is significant in two situations: first, Teeth mesial and distal to a displaced tooth, which was discussed earlier. Second, when a tooth is sliding along an archwire, let us consider the following example (Figure 6-3 a) to elaborate on the second situation. A cuspid is being retracted along an archwire. More often than not, the retracting force is applied to the bracket at a distance from the center of resistance of the cuspid, therefore, the initial cuspid movement is tipping until the bracket slot walls contact the archwire. Further retraction of the cuspid will be resisted by (a) the ligation method (b) friction between the bracket slot walls and the archwire. Now let us consider Figure 6-3b, the wire will have to slide through a number of brackets, the axial angulations of the teeth are not being altered as no forces are being applied to those teeth, therefore, no tooth tipping takes place, and the bracket walls are not actively pushed against the surface of the wire. Therefore, in this example the friction of the ligation mechanism is the only source of the resistance to sliding. Situations similar to Figure 6-3a usually involve sliding of a single tooth along an archwire such as cuspid retraction, or on brackets mesial and distal to a displaced tooth. Situations similar to Figure 6-3b involve initial alignment and overjet correction where the archwire is pushed through the brackets by either the aligning forces (Fr) or the retraction forces. We believe that when studying friction and binding, there should be distinction between a tooth sliding along an archwire and a wire sliding through multiple brackets.

Bracket/archwire contact during cuspid retraction

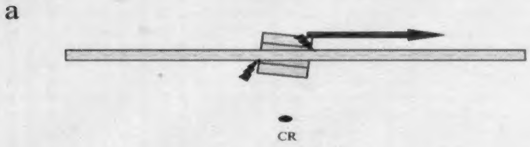

Bracket/archwire contact during initial alignment

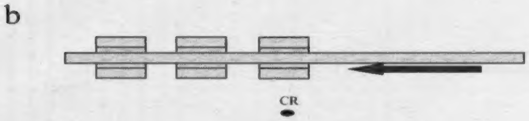

Figure 6-2: two types of sliding in orthodontics

It seems logical that low friction is preferable to high friction, we conclude that the effect of an increase in the resistance to sliding goes beyond the potential to slow down tooth movement, which is debatable, as we still see tooth movement and archwire sliding even with high friction mechanics (elastic ligation). This is most likely facilitated by intra-oral vibrations that negate this resistance to sliding. Based on our preliminary study and subject to confirmation through more follow-up studies it seems that the introduction of resistance to sliding can profoundly alter the orthodontic force system. We saw earlier that the increased resistance to sliding tends to propagate and carry on throughout the dental arch, and surprisingly causes profound changes to the buccolingual force patterns in the absence of bucco-lingual tooth displacements. Moreover, it can produce some effects on the moments generated.

Orthodontists recognize that the ideal force system is not possible, however they strive to design their mechanics in a way that would produce the required forces while minimizing the unwanted forces. It seems that all other factors being equal, higher friction is a disadvantage, it is hard to assess the loss of clinical performance that arises from a certain level of increased friction. It is logical however to conclude that lower friction produces less resistance to sliding, and therefore produces less unwanted forces and moments, and higher friction is more likely to produce unwanted forces and moments.

6.3 Future research

The development of the current OSIM is far from complete. A number of modifications are required to improve this method. Our objective was not to accurately simulate the oral environment and control for all possible variables, which include moisture, lip pressures, tongue pressures, PDL compliance, pressure distribution within the PDL, alveolar bone level and geometry, and a multitude of individual biological variations. Our objective was to understand the biomechanical force system at the bracket/wire interface.

6.3.1 PDL compliance simulation:

It is recognized that the PDL compliance causes minor movements within the bracket/wire interface and can play a role in determining the resultant force system. However, PDL simulation is a complicated process due to the wide variation of data in literature ([18,156,157,158]). In the future, we plan to use an elastomeric material or oil immersed leather as an interface between the brackets and the load cells to simulate the visco-elastic properties of the PDL. The connectors on our device already have a small amount of compliance. We plan to measure the compliance of new redesigned tooth connectors and determine how much more need to be added to approximate the true PDL compliance. The fact that the PDL compliance is non-linear and the fact that it is higher in the buccolingual direction than the mesiodistal direction complicate this further.

6.3.2 Horizontal connector modification:

In the current OSIM setup, modifying the horizontal micrometer reading produces buccoligual and mesiodistal positional changes concurrently; this is due to the orientation of the horizontal micrometer relative to the dental arch. Ideally, we would like to have a set up where the horizontal micrometer is perpendicular to a tangent of the dental arch, this allows the horizontal micrometer changes to produce buccoligual changes only. In order to do so we will need to reengineer the horizontal tooth connectors and incorporate a horizontal offset to allow perpendicular orientation of the micrometers to the archform. This horizontal offset will cause interferences between the connectors, therefore vertical offsets will be necessary to avoid those interferences. In the new designs, we will try to position the loadcells in closer proximity to the point of application in order to reduce the moment errors in the OSIM.

6.3.3 Motorizing the micrometers:

The OSIM contains 28 micrometers (14 vertical and 14 horizontal). Changing the positions of the teeth is a manual process therefore real-time data gathering (gathering force system data during tooth movement) is only possible if one or two teeth are being moved. Moreover, discrete data gathering (gathering force system data between incremental tooth movements) is very labor intensive depending on the number of teeth being moved. Replacing the current manual micrometers with motor driven micrometers can solve this problem. The OSIM software package and LabView can be used to control the micrometers.

This development provides the potentially promising feature of a continuous feedback setup of the OSIM, where the OSIM software can change the positions of the teeth according to the forces acting on those teeth. In addition, it provides the means of simulating complex malocclusions where multiple tooth movements occur. We will soon begin the OSIM modifications discussed above, starting with reengineering the tooth connectors and motorizing the micrometers.

6.3.4 Future experiments:

The high cuspid simulation experiment was conducted to begin to understand the force system produced during loading and unloading. However, in order to completely understand this force system we will need to replicate this experiment and change a few variables, I present a few potential experiments:

- Using the OSIM to record the force system during unloading only can provide more insight into what clinically takes place. In a clinical situation the wire is ligated to the teeth in one of those possible methods:
    - The teeth are ligated starting from the anterior teeth (central incisors) proceeding to the posterior teeth in sequence
    - The teeth are ligated starting from the anterior teeth (central incisors) proceeding to the posterior teeth but skipping the cuspid which is ligated at the end.

Those two methods of ligation can conceivably produce different force systems depending on the ligation method used. The OSIM can be used to test this hypothesis.

- Use the OSIM to record the force system during unloading, while untying the ligation method and retying it at 1mm increments, to simulate archwire change appointments
- Use the OSIM to record the force system during unloading, with aged elastomeric ties, to assess whether elastomeric force decay affects the force system.
- Use the OSIM to record the force system during unloading and apply vibrations on the teeth to simulate perturbations caused by occlusal forces and tooth brushing. An electric toothbrush applied to the brackets between the incremental tooth movements can be used to simulate those perturbations.

7 Reference List

(1) Burstone CJ, Marcotte MR. Problem solving in orthodontics goal-oriented treatment strategies. Chicago: Quintessence Pub. Co; 2000.

(2) Smith RJ, Burstone CJ. Mechanics of tooth movement. Am J Orthod. 1984;85:294-307.

(3) Burstone CJ, Koenig HA. Force systems from an ideal arch. Am J Orthod. 1974;65:270-289.

(4) Burstone CJ, Pryputniewicz RJ, Bowley WW. Holographic measurement of tooth mobility in three dimensions. J Periodontal Res. 1978;13:283-94.

(5) Burstone CJ, Pryputniewicz RJ. Holographic determination of centers of rotation produced by orthodontic forces. Am J Orthod. 1980;77:396-409.

(6) Burstone, C. J., Pryputniewicz, R. J., and Weeks, R. centers of resistance of the human mandibular molars. J.Dent.Res. 60, 515. 1981.

(7) Christiansen RL, Burstone CJ. Centers of rotation within the periodontal space. Am J Orthod. 1969;55:353-69.

(8) Tanne K, Burstone CJ, Sakuda M. Biomechanical responses of tooth associated with different root lengths and alveolar bone heights: changes of stress distributions in the PDL. J Osaka Univ Dent Sch. 1989;29:17-24.

(9) Braun S, Winzler J, Johnson BE. An analysis of orthodontic force systems applied to the dentition with diminished alveolar support. Eur J Orthod. 1993;15:73-77.

(10) Cobo J, Arguelles J, Puente M, Vijande M. Dentoalveolar stress from bodily tooth movement at different levels of bone loss. Am J Orthod Dentofacial Orthop. 1996;110:256-62.

(11) Kusy RP, Tulloch JF. Analysis of moment/force ratios in the mechanics of tooth movement. Am J Orthod Dentofacial Orthop. 1986;90:127-31.

(12) Nagerl H, Burstone CJ, Becker B, Kubein-Messenburg D. Centers of rotation with transverse forces: an experimental study. Am J Orthod Dentofacial Orthop. 1991;99:337-45.

(13) Yoshida N, Jost-Brinkmann PG, Koga Y, Mimaki N, Kobayashi K. Experimental evaluation of initial tooth displacement, center of resistance, and center of rotation under the influence of an orthodontic force. Am J Orthod Dentofacial Orthop. 2001;120:190-197.

(14) Graber TM, Vanarsdall RL. Orthodontics
current principles and techniques, Application of Bioengineering to Clinical Orthodontics. 3rd ed ed. St. Louis: Mosby; 2000: 259-92.

(15) Proffit WR, Fields HW. Contemporary orthodontics. 3rd ed ed. St. Louis: Mosby; 2000.

(16) Lindauer SJ, Isaacson RJ. One-couple orthodontic appliance systems. Semin Orthod. 1995;1:12-24.

(17) Pryputniewicz RJ, Burstone CJ. The effect of time and force magnitude on orthodontic tooth movement. J Dent Res. 1979;58:1754-64.

(18) van Driel WD, van Leeuwen EJ, Von den Hoff JW, Maltha JC, Kuijpers-Jagtman AM. Time-dependent mechanical behaviour of the periodontal ligament. Proc Inst Mech Eng [H]. 2000;214:497-504.

(19) Iwasaki LR, Haack JE, Nickel JC, Morton J. Human tooth movement in response to continuous stress of low magnitude. Am J Orthod Dentofacial Orthop. 2000;117:175-83.

(20) Quinn RS, Yoshikawa DK. A reassessment of force magnitude in orthodontics. Am J Orthod. 1985;88:252-60.

(21) King GJ, Keeling SD, McCoy EA, Ward TH. Measuring dental drift and orthodontic tooth movement in response to various initial forces in adult rats. Am J Orthod Dentofacial Orthop. 1991;99:456-65.

(22) Pilon JJ, Kuijpers-Jagtman AM, Maltha JC. Magnitude of orthodontic forces and rate of bodily tooth movement. An experimental study. Am J Orthod Dentofacial Orthop. 1996;110:16-23.

(23) Konoo T, Kim YJ, Gu GM, King GJ. Intermittent force in orthodontic tooth movement. J Dent Res. 2001;80:457-60.

(24) Baumrind S. A reconsideration of the propriety of the "pressure-tension" hypothesis. Am J Orthod. 1969;55:12-22.

(25) Sandy JR. Tooth eruption and orthodontic movement. Br Dent J. 1992;172:141-49.

(26) Tanne K, Yoshida S, Kawata T, Sasaki A, Knox J, Jones ML. An evaluation of the biomechanical response of the tooth and

periodontium to orthodontic forces in adolescent and adult subjects. Br J Orthod. 1998;25:109-15.

(27) Lee BW. The force requirements for tooth movement. Part III: The pressure hypothesis tested. Aust Orthod J. 1996;14:93-97.

(28) Lee BW. The force requirements for tooth movement, Part I: Tipping and bodily movement. Aust Orthod J. 1995;13:238-48.

(29) Fortin JM. Translation of premolars in the dog by controlling the moment-to-force ratio on the crown. Am J Orthod. 1971;59:541-51.

(30) Boester CH, Johnston LE. A clinical investigation of the concepts of differential and optimal force in canine retraction. Angle Orthod. 1974;44:113-19.

(31) Tanne K, Koenig HA, Burstone CJ, Sakuda M. Effect of moment to force ratios on stress patterns and levels in the PDL. J Osaka Univ Dent Sch. 1989;29:9-16.

(32) Middleton J, Jones ML, Wilson AN. Three-dimensional analysis of orthodontic tooth movement. J Biomed Eng. 1990;12:319-27.

(33) Yoshikawa DK. Biomechanical principles of tooth movement. Dent Clin North Am. 1981;25:19-26.

(34) Ren Y, Maltha JC, Kuijpers-Jagtman AM. Optimum force magnitude for orthodontic tooth movement: a systematic literature review. Angle Orthod. 2003;73:86-92.

(35) Koenig HA, Burstone CJ. Force systems from an ideal arch--large deflection considerations. Angle Orthod. 1989;59:11-16.

(36) Halazonetis DJ. Ideal arch force systems: a center-of-resistance perspective. Am J Orthod Dentofacial Orthop. 1998;114:256-64.

(37) Ronay F, Kleinert W, Melsen B, Burstone CJ. Force system developed by V bends in an elastic orthodontic wire. Am J Orthod Dentofacial Orthop. 1989;96:295-301.

(38) Burstone CJ, Koenig HA. Creative wire bending--the force system from step and V bends. Am J Orthod Dentofacial Orthop. 1988;93:59-67.

(39) Andrews LF. The straight-wire appliance. Explained and compared. J Clin Orthod. 1976;10:174-95.

(40) Creekmore TD. The new torqued appliance. J Clin Orthod. 1973;7:553-62.

(41) Andrews LF. The six keys to normal occlusion. Am J Orthod. 1972;62:296-309.

(42) Ricketts RM. Bioprogressive therapy as an answer to orthodontic needs. Part I. Am J Orthod. 1976;70:241-68.

(43) Hanson GH. The SPEED system: a report on the development of a new edgewise appliance. Am J Orthod. 1980;78:243-65.

(44) Alexander RG. The vari-simplex discipline. Part 1. Concept and appliance design. J Clin Orthod. 1983;17:380-392.

(45) McLaughlin RP, Bennett JC, Trevisi H. Systemized orthodontic treatment mechanics. London: Mosby; 2001.

(46) Andreasen GF, Brady PR. A use hypothesis for 55 Nitinol wire for orthodontics. Angle Orthod. 1972;42:172-77.

(47) Tonner RI, Waters NE. The characteristics of super-elastic Ni-Ti wires in three-point bending. Part II: Intra-batch variation. Eur J Orthod. 1994;16:421-25.

(48) Tonner RI, Waters NE. The characteristics of super-elastic Ni-Ti wires in three-point bending. Part I: The effect of temperature. Eur J Orthod. 1994;16:409-19.

(49) Segner D, Ibe D. Properties of superelastic wires and their relevance to orthodontic treatment. Eur J Orthod. 1995;17:395-402.

(50) Miura F, Mogi M, Ohura Y, Hamanaka H. The super-elastic property of the Japanese NiTi alloy wire for use in orthodontics. Am J Orthod Dentofacial Orthop. 1986;90:1-10.

(51) Miura F, Mogi M, Okamoto Y. New application of superelastic NiTi rectangular wire. J Clin Orthod. 1990;24:544-48.

(52) Santoro M, Nicolay OF, Cangialosi TJ. Pseudoelasticity and thermoelasticity of nickel-titanium alloys: a clinically oriented review. Part II: Deactivation forces. Am J Orthod Dentofacial Orthop. 2001;119:594-603.

(53) Santoro M, Nicolay OF, Cangialosi TJ. Pseudoelasticity and thermoelasticity of nickel-titanium alloys: a clinically oriented review. Part I: Temperature transitional ranges. Am J Orthod Dentofacial Orthop. 2001;119:587-93.

(54) Ricketts RM. The wisdom of the bioprogressive philosophy. Semin Orthod. 1998;4:201-9.

(55) Odegaard J, Meling T, Meling E. An evaluation of the torsional moments developed in orthodontic applications. An in vitro study. Am J Orthod Dentofacial Orthop. 1994;105:392-400.

(56) Meling TR, Odegaard J, Seqner D. On bracket slot height: a methodologic study. Am J Orthod Dentofacial Orthop. 1998;113:387-93.

(57) Meling TR, Odegaard J. On the variability of cross-sectional dimensions and torsional properties of rectangular nickel-titanium arch wires. Am J Orthod Dentofacial Orthop. 1998;113:546-57.

(58) Siatkowski RE. Loss of anterior torque control due to variations in bracket slot and archwire dimensions. J Clin Orthod. 1999;33:508-10.

(59) Hixson ME, Brantley WA, Pincsak JJ, Conover JP. Changes in bracket slot tolerance following recycling of direct-bond metallic orthodontic appliances. Am J Orthod. 1982;81:447-54.

(60) Sebanc J, Brantley WA, Pincsak JJ, Conover JP. Variability of effective root torque as a function of edge bevel on orthodontic arch wires. Am J Orthod. 1984;86:43-51.

(61) Meling TR, Odegaard J, Meling EO. On mechanical properties of square and rectangular stainless steel wires tested in torsion. Am J Orthod Dentofacial Orthop. 1997;111:310-320.

(62) Meling TR, Odegaard J. The effect of second-order couple on the application of torque. Am J Orthod Dentofacial Orthop. 1998;113:256-62.

(63) Flores DA, Choi LK, Caruso JM, Tomlinson JL, Scott GE, Jeiroudi MT. Deformation of metal brackets: a comparative study. Angle Orthod. 1994;64:283-90.

(64) Kapur R, Sinha PK, Nanda RS. Comparison of load transmission and bracket deformation between titanium and stainless steel brackets. Am J Orthod Dentofacial Orthop. 1999;116:275-78.

(65) Balut N, Klapper L, Sandrik J, Bowman D. Variations in bracket placement in the preadjusted orthodontic appliance. Am J Orthod Dentofacial Orthop. 1992;102:62-67.

(66) Germane N, Bentley BE, Jr., Isaacson RJ. Three biologic variables modifying faciolingual tooth angulation by straight-wire appliances. Am J Orthod Dentofacial Orthop. 1989;96:312-19.

(67) Miethke RR, Melsen B. Effect of variation in tooth morphology and bracket position on first and third order correction with preadjusted appliances. Am J Orthod Dentofacial Orthop. 1999;116:329-35.

(68) Levason JA. Simple controlled tooth movement with the Edgewise appliance. Br J Orthod. 1978;5:5-12.

(69) Lang RL, Sandrik JL, Klapper L. Rotation of rectangular wire in rectangular molar tubes. Part II. Pretorqued molar tubes. Am J Orthod. 1982;81:22-31.

(70) Burstone CJ, Koenig HA. Optimizing anterior and canine retraction. Am J Orthod. 1976;70:1-19.

(71) Mulligan TF. Common sense mechanics. J Clin Orthod. 1979;13:676-83.

(72) Isaacson RJ, Lindauer SJ, Rubenstein LK. Moments with the edgewise appliance: incisor torque control. Am J Orthod Dentofacial Orthop. 1993;103:428-38.

(73) Isaacson RJ, Rebellato J. Two-couple orthodontic appliance systems: torquing arches. Semin Orthod. 1995;1:31-36.

(74) Isacson RJ, Lindauer SJ, Conley P. Responses of 3-dimensional arch wires to vertical v-bends: comparisons with existing 2-dimensional data in the lateral view. Semin Orthod. 1995;1:57-63.

(75) Parkhouse RC. Rectangular wire and third-order torque: a new perspective. Am J Orthod Dentofacial Orthop. 1998;113:421-30.

(76) Schudy GF, Schudy FF. Intrabracket space and interbracket distance: critical factors in clinical orthodontics. Am J Orthod Dentofacial Orthop. 1989;96:281-94.

(77) Dellinger EL. A scientific assessment of the straight-wire appliance. Am J Orthod. 1978;73:290-299.

(78) Schwaninger B. Evaluation of the straight arch wire concept. Am J Orthod. 1978;74:188-96.

(79) Creekmore TD. Dr. Thomas D. Creekmore on torque. J Clin Orthod. 1979;13:305-10.

(80) Hocevar RA. Understanding, planning, and managing tooth movement: orthodontic force system theory. Am J Orthod. 1981;80:457-77.

(81) Hocevar RA. Why edgewise? A compendium of means to gentle resilient fixed appliances. Am J Orthod. 1981;80:237-55.

(82) Raphael E, Sandrik JL, Klapper L. Rotation of rectangular wire in rectangular molar tubes. Part I. Am J Orthod. 1981;80:136-44.

(83) McKnight MM, Jones SP, Davies EH. A study to compare the effects of simulated torquing forces on pre-adjusted orthodontic brackets. Br J Orthod. 1994;21:359-65.

(84) Taylor RM. Variation in form of human teeth. II. An anthropologic and forensic study of maxillary canines. J Dent Res. 1969;48:173-82.

(85) Taylor RM. Variation in form of human teeth: I. An anthropologic and forensic study of maxillary incisors. J Dent Res. 1969;48:5-16.

(86) Delivanis HP, Kuftinec MM. Variation in morphology of the maxillary central incisors found in class II, division 2 malocclusions. Am J Orthod. 1980;78:438-43.

(87) Bryant RM, Sadowsky PL, Hazelrig JB. Variability in three morphologic features of the permanent maxillary central incisor. Am J Orthod. 1984;86:25-32.

(88) Bjorndal AM, Henderson WG, Skidmore AE, Kellner FH. Anatomic measurements of human teeth extracted from males between the ages of 17 and 21 years. Oral Surg Oral Med Oral Pathol. 1974;38:791-803.

(89) Vardimon AD, Lambertz W. Statistical evaluation of torque angles in reference to straight-wire appliance (SWA) theories. Am J Orthod. 1986;89:56-66.

(90) Carlsson R, Ronnerman A. Crown-root angles of upper central incisors. Am J Orthod. 1973;64:147-54.

(91) Harradine NW. Self-ligating brackets: where are we now? J Orthod. 2003;30:262-73.

(92) Henao SP, Kusy RP. Evaluation of the frictional resistance of conventional and self-ligating bracket designs using standardized archwires and dental typodonts. Angle Orthodontist 74(2):202-11. 2004.

(93) Shivapuja PK, Berger J. A comparative study of conventional ligation and self-ligation bracket systems. Am J Orthod Dentofacial Orthop. 1994;106:472-80.

(94) Harradine NW. Self-ligating brackets and treatment efficiency. Clin Orthod Res. 2001;4:220-227.

(95) Thorstenson GA, Kusy RP. Resistance to sliding of self-ligating brackets versus conventional stainless steel twin brackets with second-order angulation in the dry and wet (saliva) states. American Journal of Orthodontics & Dentofacial Orthopedics 120(4):361-70. 2001.

(96) Thorstenson GA, Kusy RP. Comparison of resistance to sliding between different self-ligating brackets with second-order angulation in the dry and saliva states. Am J Orthod Dentofacial Orthop. 2002;121:472-82.

(97) Khambay B, Millett D, McHugh S. Evaluation of methods of archwire ligation on frictional resistance. Eur J Orthod. 2004;26:327-32.

(98) Khambay B, Millett D, McHugh S. Archwire seating forces produced by different ligation methods and their effect on frictional resistance. Eur J Orthod. 2005;27:302-8.

(99) Baccetti T, Franchi L. Friction produced by types of elastomeric ligatures in treatment mechanics with the preadjusted appliance. Angle Orthod. 2006;76:211-16.

(100) Chimenti C, Franchi L, Di Giuseppe MG, Lucci M. Friction of orthodontic elastomeric ligatures with different dimensions. Angle Orthodontist 75(3):421-5. 2005.

(101) Griffiths HS, Sherriff M, Ireland AJ. Resistance to sliding with 3 types of elastomeric modules. Am J Orthod Dentofacial Orthop. 2005;127:670-675.

(102) Thorstenson GA, Kusy RP. Effects of ligation type and method on the resistance to sliding of novel orthodontic brackets with second-order angulation in the dry and wet states. Angle Orthod. 2003;73:418-30.

(103) Thomas S, Sherriff M, Birnie D. A comparative in vitro study of the frictional characteristics of two types of self-ligating brackets and two types of pre-adjusted edgewise brackets tied with elastomeric ligatures. Eur J Orthod. 1998;20:589-96.

(104) Henao SP, Kusy RP. Frictional evaluations of dental typodont models using four self-ligating designs and a conventional design. Angle Orthod. 2005;75:75-85.

(105) Redlich M, Mayer Y, Harari D, Lewinstein I. In vitro study of frictional forces during sliding mechanics of "reduced-friction" brackets. Am J Orthod Dentofacial Orthop. 2003;124:69-73.

(106) Loftus BP, Artun J, Nicholls JI, Alonzo TA, Stoner JA. Evaluation of friction during sliding tooth movement in various bracket-arch wire combinations. Am J Orthod Dentofacial Orthop. 1999;116:336-45.

(107) Thorstenson GA, Kusy RP. Effect of archwire size and material on the resistance to sliding of self-ligating brackets with second-order angulation in the dry state. American Journal of Orthodontics & Dentofacial Orthopedics 122(3):295-305. 2002.

(108) Sayeh Ehsani. Frictional resistance in self-ligating orthodontic brackets and conventionally ligated brackets. American Journal of Orthodontics & Dentofacial Orthopedics 98(2):117-26. 2008.

(109) Braun S, Bluestein M, Moore BK, Benson G. Friction in perspective. Am J Orthod Dentofacial Orthop. 1999;115:619-27.

(110) O'Reilly D, Dowling PA, Lagerstrom L, Swartz ML. An ex-vivo investigation into the effect of bracket displacement on the resistance to sliding. Br J Orthod. 1999;26:219-27.

(111) Scott P, DiBiase AT, Sherriff M, Cobourne MT. Alignment efficiency of Damon3 self-ligating and conventional orthodontic bracket systems: a randomized clinical trial. Am J Orthod Dentofacial Orthop. 2008;134:470-478.

(112) Tecco S, Festa F, Caputi S, Traini T, Di Iorio D, D'Attilio M. Friction of conventional and self-ligating brackets using a 10 bracket model. Angle Orthod. 2005;75:1041-45.

(113) Hain M, Dhopatkar A, Rock P. The effect of ligation method on friction in sliding mechanics. American Journal of Orthodontics & Dentofacial Orthopedics 123(4):416-22. 2003.

(114) Read-Ward GE, Jones SP, Davies EH. A comparison of self-ligating and conventional orthodontic bracket systems. Br J Orthod. 1997;24:309-17.

(115) Pizzoni L, Ravnholt G, Melsen B. Frictional forces related to self-ligating brackets. Eur J Orthod. 1998;20:283-91.

(116) Sims AP, Waters NE, Birnie DJ, Pethybridge RJ. A comparison of the forces required to produce tooth movement in vitro using two self-ligating brackets and a pre-adjusted bracket employing two types of ligation. European Journal of Orthodontics 15(5):377-85. 1993.

(117) Gioka C, Eliades T. Materials-induced variation in the torque expression of preadjusted appliances. Am J Orthod Dentofacial Orthop. 2004;125:323-28.

(118) Thomas M.Graber, Robert L.Vanarsdall Jr. *Orthodontics: Current Principles and Techniques*. St. Louise, Missouri: Mosby, Inc; 2000.

(119) Tanne K, Nagataki T, Inoue Y, Sakuda M, Burstone CJ. Patterns of initial tooth displacements associated with various root lengths and alveolar bone heights. Am J Orthod Dentofacial Orthop. 1991;100:66-71.

(120) Tanne K, Sakuda M, Burstone CJ. Three-dimensional finite element analysis for stress in the periodontal tissue by orthodontic forces. Am J Orthod Dentofacial Orthop. 1987;92:499-505.

(121) Solonche DJ, Burstone CJ, Vanderby R, Jr. A device for determining the mechanical behavior of orthodontic appliances. IEEE Trans Biomed Eng. 1977;24:538-39.

(122) O'Higgins EA, Kirschen RH, Lee RT. The influence of maxillary incisor inclination on arch length. Br J Orthod. 1999;26:97-102.

(123) Gmyrek H, Bourauel C, Richter G, Harzer W. Torque capacity of metal and plastic brackets with reference to materials, application, technology and biomechanics. J Orofac Orthop. 2002;63:113-28.

(124) Reitan, K. some factors determining the evaluation of forces in orthodontics. Am.J.Orthod. 32-45. 1-1-1957.
Ref Type: Abstract

(125) Burstone CJ. The segmented arch approach to space closure. Am J Orthod. 1982;82:361-78.

(126) Cash AC, Good SA, Curtis RV, McDonald F. An evaluation of slot size in orthodontic brackets--are standards as expected? Angle Orthod. 2004;74:450-453.

(127) Menghi C, Planert J, Melsen B. 3-D experimental identification of force systems from orthodontic loops activated for first order corrections. Angle Orthod. 1999;69:49-57.

(128) Friedrich D, Rosarius N, Rau G, Diedrich P. Measuring system for in vivo recording of force systems in orthodontic treatment-concept and analysis of accuracy. J Biomech. 1999;32:81-85.

(129) Friedrich D, Rosarius N, Schwindke P, Rau G, Diedrich P. In vitro testing of a measuring system for in vivo recording of orthodontically applied forces and moments in the multiband technique. Part II. J Orofac Orthop. 1998;59:82-89.

(130) Kuo B, Takakuda K, Miyairi H. Development of an orthodontic simulator for measurement of orthodontic forces. J Med Dent Sci. 2001;48:15-21.

(131) Lapatki BG, Bartholomeyczik J, Ruther P, Jonas IE, Paul O. Smart bracket for multi-dimensional force and moment measurement. J Dent Res. 2007;86:73-78.

(132) Bourauel C, Drescher D, Thier M. An experimental apparatus for the simulation of three-dimensional movements in orthodontics. J Biomed Eng. 1992;14:371-78.

(133) Drescher D, Bourauel C, Thier M. Application of the orthodontic measurement and simulation system (OMSS) in orthodontics. Eur J Orthod. 1991;13:169-78.

(134) Felton JM, Sinclair PM, Jones DL, Alexander RG. A computerized analysis of the shape and stability of mandibular arch form. Am J Orthod Dentofacial Orthop. 1987;92:478-83.

(135) Eliades T, Eliades G, Silikas N, Watts DC. In vitro degradation of polyurethane orthodontic elastomeric modules. J Oral Rehabil. 2005;32:72-77.

(136) Taloumis LJ, Smith TM, Hondrum SO, Lorton L. Force decay and deformation of orthodontic elastomeric ligatures. Am J Orthod Dentofacial Orthop. 1997;111:1-11.

(137) Franchi L, Baccetti T. Forces released during alignment with a preadjusted appliance with different types of elastomeric ligatures. Am J Orthod Dentofacial Orthop. 2006;129:687-90.

(138) Rhee JN, Chun YS, Row J. A comparison between friction and frictionless mechanics with a new typodont simulation system. American Journal of Orthodontics & Dentofacial Orthopedics 119(3):292-9. 2001.

(139) Hain M, Dhopatkar A, Rock P. A comparison of different ligation methods on friction. Am J Orthod Dentofacial Orthop. 2006;130:666-70.

(140) Kusy RP, Whitley JQ. Friction between different wire-bracket configurations and materials. Semin Orthod. 1997;3:166-77.

(141) Clocheret K, Willems G, Carels C, Celis JP. Dynamic frictional behaviour of orthodontic archwires and brackets. European Journal of Orthodontics 26(2):163-70. 2004.

(142) Dickson JA, Jones SP, Davies EH. A comparison of the frictional characteristics of five initial alignment wires and stainless steel brackets at three bracket to wire angulations--an in vitro study. British Journal of Orthodontics 21(1):15-22. 1994.

(143) Downing A, McCabe J, Gordon P. A study of frictional forces between orthodontic brackets and archwires. British Journal of Orthodontics 21(4):349-57. 1994.

(144) Bednar JR, Gruendeman GW, Sandrik JL. A comparative study of frictional forces between orthodontic brackets and arch wires. Am J Orthod Dentofacial Orthop. 1991;100:513-22.

(145) Drescher D, Bourauel C, Schumacher HA. Frictional forces between bracket and arch wire. American Journal of Orthodontics & Dentofacial Orthopedics 96(5):397-404. 1989.

(146) Kapila S, Angolkar PV, Duncanson MG, Jr., Nanda RS. Evaluation of friction between edgewise stainless steel brackets and orthodontic wires of four alloys. American Journal of Orthodontics & Dentofacial Orthopedics 98(2):117-26. 1990.

(147) Gurgel JA, Kerr S, Powers JM, LeCrone V. Force-deflection properties of superelastic nickel-titanium archwires. Am J Orthod Dentofacial Orthop. 2001;120:378-82.

(148) Gurgel JA, Kerr S, Powers JM, Pinzan A. Torsional properties of commercial nickel-titanium wires during activation and deactivation. Am J Orthod Dentofacial Orthop. 2001;120:76-79.

(149) Hazel RJ, Rohan GJ, West VC. Force relaxation in orthodontic arch wires. Am J Orthod. 1984;86:396-402.

(150) Lundgren D, Owman-Moll P, Kurol J, Martensson B. Accuracy of orthodontic force and tooth movement measurements. Br J Orthod. 1996;23:241-48.

(151) Cattaneo PM, Dalstra M, Melsen B. The finite element method: a tool to study orthodontic tooth movement. Journal of Dental Research 84(5):428-33. 2005.

(152) Chang YI, Shin SJ, Baek SH. Three-dimensional finite element analysis in distal en masse movement of the maxillary dentition with the multiloop edgewise archwire. European Journal of Orthodontics 26(3):339-45. 2004.

(153) Clement R, Schneider J, Brambs HJ, Wunderlich A, Geiger M, Sander FG. Quasi-automatic 3D finite element model generation for individual single-rooted teeth and periodontal ligament. Computer Methods & Programs in Biomedicine 73(2):135-44. 2004.

(154) Dorow C, Sander FG. Development of a model for the simulation of orthodontic load on lower first premolars using the finite element method. Journal of Orofacial Orthopedics 66(3):208-18. 2005.

(155) Fotos PG, Spyrakos CC, Bernard DO. Orthodontic forces generated by a simulated archwire appliance evaluated by the finite element method. Angle Orthod. 1990;60:277-82.

(156) Dorow C, Krstin N, Sander FG. Experiments to determine the material properties of the periodontal ligament. J Orofac Orthop. 2002;63:94-104.

(157) McGuinness NJ, Wilson AN, Jones ML, Middleton J. A stress analysis of the periodontal ligament under various orthodontic loadings. Eur J Orthod. 1991;13:231-42.

(158) Cronau M, Ihlow D, Kubein-Meesenburg D, Fanghanel J, Dathe H, Nagerl H. Biomechanical features of the periodontium: an experimental pilot study in vivo. Am J Orthod Dentofacial Orthop. 2006;129:599-21.

8 Appendix

8.1 OSIM 0.014" Display

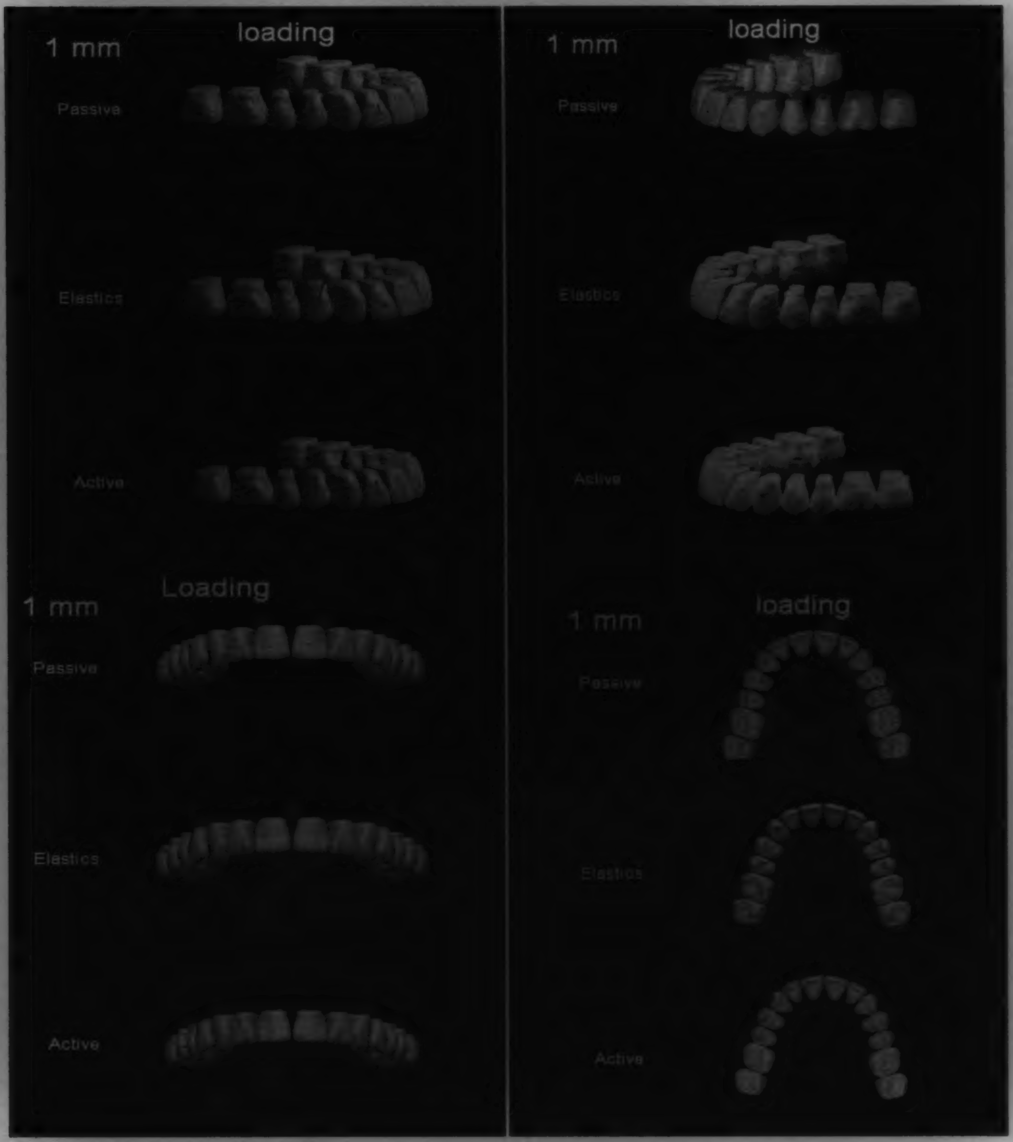

Figure 8-1: 0.014" 1mm loading OSIM display

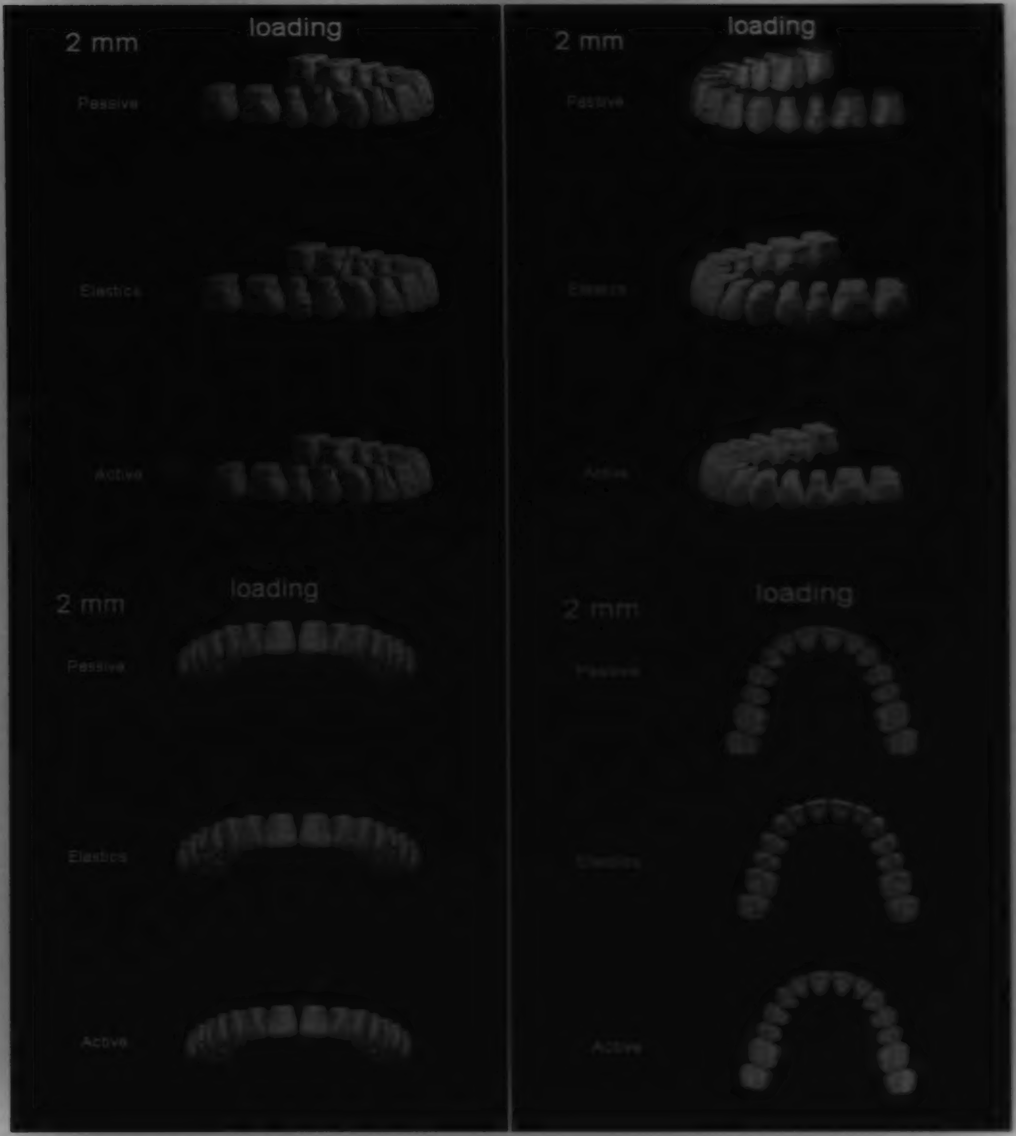

Figure 8-2: 0.014" 2mm loading OSIM display

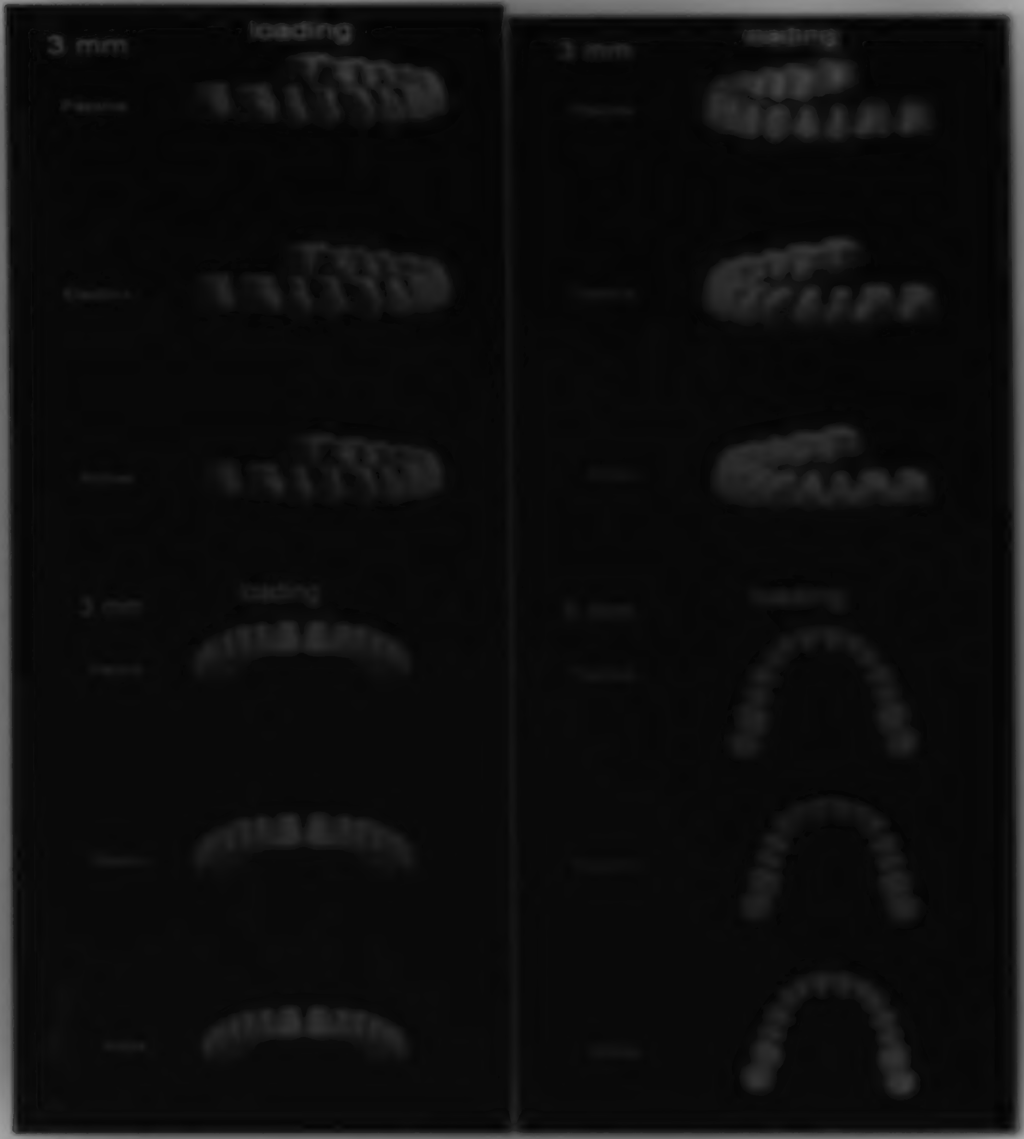

Figure 8-3: 0.014" 3mm loading OSIM display

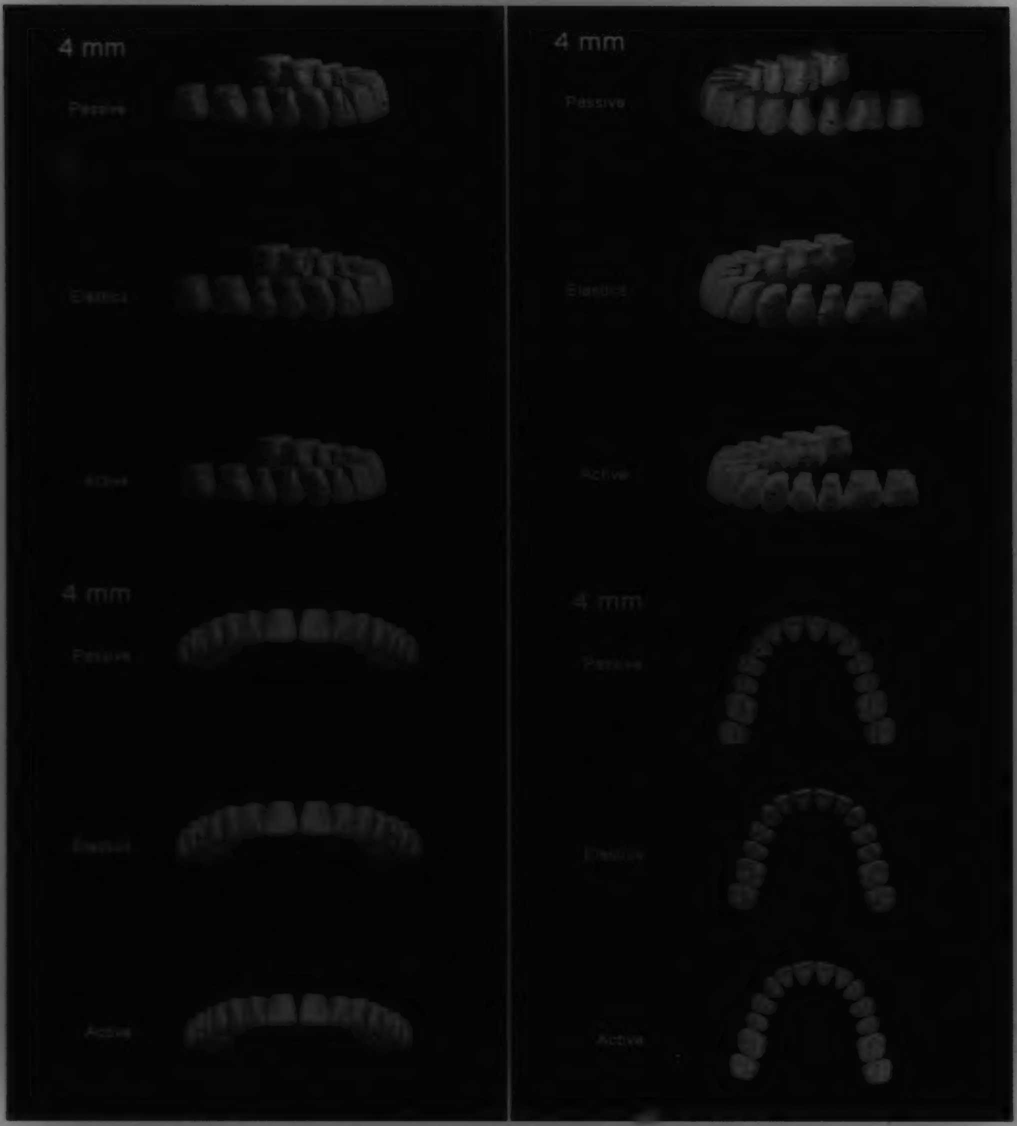

Figure 8-4: 0.014" 4mm OSIM display

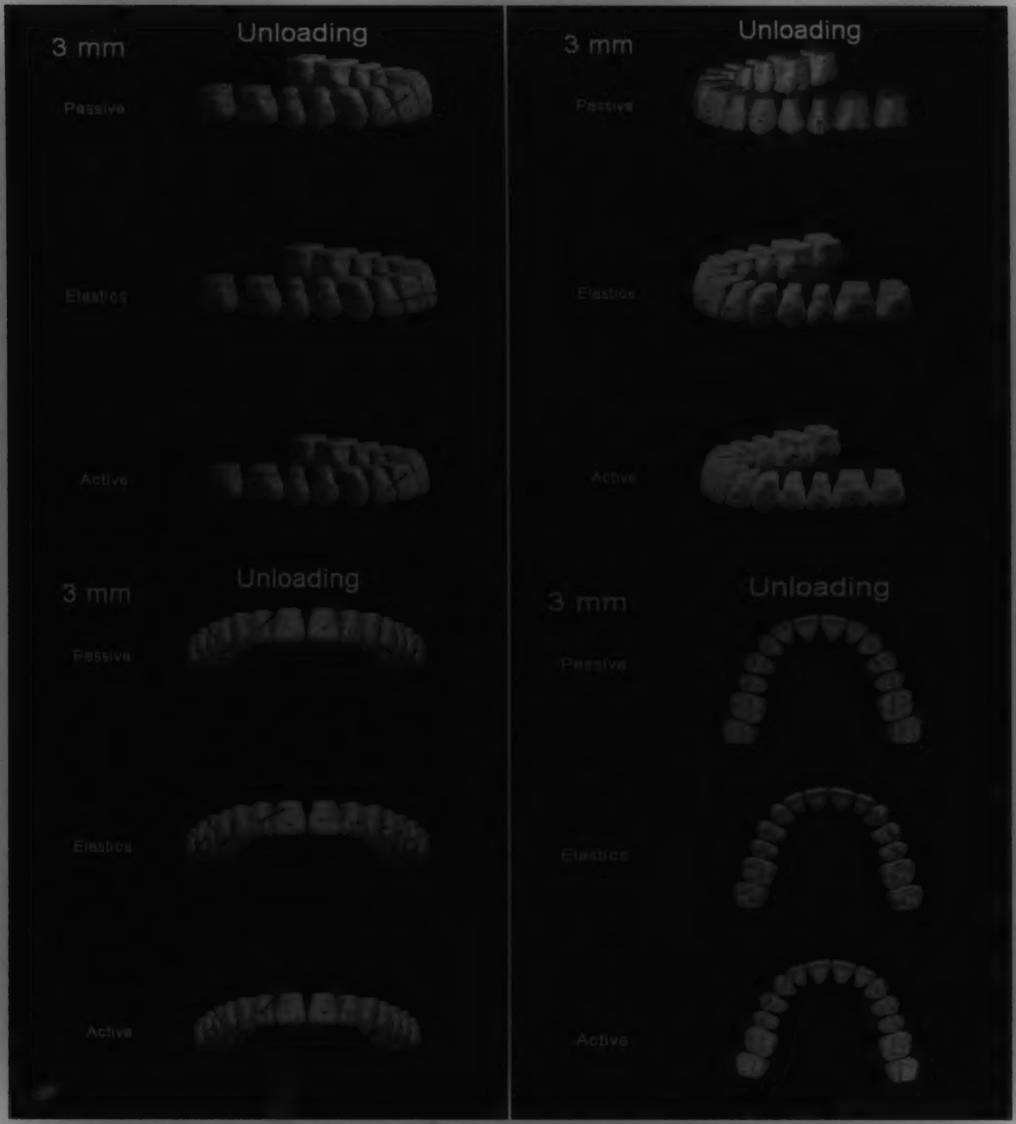

Figure 8-5: 0.014” 3mm unloading OSIM display

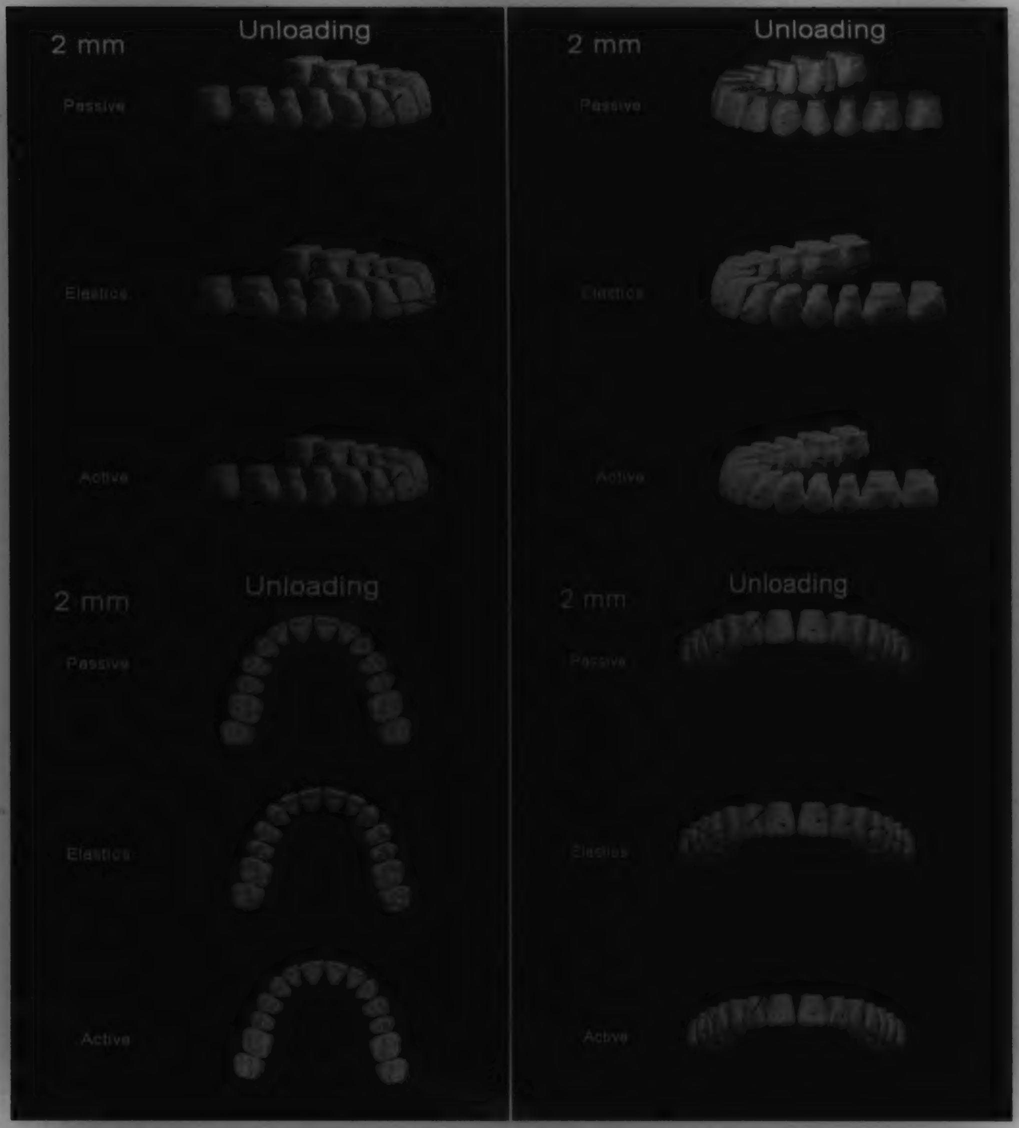

Figure 8-6: 0.014" 2mm unloading OSIM display

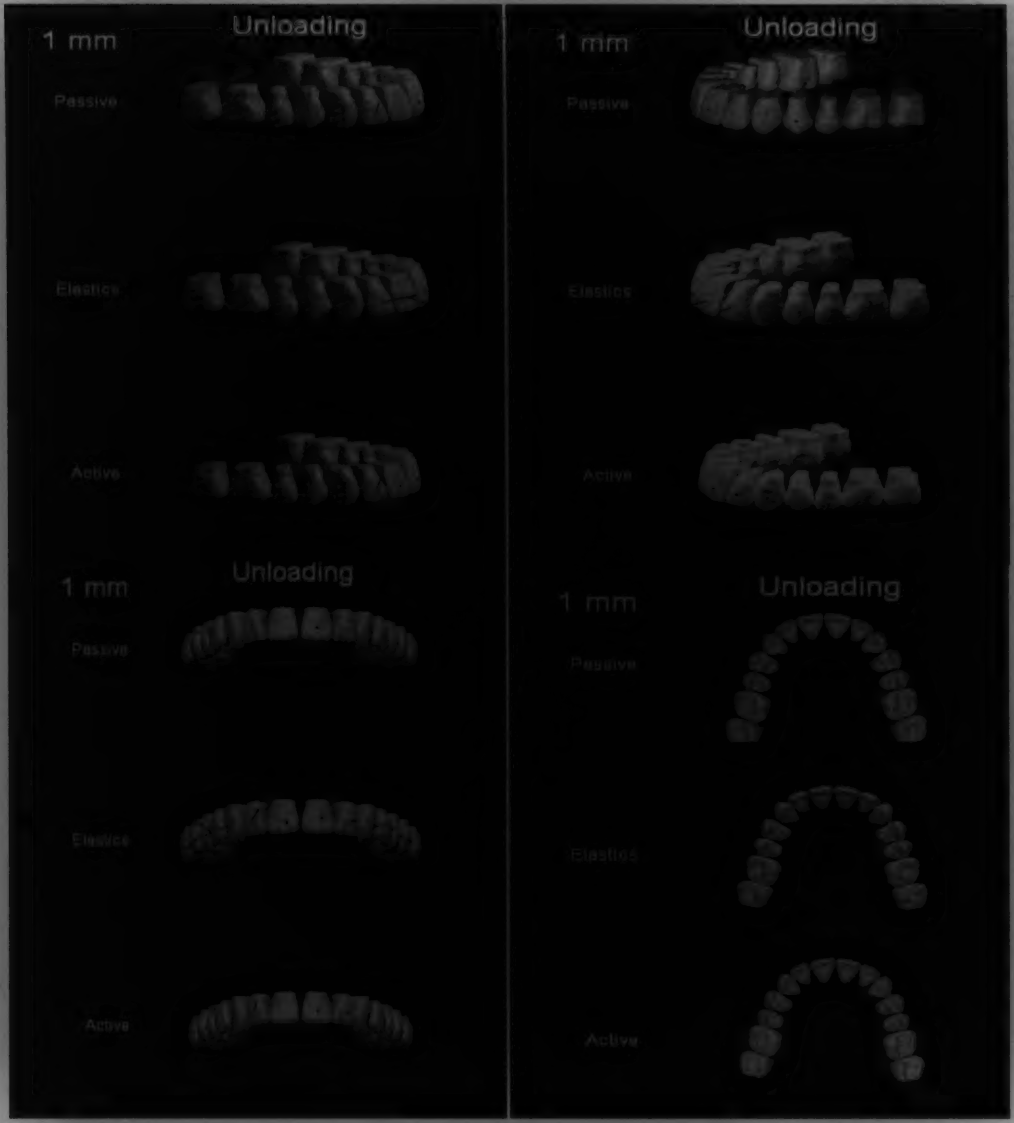

Figure 8-7: 0.014” 1mm unloading OSIM display

8.2 OSIM 0.018” Display

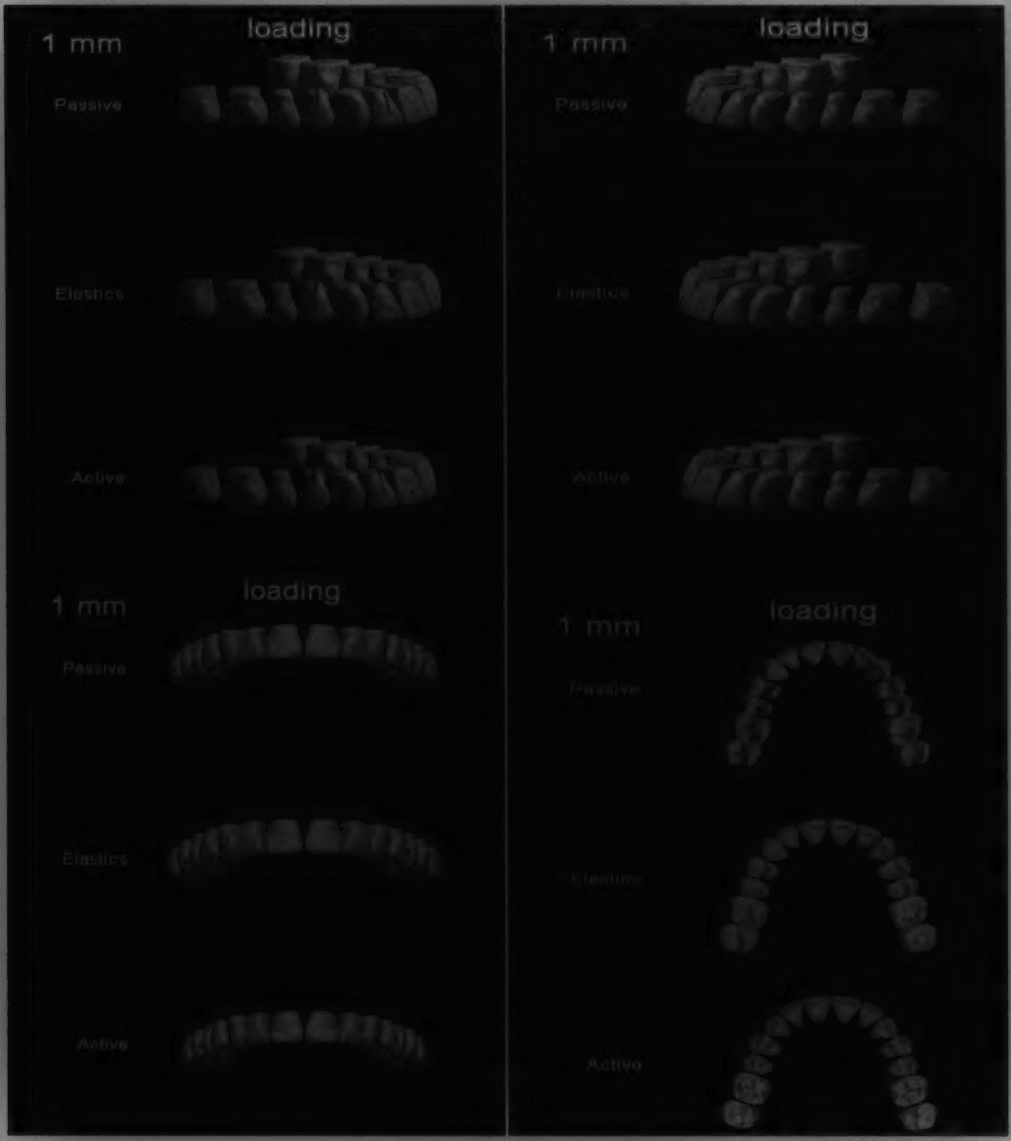

Figure 8-8: 0.018” 1mm loading OSIM display

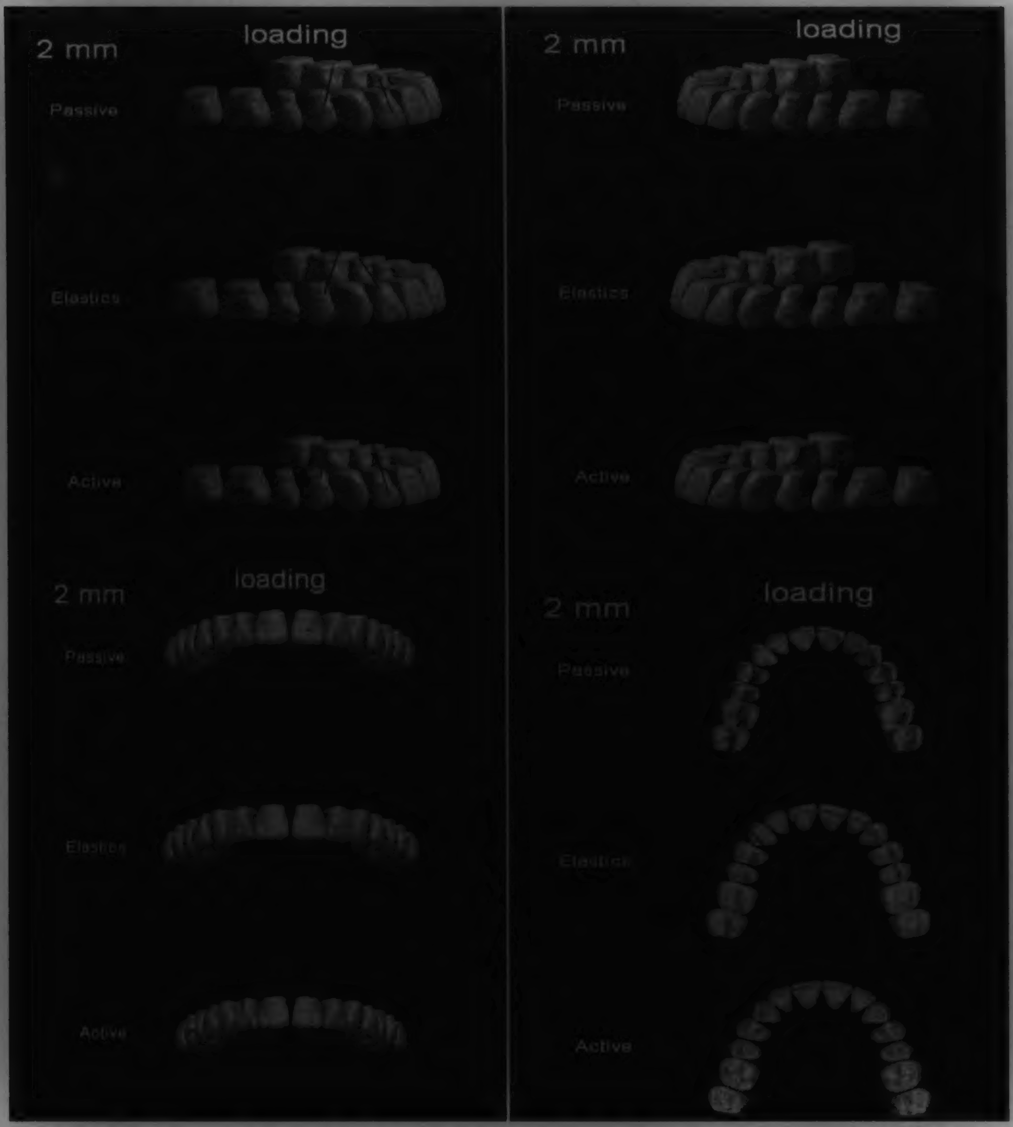

Figure 8-9: 0.018" 2mm loading OSIM display

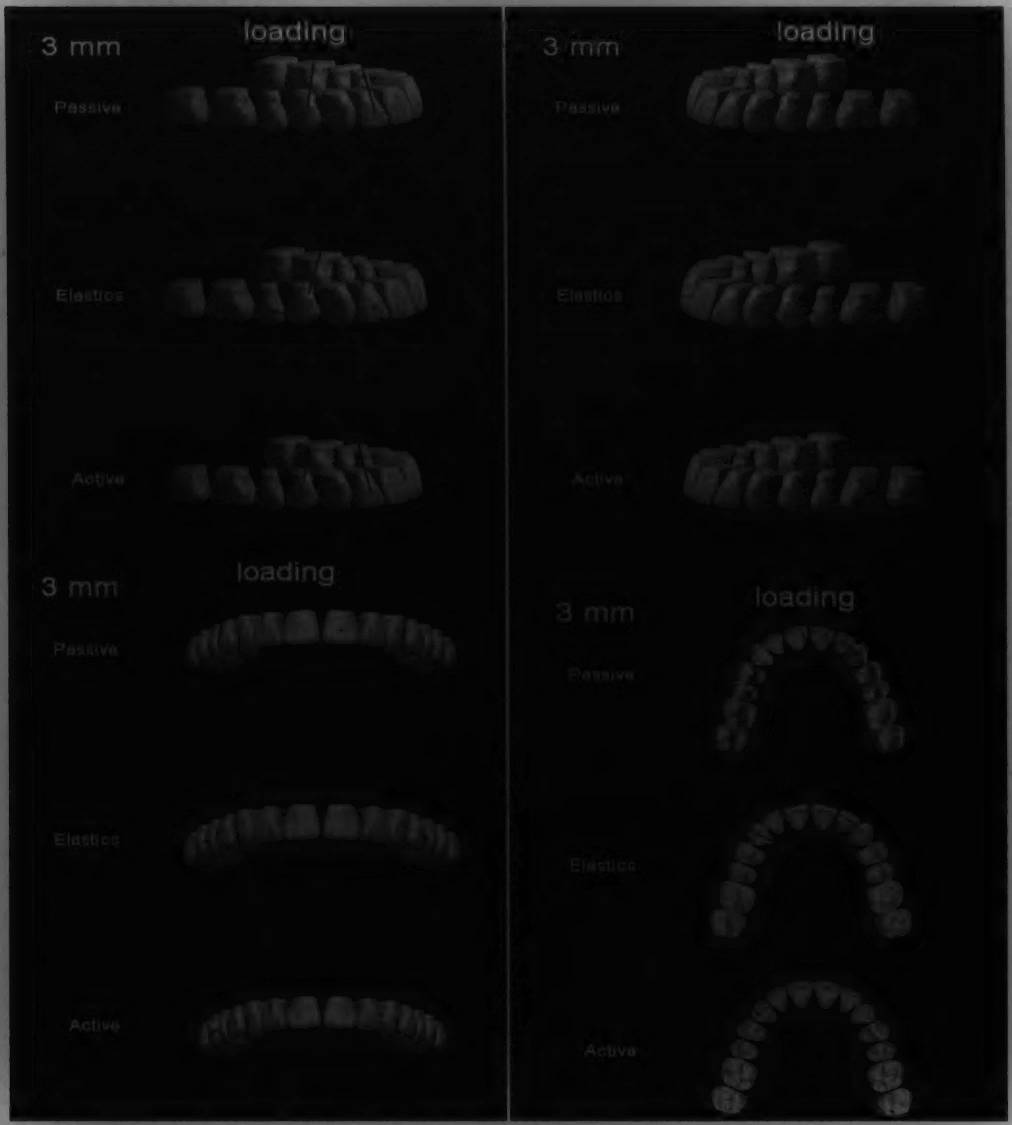

Figure 8-10: 0.018” 3mm loading OSIM display

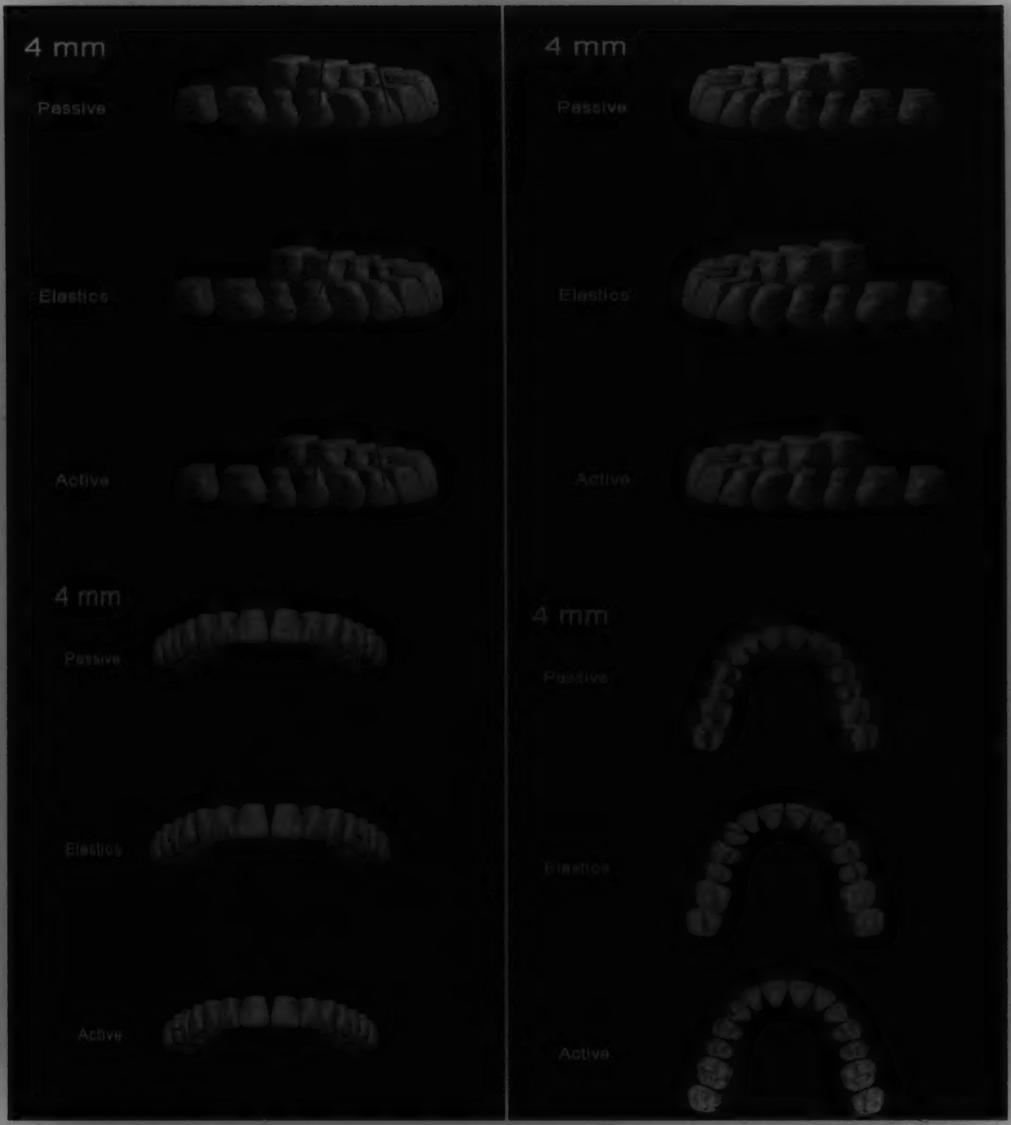

Figure 8-11: 0.018" 4mm OSIM display

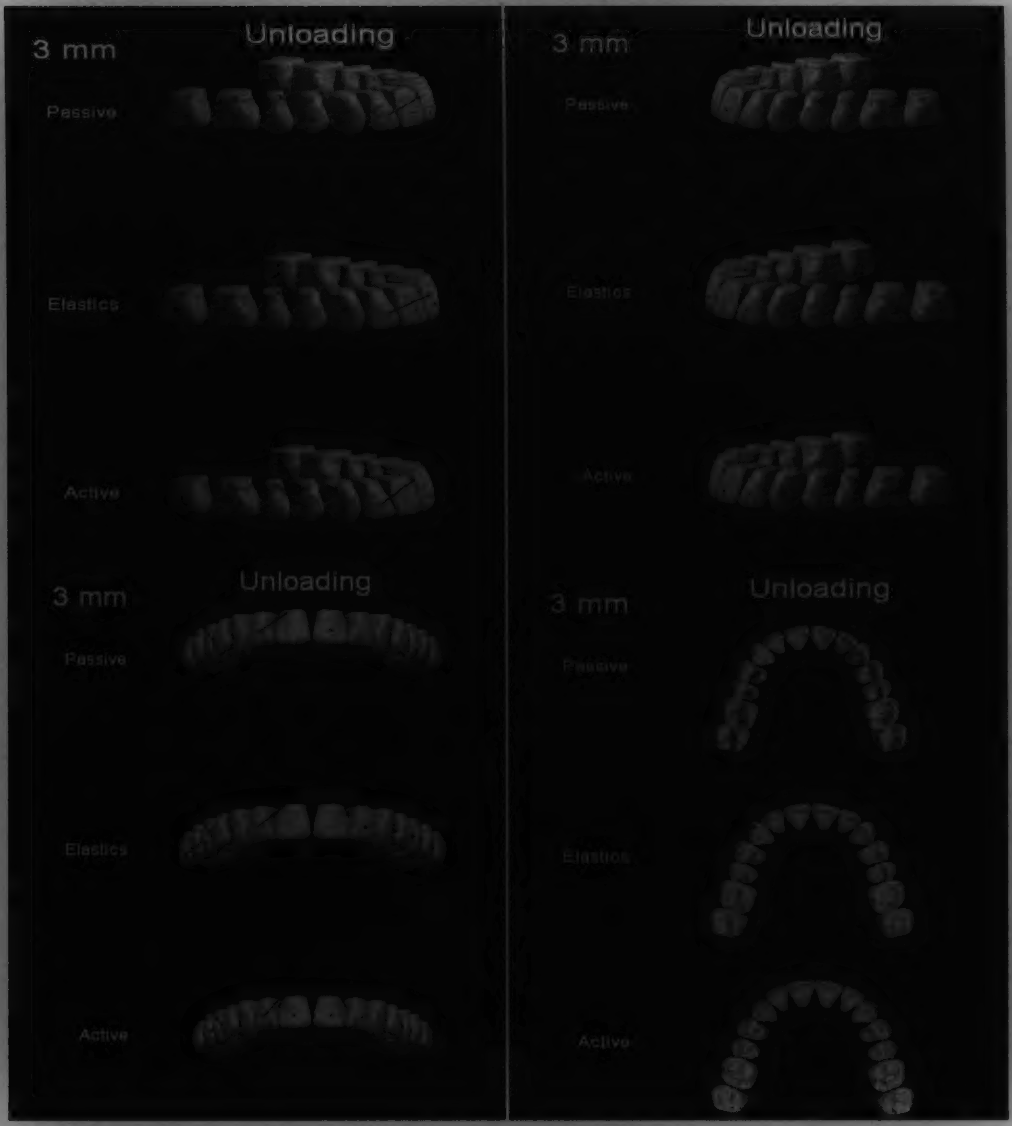

Figure 8-12: 0.018” 3mm unloading OSIM display

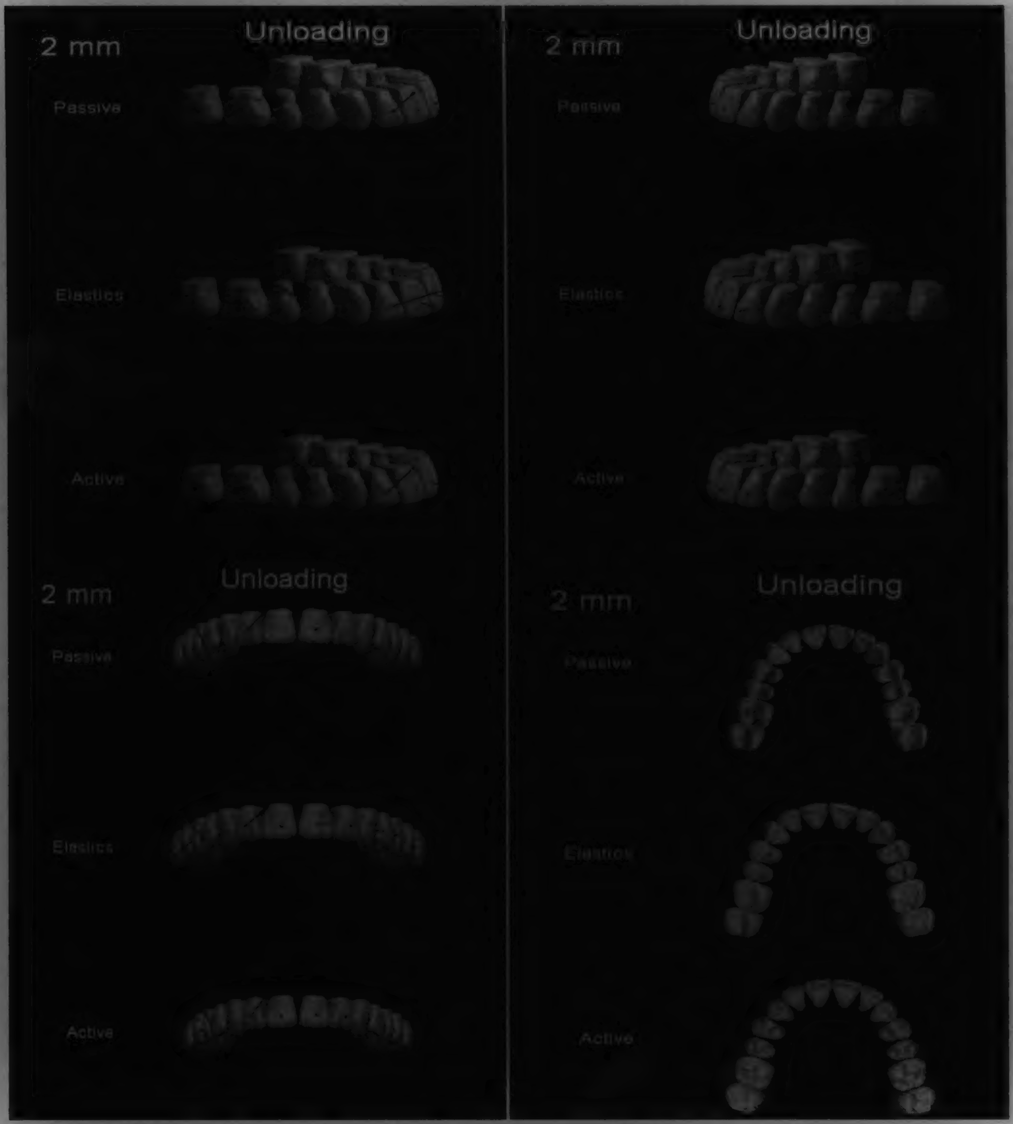

Figure 8-13: 0.018” 2mm unloading OSIM display

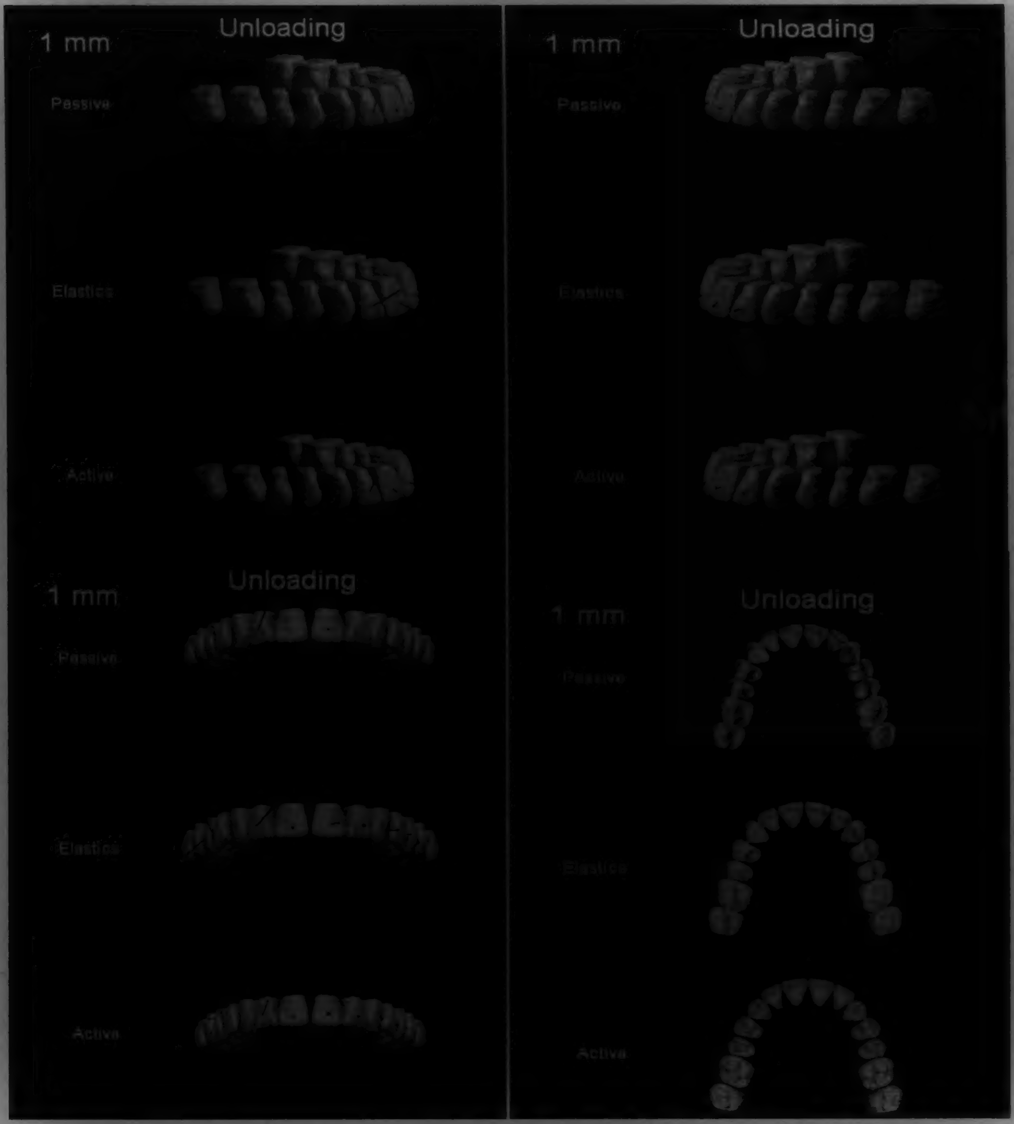

Figure 8-14: 0.018" 1mm unloading OSIM display

8.3 OSIM 14x25 Display

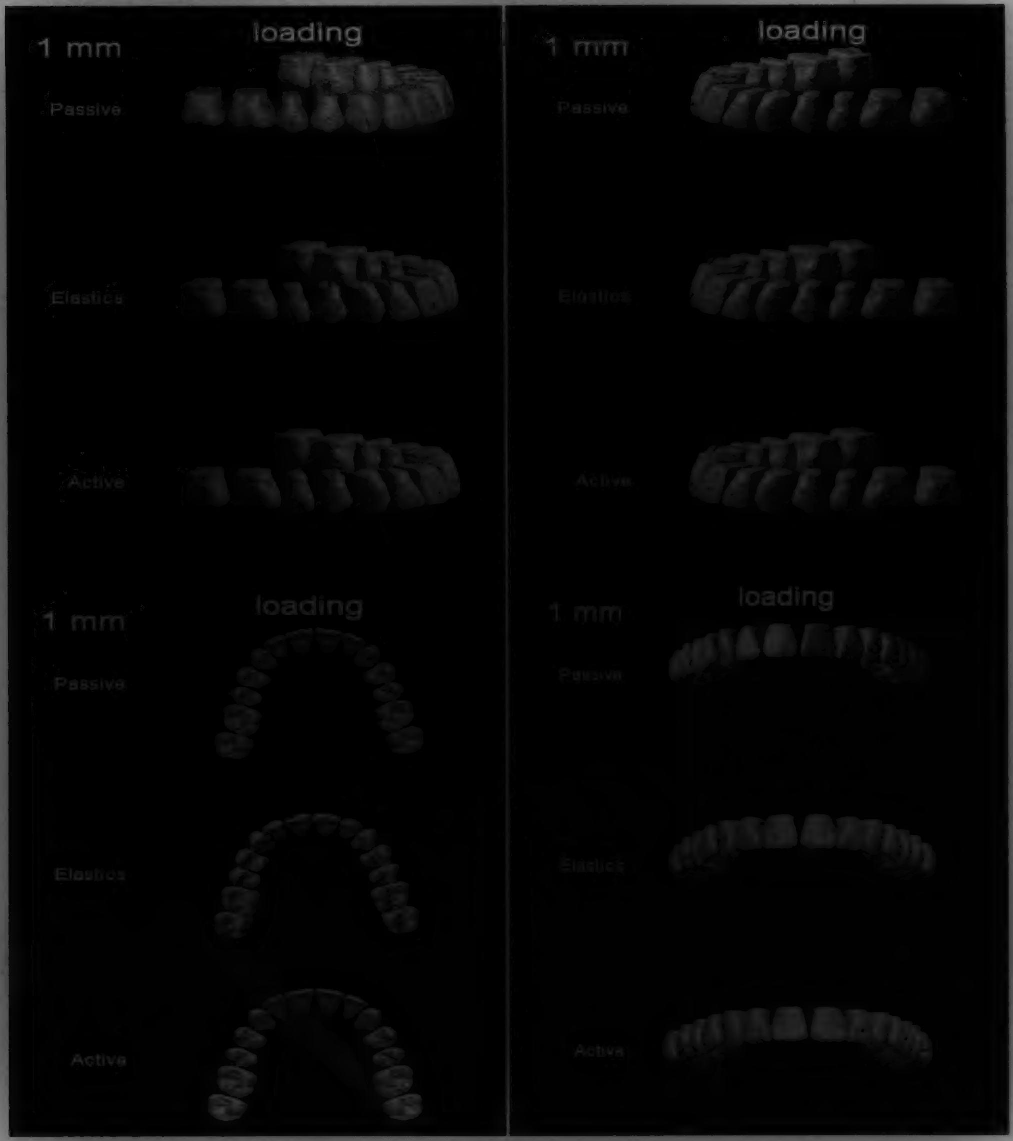

Figure 8-15: 14x25 1mm loading OSIM display

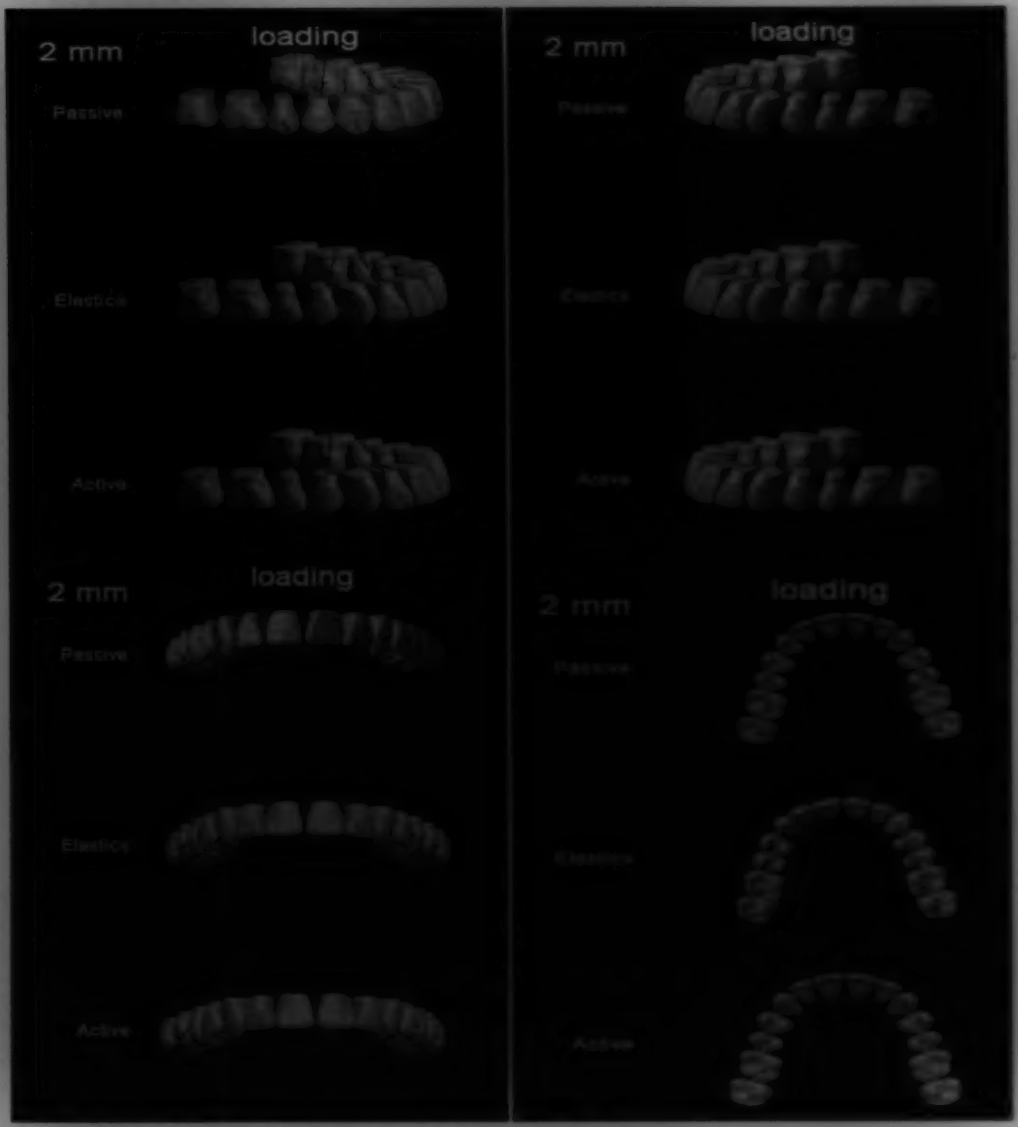

Figure 8-16: 14x25 2mm loading OSIM display

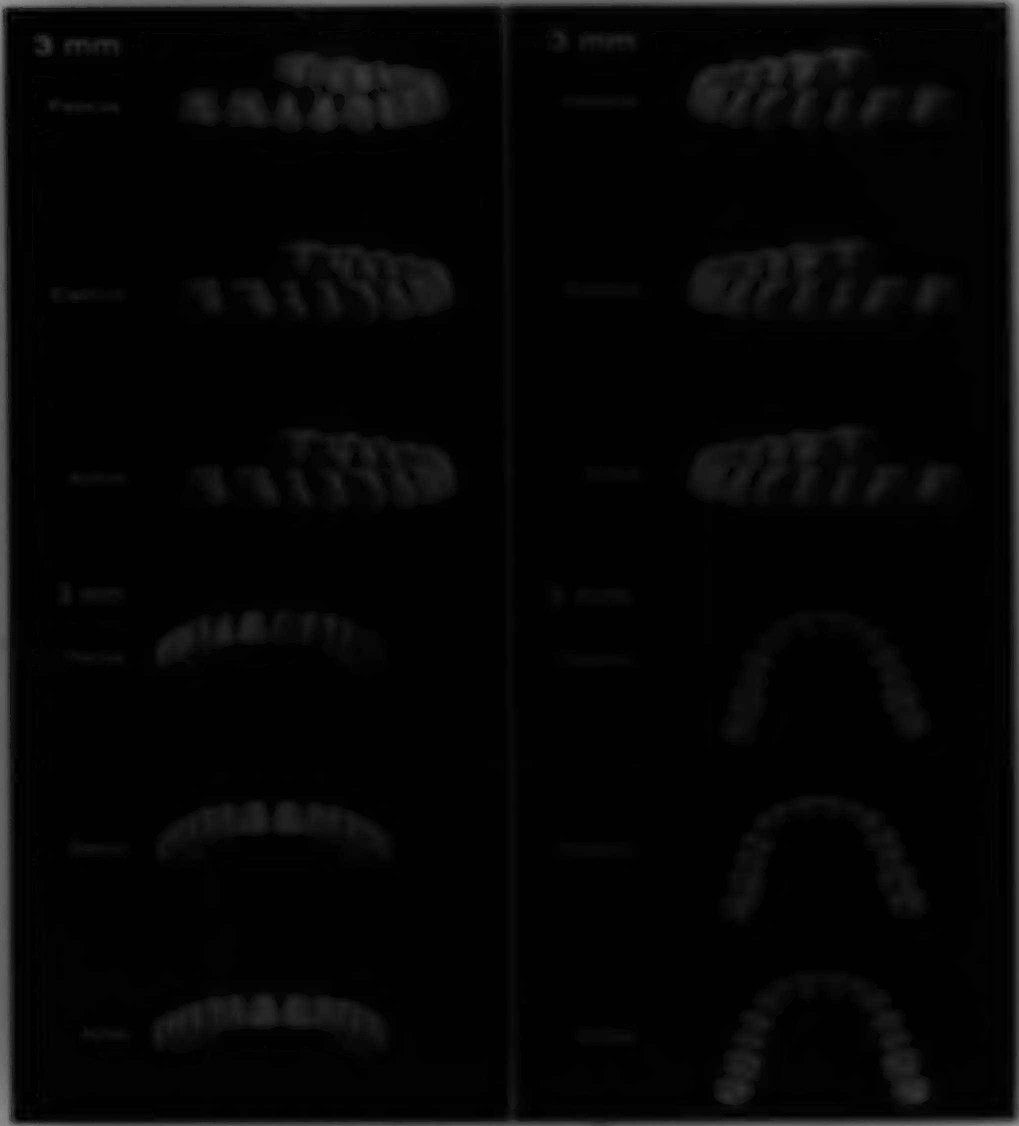

Figure 8-17: 14x25 3mm OSIM display

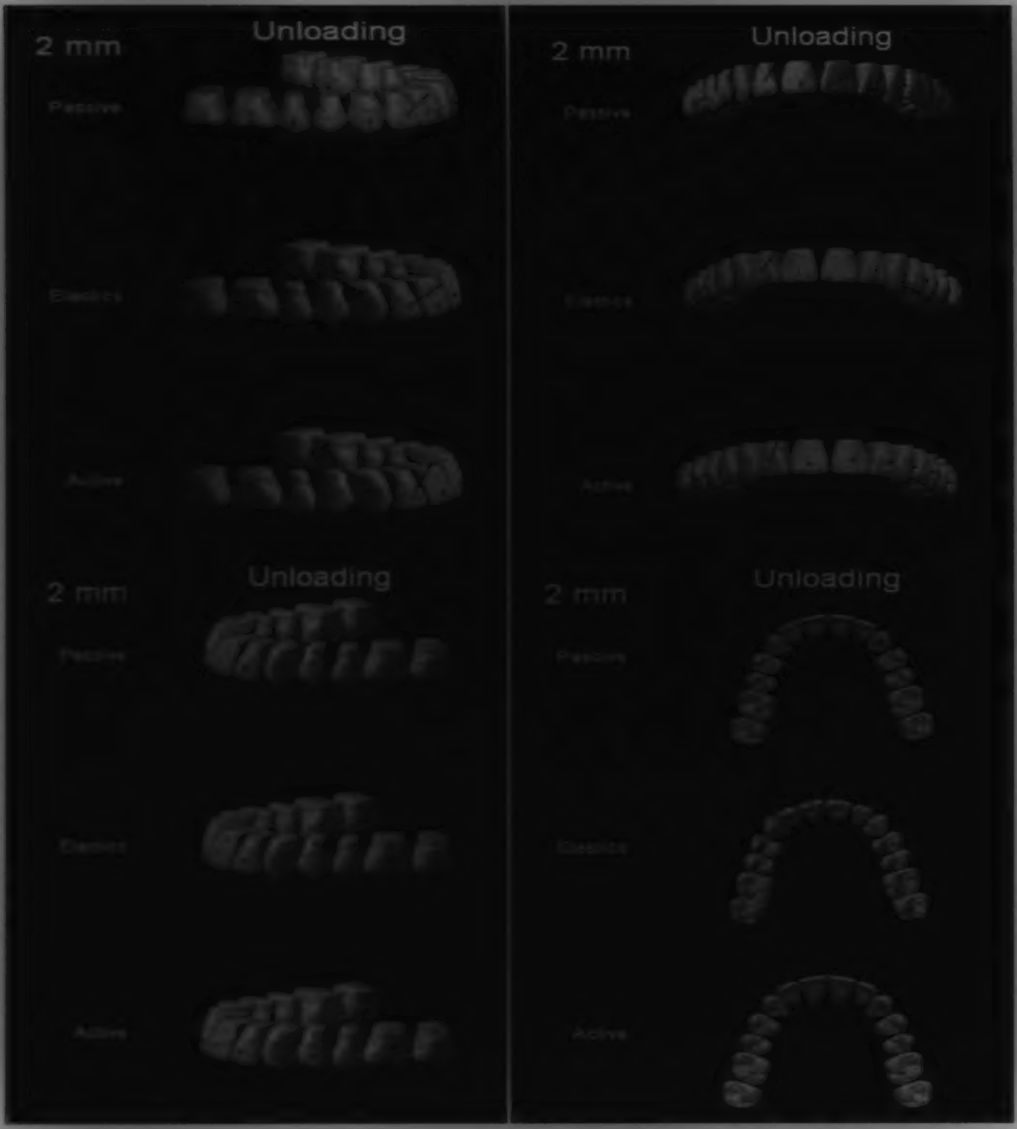

Figure 8-18: 14x25 2mm unloading OSIM display

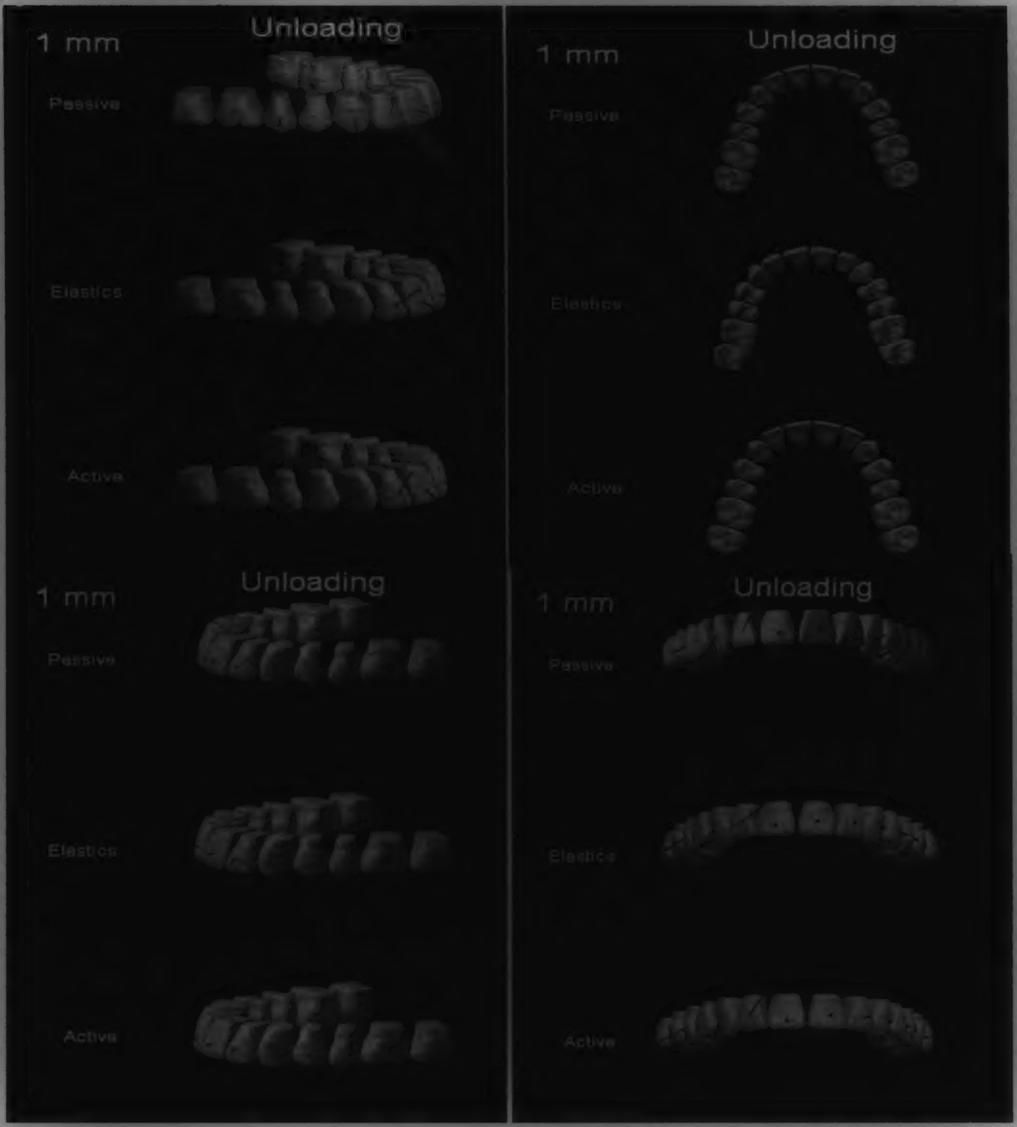

Figure 8-19: 14x25 1mm unloading OSIM display